

Implementation of Improved EDC Combustion Model in the Open LES Code FDS

David R.U. Johansen



Master's thesis in Process Safety
University of Bergen
Department of Physics and Technology
Bergen, Norway

August 2011

Preface

This thesis is submitted as the final part of the degree Master of Science in Process Safety Engineering at the University of Bergen. The work has been carried out at Stord/Haugesund University College throughout the whole period. To work with this thesis has been both challenging and time consuming. Still, it has been a valuable experience and really exciting.

The major challenge of this thesis has not been to implement the code in FDS, but to adapt it to the rest of the code and to orientate in the in the jungle of modules and subroutines. To handle the large amount of numbers requires systematic work and has also been challenging. Unfortunately, the experiments at Lund University gave unsuccessful PIV data. However, the main goal with the experiments was to gain more knowledge to experimental work and not validate the implemented code.

To be able to quantify such complex physical and chemical phenomenon as a fire, and also fluid flow in general with CFD, is truly fascinating me. Since the use of CFD requires a broad knowledge in scientific topics makes it extra interesting. Through this project I have linked loose ends of knowledge together from earlier courses and learned how to apply it in the context of CFD. I have also gained more knowledge to numerical methods and experimental work. However, it is still much more to learn. To work with this thesis has encouraged me to continue to work in the field of fire research.

Acknowledgements

I would like to express my sincere gratitude to my supervisor Associate Professor Bjarne P. Husted at Stord/Haugesund University College. He has been a great inspiration and encouraging to work with. Throughout the process of my work, Bjarne P. Husted has been providing me with expert advice on CFD, fire dynamics, computer science, numerical methods and experimental work. I really appreciate that he linked me up to the pool fire project and even joined the experiments at Lund University.

I appreciate that the staff at Lund University let me take part of the pool fire project, and at the same time let me to do experiments relating my Master's thesis. I would like to particularly thank Mr. Per Petersson for operating PIV measurements, Professor Patrick van Hees for leading the experiments and PhD student Jonathan Wahlquist who helped with set up.

Other people I would like to thank are:

- Dr. Balram Panjwani (Norwegian University of Science and Technology) who e-mailed me his PhD thesis and answered questions regarding LES-EDC
- Ms. Mari Ueland and Ms. Siri H. Walaker for feedbacks on my report
- my older brother Mr. Remi Johansen who helped me with Linux, MatLab and L^AT_EX
- Dr. Monika Metallinou who arranged an office for me at Stord/Haugesund University College
- Professor Bjørn Arntzen at the University of Bergen and fellow Master student Ms. Natalja Pedersen for discussion of EDC
- PhD student Bjarne Chr. Hagen (Stord/Haugesund University College) and fellow Master student Mr. Einar Kolstad for general discussion and advice
- Dr. Alf Reidar Nilsen (Stord/Haugesund University College and Statoil) for letting me use his computers for simulations
- Mr. Arjen Kraaijeveld (Stord/Haugesund University College) for advices regarding experimental work

Summary

In this thesis, Magnussen's and Hjertager's Eddy Dissipation Concept (EDC) Combustion Model [1][2][3] has been implemented in the CFD code Fire Dynamics Simulator (FDS) [4]. FDS is an open source non-commercial Large Eddy Simulation (LES) code mainly developed by the National Institute of Standards and Technology (NIST). EDC is developed for Reynolds Average Navier Stokes (RANS) equations where fluctuating values caused by turbulence are modeled. The reaction rate in EDC is predicted by RANS quantities such as Turbulent Kinetic Energy (TKE) and Dissipation of Turbulent Kinetic Energy, which is not solved explicitly in LES codes. A promising extension of EDC to LES was proposed Panjwani *et al.* treating eddy viscosity and strain rate instead [5][6]. In their validation work a model constant was established for jet flames for the Smagorinsky turbulence model. However, the main purpose of FDS is studying smoke spread, fire detection and smoke ventilation in building fires. Such fires involves low Mach number flows driven by buoyancy, in contrast to jet fire that are strongly influenced by the momentum fuel release and are highly turbulent.

The first motivation of this thesis has been to implement LES-EDC in FDS, and second to establish a model constant for buoyancy driven fires and evaluate whether a static constant is sufficient or a dynamic constant is necessary. This is solved by validate the code against velocity profiles in Sandia plume experiments, Heskestad flame height correlation, McCaffery centerline temperature and velocity correlation. Results are also compared with the existing combustion model in FDS for the default turbulence model, Deardorff, in the unofficial version 6.

Experiments with square pipes inserted in the persistent flame region were performed at Lund University. Particle Image Velocimetry (PIV) technique was applied to measure the velocity vector field above the pipes. The goal was to study the affected of generated turbulence from the pipes and perhaps be able to investigate how the turbulence effected the LES-EDC model constant. Unfortunately, the experiments gave unsatisfactory results for CFD validation. During the experiments it was some technical problems with the shutter on the camera occurred as well as the seeding of particles turned out to be quite challenging. Therefore, this part of the thesis must be regarded as a contribution to the project *Prediction and validation of pool fire developed in enclosures by means of CFD models for risk assessment of nuclear power plants* which the experiments were linked up to, and not validation of FDS-EDC.

A model constant of 0.015 gave satisfactory results for all the chosen validation cases. But a somewhat smaller constant is preferable for the centerline temperature and velocity profiles in the McCaffery simulations. With $C_{LES} = 0.015$ the maximum temperature is over estimated. The slope change in flame height around $Q^* \approx 1$ was not captured by the Vreman and Deardorff turbulence model. The already existing combustion had the same difficulties. LES-EDC with the Smagorinsky model in addition to the existing combustion did also capture the dip for vertical velocity profile in the Sandia plume experiment test 17. But the disadvantage with the Smagorinsky model is the CPU clock times compared with the two other turbulence models.

The errors of the implemented code (referred as FDS-EDC) are in most cases less or the same as for the existing model. The models are also about the same computational expensive. In contrast to the existing model, the implemented code is strongly grid dependent. So before FDS-EDC can be applied in fire analysis the model must be modified to be grid independent. A dynamic constant is not necessary for buoyancy-driven fires in fire engineering application but a more accurate constant is recommended to be established. Temperature and velocity should in further work be validated in a wider range of Q^* for practical fire sizes than in this thesis.

Nomenclature

A	number of collisions	[-]
a	number of nitrogen atoms	[-]
C	model constant	[-]
C	concentration	[mol/m ³]
C_D	Deardorff model constant	[-]
C_{LES}	EDC-LES model constant	[-]
C_S	Smagorinsky model constant	[-]
C_V	Vreman model constant	[-]
c_p	heat capacity	[J/kg·K]
c	speed of light	[m/s]
D	mass diffusivity	[m ² /s]
D	diameter	[m]
D^*	non-dimensional fire diameter	[-]
Da	the turbulent Damköhler number	[-]
E_a	activation energy	[J]
E	thermal radiative energy	[W/m ²]
f	acceleration	[m/s ²]
Fr	Froude number	[-]
g	gravitational constant	[m/s ²]
H	heat	[kJ]
ΔH_c	heat of combustion	[kJ/kg]
h	specific enthalpy	[kJ/kg]
h	convective heat transfer coefficient	[W/m ² K]
h	Planck's constant	[Js]
j	diffusiv mass flux	[kg/m ² s]
k	number of reactions each second	[s ⁻¹]
k	model constant	[-]
k	turbulent kinetic energy	[kJ/kg]
k	thermal conductivity	[W/m·K]
k	Boltzman constant	[J/K]
Ka	the turbulent Karlovitz number	[-]
L	characteristic length scale	[m]
L	length	[m]

L_v	heat required to produce volatiles	[kJ/g]
l	length scale	[m]
M	mass	[kg]
M	molar mass	[g/mol]
Ma	Mack number	[-]
m	mass	[kg]
N	number of species	[-]
Nu	Nusselt number	[-]
p	pressure	[N/m ²]
\dot{Q}_c	heat release rate (HRR)	[W]
\dot{Q}_r	radiative heat transfer	[W]
Q^*	dimensionless heat release rate	[-]
q	heat	[kJ/kg]
R	universal gas constant	[J/mol·K]
R	reaction rate	[kg/s]
Re	Reynolds number	[-]
R_t	turbulent Reynolds number	[-]
S	strain rate	[s ⁻¹]
S	source term	
Sc	Schmidt number	[-]
s	stoichiometric coefficient	[-]
T	temperature	[K]
t	time	[s]
U	internal energy	[J]
u	velocity	[m/s]
W	molecular wight	[kg/kmol]
w	mechanical work	[kJ/kg]
x	direction x	
x	number of carbon atoms	[-]
Y	mass fraction	[kg/kg]
y	direction y	
y	number of hydrogen atoms	[-]
Z	mixture fraction	[kg/kg]
z	direction z	
z	number of oxygen atoms	[-]
z	height	[m]

Greek symbols

α	thermal diffusivity	[m ² /s]
β	model constant	[-]
γ_λ	ratio of fine structure mass between large eddies to the total mass	[kg/kg]
γ^*	ratio of fine structure mass to the total mass	[kg/kg]
Δ	grid cell size	[m]
δ_{ij}	Kronecker-delta ($i = j \rightarrow \delta_{ij} = 1$ and $i \neq j \rightarrow \delta_{ij} = 0$)	[-]
ϵ	dissipation rate of turbulent kinetic energy k	[W/kg]
η	model constant	[-]
λ	wave length	[m]
μ	dynamic molecular viscosity	[kg/m·s]
ν	kinematic molecular viscosity	[m ² /s]
ν	yield	[kg/kg]
ρ	density	[kg/m ³]
σ_k	Schmidt number for turbulent kinetic energy k	[-]
σ_ϵ	Schmidt number for dissipation rate of turbulent kinetic energy ϵ	[-]
σ	Stefan-Boltzman constant	[W/m ² K ⁴]
τ	viscous shear tensor	[N/m ²]
τ	time scale	[s]
φ	variable in transport equation or filtered value	[-]
χ	efficient coefficient	[-]
$\dot{\omega}$	reaction rate	[kg/s]
ω	strain	[s ⁻¹]

Superscripts

'	fluctuating value
''	characteristic turbulent scale
''	per m^2
-	favre average value
~	filtered value
·	per second
*	fine structure
0	surrounding

Subscripts

0	integral length scale
0	centerline
∞	ambient
a	number of nitrogen atoms
d	diffusion
F	fuel
F	flame
f	formation
f	flame
f	fluid
g	gravitational
i	component in x -direction
j	species j
j	component in y -direction
k	component in z -direction
k	species k
k	turbulent kinetic energy
K	Kolmogorov (length scale)
LFT	lower flame temperature
L	laminar
L	loss
n	number
P	products
r	radiation
SGS	subgrid scale
S	soot
s	surface
T	Taylor (length scale)
T	Turbulent
t	turbulent
u	turbulent
v	vapourizing

x number of carbon atoms
 y number of hydrogen atoms
 z number of oxygen atoms
 α number
 ϵ dissipation rate of turbulent kinetic energy

Contents

1	Introduction	5
2	Theory	7
2.1	Computational Fluid Dynamics	7
2.1.1	Governing Equations	7
2.1.2	Reacting Flows	8
2.1.3	Turbulence and Turbulence Modeling	9
2.2	Combustion	13
2.2.1	Chemical Kinetics	15
2.2.2	Heat Release Rate (HRR) and Reaction Rate	15
2.3	Flame Characteristics and Fire Plumes	17
2.3.1	Borghini Diagram	18
2.3.2	Flame Height	19
2.3.3	Centerline Flame Temperature and Velocity	20
2.4	Heat Transfer	21
2.4.1	Conduction	22
2.4.2	Convection	22
2.4.3	Radiation	23
2.5	Eddy Dissipation Concept (EDC)	23
2.5.1	Energy Cascade	23
2.5.2	Fine Structures and Mass Exchange	25
2.5.3	Perfectly Stirred Reactor (PSR)	26
3	Fire Dynamics Simulator (FDS)	28
3.1	Local Heat Release Rate (HRR) and Reaction Rate	28
3.2	Mult-Parameter Mixture Fraction	30
3.2.1	Two parameter single-step reaction	31
3.2.2	Three parameter two-step reaction	32
3.3	Extinction Criteria	34
3.4	Grid Resolution	34

4	Implementation of LES-EDC in FDS	35
4.1	LES-EDC	35
4.2	Numerical Procedure	36
4.3	The Implemented Code	37
5	Validation of FDS-EDC	40
5.1	McCaffery's Plume Correlation, Velocity and Temperature Profiles	42
5.2	Heskestad Flame Height Correlation	60
5.3	Sandia Plume	65
5.3.1	Methane Fire, Test 14	66
5.3.2	Methane Fire, Test 17	76
5.3.3	Methane Fire, Test 24	86
5.3.4	CPU clock time	96
5.4	Discussion	100
5.4.1	McCaffery's Plume Correlation, Velocity and Temperature Profiles	100
5.4.2	Heskestad Flame Height Correlation	101
5.4.3	Sandia Plume	104
6	Flow Field Above Obstacle Inserted in Fire Plume	107
6.1	Designing Experiments for CFD Validation	108
6.2	Measurement Techniques	109
6.2.1	Particle Image Velocimetry (PIV)	109
6.2.2	Thermocouples	110
6.3	Experiments	111
6.3.1	Summary of the experiments	113
7	Conclusion	116
7.1	Further Work	117
A	FDS input files	121
A.1	Sandia test 14	121
A.2	Sandia test 17	126
A.3	Sandia test 24	132
A.4	Heskestad	138
A.5	McCaffery	138
B	Implemented code	140
B.1	fire.f90	140
B.2	velo.f90	165
B.3	mesh.f90	174
B.4	init.f90	181
C	Flame Height Calculation, post-processing	210

List of Figures

2.1	Vortex Stretching	10
2.2	Energy Cascade of TKE	10
2.3	Physical processes involved in a fire	14
2.4	Potential Energy	16
2.5	Borghi diagram	19
2.6	Flame Length	20
2.7	Fire Plume Regimes	21
2.8	Energy Cascade	24
2.9	Reactor model	26
3.1	Finite Rate Reaction and Infinitely fast Reaction	29
3.2	The threshold temperature	30
4.1	Numerical Procedure in FDS Combustion Model	36
5.1	McCaffery 14 kW Deardorff	43
5.2	McCaffery 22 kW Deardorff	44
5.3	McCaffery 33 kW Deardorff	45
5.4	McCaffery 45 kW Deardorff	46
5.5	McCaffery 57 kW Deardorff	47
5.6	McCaffery 14 kW Smagorinsky	48
5.7	McCaffery 22 kW Smagorinsky	49
5.8	McCaffery 33 kW Smagorinsky	50
5.9	McCaffery 45 kW Smagorinsky	51
5.10	McCaffery 57 kW Smagorinsky	52
5.11	McCaffery 14 kW Vreman	53
5.12	McCaffery 22 kW Vreman	54
5.13	McCaffery 33 kW Vreman	55
5.14	McCaffery 45 kW Vreman	56
5.15	McCaffery 57 kW Vreman	57
5.16	McCaffery FDS6	58
5.17	McCaffery FDS6	59
5.18	Flame Height Heskestad	61

5.19	Flame Height Smagorinsky	62
5.20	Flame Height Vreman	63
5.21	Flame Height comparison, FDS6	64
5.22	Sandia test 14 Deardorff $z = 0.3$ m	66
5.23	Sandia test 14 Deardorff $z = 0.5$ m	67
5.24	Sandia test 14 Deardorff $z = 0.9$ m	68
5.25	Sandia test 14 Smagorinsky $z = 0.3$ m	69
5.26	Sandia test 14 Smagorinsky $z = 0.5$ m	70
5.27	Sandia test 14 Smagorinsky $z = 0.9$ m	71
5.28	Sandia test 14 Vreman $z = 0.3$ m	72
5.29	Sandia test 14 Vreman $z = 0.5$ m	73
5.30	Sandia test 14 Vreman $z = 0.9$ m	74
5.31	Sandia test 14 FDS6	75
5.32	Sandia test 17 Deardorff $z = 0.3$ m	76
5.33	Sandia test 17 Deardorff $z = 0.5$ m	77
5.34	Sandia test 17 Deardorff $z = 0.9$ m	78
5.35	Sandia test 17 Smagorinsky $z = 0.3$ m	79
5.36	Sandia test 17 Smagorinsky $z = 0.5$ m	80
5.37	Sandia test 17 Smagorinsky $z = 0.9$ m	81
5.38	Sandia test 17 Vreman $z = 0.3$ m	82
5.39	Sandia test 17 Vreman $z = 0.5$ m	83
5.40	Sandia test 17 Vreman $z = 0.9$ m	84
5.41	Sandia test 17 FDS6	85
5.42	Sandia test 24 Deardorff $z = 0.3$ m	86
5.43	Sandia test 24 Deardorff $z = 0.5$ m	87
5.44	Sandia test 24 Deardorff $z = 0.9$ m	88
5.45	Sandia test 24 Smagorinsky $z = 0.3$ m	89
5.46	Sandia test 24 Smagorinsky $z = 0.5$ m	90
5.47	Sandia test 24 Smagorinsky $z = 0.9$ m	91
5.48	Sandia test 24 Vreman $z = 0.3$ m	92
5.49	Sandia test 24 Vreman $z = 0.5$ m	93
5.50	Sandia test 24 Vreman $z = 0.9$ m	94
5.51	Sandia test 24 FDS6	95
5.52	Sandia plume CPU clock time, $dx = 1.5$ cm	96
5.53	Sandia plume CPU clock time, $dx = 3$ cm	97
5.54	Sandia plume CPU clock time, $dx = 6$ cm	98
5.55	Sandia plume CPU clock time, comparison between FDS6 and FDS-EDC	99
5.56	Temperature and velocity contours for McCaffery 57 kW	101
5.57	Heskestad Percentage Error, Smagorinsky	102
5.58	HRRPUV Slice File Smagorinsky	103
5.59	Temperature contours for FDS6 test 14	105
6.1	CFD road map	108

6.2	Numbering of thermal couples in the pipes.	109
6.3	Particle Image Velocimetry (PIV)	110
6.4	Thermocouple measurement circuit.	111
6.5	Experimental setup	112
6.6	Calibration of the camera.	114

List of Tables

2.1	Chemical Reactions	15
2.2	Flame types	17
2.3	McCaffery Empirical Constants	22
5.1	Heskestad Flame Height Simulations	60
5.2	Sandia plume experiment simulations.	65
6.1	Experimental scenarios.	112

Chapter 1

Introduction

Accidental fires and explosions are a severe threat to human life and expensive process equipment in the process industries. To obtain an acceptable risk when handling flammable gas and liquid, knowledge to the physical processes involved in a fire or explosion is required for safety designing. Computational Fluid Dynamics (CFD) is a useful engineering tool to evaluate potential consequences, such as heat loads on process equipment or gas dispersion from accidental leaks, detector and mitigation optimization. Over the last decades, the use of CFD has increased as a result of increased computational power. Increasing computational power is also allowing continuously development of CFD.

Several commercial and non-commercial CFD codes exist for different use. Mainly the codes are divided in which way the turbulence is modeled. Fire Dynamic Simulator (FDS) is a non-commercial Large Eddy Simulation (LES) code developed by NIST (National Institute of Standard and Technology) appropriate for indoor building fire analysis [4]. FDS is limited to simulations of thermal driven flows as buoyancy-driven fires, i.e FDS is unsuitable for jet fire and explosion simulations.

Correct modeling of the combustion process in CFD is crucial to achieve reliable results. Combustion models are based on certain assumptions related to the simulated flame type. The Eddy Dissipation Concept (EDC) proposed by Magnussen and Hjertager, is based on the turbulent mixing to model the reaction rate [1][2][3]. The model assumes that the chemical reaction occurs where reactants and hot products are molecularly mixed. The mixing process is located where the kinetic energy is dissipated into heat. These regions, referred as fine structure, are treated as a perfectly stirred reactor.

EDC in its original form assumes full turbulence cascading in each numerical cell, as the way turbulence is modeled in the Reynolds Average Navier Stokes (RANS). Extension of EDC to LES has been performed by Hu *et al.* and Zhou *et al.*, both with unsatisfactory predictions [7][8]. The reason for the unsatisfactory predictions was that RANS model constants were used. Panjwani *et al.* proposed two approaches to LES-EDC, where the fine structure regions are based on subgrid viscosity instead of turbulent kinetic energy (TKE) and dissipation, because they are usually not solved explicitly in

LES codes [5][6]. A parameter study in their validation showed that the model constant $C_{LES} = 0.25$ was satisfactory for the Smagorinsky turbulence model. However, this was for a jet fire strongly influenced by momentum. The Froude number for the jet flames Panjwani *et al.* studied were in order of 10^4 while fires interested in context of buildings are in order of less than 10^{-3} .

The objective of this thesis has been to implement LES-EDC in FDS and validate the implemented code (hereafter referred as FDS-EDC) to the application area of FDS. More precisely the objective has been to:

- establish a model constant for thermal buoyancy-driven fires and evaluate whether a static constant is sufficient with respect to different fire sizes or a dynamic constant is necessary
- establish a model constant for all supported turbulence models in FDS6; Vreman, Smagorinsky and Deardorff
- evaluate if LES-EDC can replace the already existing combustion model in FDS (hereafter referred as FDS6)

The simulations were limited to two parameter mixture fraction with a infinitely fast single-step reactions for non-premixed flames, i.e detailed kinetics are outside the scope of this thesis.

Chapter 2

Theory

2.1 Computational Fluid Dynamics

Computational fluid dynamics (CFD) is a powerful engineering tool, which is used to analyze fluid flow problems. CFD is used in a wide range of engineering disciplines, from designing airplanes, studying pipeline flows to fire engineering applications. Ever-increasing computational power leads to continuously development of CFD, which over time allows implementing of more complex algorithms. Because of inaccuracy in numerical techniques and limited precision in representation of numbers in a computer, CFD should always be considered as a supplement for experimental investigation and not a substitute [9]. In general, CFD is deterministic and is the reason why results are totally dependent on input values as boundary conditions and specified transient behavior in the computational domain. This leads to correct assumptions has to be taken into account. Therefore, CFD requires expert knowledge in physics, chemistry, computer science and numerical methods [10].

2.1.1 Governing Equations

In CFD, the finite volume method is applied by dividing a computational domain in to several sub volumes, a grid, where partial differential equations are solved in center of each sub volume or grid cell. The partial differential equations (PDE) are based on conservation of mass, momentum, energy and other static variables, φ . A general flow equation is given by

$$\underbrace{\frac{\partial}{\partial t}(\rho\varphi)}_{\text{accumulation}} + \underbrace{\frac{\partial}{\partial x_j}(\rho\varphi u_j)}_{\text{convective transport}} = \underbrace{\frac{\partial}{\partial x_j}(-j_{\varphi,j})}_{\text{diffusive transport}} + \underbrace{S_\varphi}_{\text{source term}} \quad (2.1)$$

The first term is accumulation of φ , the second is convective transport of φ , the third term is diffusive transport of φ and the last is the source term. Since an analytical solution on these equations does not exist, the equations are solved numerically. Taylor

expansions series is the most common technique to solve these partial differential equations [9]. The governing equations are:

Conservation of mass (Continuity Equation)

$$\frac{\partial \rho}{\partial t} + \frac{\partial}{\partial x_j}(\rho u_j) = 0 \quad (2.2)$$

Conservation of momentum (Newton's Second Law)

$$\frac{\partial}{\partial t}(\rho u_j) + \frac{\partial}{\partial x_j}(\rho u_i u_j) = -\frac{\partial p}{\partial x_i} + \frac{\partial \tau_{ij}}{\partial x_j} + \rho f_i \quad (2.3)$$

Conservation energy (First Law of Thermodynamics)

$$\frac{\partial}{\partial t}(\rho h) + \frac{\partial}{\partial x_j}(\rho u_i h) = \frac{\partial}{\partial x_j} \left(\rho \alpha \frac{\partial h}{\partial x_j} \right) + \dot{Q}_r + \rho \dot{\omega} Y_f \Delta H_c \quad (2.4)$$

These five partial differential equation consist six solution vectors: density ρ , temperature T , pressure p , three velocity components u_i , u_j and u_k . Note that it is three equations for conservation of momentum, one in each direction. The enthalpy is given as a function of temperature; $h = \int_{T_0}^T c_p T dT$. Pressure is calculated from the equation of state

$$p = \frac{\rho R T}{M} \quad (2.5)$$

Additional sub models are needed for closing the source terms, e.g radiation, Reynolds Stresses and combustion.

2.1.2 Reacting Flows

For reacting flows or multi-species flows, mass fractions for each species, k , is conserved

$$\frac{\partial}{\partial t}(\rho Y_k) + \frac{\partial}{\partial x_j}(\rho u_i Y_k) = \frac{\partial}{\partial x_j} \left(\rho D \frac{\partial Y_k}{\partial x_j} \right) + R_k \quad (2.6)$$

From the relation $\sum_k Y_k = 1$ the last species can be calculated, hence $N - 1$ partial differential equations are necessary for a total number N species.

PDE are expensive to compute. So to reduce the number of PDE when computing reacting flow, the mixture fraction can be computed instead of mass fractions:

$$\frac{\partial}{\partial t}(\rho Z_k) + \frac{\partial}{\partial x_j}(\rho u_i Z_k) = \frac{\partial}{\partial x_j} \left(\rho D \frac{\partial Z_k}{\partial x_j} \right) + R_k \quad (2.7)$$

Considering two streams mixing together, Z kg with property φ_1 in stream 1 and $(1 - Z)$ kg with property φ_2 in stream 2 giving 1 kg mixture $\varphi_{mix} = Z\varphi_1 + (1 - Z)\varphi_2$. The mixture fraction is then

$$Z = \frac{\varphi_{mix} - \varphi_2}{\varphi_1 - \varphi_2} \quad (2.8)$$

Assuming no sink or source, this expression can be used for all kinds of scalars [11]. In combustion modeling, stream 1 could be fuel and stream 2 air with property mass fractions $(Y_k)_{mix} = Z(Y_k)_1 + (Z - 1)(Y_k)_2$. Assuming stoichiometric infinitely fast chemistry of



”mixed is burned”, i.e oxygen and fuel cannot coexist, the scalar $Y_F - \frac{1}{s}Y_{O_2}$ is conserved for a complete reaction. Y_F and Y_{O_2} are mass fractions for fuel and oxygen respectively, and s is the stoichiometric coefficient. At stoichiometric condition, the mixture fraction is

$$Z_{stoich} = \frac{(Y_F - \frac{1}{s}Y_{O_2})_{stoic} - (Y_F - \frac{1}{s}Y_{O_2})_2}{(Y_F - \frac{1}{s}Y_{O_2})_1 - (Y_F - \frac{1}{s}Y_{O_2})_2} = \frac{1}{s + 1} \quad (2.10)$$

Then $Y_{products} = 1$ and there is no fuel or oxygen left. In the fuel-rich region ($Z > Z_{stoich}$) no oxygen is left, and in the fuel-lean region ($Z < Z_{stoich}$) no fuel is left. Now, all mass fractions can simply be calculated.

2.1.3 Turbulence and Turbulence Modeling

To give a precise definition of turbulence is very difficult, but in fluid dynamics may turbulent flows be characterized as irregular motion of fluid where velocity is rapidly fluctuating. The underlying physical mechanism in turbulence is complex and is yet not fully understood. Turbulence remains as one of the most important unsolved physical problem, because of the fact that almost all natural flows are turbulent [12]. To evaluate whether a flow is turbulent or laminar, the dimensionless Reynolds number is calculated. The Reynolds number is the ratio of inertial forces to viscous forces. In turbulent flows inertial forces are dominating, hence the Reynolds number is large.

In turbulent flows, rotational flow structures called eddies are formed, each with different characteristic length and velocity scale (’,”,”,...,*). Eddies are formed as a consequence of shear stress (friction) generated between fluid sheets of different velocities. Turbulent flows are always dissipative [12]. Eddies are dissipating through vortex stretching caused by viscous shear stress in the flow and the kinetic energy is converted to internal energy (see Figure 2.1). Mechanic energy is transferred from the main stream to large eddies and further down to smaller eddies [13]. The eddy dissipation continues down to a level where the diffusion time across the diameter equals the time for an eddy to rotate 1/2 revolution [14]. At this level, the *length scale* of an eddy equals *Kolmogorov length scale* and is where molecular mixing dominating (see Figure 2.2). This breakdown of eddies is called the energy cascade model and is seen in Figure 2.8.

The major part of the kinetic energy is in the large eddies [14]. In turbulent flows for high turbulence Reynolds number large eddies are much larger than small eddies. According to Kolmogorov the small eddies are then not influenced by large eddies and the main stream. A typical distribution of *turbulent kinetic energy* is given in Figure 2.2.

Integral length scale, l_0 , is the largest length scale and corresponds to geometrical dimensions [14]. Large eddies has characteristic scales as the mean flow and are therefore

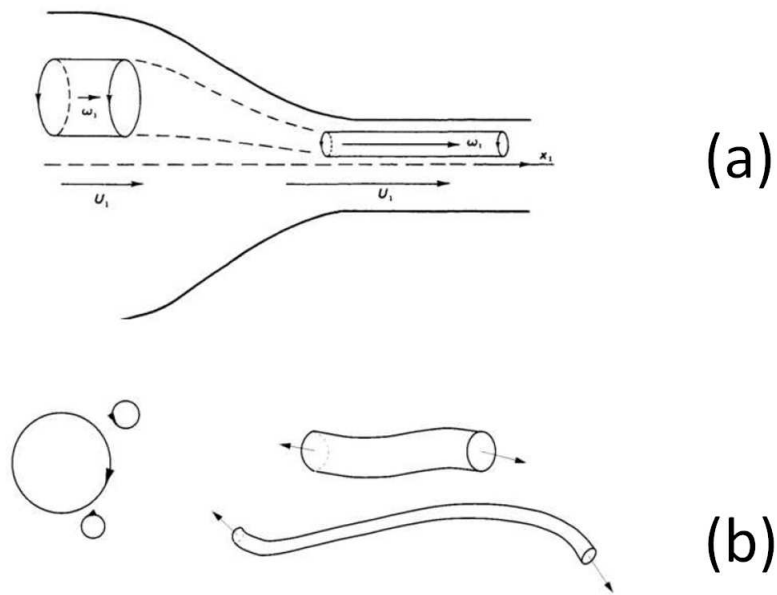


Figure 2.1: (a) Vortex stretching in wind tunnel [12]. Angular momentum is conserved. (b) Principle of vortex stretching [13].

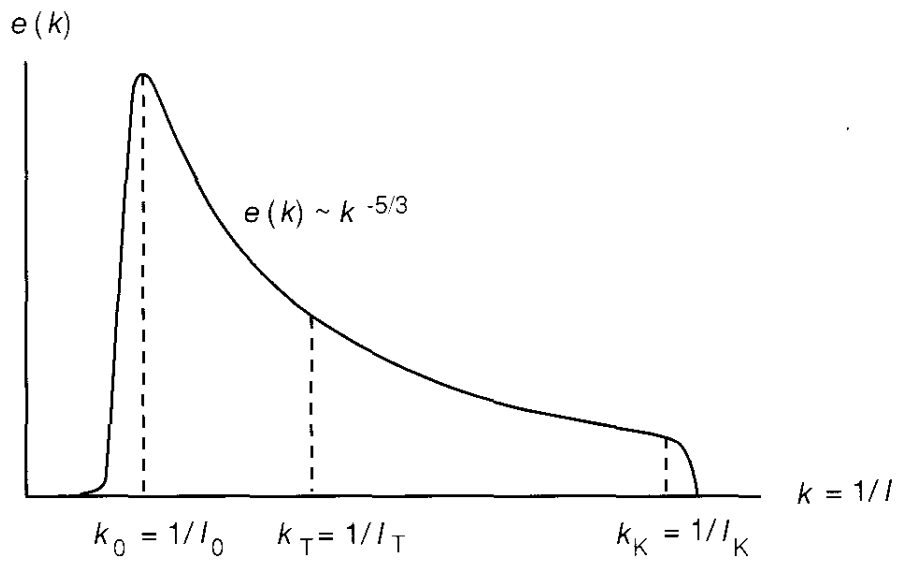


Figure 2.2: Energy cascade: Distribution of *turbulent kinetic energy* at different length scales [14]. Integral length scale, l_0 , Taylor length scale, l_T , and Kolmogorov length scale, l_K .

dominated by inertia effects [15]. I.e large eddies are inviscid in contrast to small eddies which are influenced by viscosity. For this reason, high viscosity flows are associated with few large eddies while low viscosity flows are associated with less larger eddies but a larger amount of smaller eddies. The largest length scale where viscosity affects the dynamics of turbulent eddies is called Taylor length scale, l_T .

Depending on how the turbulence is treated, CFD models are divided in

- Reynolds Average Navier-Stokes (RANS)
- Large Eddy Simulation (LES)
- Direct Numerical Simulation (DNS)

In RANS, all turbulent structures are modeled in a sub grid scale model (SGS) , in contrast to DNS where fluctuations are captured on the grid points and calculated directly by the governing equations. Between DNS and RANS, LES are capturing large eddies on the grid points while small eddies are modeled.

In the momentum equation (eq. (2.3)), the viscous stress tensor is divided in $\tau_{eff} = \tau_{mol} + \tau_{turb}$, where τ_{turb} can be regarded as an extra stress (or viscosity) caused by increased transport in turbulent flows. This extra stress is closed by a turbulence model. According to Boussinesq hypothesis, Reynolds stresses ($-\bar{\rho}u'_i u'_j$, $-\bar{\rho}u'_j h'$ and $-\bar{\rho}u'_j Y'_k$) are proportional to the mean rate of strain:

$$-\bar{\rho}u'_i u'_j + \frac{2}{3}\bar{\rho}\tilde{k}\delta_{ij} = 2\mu_t\tilde{S}_{ij} - \frac{2}{3}\mu_t\frac{\partial\tilde{u}_k}{\partial x_k}\delta_{ij} \quad (2.11)$$

where μ_t is the *turbulent viscosity*, δ_{ij} is the Kronecker delta ($i = j \rightarrow \delta_{ij} = 1$ and $i \neq j \rightarrow \delta_{ij} = 0$) and turbulent kinetic energy $\tilde{k} = \frac{1}{2}u'_i u'_i$. Bars over the variables represents favre filtered quantities (for LES) or average quantities (for RANS). The strain rate tensor is expressed as

$$\tilde{S}_{ij} = \frac{1}{2}\left(\frac{\partial\tilde{u}_i}{\partial x_j} + \frac{\partial\tilde{u}_j}{\partial x_i}\right) \quad (2.12)$$

Reynold's Average Navier-Stokes (RANS)

RANS is applied when only average values are interesting in fluid flow analysis. RANS is the least computational expensive model and is used in most commercial CFD codes. In RANS, the solution vector is split in a fluctuating term and an average term, e.g for velocity $u = \bar{u} + u'$. The most common model to close RANS equations is k - ϵ two-equation model, where two additional partial differential equations for transport of *turbulent kinetic energy*, k , and *dissipation rate* of kinetic energy, ϵ , are solved:

$$\frac{\partial(\bar{\rho}k)}{\partial t} + \frac{\partial(\bar{\rho}\bar{u}_j k)}{\partial t} = \frac{\partial}{\partial x} \left[\frac{\mu_T}{\sigma_k} \frac{\partial k}{\partial x_j} \right] - \bar{\rho}u'_i u'_j \frac{\partial\tilde{u}_i}{\partial x_j} - \bar{\rho}\epsilon \quad (2.13)$$

$$\frac{\partial(\bar{\rho}\epsilon)}{\partial t} + \frac{\partial(\bar{\rho}\bar{u}_j \epsilon)}{\partial t} = \frac{\partial}{\partial x} \left[\frac{\mu_T}{\sigma_\epsilon} \frac{\partial \epsilon}{\partial x_j} \right] - C_{\epsilon 1} \frac{\epsilon}{k} \left(\bar{\rho}u'_i u'_j \frac{\partial\tilde{u}_i}{\partial x_j} \right) - C_{\epsilon 2} \bar{\rho} \frac{\epsilon^2}{k} \quad (2.14)$$

For the two-equation model the turbulent viscosity is

$$\mu_t = \bar{\rho} C_\mu \frac{k^2}{\epsilon}, \quad (2.15)$$

where $k = \frac{1}{2} \widetilde{u'_i u'_i}$ and $\epsilon = \frac{\mu_T}{\bar{\rho}} \widetilde{\left(\frac{\partial u'_i}{\partial x_j} \right) \left(\frac{\partial u'_i}{\partial x_j} \right)}$. The constants for eq.(2.13), (2.14) and (2.15) have been established by data fittings from experiments of a broad range of turbulent flows; $C_\mu = 0.09$, $\sigma_k = 1.0$, $\sigma_\epsilon = 1.3$, $C_{\epsilon 1} = 1.44$, $C_{\epsilon 2} = 1.92$ [16]. However, the one-equation model only consist one additional partial differential equation. This equation is for conservation of *turbulent kinetic energy*. In the zero-equation model, the turbulent viscosity is calculated directly from an empirical correlation.

Other turbulence models for RANS equations may be k - ω , Menter model, and the more sophisticated Reynolds Stress Model which involves calculation of individual Reynolds stresses and gives seven additional partial differential equations.

Large Eddy Simulation (LES)

The computational time of Large Eddy Simulation is less than DNS and more than RANS. LES compute explicitly the largest structures in the flow by filtered Navier-Stokes equation, while small structures, typically smaller than the grid cell size, are modeled. The grid cell size must be in order that a sufficient amount of the turbulent energy is solved on the grid points (see Section 3.4). In 1D, large structure (low wave numbers) are filtered by

$$\tilde{\varphi}(x, t) = \int_{x-\frac{\Delta}{2}}^{x+\frac{\Delta}{2}} \varphi(r, t) dr \quad (2.16)$$

where $\tilde{\varphi}$ is the filtered quantity and Δ is the local cell size.

The most popular approach for the unresolved fluxes in LES is the Smagorinsky model:

$$\mu_t = \rho C_S^2 \Delta^{4/3} l_t^{2/3} |\bar{S}| \quad (2.17)$$

where $\Delta = (\delta x \delta y \delta z)^{\frac{1}{3}}$ and the strain rate, S , is given in eq. (2.12). The empirical constant, C_S , is usually 0.1 - 0.2. Eq. (2.17) is simplified assuming that the turbulence integral length scale is in the same order as the grid cell size, $l_t \approx \Delta$:

$$\mu_t = \rho (C_S \Delta)^2 |\bar{S}| \quad (2.18)$$

Germano et al. attempted to formulate a more universal approach, and proposed a dynamic Smagorinsky constant [17]. A detailed description of the dynamic constant is found in various litterature (e.g Theoretical and Numerical Combustion, 2005 [18]).

Another model turbulence model is the Deardorff eddy viscosity model. The eddy viscosity is expressed as

$$\mu_T = \rho C_D \Delta \sqrt{k_{SGS}}, \quad (2.19)$$

where $C_D = 0.1$ (in FDS v.6) and k_{SGS} is the sub grid scale kinetic energy.

Recently, Vreman proposed a simple turbulence model that similar to the Smagorinsky model, only needs the first-order derivatives of the velocity and the local filter width to compute the viscosity [19]:

$$\mu_T = \rho C_V \sqrt{\frac{B_\beta}{\alpha_{i,j}\alpha_{i,j}}} \quad (2.20)$$

$C_V \approx 2.5C_S$. For homogenous isotropic turbulence, the Smagorinsky constant equals 0.17 and gives $C_V = 0.07$ (default in FDS v.6) [19]. α is a 3×3 matrix with derivatives of the filtered velocity:

$$\alpha = \begin{bmatrix} \frac{\partial \tilde{u}}{\partial x} & \frac{\partial \tilde{u}}{\partial y} & \frac{\partial \tilde{u}}{\partial z} \\ \frac{\partial \tilde{v}}{\partial x} & \frac{\partial \tilde{v}}{\partial y} & \frac{\partial \tilde{v}}{\partial z} \\ \frac{\partial \tilde{w}}{\partial x} & \frac{\partial \tilde{w}}{\partial y} & \frac{\partial \tilde{w}}{\partial z} \end{bmatrix} \quad (2.21)$$

By definition, μ_T is set to zero if $\alpha_{i,j}\alpha_{i,j} = 0$. Further,

$$B_\beta = \beta_{11}\beta_{22} - \beta_{12}^2 + \beta_{11}\beta_{33} - \beta_{13}^2 + \beta_{22}\beta_{33} - \beta_{23}^2 \quad (2.22)$$

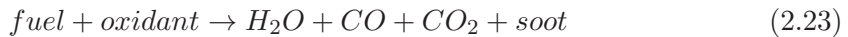
where $\beta_{i,j} = \Delta_m^2 \alpha_{m,i} \alpha_{m,j}$.

Direct Numerical Simulation (DNS)

DNS is the most computational expensive approach where the transport equations are solved numerically without any turbulence model. To capture all the spatial scales of turbulence on the numerical grid, from *Kolmogorov length scale*, l_k (smallest dissipative scales), to *integral length scale*, l_0 , a sufficient number of grid points are needed. According to J. Warnatz et al. [14] about 1000 grid points in each direction are necessary to resolve the smallest turbulent structures for a typical flow with turbulence Reynolds number $Re_l = 500$ and ratio $l_0/l_k \approx 100$. This equals for a three-dimensional simulation a total of 10^9 grid points. For RANS and LES a typical range in order of 10^5 - 10^6 grid points are sufficient. Therefore, DNS is limited to small-scale laminar bench scale flames in the matter of fire research.

2.2 Combustion

Combustion is an exothermic process where fuel and oxidant are reacting chemically involving rather complex physics and chemistry. The combustion can be seen as light, either as a flame or a glow, caused by the heat released in the reactions. Simplified, fuel and an oxidant are reacting forming carbon dioxide, carbon monoxide, soot and water vapor for combustion of hydrocarbons:



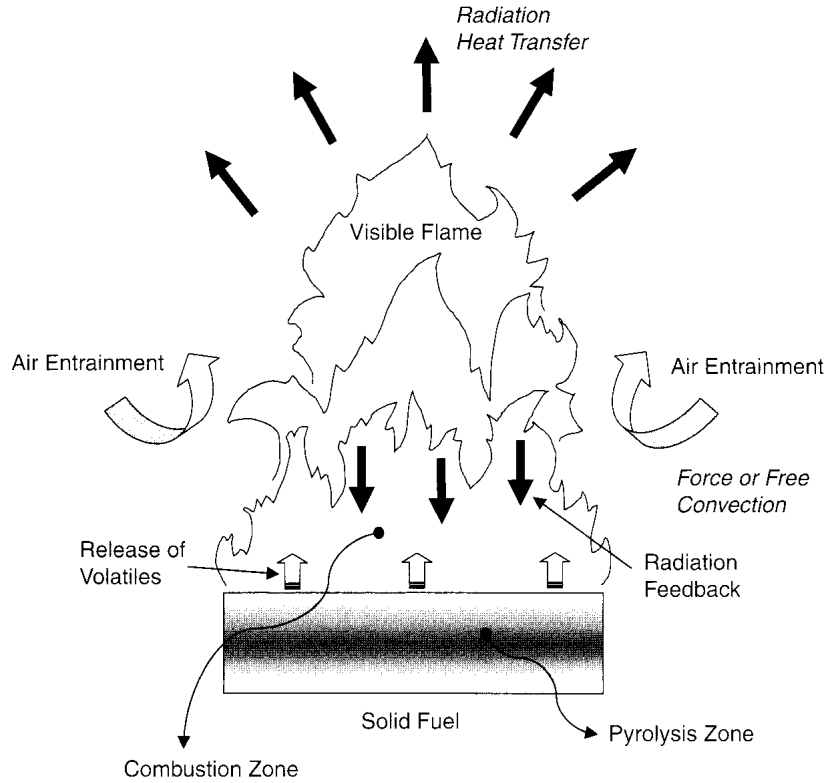


Figure 2.3: Physical processes involved in a fire [15].

In natural fires, oxygen in the air is the oxidant in the chemical reactions. The fuel can be solid, gas or liquid usually carbon-based. However, the flame is a gas phase phenomenon [20]. This means that in a combustion process involving a solid or liquid, a conversion to gaseous form is necessary. In a liquid fire the radiation from the flame is evaporating the liquid, but for most solids, a chemical decomposition or *pyrolysis* takes place instead of evaporation. *Pyrolysis* yields products light enough to volatilize from the surface before entering the combustion zone. A general mass burning rate be expressed as

$$\dot{m}'' = \frac{\dot{Q}''_F - \dot{Q}''_L}{L_v} \quad (2.24)$$

where L_v is the heat required for evaporation or *pyrolysis*, \dot{Q}''_F the heat supplied by the flame to the fire area and \dot{Q}''_L heat loss from the fuel surface. A visual description of physical processes in a fire is shown in Figure 2.3.

2.2.1 Chemical Kinetics

A combustion process consist of several chemical reactions, called *elementary reaction*. Even a simple combustion of methane in air consists 400 reactions [21]. The reactions of interest, *radical chain reactions*, are divided in *chain propagation*, *chain branching* and *chain termination*. Warnatz *et al.* considered a hydrogen combustion where the most important reactions are given in Table 2.1 [14]. An overall stoichiometric reaction for combustion of hydrogen in oxygen is:



Table 2.1: Chemical reactions with respect to hydrogen ignition (adapted from Warnatz *et al.*, 2006 [14])

Reaction number	Chemical reaction	Reaction Mechanism
0	$H_2 + O_2 = 2OH\bullet$	<i>chain initiation</i>
1	$OH\bullet + H_2 = H_2O + H\bullet$	<i>chain propagation</i>
2	$H\bullet + O_2 = OH\bullet + O\bullet$	<i>chain branching</i>
3	$O\bullet + H_2 = OH\bullet + H\bullet$	<i>chain branching</i>
4	$H\bullet = 1/2H_2$	<i>chain termination</i>
5	$H\bullet + O_2 + M = HO_2 + M$	<i>chain termination</i>

The dots in the reactions represents that the species are a free radical. Free radicals are highly reactive because of its charge and are essential to obtain the chemical reactions in a combustion process. In the first reaction, *chain initiation*; a stable species are forming one reacting species. The *chain initiation* leads to *chain propagation* (reaction 2 and 3) where a reactive species react with stable species forming another reactive species. In *chain branching steps* two reactive species are formed from a stable species and a reactive species. The last steps (reaction 4 and 5), *chain termination*; no reactive species are formed.

2.2.2 Heat Release Rate (HRR) and Reaction Rate

The heat release rate (HRR) is the most important factor to characterize a fire. Mathematically HRR can be expressed as

$$\dot{Q}_c = \chi \dot{m} \Delta H_c \quad (2.26)$$

where χ is an efficiency coefficient which takes into account that the combustion is incomplete, and heat is lost to surroundings e.g. through radiation and heat transfer to the air entrained (see figure 2.3). \dot{m} is the fuel consumption rate. The reaction rate is depended on a characteristic time scale limiting the reaction. A simple assumption

would be finite chemical reaction rate, hence the chemical time scale limits the reaction rate. Collisions between molecules is the underlying phenomena in chemical reactions, i.e the reaction rate is a function of temperature, pressure and concentration. The reaction rate may be given as

$$R_k = -k\rho^2 C_{fuel} C_{oxygen} \quad (2.27)$$

where C_{fuel} and C_{oxygen} are concentrations of fuel and oxygen respectively. k is the rate coefficient are given by *Arrhenius law* for temperature depended reactions:

$$k = Ae^{-E_a/RT} \quad (2.28)$$

A is the total number of molecular collisions and $e^{-E_a/RT}$ the fraction of collisions that leads to reactions. Figure 2.4 shows that E_a , the *activation energy*, is the energy barrier to start the reaction. R is the *universal gas constant* and T absolute temperature in Kelvin. A more sophisticated method assumes infinitely fast chemistry and would (also) involve other limiting time scale e.g turbulent time scale, diffusive timescale or acceleration time scale. See section 2.5 and 3.1.

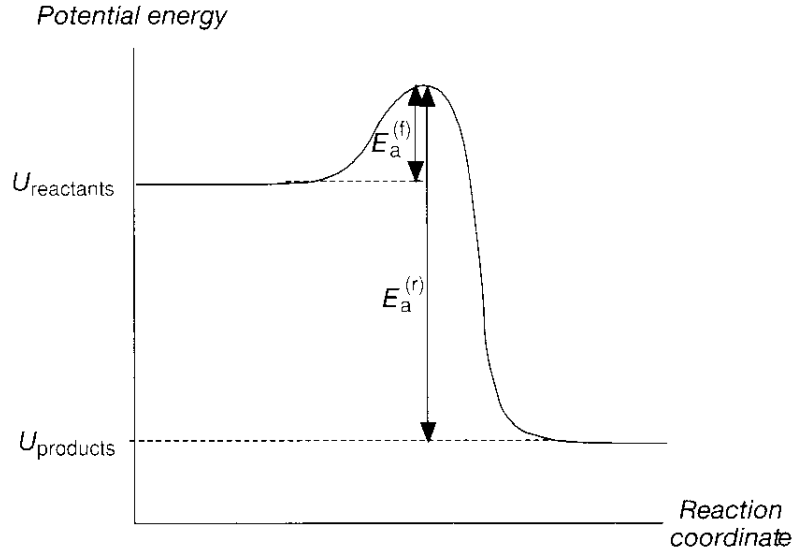


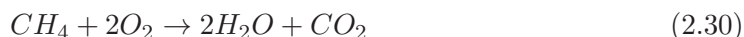
Figure 2.4: A graphical description of energy in an exothermic reaction [14]. $E_a^{(f)}$ is the energy barrier to start the reaction. Considering a combustion $\Delta H_c \approx U_{reactants} - U_{products}$.

ΔH_c is the *heat of combustion*, the energy released during combustion per unit mass or mole. Heat of combustion equals the difference in energy of species before the combustion and after the combustion. Assuming adiabatic conditions (no heat loss to surroundings), the heat of combustion can be determined experimentally in calorimeter bomb at constant volume, where temperature rise is measured. The change in enthalpy according to the first law of thermo dynamics is then

$$\Delta H = \Delta U + p\Delta V \quad (2.29)$$

From the ideal gas law (eq. (2.5)) the work done ($p\Delta V$) can be calculated. But since the work done is small compared to the increase of internal energy (ΔU), it may be neglected, leaving $\Delta H_c \approx U_{products} - U_{reactants}$, as shown in Figure 2.4.

When a compound is formed under standard state (1 atm. pressure and 298 K), the change of enthalpy is by definition, the same as heat of formation (ΔH_f) [20]. Considering stoichiometric combustion of methane, the balanced reaction is



The heat of combustion may be calculated by definition of heat of formation

$$\Delta H_c(CH_4) = (2\Delta H_f(H_2O) + \Delta H_f(CO_2)) - (2\Delta H_f(O_2) + \Delta H_f(CH_4)) \quad (2.31)$$

ΔH_f for reactants and products are found in various literature.

2.3 Flame Characteristics and Fire Plumes

Flames are categorized in four different types given in Table 2.2. When fuel and the oxidant are mixed and burned simultaneously, the flame is *non-premixed*. If the fuel and oxidant are mixed before the combustion it is called a *premixed* flame. Non-premixed and premixed flames are either turbulent or laminar. As flows in general, most flames are also turbulent. Rapid mixing of reactants in the combustion zone for turbulent flames increases the reaction rate and is characterized by an irregular flame sheet.

Table 2.2: Flame types (adapted from Warnatz *et al.*, 2006 [14]).

Fuel/Oxidizer Mixing	Fluid Motion	Example
premixed	laminar	flat flame Bunsen burner
	turbulent	gasoline engine and gas turbines
nonpremixed	laminar	wood fire and candles
	turbulent	aircraft turbine, diesel engine and coal combustion

Froude number is a way to characterize a fire and is expressed as

$$Fr = \frac{U^2}{gD} \quad (2.32)$$

and is the ratio of momentum forces and buoyancy forces. U is the gas velocity, D fire diameter or a characteristic length and g gravitational constant. The velocity is estimated by

$$U = \frac{\dot{Q}_c}{\Delta H_c \rho (\pi D^2 / 4)} \quad (2.33)$$

where $(\pi D^2/4)$ is the diameter, \dot{Q}_c the HRR, ΔH_c the heat of combustion and D the fire diameter. Dimensionless HRR is a function of the Froude number and is in fire dynamics often replaced by the Froude number. The dimensionless heat release rate was first introduced by Zukoski and others and is expressed as

$$Q_c^* = \frac{\dot{Q}_c}{\rho_\infty c_p T_\infty \sqrt{gD} D^2} \quad (2.34)$$

where ρ is the density, c_p the heat capacity and T the temperature. The indexes, ∞ , represent the ambient value.

Flames dominated by high momentum (high Froude numbers or $Q_c^* > 10^5$, region V in Figure 2.6) fuel release and in practice highly turbulent are called jet flames. Such flames can occur from accidental leaks in pressurized pipelines or vessels at process plants, where hydrocarbons are processed.

In natural fires, buoyancy caused by density difference between rising hot gases in the fire plume and ambient air is the dominant driving force. The buoyancy force, in contrast to the momentum from the fuel flow in jet flames, is resisted by viscous drag working in opposite direction, leads to shear stress in the flame sheet. As a consequence eddies are formed if the buoyancy force is large enough. In this process air is *entrained* in the fire plume and mixes fuel with the air. The flame itself is not influenced by the momentum from the fuel release as for jet flames. Natural fires are associated with relatively low velocity since the radiation from the flame is controlling the fuel release (evaporation or pyrolysis) [22]. As the fire diameter increase the radiation also increases, generally resulting in a larger and more turbulent flame.

2.3.1 Borghi Diagram

The Borghi diagram is a diagram for characterizing of flame regimes, seen in Figure 2.5. u'/u_L versus l_0/l_L is plotted with log-log axis where u' is the velocity fluctuation, u_L the laminar burning velocity, l_0 the integral length scale and l_L the laminar flame thickness.

The diagram is divided by three diagonal lines which represents where the dimensionless numbers Da , Ka and Re_T are unity. $Re_l = Re_T^2$ where the turbulent Reynolds number is

$$Re_l = \frac{u'l_0}{\nu} \quad (2.35)$$

ν is the kinematic viscosity $\nu = \mu/\rho$. The turbulent Damköhler number, Da , is large for a fast reaction and small for slow reaction. The number denotes the ratio between macroscopic time scale and the chemical times scale given by

$$Da = \frac{t_0}{t_L} = \frac{l_0 u_L}{l_L u'} \quad (2.36)$$

The turbulent Karlovitz number is expressed as

$$Ka = \frac{t_L}{t_K} \quad (2.37)$$

Borghi Diagram

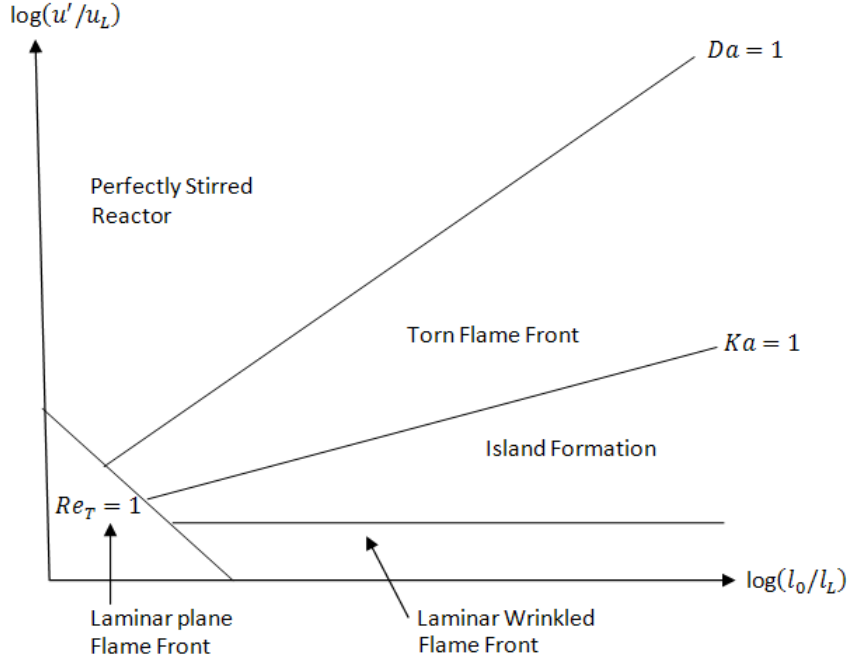


Figure 2.5: Borghi diagram.

where $t_l = l_L/v_L$ and $t_K = \sqrt{\nu/\epsilon}$. t_l and t_K is the time scales of laminar flame and Kolomogorov, respectively.

In the laminar regime $Re_T > 1$, the flame sheet has a thin and a flat reaction zone. Moving in positive x-direction in the Borghi diagram, the turbulence is increasing forming a wrinkled flame front. In the turbulent regime where $Ka < 1$ island of burning fuel in the and air in the flame sheet is observed. Between $Da = 1$ and $Ka = 1$ the chemical time is larger than change of fluid motion [14]. Still, the chemical time is not so large compared to the fluid motion that island formations occur. Above $Da = 1$ the turbulence is so intense compared to the chemical time, allowing a perfect mix fuel and oxidant before the reaction occurs. This regime is referred as *perfectly stirred reactor* as in Section 2.5.3 in the EDC combustion model.

2.3.2 Flame Height

Flame height is an important parameter in fire safety engineering, for example to determine the distance where the radiant heat is sufficient to ignite combustible items. The

correlation by Heskestad for buoyancy flames is given by [23]

$$\frac{L_f}{D} = 3.7(\dot{Q}_c^*)^{2/5} - 1.02 \quad (2.38)$$

where L_f is the flame height and D is fire area diameter. The dimensionless heat release rate is given in eq. (2.34). The dimensionless flame length, l_f/D , as a function of the dimensionless heat release rate is seen in Figure 2.6. Fire types are divided in five regions. Turbulent buoyancy driven diffusion flames are in regions I and II while jet flame is in region V. For natural fires (i.e not jet fires), Q^* is less than 10 in most situations [10].

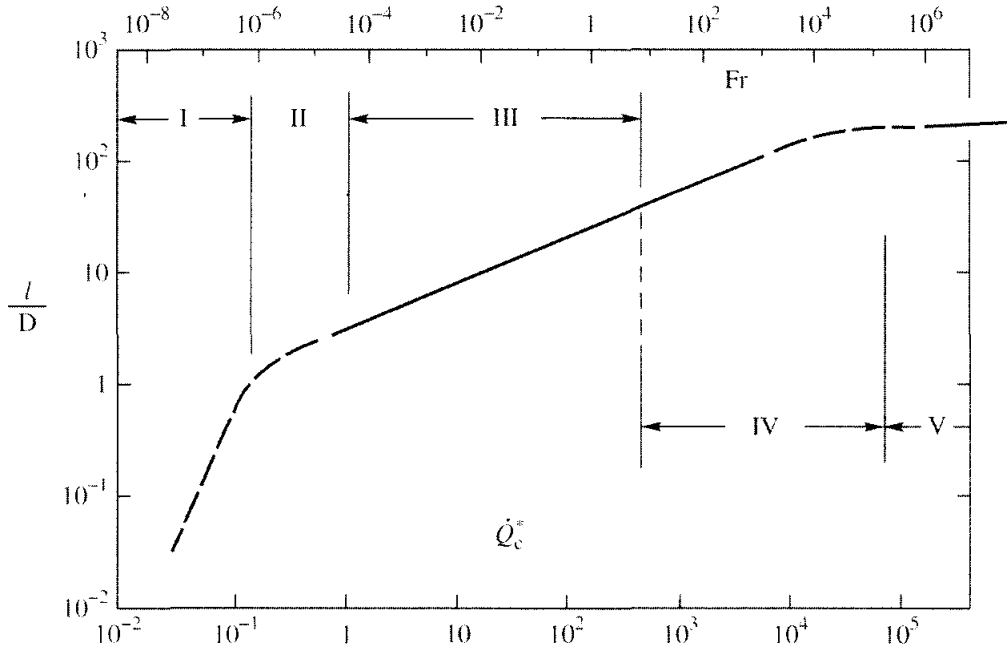


Figure 2.6: The figure is showing the dimensionless flame length, l_f/D , as a function of the dimensionless heat release rate and the Froude number [20].

2.3.3 Centerline Flame Temperature and Velocity

In 1979, McCaffery measured centerline temperature and velocity profiles above 0.3 m square burner [24]. The fuel was methane corresponding to five HRR ranging from 14 kW - 57 kW. McCaffery divided the fire plume in three regimes (in Figure 2.7):

- Persistent flame: accelerating flow
- Intermittent flame: nearly constant flow velocity
- Buoyant plume: decreasing velocity and temperature with respect to height

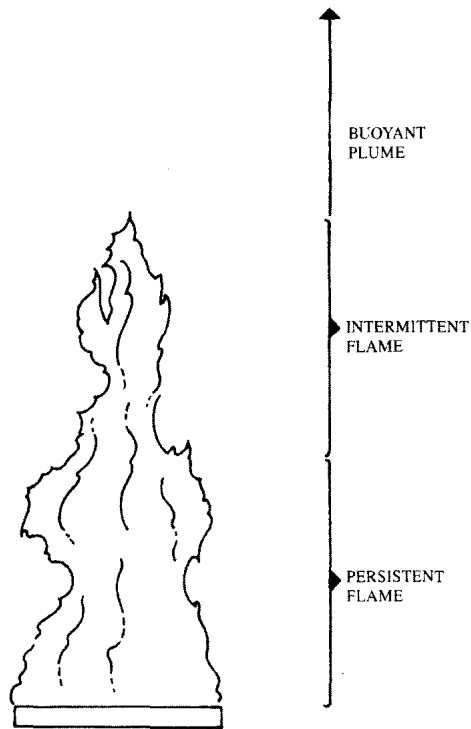


Figure 2.7: McCaffery's fire plumes regimes [20].

From the experiments, McCaffery proposed empirical correlation to centerline velocity, u_0 ,

$$\frac{u_0}{\dot{Q}_c^{1/5}} = k \left(\frac{z}{\dot{Q}_c^{2/5}} \right)^\eta \quad (2.39)$$

and centerline temperature, T_0 ,

$$\frac{2g\Delta T_0}{T_0} = \left(\frac{k}{C} \right)^2 \left(\frac{z}{\dot{Q}_c^{2/5}} \right)^{2\eta-1} \quad (2.40)$$

where Q_c is HRR, z is the height above the fire, ΔT_0 is the temperature difference between the centerline temperature and ambient temperature. k , η and C are empirical constants given in Table 2.3.

2.4 Heat Transfer

Heat can be transferred in three different ways: *conduction*, *convection* and *radiation* - all involved in a fire.

2.4.1 Conduction

Heat transfer through a solid or non-moving fluid, due to a temperature gradient, is called conduction. The physical nature of heat is vibrations of molecules, and spreads from regions of higher temperatures to regions of lower temperature, by collisions and diffusion of molecules. According to Fourier's law of conduction, the steady state one-dimensional heat rate transfer through an area is proportional to the negative temperature gradient

$$\dot{q}_x'' = -k \frac{dT}{dx} \quad (2.41)$$

The thermal conductivity, k , is a measure of how well a material can transfer heat. In transient phenomenas such as fires, the non-steady state conduction is expressed as

$$\rho c_p \frac{\partial T}{\partial t} = \frac{\partial}{\partial x} \left(k \frac{\partial T}{\partial x} \right) \quad (2.42)$$

where c_p is the heat capacity. Eq. (2.41) and (2.42) assumes constant thermal conductivity, heat capacity and density that in reality is a function of temperature.

2.4.2 Convection

Convection is heat exchange between a moving liquid or gas and a solid and is given by Newton's law of cooling

$$\dot{q}'' = h(T_s - T_\infty) \quad (2.43)$$

where h is the convective heat transfer, T_s the temperature at the surface and T_∞ the surrounding temperature. From the ratio of convective heat transfer coefficient to conductive heat transfer, also known as the dimensionless Nusselt number, the convective heat transfer is determined

$$Nu = \frac{hL}{k_f} \quad (2.44)$$

L is the characteristic length and k_f conductivity of the fluid. The Nusselt number is depended on the fluid property, the thickness of boundary layer created by the shear stress and the flow property. Hence convection involving buoyancy-driven flows as a consequence of temperature gradients are referred as natural convection is distinguished from forced convection involving external forces.

Table 2.3: Empirical constants in McCaffery's centerline temperature and velocity profile

Region	k	η [-]	$z/\dot{Q}^{2/5}$ [m/kW ^{2/5}]	C [-]
Persistent flame	6.8 m ^{1/2} /s	1/2	<0.08	0.9
Intermittent flame	1.9 m/kW ^{1/5} .s	0	0.08-0.2	0.9
Buoyant plume	1.1 m ^{4/3} /kW ^{1/3} .s	-1/3	>0.2	0.9

2.4.3 Radiation

Heat transferred by electromagnetic waves is called radiation. From Planck's law, energy emitted by a black body per unit area at a given temperature, T , within a narrow band of wavelengths, λ , is

$$E_{b,\lambda} = \frac{2\pi c^2 h \lambda^{-5}}{\exp(ch/\lambda kT) - 1} \quad (2.45)$$

where c is the speed of light, h the Planck's constant and k the Boltzman constant. Integrating eq. (2.45) over the whole spectrum of wavelengths gives

$$E_b = \int_0^\infty E_{b,\lambda} d\lambda = \frac{2\pi^5 k^4 T^4}{15c^2 h^3} \quad (2.46)$$

The emissivity, ϵ , is not unity for surfaces other than for black bodies and is defined as

$$\epsilon = \frac{E_\lambda}{E_{b,\lambda}} \quad (2.47)$$

Rewriting eq. (2.46) gives

$$E = \epsilon \sigma T^4 \quad (2.48)$$

where σ is the Stefan-Boltzman constant.

2.5 Eddy Dissipation Concept (EDC)

This section is based on Ertesvågs presentation of the Eddy Dissipation Concept (EDC) in *Turbulent Flow and Combustion* [13] (in Norwegian: *Turbulent Strøyming og Forbrenning*, pp. 171-189).

The Eddy Dissipation Concept (EDC) was proposed by Magnussen and Hjertager and has been developed for decades [1][2][3]. EDC model assumes that the chemical reaction in a turbulent flow takes place where reactants and hot products are molecularly mixed. As described in Section 2.1.3, the molecular mixing occurs where the time of diffusion over the diameter of an eddy is shorter than the time an eddy takes to rotate 1/2 revolution. These locations are referred as fine structures and are also the place where TKE is dissipated into heat.

2.5.1 Energy Cascade

The EDC model is developed for RANS, which treats average values and is taken into account in the energy cascade shown in Figure 2.8. Mechanical energy, w' , from the mean flow is transferred to the largest eddies with a characteristic length scale L' , velocity scale u' and a frequency or strain rate $\omega' = u'/L'$. On the next level in the cascade, the characteristic frequency is $\omega'' = 2\omega'$ and length L'' . Further, on the n -th level, the characteristic scales are $\omega_n = 2\omega_{n-1}$, L_n and $\omega_n = u_n/L_n$. The energy transfer continues down to the smallest level, equals Kolmogorov scale ω^* , u^* and L^* . A total

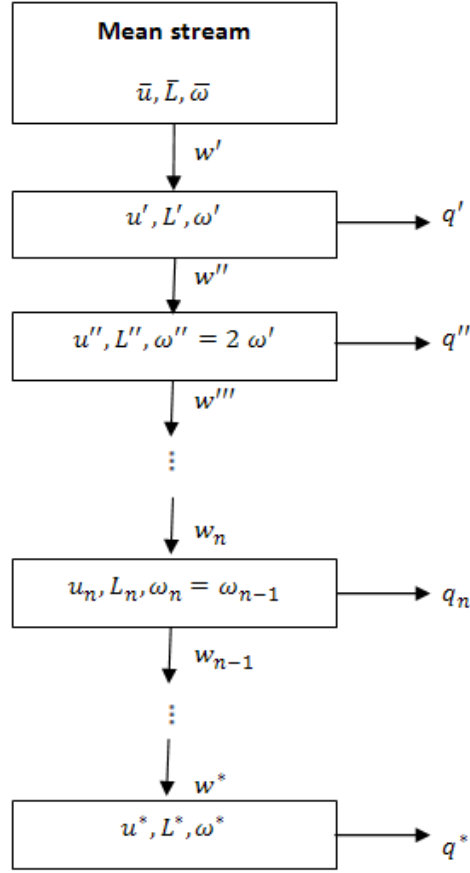


Figure 2.8: Energy cascade (adapted from Ertesvåg, 2000 [13]).

eddy dissipation for the whole cascade equal the energy transferred from the largest eddies, $\epsilon = q' + w''$. Production of TKE equals the mechanical energy transferred from the main flow to the largest eddies and is the source term in eq. (2.13) $\left(w' = \bar{\rho} \widetilde{u'_i u'_j} \frac{\partial \bar{u}_i}{\partial x_j}\right)$.

Dissipation of TKE on the first level in the cascade is proportional to the viscosity and the strain rate:

$$w'' = \frac{3}{2} C_{D1} \omega' 2u''^2 \quad (2.49)$$

and

$$q' = C_{D2} \nu \omega'^2 \quad (2.50)$$

C_{D1} and C_{D2} are model constants. It is assumed that w and q are equal on all levels [1]. By inserting $\omega'' = 2\omega'$ or $\omega_n = 2\omega_{n-1}$, the received and dissipated energy on n -th level yields

$$w_n = \frac{3}{2} C_{D1} \omega_n u_n^2 \quad (2.51)$$

and

$$q_n = C_{D2} \nu \omega_n^2 \quad (2.52)$$

An energy balance gives $w_n = q_n + w_{n+1}$. In turbulent flows with high Reynolds number $q_n \ll w_n$ and $w_n \approx w_{n+1}$ for small steps, n , and $w''^2 = \frac{1}{2}u'^2$ yields

$$w'' = \frac{3}{2}C_{D1}\omega'u'^2 = C_{D1}\omega'k \quad (2.53)$$

and

$$q' = C_{D2}\nu\omega'^2 \quad (2.54)$$

On the final step of the cascade, in the fine structure, $w^* = q^*$ and

$$w^* = \frac{3}{2}C_{D1}\omega^*u^{*2} \quad (2.55)$$

and

$$q^* = C_{D2}\nu\omega^{*2} \quad (2.56)$$

At one level in the cascade, the dissipation rate is 1/4 of the dissipation rate on the level below [13]. Nearly no turbulence energy is dissipated into heat in the largest eddies and according to the model, 3/4 of the dissipation takes place in the fine structure [1]. 98% of the dissipated heat takes places in the last three steps of the cascade [13]. In flows with high Reynolds number $\epsilon \approx w''$ and $\epsilon = \frac{4}{3}q^*$, since w' is far greater than q' :

$$\epsilon = w'' = \frac{3}{2}C_{D1}\frac{u'^3}{L'} \quad (2.57)$$

$$\epsilon = \frac{4}{3}q^* = \frac{4}{3}C_{D2}\nu\frac{u^{*2}}{L^{*2}} \quad (2.58)$$

A balance for last level, the fine structure is

$$\epsilon = \frac{4}{3}w^* = 2C_{D1}\frac{u^{*3}}{L^*} \quad (2.59)$$

Now, the characteristic scales for the fine structures may be expressed as

$$L^* = \frac{2}{3} \left(\frac{3C_{D2}^3}{C_{D1}^2} \right)^{1/4} \left(\frac{\nu^3}{\epsilon} \right)^{1/4} \quad (2.60)$$

$$u^* = \left(\frac{C_{D2}}{3C_{D1}^2} \right)^{1/4} (\nu\epsilon)^{1/4} \quad (2.61)$$

2.5.2 Fine Structures and Mass Exchange

The modeled ratio of fine structure mass to the total mass is

$$\gamma^* = \left(\frac{u^*}{u'} \right)^3 = \left(\frac{3C_{D2}}{4C_{D1}^2} \right)^{3/4} \left(\frac{\nu\epsilon}{k^2} \right)^{3/4} = 9.8 \left(\frac{\nu\epsilon}{k^2} \right)^{3/4} \quad (2.62)$$

The ratio can be seen as a thin layer of fine structure, L^* , on a cylinder representing an eddy of diameter L' , where the ratio is $\gamma^* \approx \frac{L^*}{L'}$ [13]. In between large eddies, regions of fine structures appears. The ratio of this mass to the total mass is

$$\gamma_\lambda = \frac{u^*}{u'} = \left(\frac{3C_{D2}}{4C_{D1}^2} \right)^{1/4} \left(\frac{\nu\epsilon}{k^2} \right)^{1/4} = 2.1 \left(\frac{\nu\epsilon}{k^2} \right)^{1/4} \quad (2.63)$$

Mass exchange between the fine structure to the surroundings, divided on the mass of the fine structure is expressed as

$$\dot{m}^* = 2 \frac{u^*}{L^*} = \left(\frac{3}{C_{D2}} \right)^{1/2} \left(\frac{\epsilon}{\nu} \right)^{1/2} = 2.5 \left(\frac{\epsilon}{\nu} \right)^{1/2} \quad (2.64)$$

Then, the mass exchange between the fine structure to the surroundings, divided on the total mass must be $\dot{m} = \dot{m}^* \gamma^*$:

$$\dot{m} = \frac{3}{4C_{D1}} \left(\frac{12C_{D2}}{C_{D1}^2} \right)^{1/4} \left(\frac{\nu\epsilon}{K^2} \right)^{1/4} \frac{\epsilon}{k} = 24 \left(\frac{\nu\epsilon}{k^2} \right)^{1/4} \frac{\epsilon}{k} \quad (2.65)$$

The duration of mixing must be long enough that the hot products starts the reaction between fuel and oxygen. This time is given by

$$\tau^* = \frac{1}{\dot{m}^*} \quad (2.66)$$

2.5.3 Perfectly Stirred Reactor (PSR)

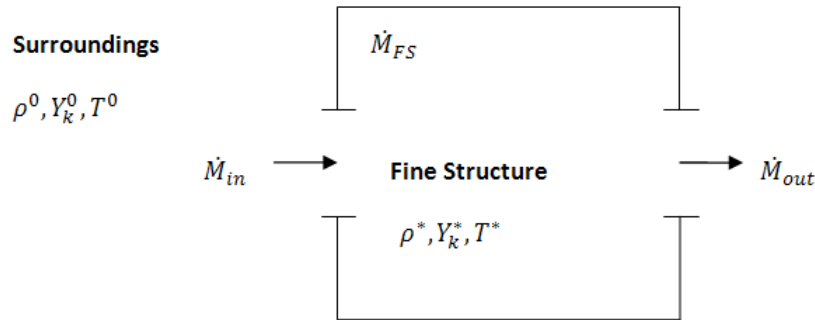


Figure 2.9: Reactor model (adapted from Ertesvåg, 2000 [13]).

The fine structures, where the reaction occurs, are treated as perfectly stirred reactor (PSR) which means that the reactants are perfectly mixed and the mass is constant at each time step [5]. The combustion in the reactor can be modeled with fast chemistry, equilibrium or chemical kinetics. Mass balance in the reactor may be expressed as

$$\dot{M}_{in} Y_k^0 - \dot{M}_{out} Y_k^* = -R_k^* \frac{\dot{M}_{FS}}{\rho^*} \quad (2.67)$$

where R_k^* is the reaction rate of the fine structure, the superscripts 0 and * represents values for surroundings and fine structure, respectively (Figure 2.9). At stationary conditions $\dot{M}_{in} = \dot{M}_{out} = \dot{M}$. Inserting $\dot{m}^* = \frac{\dot{M}}{M_{FS}}$ in eq. (2.67) yields

$$-R_k^* = \rho^* \dot{m}^* (Y_k^0 - Y_k^*) \quad (2.68)$$

The average reaction rate is

$$\bar{R}_k = \left(R_k^* \frac{M_{FS}}{\rho^*} \right) \left(\frac{M_{tot}}{\bar{\rho}} \right)^{-1} = \frac{\bar{\rho}}{\rho^*} \gamma^* R_k^* \quad (2.69)$$

Not all of the fine structures are reacting, so a reaction fraction is given by a probability function χ :

$$\bar{R}_k = \frac{\bar{\rho}}{\rho^*} \chi \gamma^* R_k^* \quad (2.70)$$

Using $\dot{m} = \gamma^* \dot{m}^*$ and inserting eq. (2.68) in eq. (2.70) yields

$$-\bar{R}_k = \bar{\rho} \dot{m} \chi (Y_k^0 - Y_k^*) \quad (2.71)$$

As mentioned previously, RANS is treating average values. Therefore must eq. (2.71) must be expressed by an average mass fraction:

$$-\bar{R}_k = \frac{\bar{\rho} \dot{m} \chi}{1 - \gamma^* \chi} (\tilde{Y}_k - Y_k^*) \quad (2.72)$$

A detailed description of averaging is found in *Turbulent Flow and Combustion* by Ertesvåg [13]. When assuming fast chemistry, the reaction rate is

$$-\bar{R}_F = \frac{\bar{\rho} \dot{m} \chi}{1 - \gamma^* \chi} Y_{min} \quad (2.73)$$

where

$$Y_{min} = \min \left(Y_F, \frac{Y_{O_2}}{s} \right); s = \frac{W_f}{\nu_{O_2} W_{O_2}} \quad (2.74)$$

The probability function consists three parameters

$$\chi = \chi_1 \cdot \chi_2 \cdot \chi_3 \quad (2.75)$$

where χ_1 is the probability of coexistence of reactants

$$\chi_1 = \frac{\left(\tilde{Y}_{min} + \tilde{Y}_P / (1 + s) \right)^2}{\left(\tilde{Y}_F + \tilde{Y}_P / (1 + s) \right) \left(\tilde{Y}_{O_2} / s + \tilde{Y}_P / (1 + s) \right)} \quad (2.76)$$

χ_2 the degree of heating

$$\chi_2 = \min \left[\frac{1}{\gamma_\lambda} \cdot \frac{\tilde{Y}_P / (1 + s)}{\tilde{Y}_P / (1 + s) + \tilde{Y}_{min}}, 1 \right] \quad (2.77)$$

and χ_3 the limitation due to lack of reactants

$$\chi_3 = \min \left[\frac{\gamma_\lambda \left(\tilde{Y}_P / (1 + s) + \tilde{Y}_{min} \right)}{\tilde{Y}_{min}}, 1 \right] \quad (2.78)$$

Chapter 3

Fire Dynamics Simulator (FDS)

The Fire Dynamics Simulator (FDS) is an open source CFD code used world wide in fire engineering applications and science. For almost 25 years FDS has been developed, mainly by the National Institute of Standards and Technology (NIST) and is today accepted as industrial standard. However, the first public release was in February 2000 [4]. The main purposes of FDS are to study smoke spread, smoke venting and activation of detectors in natural building fires.

FDS calculation consists three parts: pre-processing, processing and post-processing. In the pre-processing part, a text file is written in a plain text editor where input values as boundary conditions and other initial conditions as temperature, pressure, HRR are specified. The processing part is the calculation itself, solved with FDS. In Smokeview, the post-processor, animations and images of output values can be analyzed. Output values may also be exported to Excel, MatLab or similar softwares. Third party softwares exist for pre-processing and/or post-processing. The most popular commercial software is PyroSim.

FDS solves numerically the Navier-Stokes equations with low Mach number approximation, $Ma < 0.3$, on a (uniform) cartesian grid. This limits simulations to thermally-driven flows with low pressure differences. The equations are solved explicitly in second order central difference schemes in space and time [25]. Reynolds stresses are closed either with Deardorff SGS Model (current default), Smagorinsky SGS model (constant or dynamic coefficient) or Vreman (in the unofficial version 6).

3.1 Local Heat Release Rate (HRR) and Reaction Rate

The reaction rate in a combustion process is assumed to be limited by either the chemical reaction time (finite-rate reaction) or by mixing time of fuel, oxygen and hot products (infinitely fast reaction). When using LES the grid resolution is too coarse to compute the reaction rate directly because the flame sheet is much thinner than a grid cell [25]. I.e combustion is a subgrid phenomenon and need to be modeled. If the condition in a grid cell meets certain criteria and the reactants of the reaction are present, the local

HRR is modeled as

$$\dot{Q}_c = \rho \min \left(Y_F, \frac{Y_{O_2}}{s}, \beta \frac{Y_P}{1+s} \right) (1 - e^{-\delta t/\tau}) \Delta H_c \quad (3.1)$$

if simple chemistry (one-step reaction) and eddy dissipation is specified in the input file, else HRR is

$$\dot{Q}_c = \rho \min \left(Y_F, \frac{Y_{O_2}}{s}, \beta \frac{Y_P}{1+s} \right) \left(\frac{1}{\tau} \right) \Delta H_c \quad (3.2)$$

where Y_F , Y_{O_2} and Y_P are mass fractions of fuel, oxygen and products, respectively. The empirical parameter β is equal 1, δt is the time step and $s = \frac{W_f}{\nu_{O_2} W_{O_2}}$. τ is a characteristic mixing time given by

$$\tau = \max (\tau_{chem}, \min (\tau_d, \tau_u, \tau_g, \tau_{flame})) \quad (3.3)$$

where the diffusion time scale, turbulent time scale and acceleration time scale are

$$\tau_d = \frac{Sc_t \rho \Delta^2}{\mu}; \tau_u = \frac{\Delta}{\sqrt{2k_{sgs}}}; \tau_g = \sqrt{\frac{2\Delta}{g}} \quad (3.4)$$

Sc is the dimensionless Schmidt number, defined as the ratio of viscous diffusion rate and molecular diffusion rate (default is 0.5 [25]). The subgrid kinetic energy, k_{sgs} , is calculated by integrating a model Kolmogorov spectrum [25]. τ_g is acceleration time scale and is the time required to travel a distance Δ under a constant acceleration, $g = 9.81$ m/s². The flame time scale (large), τ_{flame} , and the chemistry time scale (small), τ_{chem} may be specified by the user. They are however, rarely the limiting mixing time. The simple mixing model used in FDS is grid depended and will overestimate the HRR when a too coarse grid resolution is applied. An upper bound on the total local heat release rate per unit volume (HRRPUV) is set to 2500 kW/m³.

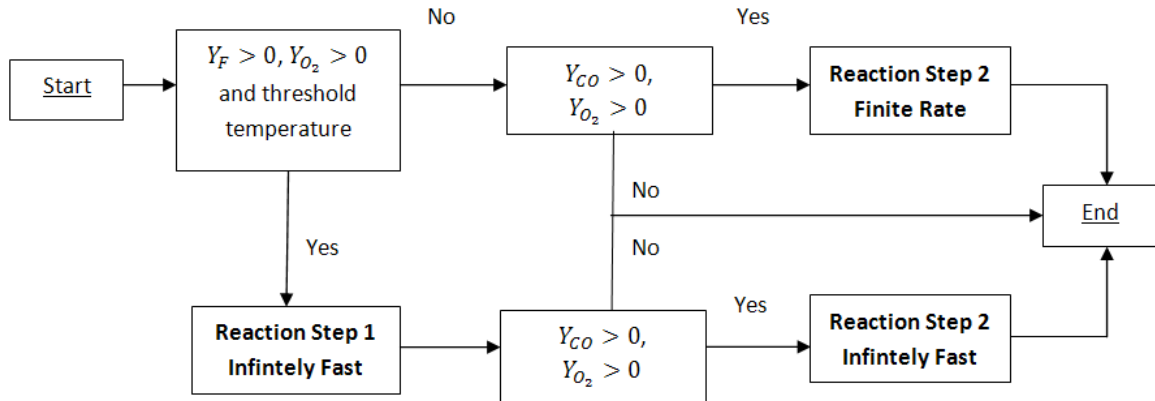


Figure 3.1: A description of how the reaction rate is computed in FDS.

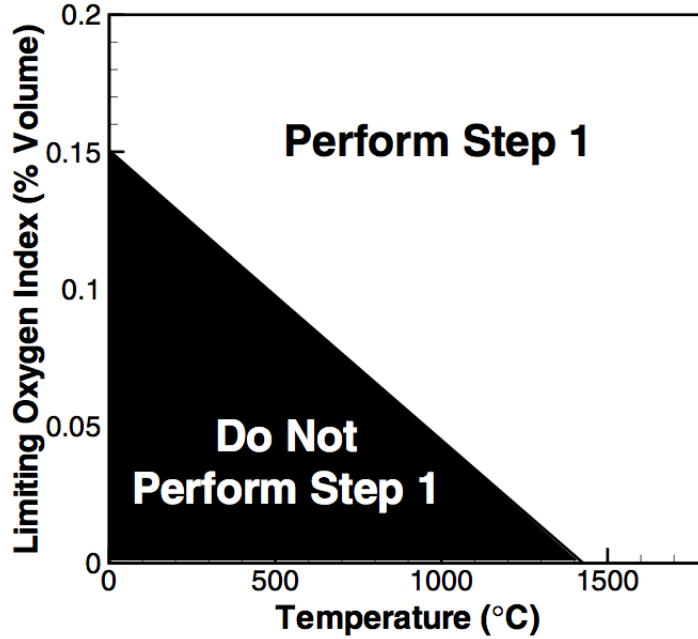


Figure 3.2: The threshold temperature for a given oxygen concentration [26].

When assuming finite rate reaction, the reaction rate is computed by Arrhenius rate, used for DNS calculations and post-flame measurements. A detailed description is found in FDS Technical Reference Guide [25].

For the two-step reaction, fuel and oxygen are reacting infinitely fast (eq. (3.1)) forming CO, soot and other products if the temperature for a given oxygen concentration fulfills Figure 3.2. Further, CO is reacting infinitely fast with oxygen if any oxygen is left in the grid cell after the first reaction. If no fuel is traced in the first reaction or the temperature is too low to support combustion, but CO is present, a finite rate is assumed. A visual description is seen in Figure 3.1.

3.2 Multi-Parameter Mixture Fraction

With a single parameter mixture fraction model information of the completeness of the reaction is not stored [26]. In FDS v4 a single parameter mixture fraction, Z , given in eq. (3.5) was used. The scalar represents the original mass of fuel before the combustion.

$$Z = Y_F + \frac{W_F}{xW_{CO_s}} Y_{CO_2} + \frac{W_f}{xW_{CO}} Y_{CO} + \frac{W_F}{xW_s} Y_s \quad (3.5)$$

In well-ventilated fires the single scalar approach is sufficient. In other cases as extinctions and under-ventilated fires resulting in incomplete reaction, a single parameter is not sufficient. In order to get information of CO and CO₂ production, multi-parameter mixture fraction model is necessary.

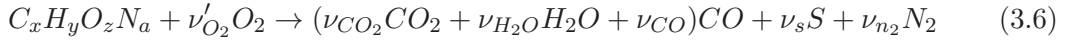
FDS supports

- two parameters single-step reaction: Z_0 , Z_1 and Z_2
- three parameters two-step reaction: Z_0 , Z_1 , Z_2 and Z_3

where $Z = \sum_{\alpha} Z_{\alpha}$. For a single step reaction fuel is reacting with oxygen and do not allow post combustion of CO. A fixed amount of CO is formed. In contrast, a two-step approach allows post combustion of CO within a hot upper layer in under-ventilated fires, post flame combustion or CO production due to fire suppression [25][26]. Note that a yield of CO (ν_{CO}) is still needed to be specified when using a two-step reaction. Also the yields of CO₂ and soot (ν_{CO_2}, ν_s) in eq. (3.25) and (3.6) must be specified by the user, for either a complete or incomplete reaction.

3.2.1 Two parameter single-step reaction

For a single-step approach, the reaction is



where x is the number of carbon atoms, y the number of hydrogen atoms, z the number of oxygen atoms and a the number of nitrogen atoms. A general form of the reaction is



The species are Z_0 for air, Z_1 for fuel and Z_2 for products. Z_1 and Z_2 are tracked explicitly while Z_0 is tracked implicitly as the background species. The mass fractions are given as [25]:

Z_0 : Air

$$Y_{N_2}(Z_0) = Y_{N_2}^{\infty} \quad (3.8)$$

$$Y_{O_2}(Z_0) = Y_{O_2}^{\infty} \quad (3.9)$$

$$Y_{CO_2}(Z_0) = Y_{CO_2}^{\infty} \quad (3.10)$$

$$Y_{H_2O}(Z_0) = Y_{H_2O}^{\infty} \quad (3.11)$$

Z_1 : Fuel

$$Y_F(Z_1) = Y_F \quad (3.12)$$

Z_2 : Products

$$Y_{N_2}(Z_2) = \frac{\nu_{air} W_{air} Y_{N_2}^{\infty} + \nu_{N_2} W_{N_2}}{W_F + \nu_{air} W_{air}} \quad (3.13)$$

$$Y_{CO_2}(Z_2) = \frac{\nu_{air} W_{air} Y_{CO_2}^{\infty} + \nu_{CO_2} W_{CO_2}}{W_F + \nu_{air} W_{air}} \quad (3.14)$$

$$Y_{H_2O}(Z_2) = \frac{\nu_{air} W_{air} Y_{H_2O}^{\infty} + \nu_{H_2O} W_{H_2O}}{W_F + \nu_{air} W_{air}} \quad (3.15)$$

$$Y_{CO}(Z_2) = \frac{\nu_{CO} W_{CO}}{W_F + \nu_{air} W_{air}} \quad (3.16)$$

$$Y_S(Z_2) = \frac{\nu_S W_S}{W_F + \nu_{air} W_{air}} \quad (3.17)$$

The species yields given as:

$$Y_\alpha(Z_0, Z_1, Z_2) = Y_\alpha(Z_0)(1 - Z_1 - Z_2) + Y_\alpha(Z_1)Z_1 + Y_\alpha(Z_2)Z_2 \quad (3.18)$$

Stoichiometric coefficients in Z_2 are:

$$\nu_{N_2} = \frac{a}{2} \quad (3.19)$$

$$\nu_{O_2} = \nu_{CO_2} + \frac{\nu_{CO} + \nu_{H_2O} - z}{2} \quad (3.20)$$

$$\nu_{CO_2} = x - \nu_{CO} - (1 - X_H)\nu_S \quad (3.21)$$

$$\nu_{H_2O} = \frac{y}{2} - X_H\nu_S \quad (3.22)$$

$$\nu_{CO} = \frac{W_F}{W_{CO}}y_{CO} \quad (3.23)$$

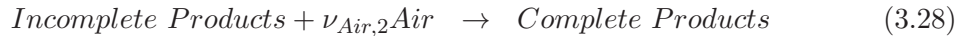
$$\nu_S = \frac{W_F}{W_S}y_S \quad (3.24)$$

3.2.2 Three parameter two-step reaction

The reactions for a two step reaction are



The species in the two-step approach are Z_0 for air, Z_1 for fuel, Z_2 for products in the incomplete reaction one and Z_2 for products in the complete reaction two. A simplified way of writing the two step reaction is



The species yields are:

Z_0 : Air

$$Y_{N_2}(Z_0) = Y_{N_2}^\infty \quad (3.29)$$

$$Y_{O_2}(Z_0) = Y_{O_2}^\infty \quad (3.30)$$

$$Y_{CO_2}(Z_0) = Y_{CO_2}^\infty \quad (3.31)$$

$$Y_{H_2O}(Z_0) = Y_{H_2O}^\infty \quad (3.32)$$

Z_1 : Fuel

$$Y_F(Z_1) = Y_F \quad (3.33)$$

Z_2 : Products of Incomplete Reaction

$$Y_{N_2}(Z_2) = \frac{\nu_{air,1}W_{air}Y_{N_2}^\infty + \nu_{N_2}W_{N_2}}{W_F + \nu_{air}W_{air}} \quad (3.34)$$

$$Y_{CO_2}(Z_2) = \frac{\nu_{air}W_{air}Y_{CO_2}^\infty}{W_F + \nu_{air}W_{air}} \quad (3.35)$$

$$Y_{H_2O}(Z_2) = \frac{\nu_{air}W_{air}Y_{H_2O}^\infty + \nu_{H_2O}W_{H_2O}}{W_F + \nu_{air}W_{air}} \quad (3.36)$$

$$Y_{CO}(Z_2) = \frac{\nu_{CO}W_{CO}}{W_F + \nu_{air}W_{air}} \quad (3.37)$$

$$Y_S(Z_2) = \frac{\nu_S W_S}{W_F + \nu_{air}W_{air}} \quad (3.38)$$

Z_3 : Products of Complete Reaction

$$Y_{N_2}(Z_3) = \frac{\nu_{air,2}W_{air}Y_{N_2}^\infty + \nu_{N_2}W_{N_2}}{W_F + \nu_{air}W_{air}} \quad (3.39)$$

$$Y_{CO_2}(Z_3) = \frac{\nu_{air}W_{air}Y_{CO_2}^\infty}{W_F + \nu_{air}W_{air}} \quad (3.40)$$

$$Y_{H_2O}(Z_3) = \frac{\nu_{air}W_{air}Y_{H_2O}^\infty + \nu_{H_2O}W_{H_2O}}{W_F + \nu_{air}W_{air}} \quad (3.41)$$

$$Y_{CO}(Z_3) = \frac{\nu_{CO}W_{CO}}{W_F + \nu_{air}W_{air}} \quad (3.42)$$

$$Y_S(Z_3) = \frac{\nu_S W_S}{W_F + \nu_{air}W_{air}} \quad (3.43)$$

The stoichiometric coefficients are:

$$\nu_{N_2} = \frac{a}{2} \quad (3.44)$$

$$\nu'_{O_2} = \frac{\nu'_{CO} + \nu_{H_2O} - z}{2} \quad (3.45)$$

$$\nu_{O_2} = \nu_{CO_2} + \frac{\nu_{CO} + \nu_{H_2O} - z}{2} \quad (3.46)$$

$$\nu_{CO_2} = x - (1 - X_H)\nu_S \quad (3.47)$$

$$\nu_M = b \quad (3.48)$$

$$\nu_{H_2O} = \frac{y}{2} - X_H\nu_S \quad (3.49)$$

$$\nu'_{CO} = x - \nu_{CO} - (1 - X_H)\nu_S \quad (3.50)$$

$$\nu'_{CO} = \frac{W_F}{W_{CO}}y_{CO} \quad (3.51)$$

$$\nu_S = \frac{W_F}{W_S}y_S \quad (3.52)$$

3.3 Extinction Criteria

The model for local extinction in FDS consists two parts. First, the local temperature in a grid cell has to be above auto-ignition temperature to the fuel. Second, the local temperature rise must exceed the lower flame temperature, T_{LFT} , from the energy released when maximum limiting available amount of fuel or oxygen, in terms of fuel are consumed:

$$\Delta Z_{air} h_{air}(T) + \Delta Z_F (h_F(T) + \Delta H_F) > \Delta Z_{air} h_{air}(T_{LFT}) + \Delta Z_F h_F(T_{LFT}) \quad (3.53)$$

3.4 Grid Resolution

To find the correct grid resolution is not straightforward. It depends on input values in the calculation and no accepted manual to this exist in the CFD community. Bjarne P. Husted *et al.* recommended that the grid cell size should be in such order that 90-99% of the turbulent energy is solved on the grid points [27]. In FDS User's Manual a somewhat lower value on at least 80% is recommended. Generally, the correct grid cell size is found by simulating the scenario with relative coarse grid and then gradually refine it until only minor differences in the results are observed. This procedure is called a grid sensitivity analysis. For low Mach number LES approximation, D^*/dx is a measure on how well the flow field is resolved. The ratio D^*/dx may also be used to predict the correct grid cell size. The non-dimensional fire diameter is

$$D^* = \left(\frac{\dot{Q}}{\rho_\infty c_p T_\infty \sqrt{g}} \right)^{\frac{2}{3}} \quad (3.54)$$

and dx is the grid cell size. The ratio D^*/dx should be between 4 and 16 [25][4]. T_∞ is the ambient temperature and ρ_∞ is the ambient density. Since CFD modeling is time consuming, it is desirable to not use a finer grid than necessary to obtain satisfactory results. It is worth noting that doubling the number of nodes in each direction, reduces the discretization error by a factor of 4. Furthermore, the computing time increases by a factor of 16 (a factor of 2 for the temporal and each spatial dimension) [28]. To enhance the calculation with respect to time, the domain can be divided in several grids and *Multi Processor Interface* (MPI) may be applied to calculate the grids in parallel.

Chapter 4

Implementation of LES-EDC in FDS

4.1 LES-EDC

Extension of EDC to LES is not a straightforward task and requires customizing. In LES, partial turbulence cascading or no cascading occurs. However, the fine structure regions are calculated based on full energy cascading in each grid cell in RANS-EDC. Panjwani *et al.* proposed two approaches for formulating the fine structure regions [5][6]. In contrast to RANS, the turbulent kinetic energy and dissipation are rarely computed explicitly (i.e no conservation) in LES. Thus, the fine structure regions are formulated from the subgrid viscosity. The first approach is based on volume fraction of small structures, the second on inhomogenous distribution of the fine structure regions, both ending up with the expression

$$\gamma_\lambda = C_{LES} \left(\frac{\nu}{\nu_{sgs}} \right)^{\frac{1}{4}} \quad (4.1)$$

where the subgrid viscosity, ν_{sgs} , is tracked from the turbulence model. In case of larger fine structure velocity than subgrid velocity, $\gamma_\lambda < 1$ is used [5]. The proposed EDC-LES model assumes that the fine structures are localized in nearly constant energy regions so that $\gamma^* = \gamma_\lambda^2$. Furthermore, the time scale is reformulated [29]:

$$\tau^* = \frac{1}{|\bar{S}|} \quad (4.2)$$

where \bar{S} is the strain rate. The reaction rate is computed as

$$\omega_k = \frac{\gamma_\lambda^2 \chi}{\tau^*} \left(\tilde{Y}_k^0 - \tilde{Y}_k^* \right) \quad (4.3)$$

where Y_k^0 is the surrounding mass fraction and Y_k^* the mass fraction of the fine structures, see Figure 2.9. In terms of limiting concentration of fuel or oxygen, the reaction rate is

$$\omega_k = \frac{\chi}{\tau^* (1 - \chi \gamma_\lambda^2)} Y_{min} \quad (4.4)$$

where

$$Y_{min} = \min \left(Y_F, \frac{Y_{O_2}}{s} \right); s = \frac{W_f}{\nu_{O_2} W_{O_2}} \quad (4.5)$$

The probability function, χ , is computed as fo RANS-EDC given in eq. (2.76) - (2.78).

4.2 Numerical Procedure

FDS is a non-commercial code written in FORTRAN 90/95 and is available on the website <http://code.google.com/p/fds-smv/>. Minor releases or subversions of FDS are accessed through a Subversion Client (SVN), while major releases are published on NIST's official website (<http://fire.nist.gov/fds/>).

The FDS code is divided in modules and subroutines as CFD in general. In this thesis the subroutine "Eddy Dissipation" (infinitely fast reaction, eq. (3.1)) in module "Fire" (fire.f90 Appendix B.1) is substituted with the EDC combustion model modified for LES described in section 4.1. In addition, other suroutines were adapted to changes implemented in the combustion model. A schematic diagram of the subroutines in the module "Fire" is presented in Figure 4.1.

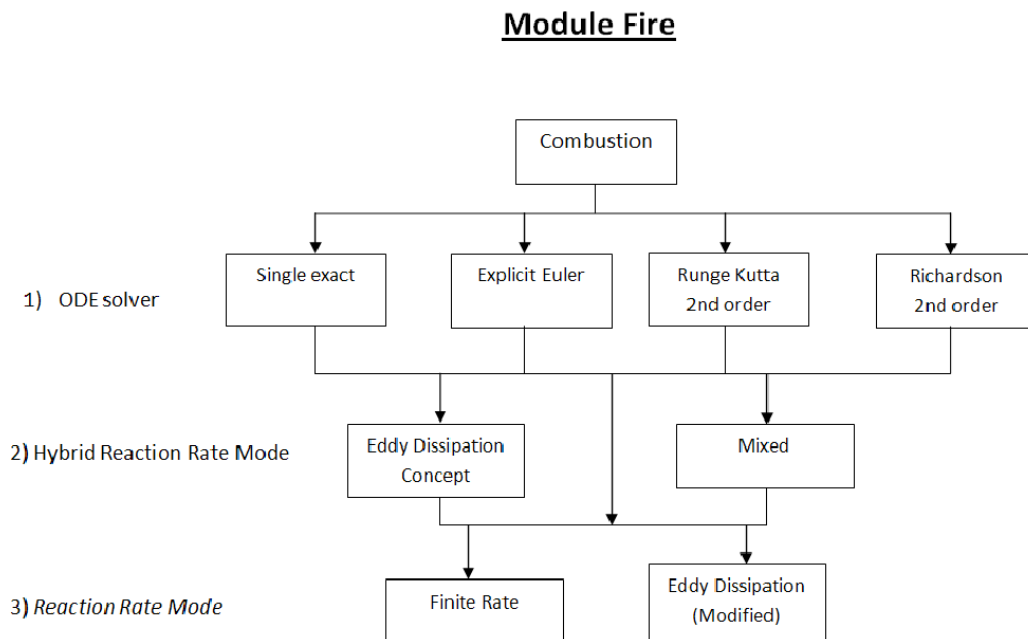


Figure 4.1: Numerical Procedure in FDS combustion model (fire.f90 in Appendix B.1).

- **Combustion:** First, the upper HRR in the grid cell is calculated, set to 2500 kW/m³. If reactants are present, an ordinary differential equation (ODE) solver is

chosen. The temperature is calculated by the energy released from the combustion, which is reported back from the ODE solver. Mixture fractions are also reported back from the ODE solver before the divergence term is updated.

- **ODE solver:** If simple chemistry (single-step reaction) and "Eddy Dissipation" reaction rate is specified in the input file, the "Single Exact" ODE solver is chosen. Otherwise, "Explicit Euler" is chosen. Use of other ODE solvers must be specified in the input file. The ODE solver reads the number of reaction steps before finding the limiting reactant in terms of fuel. The mixing time is reported from the reaction rate mode and HRR is calculated from eq. (3.1) in the "Single Exact" solver or eq. (3.2) for the other solvers. Then fuel consumption is calculated.
- **Hybrid Reaction Rate Mode:** The "Mixed" mode is following the description in Figure 3.1 and 3.2. For DNS calculations, finite rate reaction is assumed. "Eddy_Dissipation_Concept" is calculating both "Finite Rate" (RATE_CONSTANT_FR) and "Eddy Dissipation" (RATE_CONSTANT_ED). The reaction rate is then

$$(RATE_CONSTANT_ED \times RATE_CONSTANT_FR) / (RATE_CONSTANT_ED + RATE_CONSTANT_FR).$$

"Eddy Dissipation" is supporting co-existing of fuel and oxygen in the same grid cell by a function called extinction, see section 3.3.

4.3 The Implemented Code

The major part of the changes are done in the module "fire.f90", under "Eddy Dissipation":

- First the kinematic viscosity is calculated, $\nu = \mu/\rho$, because it is not a global variable in FDS.
- The fine structure is computed by eq. (4.1), an upper value value is set $\gamma_\lambda < 1$.
- Mass fractions for oxygen and fuel are tracked from the subroutine GET_MASS_FRACTION, and mass fraction for products is found from the relation $Y_{products} = 1 - (Y_{O_2} + Y_{fuel})$.
- Stoichiometric coefficient is computed.
- The probability function is computed by eq. (2.75), (2.76), (2.77) and (2.78).
- Rate constant is computed by eq. (4.3).

!The Eddy Dissipation Concept (EDC) Combustion Model (by Hjertager and Magnussen) for LES proposed by Balram et al.

```

NU = MU(I , J ,K) /RHO(I , J ,K)

C_LES = 0.15_EB

GAMMALAMBDA = C_LES*(NU/NU_EDDY(I , J ,K) )**0.25_EB
IF (GAMMALAMBDA > 1._EB) THEN
    GAMMALAMBDA = 1._EB
END IF

CALL GET_MASS_FRACTION(ZZ_GET , FUEL_INDEX , Y_FUEL) !
    ADDED
CALL GET_MASS_FRACTION(ZZ_GET , O2_INDEX , Y_O2) !ADDED
Y_PRODUCT = 1._EB - (Y_FUEL + Y_O2)

S = SPECIES(FUEL_INDEX)%MW/(RN%NU_O2*SPECIES(O2_INDEX)
    %MW)
Y_O2 = Y_O2/S
Y_PRODUCT = Y_PRODUCT/(1._EB + S)
CHI_1 = ((YY_F_LIM + Y_PRODUCT)**2)/((Y_FUEL +
    Y_PRODUCT)*(Y_O2 + Y_PRODUCT))
CHI_2 = MIN(Y_PRODUCT/(GAMMALAMBDA*(YY_F_LIM +
    Y_PRODUCT)) , 1._EB)
CHI_3 = MIN(GAMMALAMBDA*(YY_F_LIM + Y_PRODUCT)/
    YY_F_LIM , 1._EB)
CHI = CHI_1*CHI_2*CHI_3

RATE_CONSTANT = YY_F_LIM*CHI/(MIX_TIME(I , J ,K) *(1._EB -
    CHI*GAMMALAMBDA**2))
!RATE_CONSTANT = YY_F_LIM*CHI*GAMMALAMBDA**2/(
    MIX_TIME(I , J ,K) *(1._EB - CHI*GAMMALAMBDA**2))

```

The mixing time (eq. 4.2) is computed further up in the module. Other changes are done in modules "velo.f90", "mesh.f90" and "init.f90". Since the strain rate is only computed in the Smagorinsky turbulence model (eq. (2.18)), the subroutine COMPUTE_STRAIN_RATE is added in the subroutine COMPUTE_VISCOSITY for the Deardorff (eq. (2.19)) and Vreman (eq. (2.20)) turbulence model in "velo.f90". The strain rate and the subgrid viscosity are made global variables by modifications in "mesh.f90" and "init.f90". Furthermore, parts of the code are commented out, so that they do not conflict with the implemented part. The ODE solve "Single Exact" is

adapted to eq. (3.1) only, and are for that reason substituted by the "Explicit Euler". Limiting mass fraction in terms of fuel, Y_{min} , is part of the original code. The module `fire.f90` is found in its full length in Appendix B.1. Other modified subroutines are found in Appendix B while their full length is found at <http://code.google.com/p/fds-smv/>.

Chapter 5

Validation of FDS-EDC

An important aspect when implementing a new model in a CFD model is to validate this. Validation can be done by comparing simulations with experiments or other numerical tools that computes the exact physics instead of modeling it (typically DNS). In some cases CFD models are validated with flows which can be solved analytically, e.g velocity profile in Couette flow.

The Standard Guide for Evaluating the Predictive Capability of Deterministic Fire Models ASTM E 1355[30] defines verification as

-The process of determining the degree to which a calculation method is an accurate representation of the real world from the perspective of the intended uses of the calculation method.

and verification as

- The process of determining that the implementation of a calculation method accurately represents the developer's conceptual description of the calculation method and the solution to the calculation method.

In FDS verification guide it is putted in a simple way and stated that verification is to check the math and validation to check the physics [31]. The choice of validation cases must be within the limits of CFD code and related to its purpose. In the matter of combustion model validation the quantities must be related to the local HRR. The energy released in the combustion increases the temperature, and through thermal expansion and buoyancy caused by density differences the flow is forced in an upward direction. The type of fire must equal those FDS is limited to and about the same size. There are several fire scenarios to consider and many ways to validate a CFD code. The selected scenarios in this thesis are identical to some of those in FDS validation guide [32], so that results in this thesis may in further work be compared with earlier and future versions of FDS. Based on the given arguments McCaffery centerline velocity and temperature profile [24], Heskestad flame height correlation [23] and velocity profile in

Sandia plume experiments [33][34] are considered in this thesis. Temperature, velocity and flame height are important quantities for flames and are all influenced by local HRR which is calculated in the implemented code. Flame height validation is a way to check if the fuel consumed over the correct travelled distance while the center line temperature and velocity profile is a way to check the local fuel consumption is correct. Even though all the fuel is consumed after traveling the distance equal the flame height the local fuel consumption do not necessarily has to be correct. Correct modeling of the lower flame region is crucial to be able to model a flame correctly. The lower flame region, called the persistent flame, is where the flow is accelerating. Above, in the intermittent region, the flow is nearly constant. An over prediction of HRR in the lower region leads to an over prediction of the velocity, hence the height of the persistent region decreases. Furthermore, the temperature is over predicted in the lower region and the flame height under predicted. An under prediction of HRR in the persistent region leads to the opposite. By velocity profiles from Sandia experiments the persistent flame region may be studied in detail. In Section 6.1, information regarding the philosophy of arranging experiments for CFD validation is found.

In total, 720 simulations are presented in this thesis; 480 simulations for the Hestekstad correlation, 150 simulations for the McCaffery correlation and 90 simulations for the Sandia plume experiments. All simulations were run with FDS v.6, SVN revision number 10231 on six different computers:

- a) 2 x Intel(R) Xenon(R) CPU X5690 Hexa Core 3.47 GHz, (48 GB memory)
- b) 2 x Intel(R) Xenon(R) CPU X5690 Hexa Core 3.47 GHz, (48 GB memory)
- c) Intel(R) Xenon(R) CPU X5570 Quad Core 2.93 GHz, (12 GB memory)
- d) Intel(R) Xenon(TM) CPU Dual Core 3.0 GHz, (4 GB memory)
- e) 2 x Intel(R) Xenon(R) CPU E5540 Quad Core 2.53 GHz, (24 GB memory)
- f) 2 x Intel(R) Xenon(R) CPU E5630 Quad Core 2.53 GHz, (8 GB memory)

The Sandia plume experiments were simulated with 4 CPU cores with computer a) and b) to be able to compare CPU clock times¹. Because of time constraint, results for the original version FDS v.6 (only referred as FDS6) were only compared with Deardorff turbulence model. Deardorff was chosen since that is the default turbulence model in the unofficial version 6 of FDS. Input for all simulations were limited to a two parameters mixture fraction with a single-step reactions for infinitely fast chemistry.

Example of input files are found in Appendix A. All input files in its full length are found at <http://code.google.com/p/fds-smv/>. Results are presented with three different C_{LES} and three different grid resolutions.

¹Test 17 with Vreman turbulence model ($dx = 1.5$ cm) was simulated with 12 CPU cores and stopped at 15 seconds because of computer crash and time constraint in the final stages of the project.

5.1 McCaffery's Plume Correlation, Velocity and Temperature Profiles

The McCaffery case is simulated with a 30 cm x 30 cm methane burner with HRR of 14 kW, 22 kW, 33 kW, 45 kW and 57 kW. Three different grids (30x30x100, 60x60x200 and 40x40x100) are applied with varying computational domain size such that $D^*/dx = 5$, $D^*/dx = 10$ and $D^*/dx = 20$. This corresponds a range of dimensionless heat release from $Q^* = 0.005$ to $Q^* = 0.02$. The centerline velocity and temperature profiles are average over the 30 seconds simulated. Ambient conditions are 20°C and atmospheric pressure. Results are presented for Deardorff, Vreman and (dynamic) Smagorinsky turbulence models with C_{LES} of 0.005, 0.01 and 0.015. An example of input file is found in Appendix A.5.

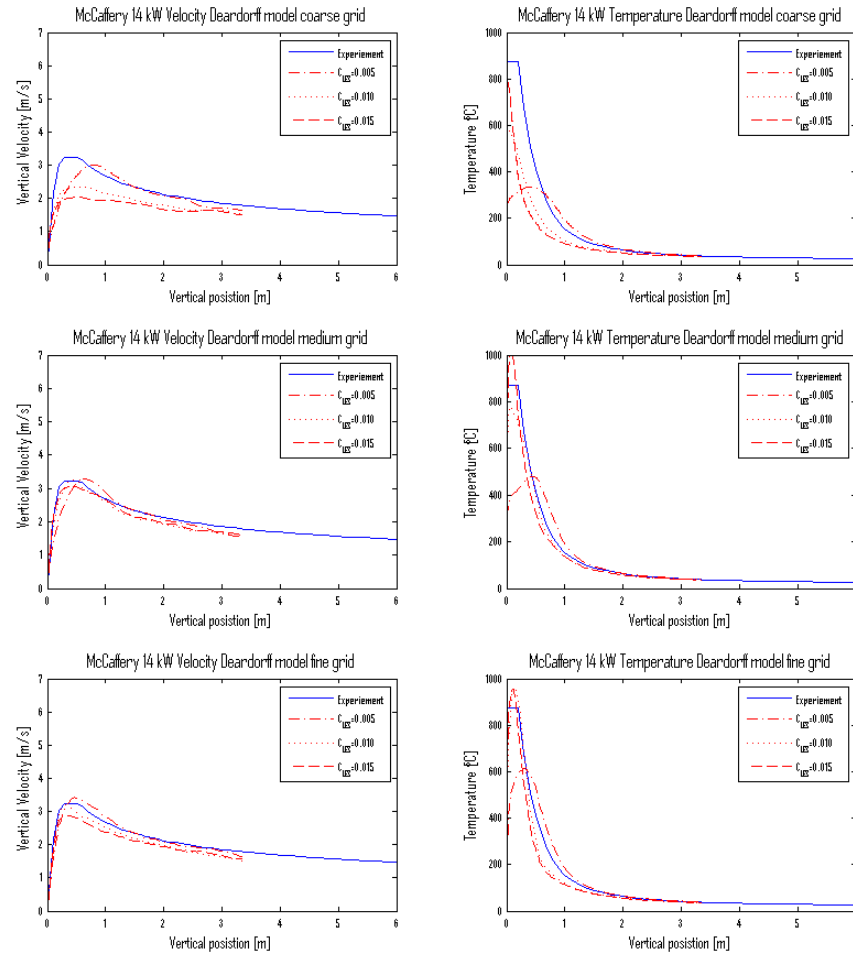


Figure 5.1: McCaffery correlation 14 kW, centerline velocity (left side) and temperature (right side) profiles with Deardorff turbulence model. Coarse grid at the top, medium grid in the middle and fine grid at the bottom.

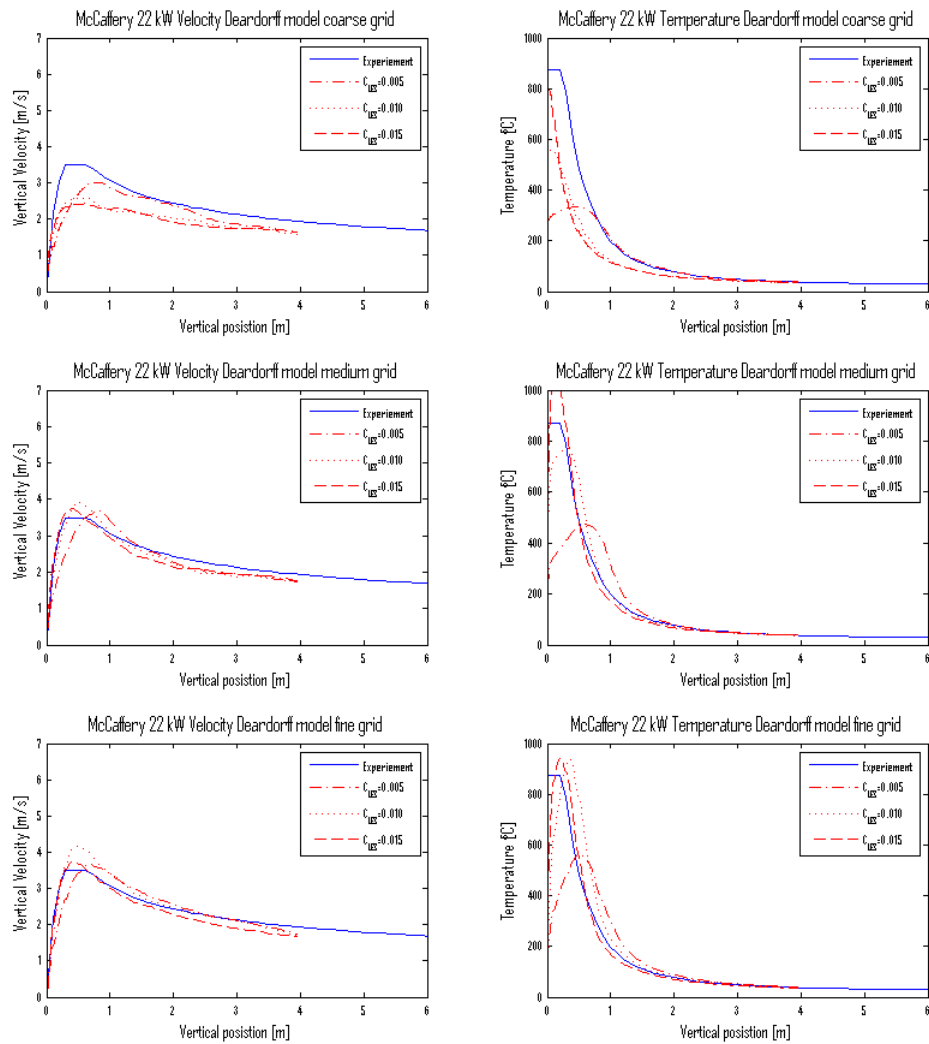


Figure 5.2: McCaffery correlation 22 kW, centerline velocity (left side) and temperature (right side) profiles with Deardorff turbulence model. Coarse grid at the top, medium grid in the middle and fine grid at the bottom.

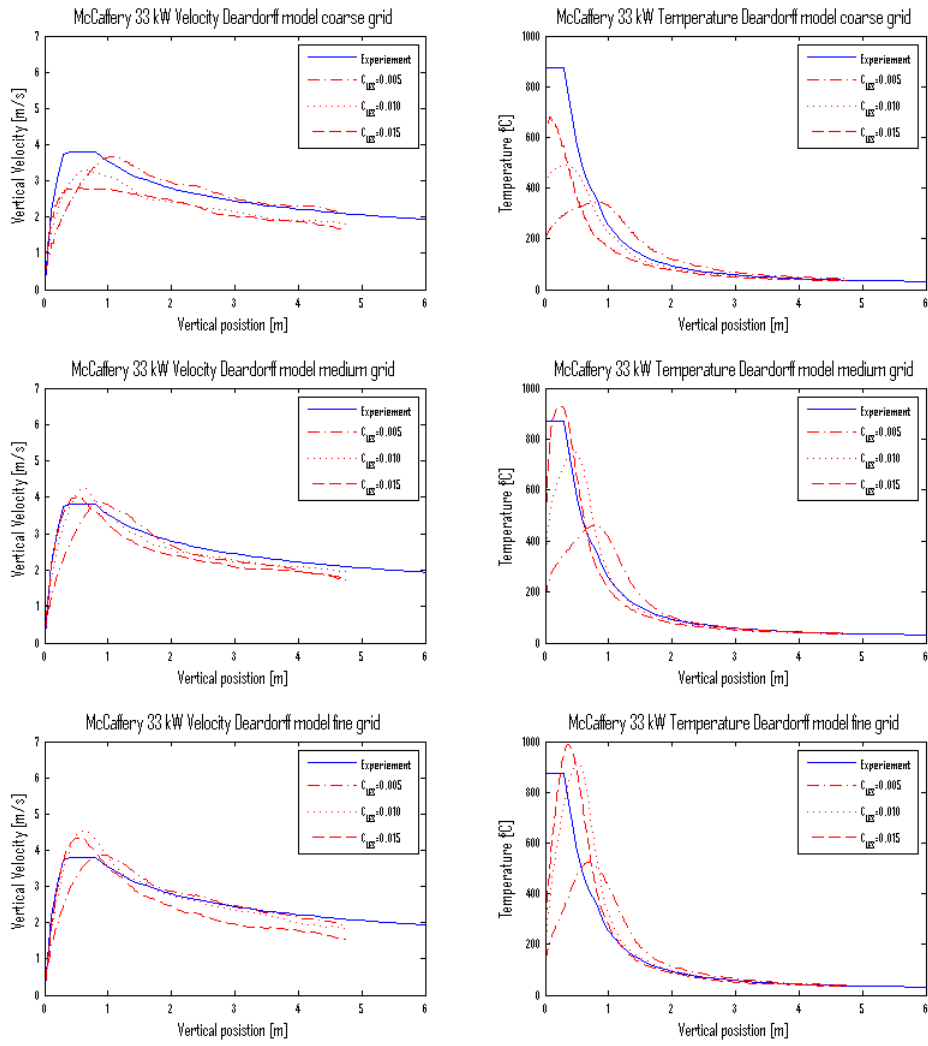


Figure 5.3: McCaffery correlation 33 kW, centerline velocity (left side) and temperature (right side) profiles with Deardorff turbulence model. Coarse grid at the top, medium grid in the middle and fine grid at the bottom.

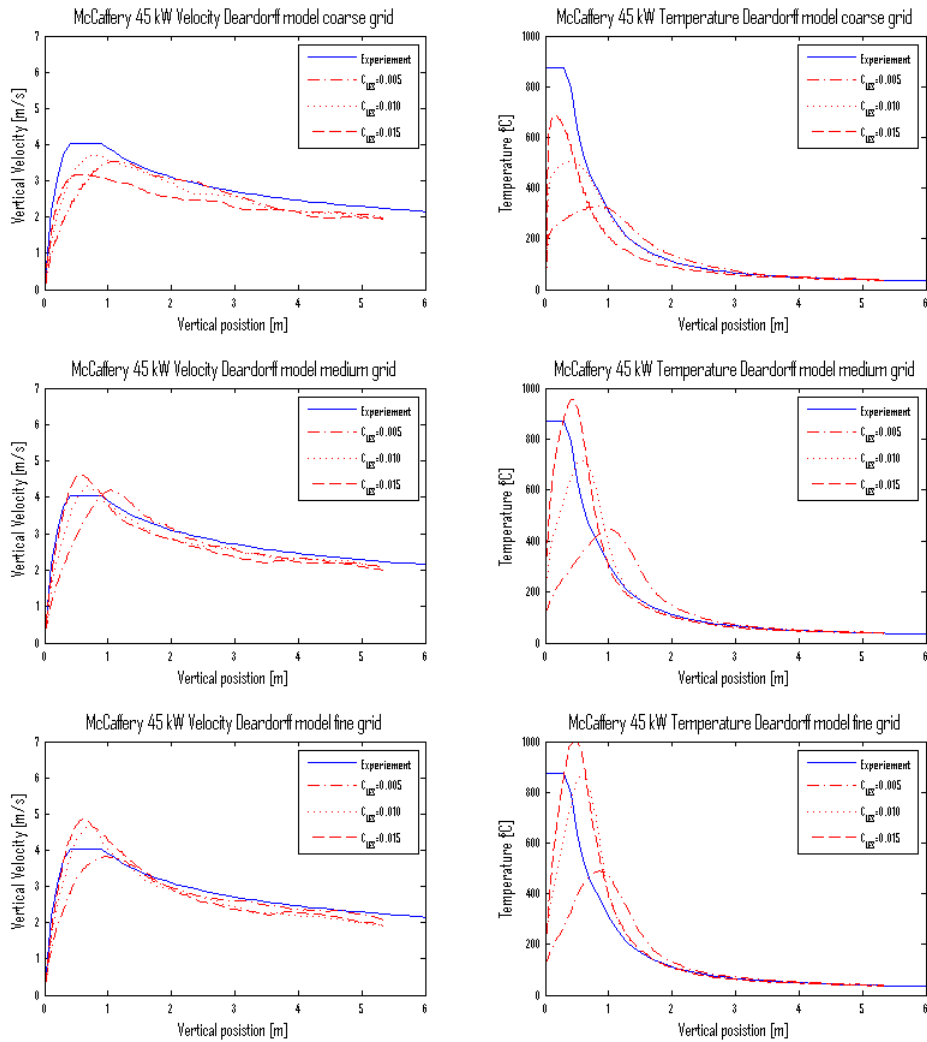


Figure 5.4: McCaffery correlation 45 kW, centerline velocity (left side) and temperature (right side) profiles with Deardorff turbulence model. Coarse grid at the top, medium grid in the middle and fine grid at the bottom.

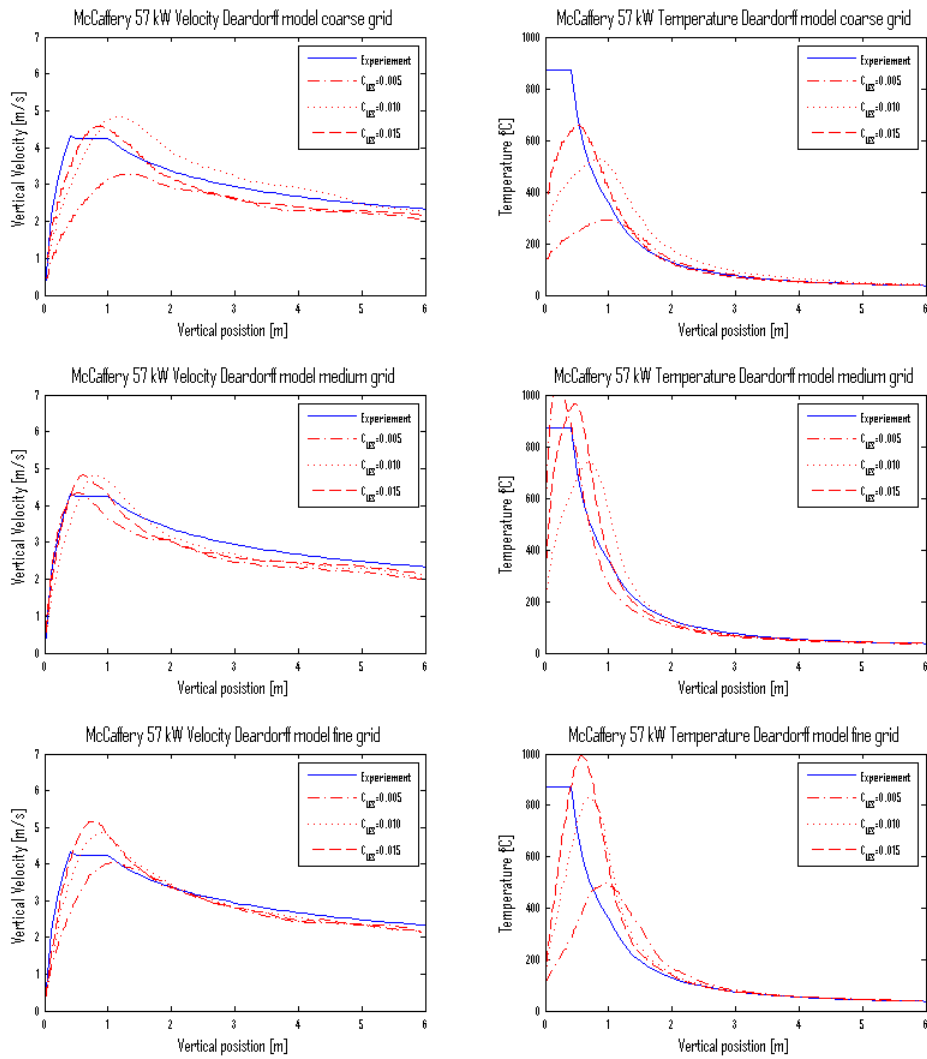


Figure 5.5: McCaffery correlation 57 kW, centerline velocity (left side) and temperature (right side) profiles with Deardorff turbulence model. Coarse grid at the top, medium grid in the middle and fine grid at the bottom.

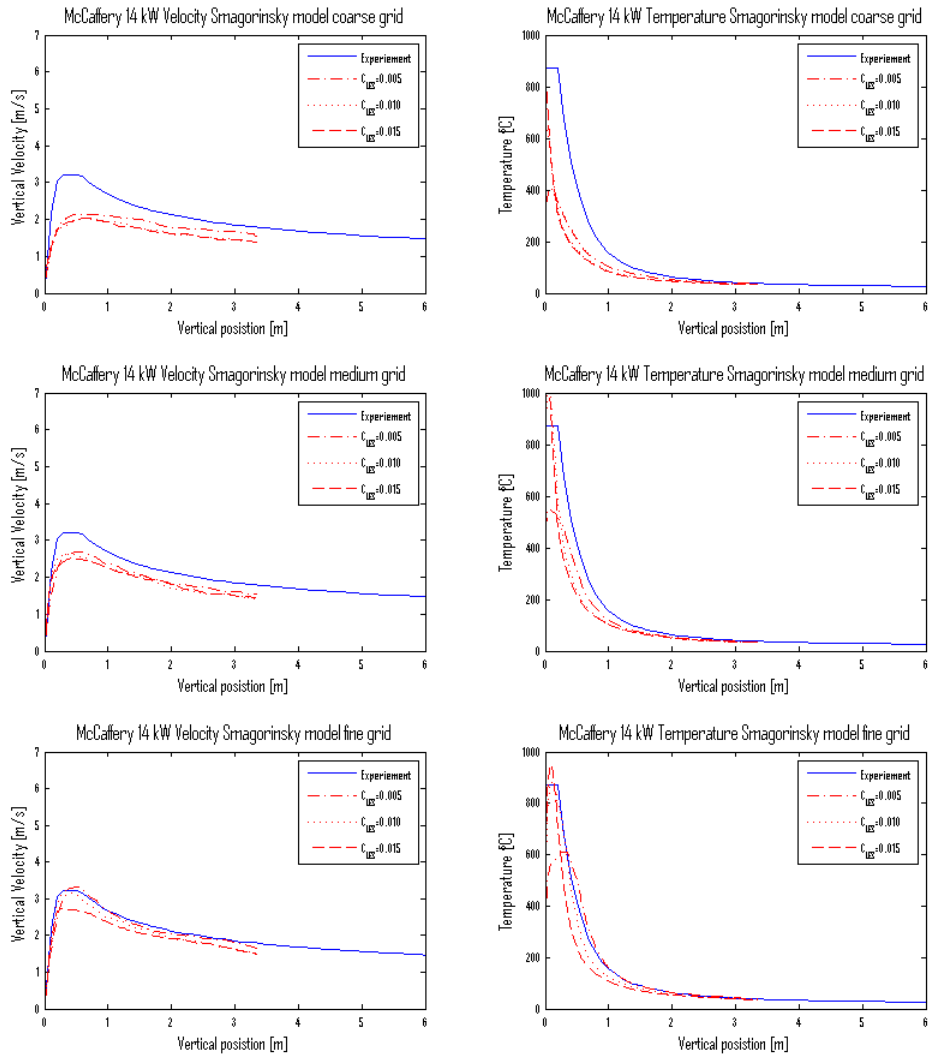


Figure 5.6: McCaffery correlation 14 kW, centerline velocity (left side) and temperature (right side) profiles with Smagorinsky turbulence model. Coarse grid at the top, medium grid in the middle and fine grid at the bottom.

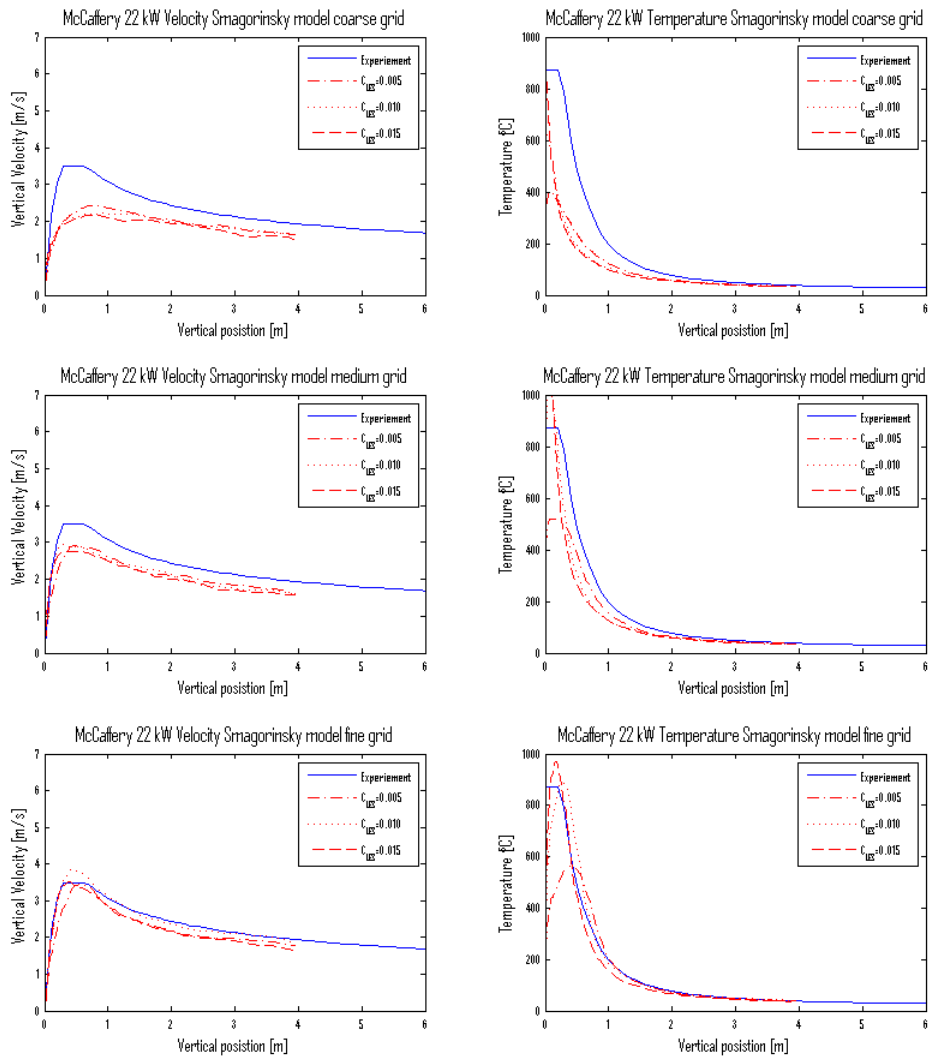


Figure 5.7: McCaffery correlation 22 kW, centerline velocity (left side) and temperature (right side) profiles with Smagorinsky turbulence model. Coarse grid at the top, medium grid in the middle and fine grid at the bottom.

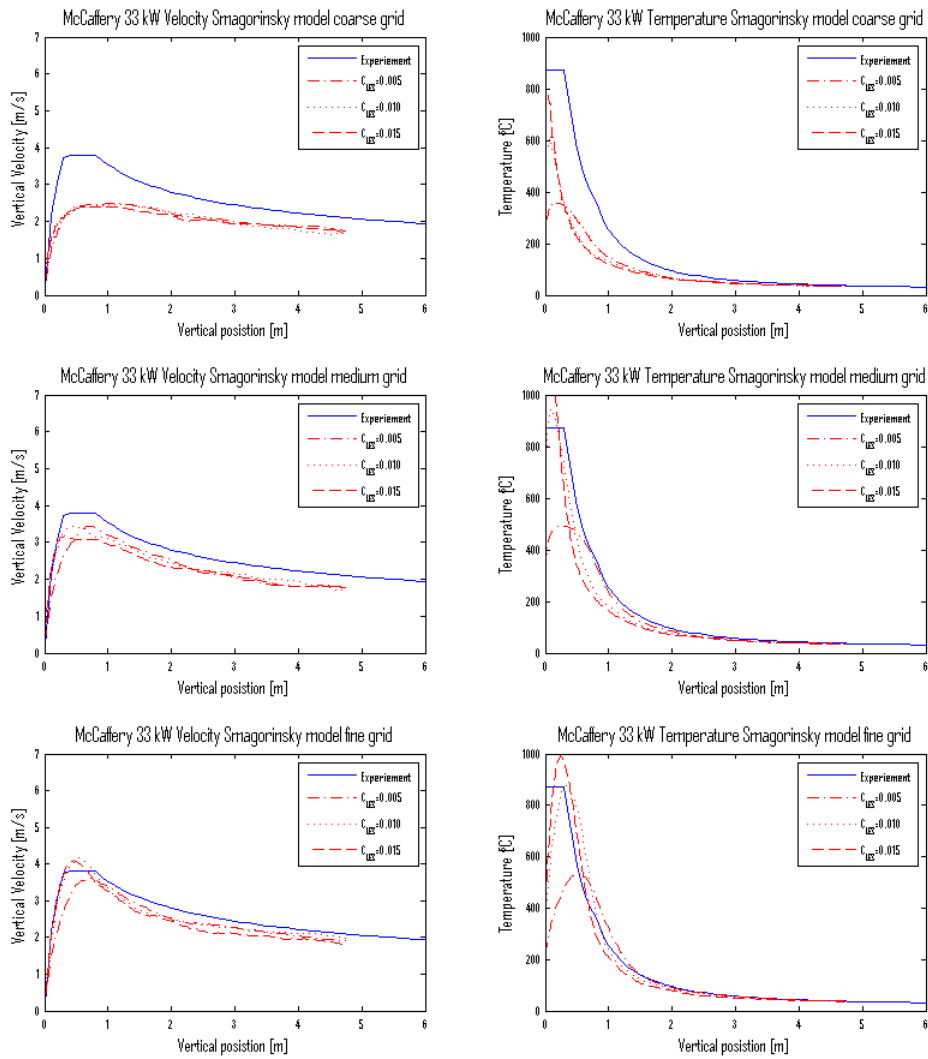


Figure 5.8: McCaffery correlation 33 kW, centerline velocity (left side) and temperature (right side) profiles with Smagorinsky turbulence model. Coarse grid at the top, medium grid in the middle and fine grid at the bottom.

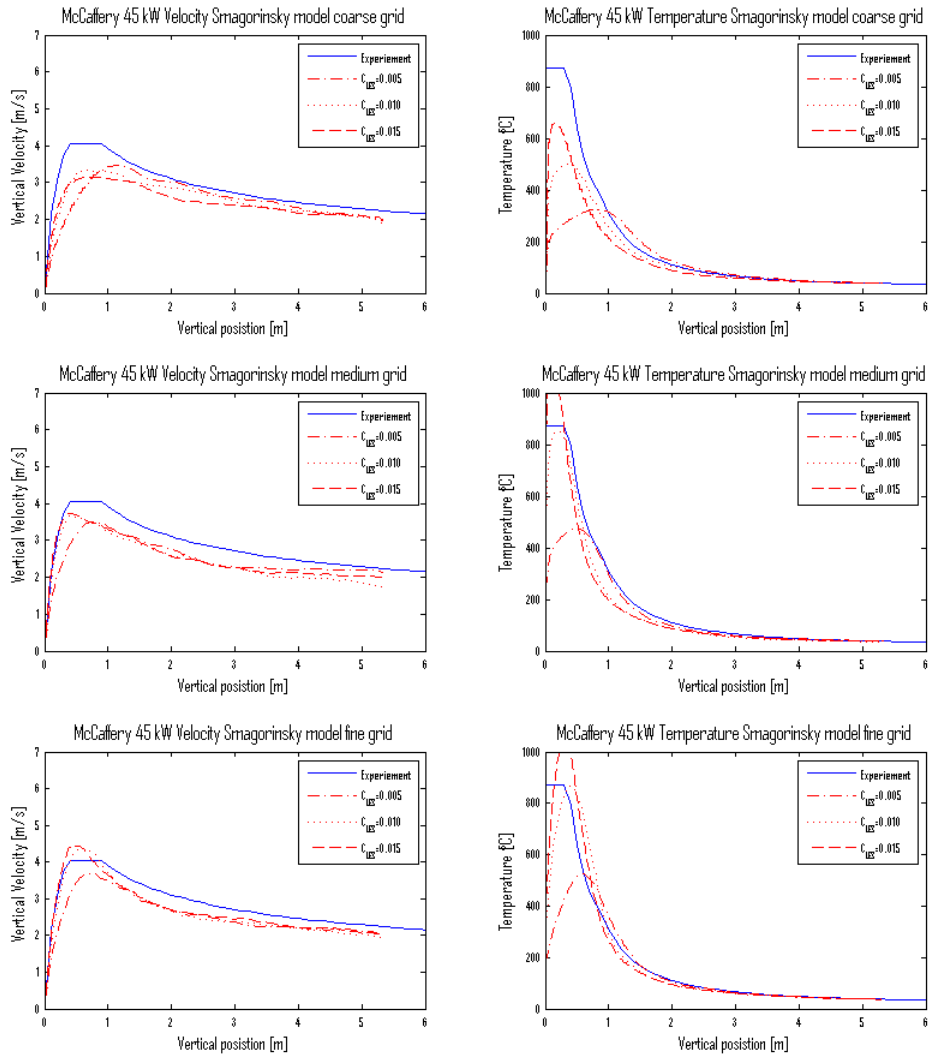


Figure 5.9: McCaffery correlation 45 kW, centerline velocity (left side) and temperature (right side) profiles with Smagorinsky turbulence model. Coarse grid at the top, medium grid in the middle and fine grid at the bottom.

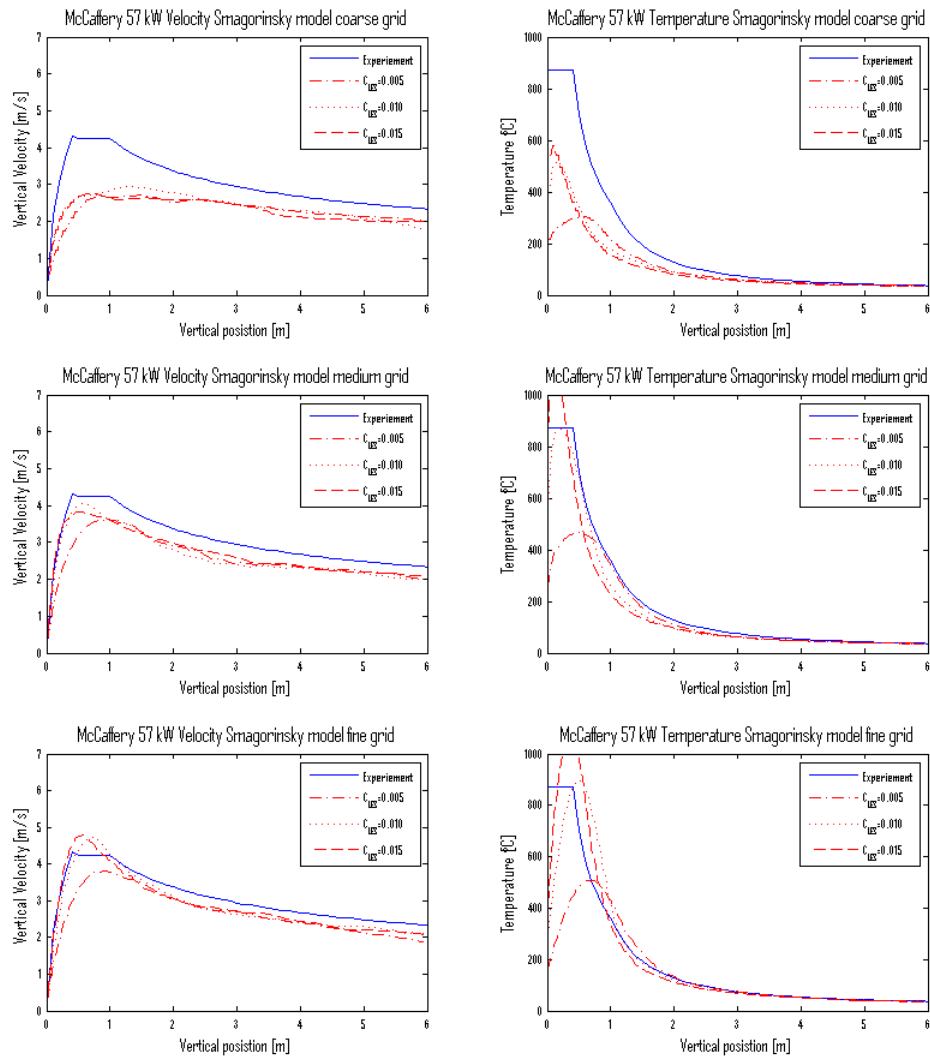


Figure 5.10: McCaffery correlation 57 kW, centerline velocity (left side) and temperature (right side) profiles with Smagorinsky turbulence model. Coarse grid at the top, medium grid in the middle and fine grid at the bottom.

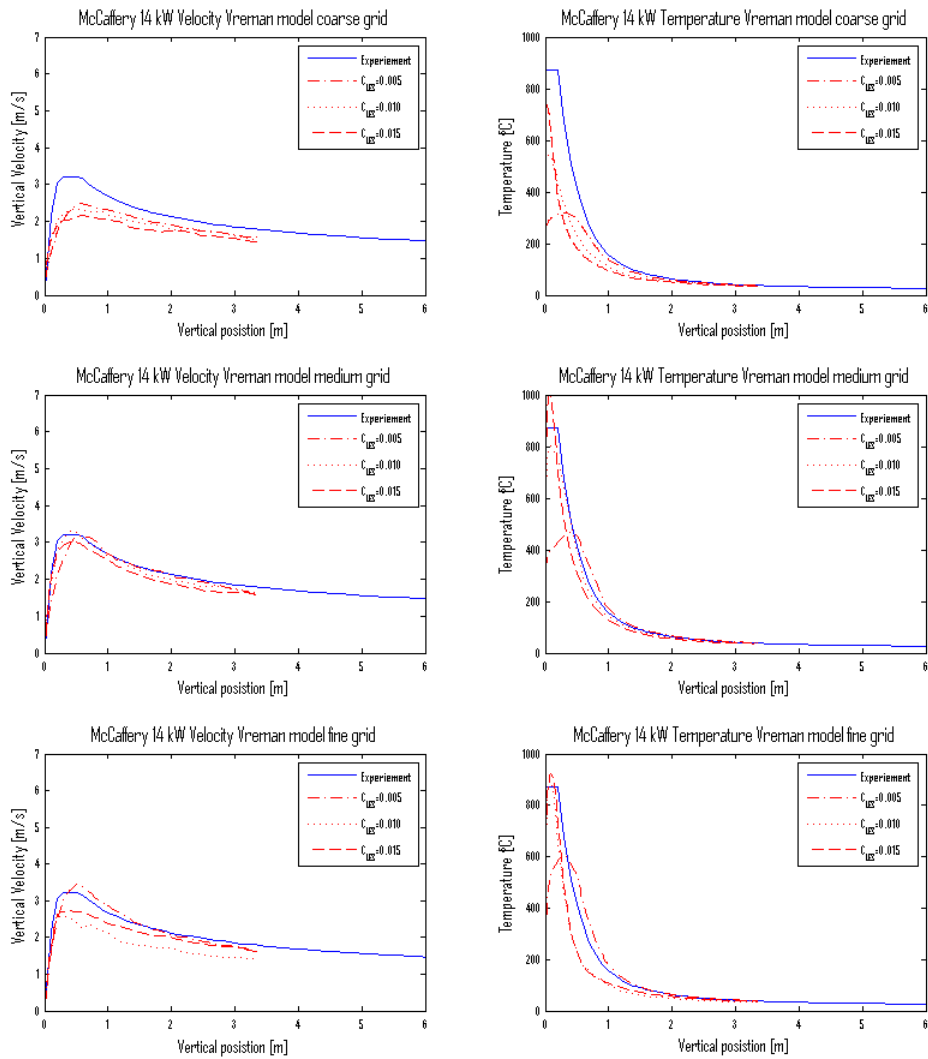


Figure 5.11: McCaffery correlation 14 kW, centerline velocity (left side) and temperature (right side) profiles with Vreman turbulence model. Coarse grid at the top, medium grid in the middle and fine grid at the bottom.

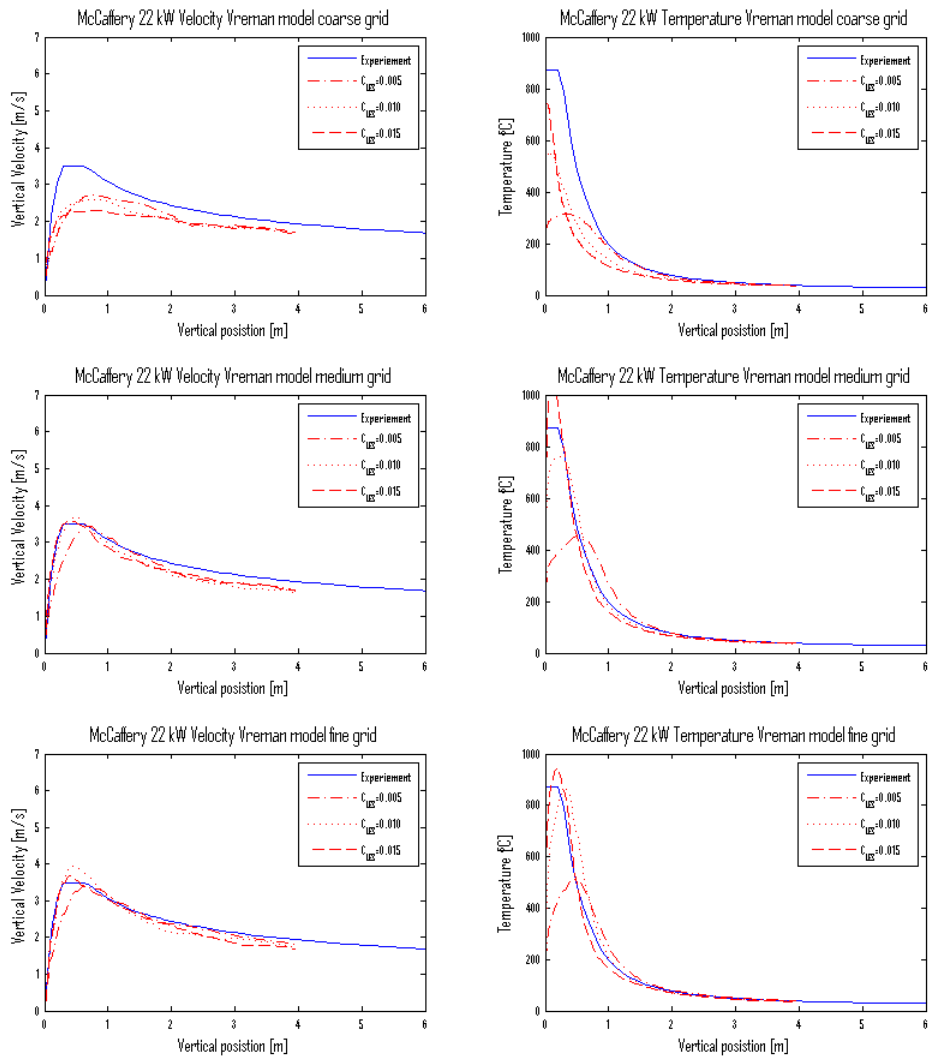


Figure 5.12: McCaffery correlation 22 kW, centerline velocity (left side) and temperature (right side) profiles with Vreman turbulence model. Coarse grid at the top, medium grid in the middle and fine grid at the bottom.

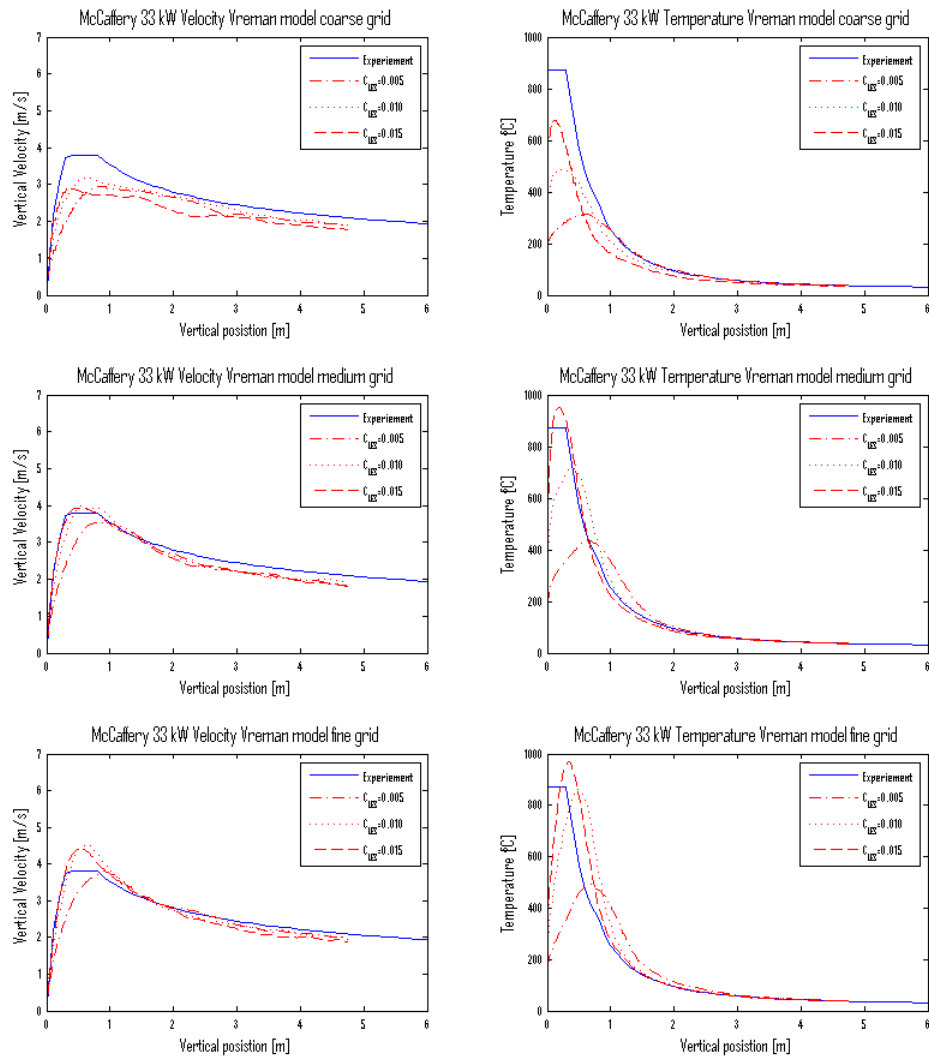


Figure 5.13: McCaffery correlation 33 kW, centerline velocity (left side) and temperature (right side) profiles with Vreman turbulence model. Coarse grid at the top, medium grid in the middle and fine grid at the bottom.

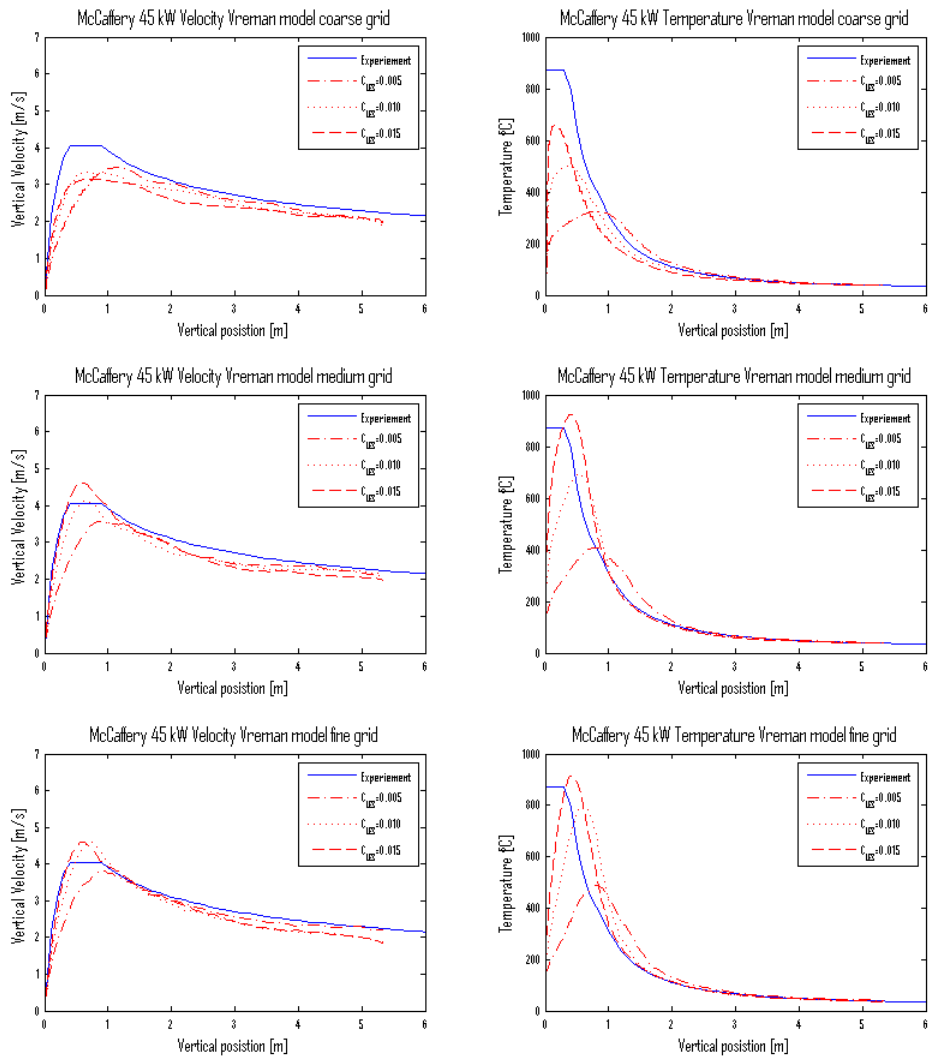


Figure 5.14: McCaffery correlation 45 kW, centerline velocity (left side) and temperature (right side) profiles with Vreman turbulence model. Coarse grid at the top, medium grid in the middle and fine grid at the bottom.

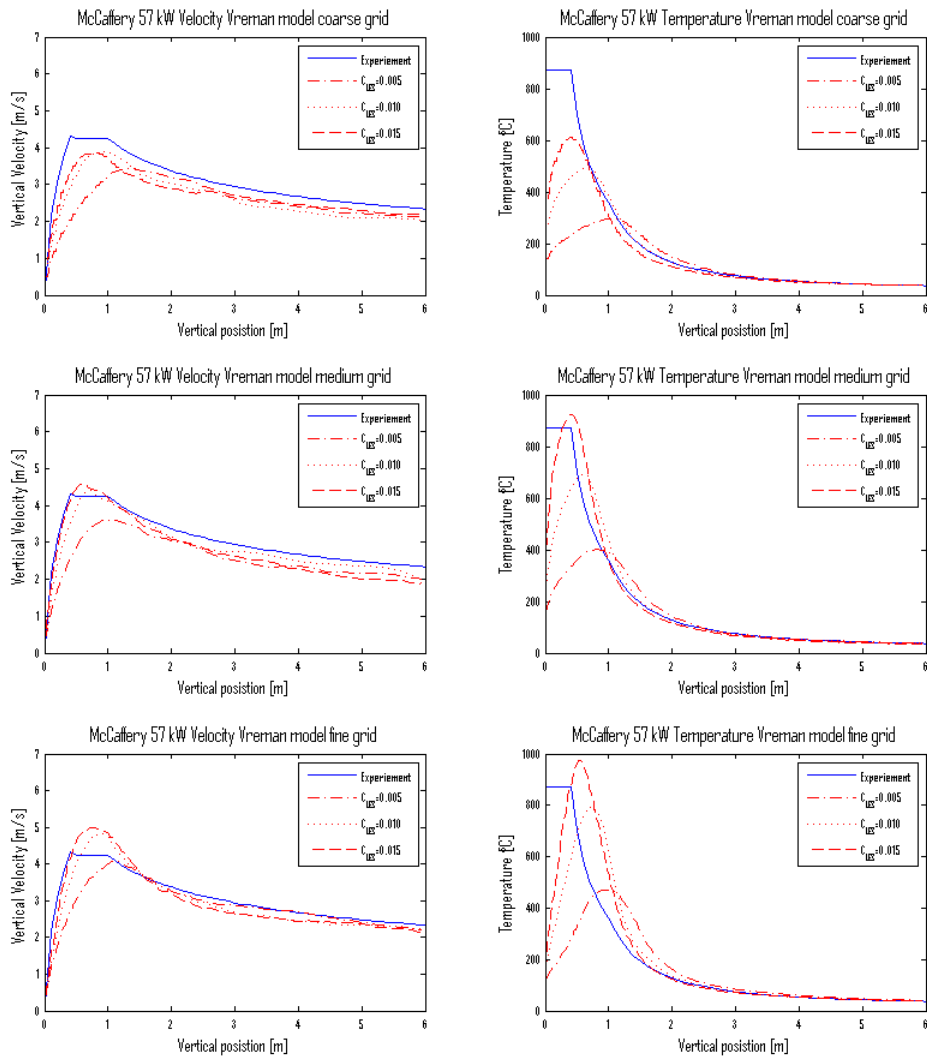


Figure 5.15: McCaffery correlation 57 kW, centerline velocity (left side) and temperature (right side) profiles with Vreman turbulence model. Coarse grid at the top, medium grid in the middle and fine grid at the bottom.

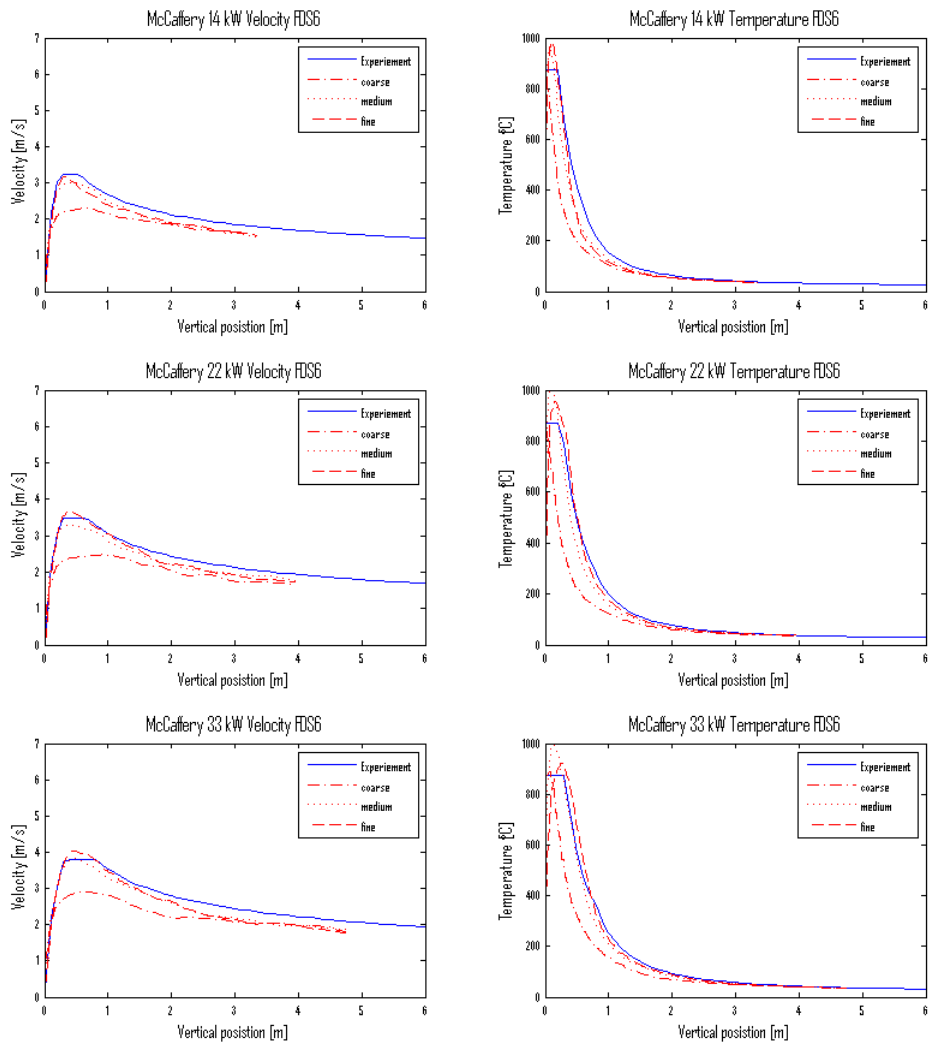


Figure 5.16: McCaffery correlation, centerline velocity (left side) and temperature (right side) profiles with FDS6 Deardorff turbulence model.

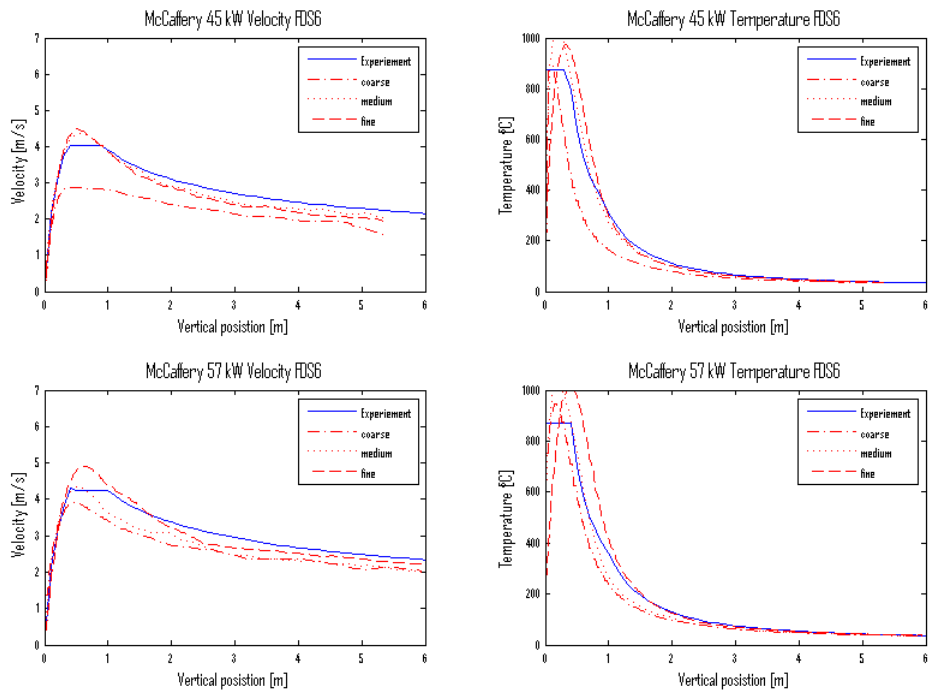


Figure 5.17: McCaffery correlation, centerline velocity (left side) and temperature (right side) profiles with FDS6 Deardorff turbulence model.

5.2 Heskestad Flame Height Correlation

The different fire cases for Heskestad validation is found in Table 5.1. Propane is used as fuel with $0.1 \leq Q^* \leq 10000$ at atmospheric pressure and 20 °C. Three different grids; 17 x 17 x 40, 33 x 33 x 80 and 65 x 65 x 160 and three different C_{LES} ; 0.005, 0.01 and 0.015 are simulated for the turbulence models Deardorff, (dynamic) Smagorinsky and Vreman. D^* and HRR is presented in Table 5.1.

Table 5.1: Heskestad Flame Height Simulations [32].

Q^*	\dot{Q} [kW]	D^* [-]	dx_{10} [m]
0.1	151	0.45	0.045
0.2	303	0.59	0.059
0.5	756	0.86	0.086
1	1513	1.13	0.113
2	3025	1.49	0.149
5	7564	2.15	0.215
10	15127	2.84	0.284
20	30255	3.75	0.375
50	75636	5.40	0.540
100	151273	7.13	0.713
200	302545	9.41	0.941
500	756363	13.6	1.36
1000	1512725	17.9	1.79
2000	3025450	23.6	2.36
5000	7563625	34.1	3.41
10000	15127250	45.0	4.50

In the validation of flame height by Heskestad correlation, outputs from the simulations must be post-processed to predict the flame height. A FORTRAN programme for this is available at <http://code.google.com/p/fds-smv/>. The output from the simulation is heat release per unit length ($HRRPUL = \int \dot{q}'' dx dy$). The flame height, L_f , is assumed to be where 99 % of fuel is consumed on average. This is the same as the height where $\sum_0^{L_f} HRRPUL = 0.99 \cdot \sum_0^\infty HRRPUL$. In line 107 in Appendix C the flame height is found through interpolation.

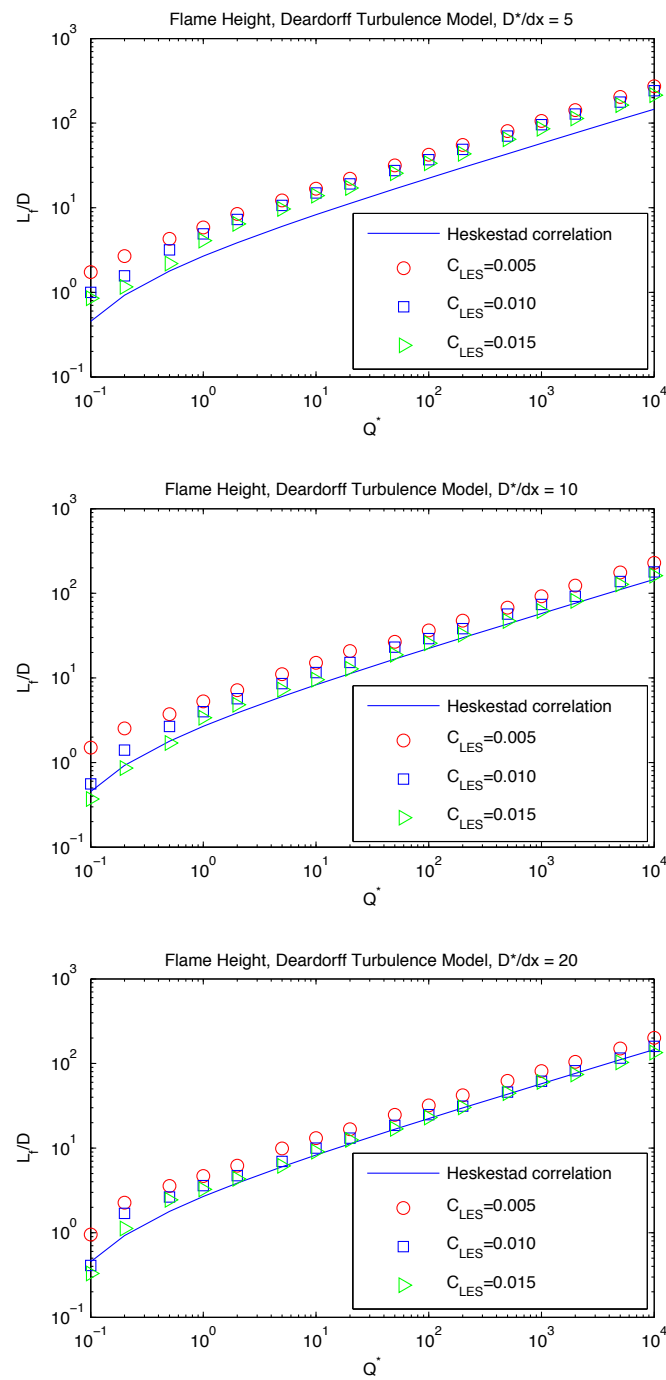


Figure 5.18: Heskestad Flame Height Correlation Deardorff Turbulence Model.

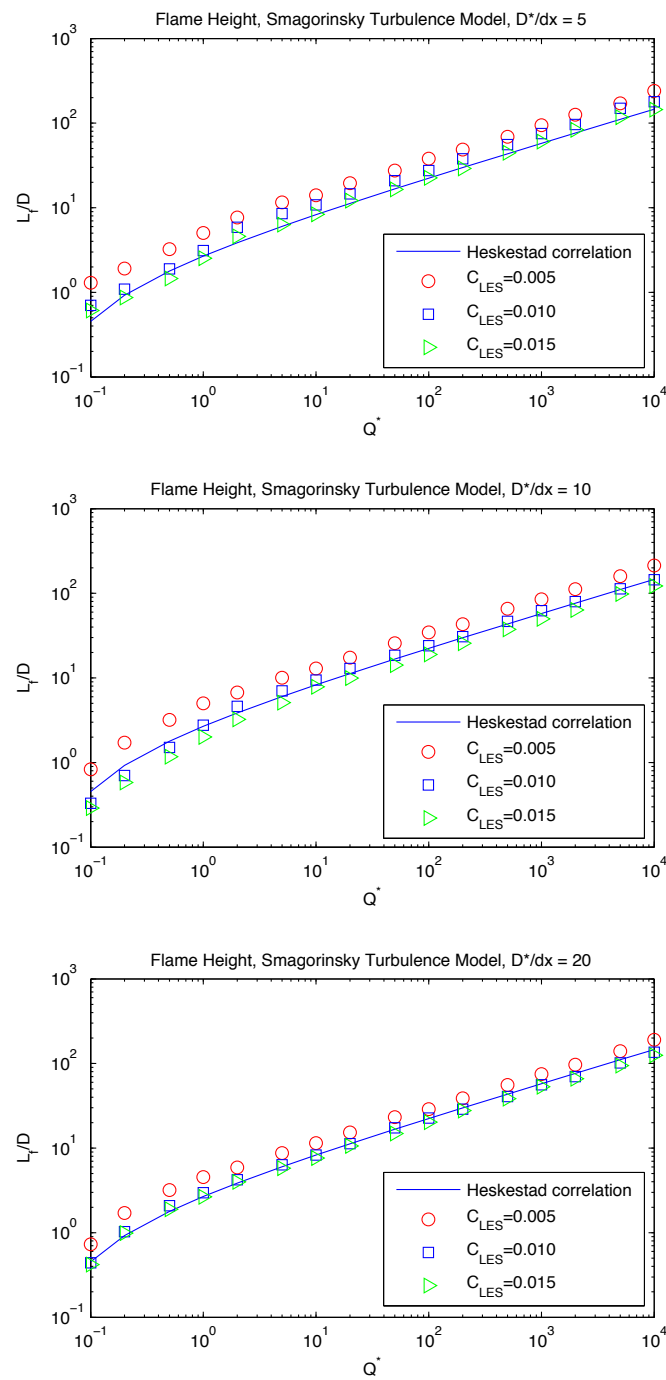


Figure 5.19: Heskestad Flame Height Correlation Smagorinsky Turbulence Model.

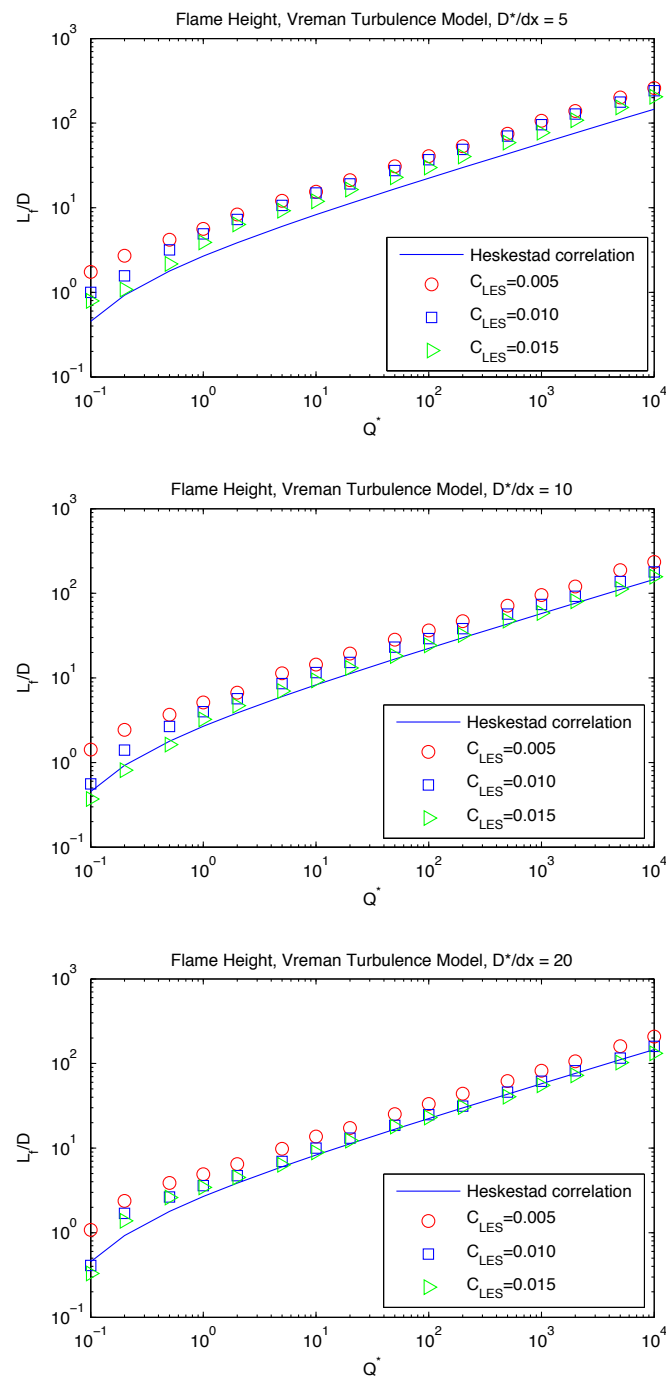


Figure 5.20: Heskestad Flame Height Correlation, Vreman Turbulence Model.

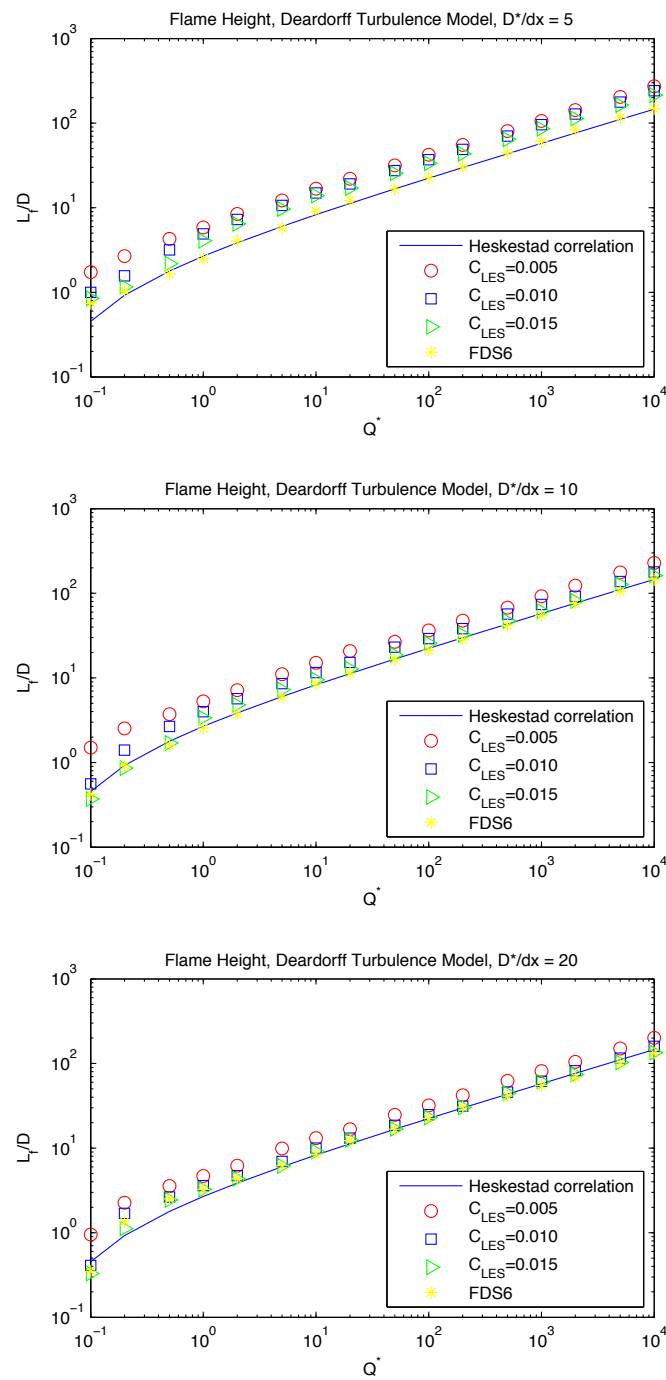


Figure 5.21: Heskestad Flame Height Correlation FDS6 compared with FDS-EDC, Deardorff Turbulence Model.

5.3 Sandia Plume

Sandia Plume experiments are specifically designed for validating CFD models involving fire plumes. The Fire Laboratory for Accreditation of Models by Experimentation (FLAME) facility is located in New Mexico and is where the experiments are performed by Tieszen *et al.* [33]. The experiments are arranged with a 0.5 m steel plane surrounding the fire area of 1 m in diameter. Average velocities profiles are measured in heights of 0.3 m, 0.5 m and 0.9 m above the fire (see Figure 5.59) with Planar Laser Induced Fluorescence (PLIF).

Simulations is compared with the average velocity profiles between 10-20 seconds in the simulations. The computational domain size is 3 m x 3 m x 4 m meters divided in uniform rectangular grid cell of 1.5 cm, 3.0 cm and 6.0 cm. This corresponds to grid resolutions of 192 x 192 x 256, 96 x 96 x 128 and 48 x 48 x 64 respectively. The fuel releases were 0.04 kg/m²s (test 14), 0.053 kg/m²s (test 24) and 0.066 kg/m²s (test 17). Dimensionless HRR and fire diameter is given in Table 5.2. Input for all cases are specified after the actual test conditions. Example of inputs for the fires are seen in Appendix A.1-A.3 [33].

Table 5.2: Sandia plume experiment simulations.

<i>Testnumber</i>	\dot{Q} [kW]	\dot{Q}^* [-]	D^* [-]
14	1590	1.35	1.13
17	2610	2.22	1.38
24	2070	1.76	1.25

5.3.1 Methane Fire, Test 14

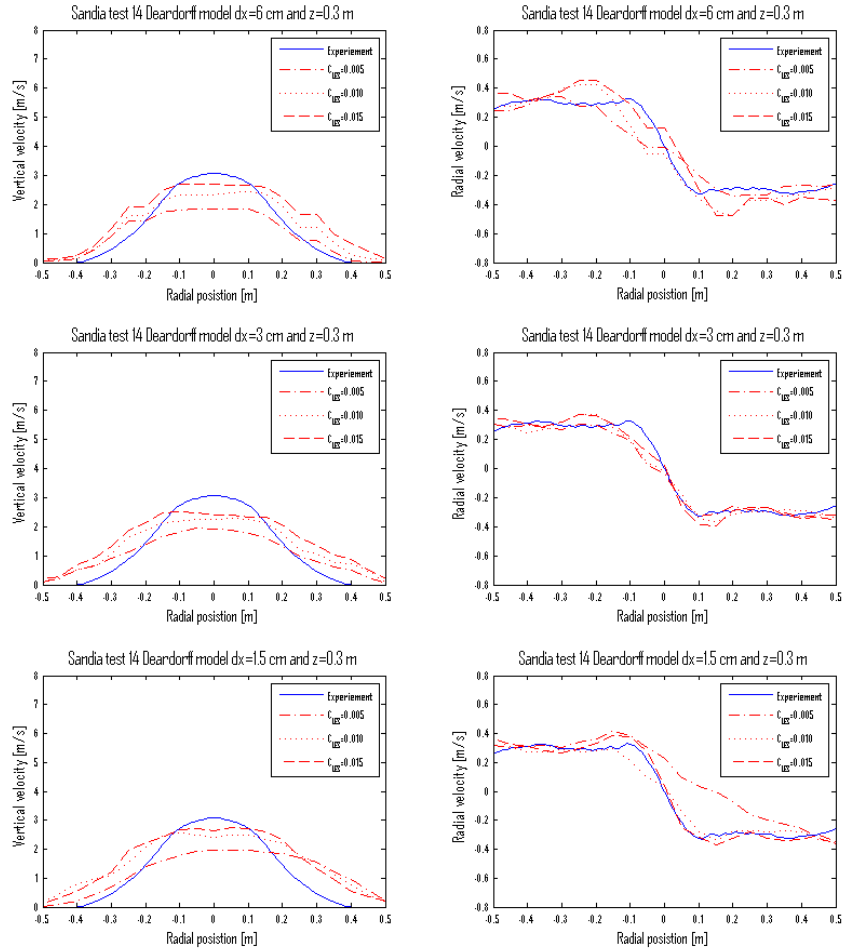


Figure 5.22: Sandia plume experiment test 14 with Deardorff turbulence model at $z = 0.3$ m. Vertical velocity to the left and radial velocity to the right. On the top the coarse grid $dx = 6$ cm, $dx = 3$ cm in the middle and $dx = 1.5$ cm at the bottom.

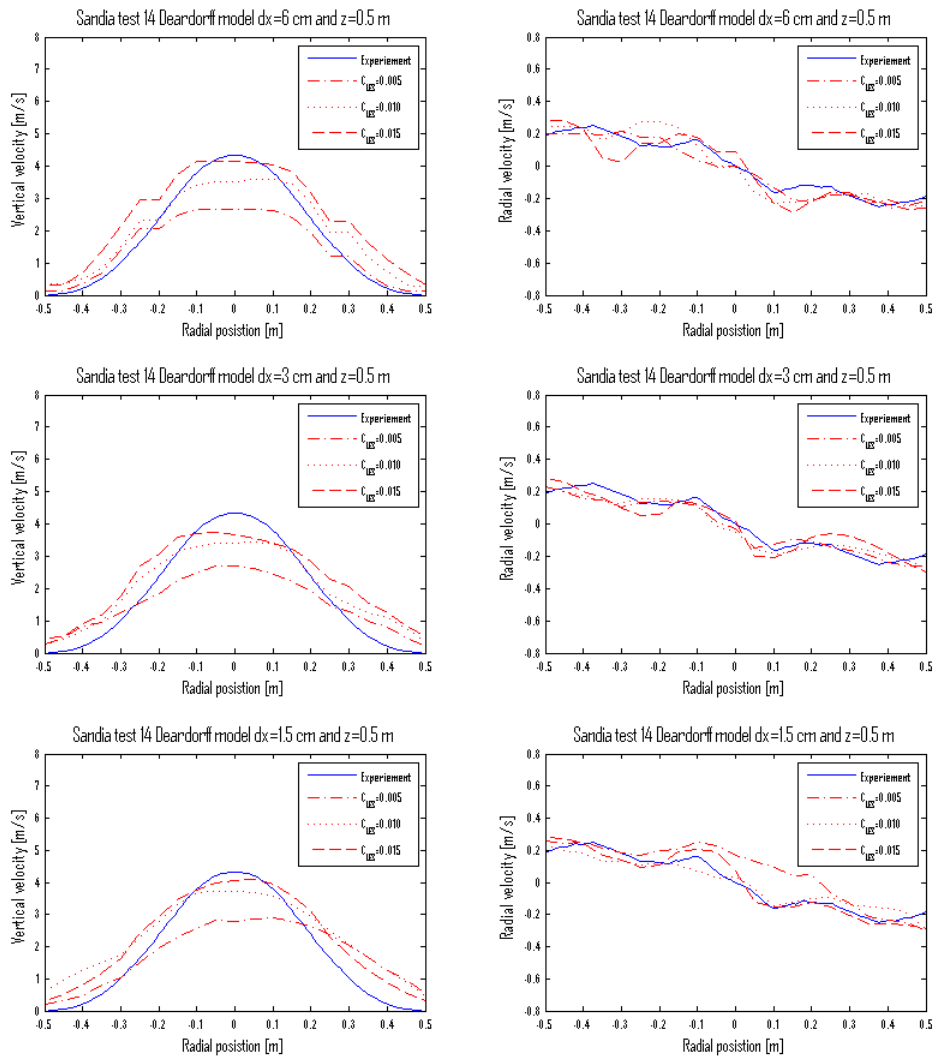


Figure 5.23: Sandia plume experiment test 14 with Deardorff turbulence model at $z = 0.5$ m. Vertical velocity to the left and radial velocity to the right. On the top the coarse grid $dx = 6$ cm, $dx = 3$ cm in the middle and $dx = 1.5$ cm at the bottom.

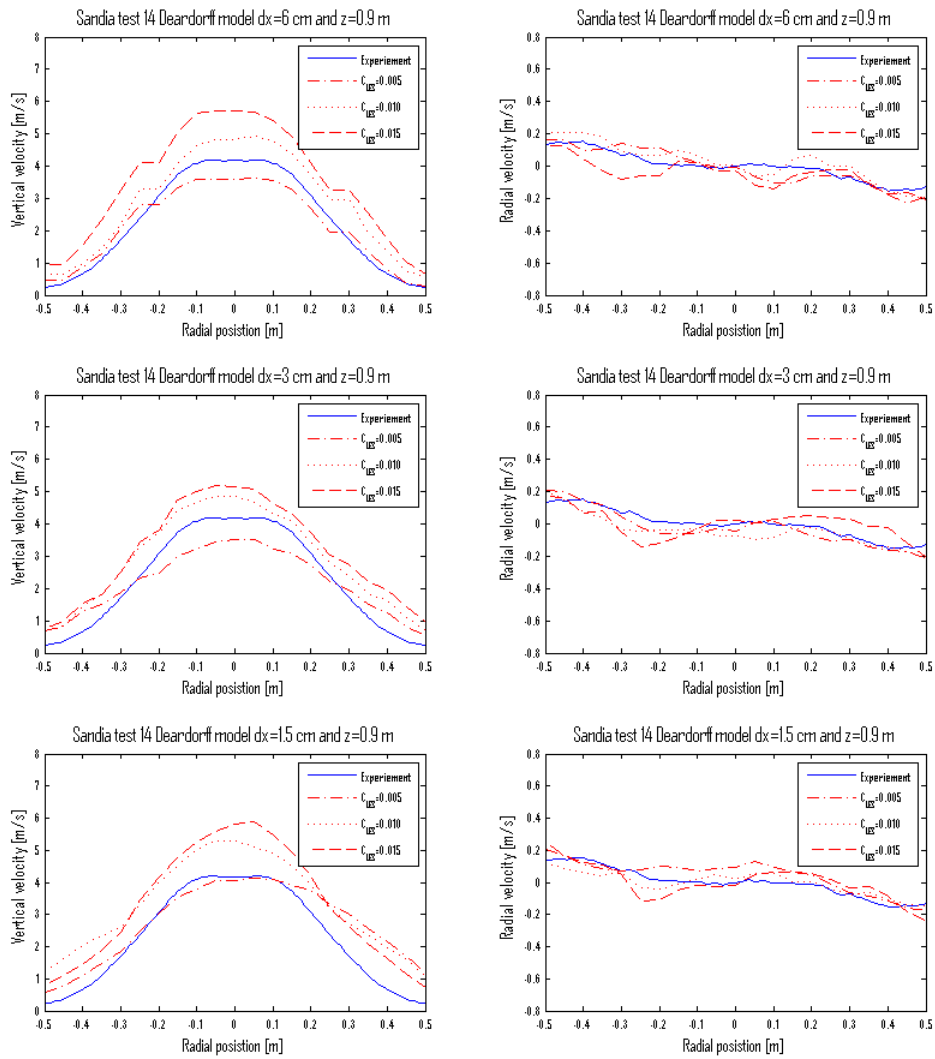


Figure 5.24: Sandia plume experiment test 14 with Deardorff turbulence model at $z = 0.9$ m. Vertical velocity to the left and radial velocity to the right. On the top the coarse grid $dx = 6$ cm, $dx = 3$ cm in the middle and $dx = 1.5$ cm at the bottom.

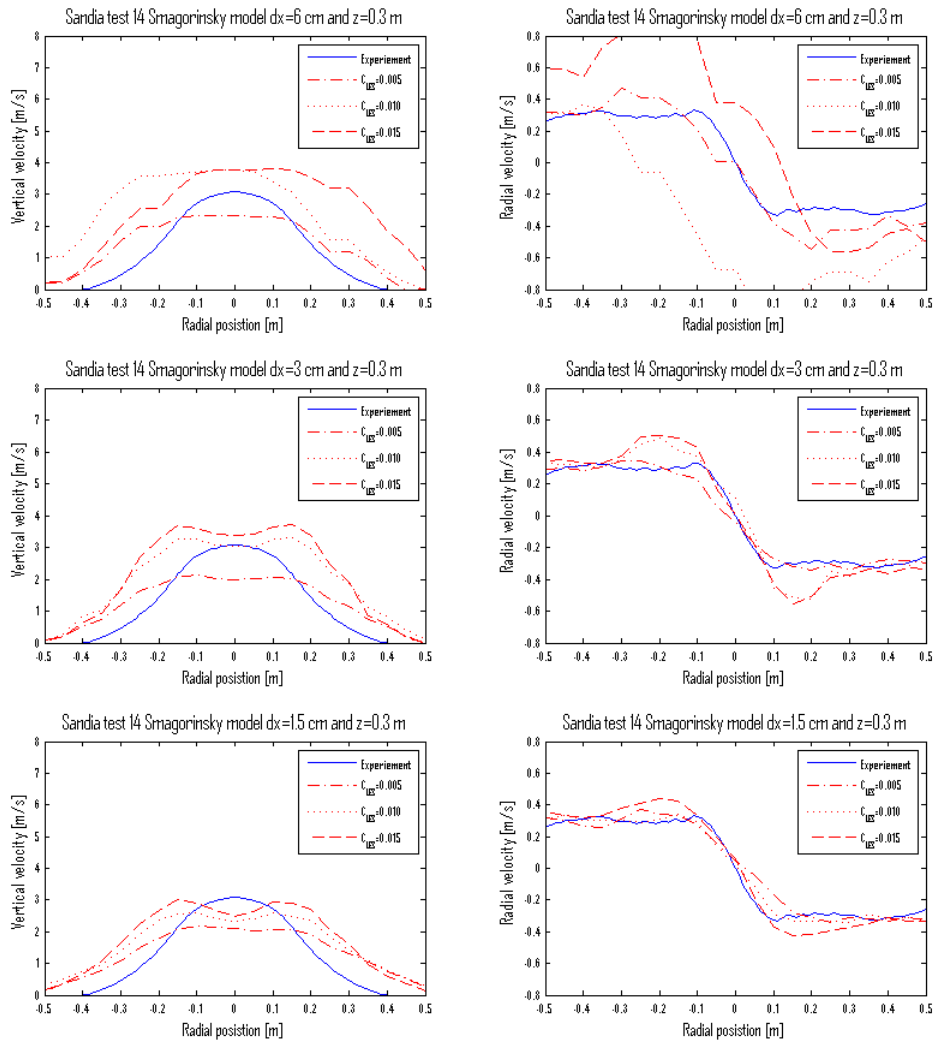


Figure 5.25: Sandia plume experiment test 14 with Smagosinsky turbulence model at $z = 0.3$ m. Vertical velocity to the left and radial velocity to the right. On the top the coarse grid $dx = 6$ cm, $dx = 3$ cm in the middle and $dx = 1.5$ cm at the bottom.

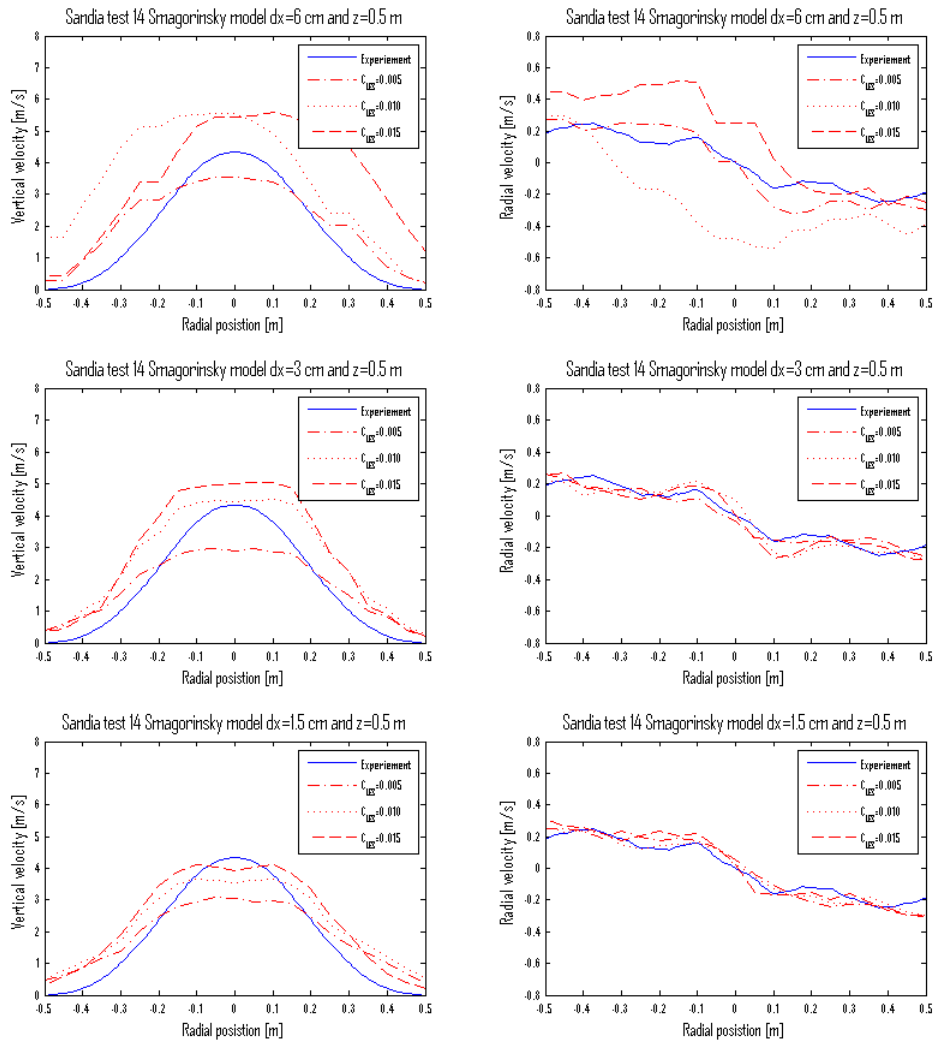


Figure 5.26: Sandia plume experiment test 14 with Smagosinsky turbulence model at $z = 0.5$ m. Vertical velocity to the left and radial velocity to the right. On the top the coarse grid $dx = 6$ cm, $dx = 3$ cm in the middle and $dx = 1.5$ cm at the bottom.

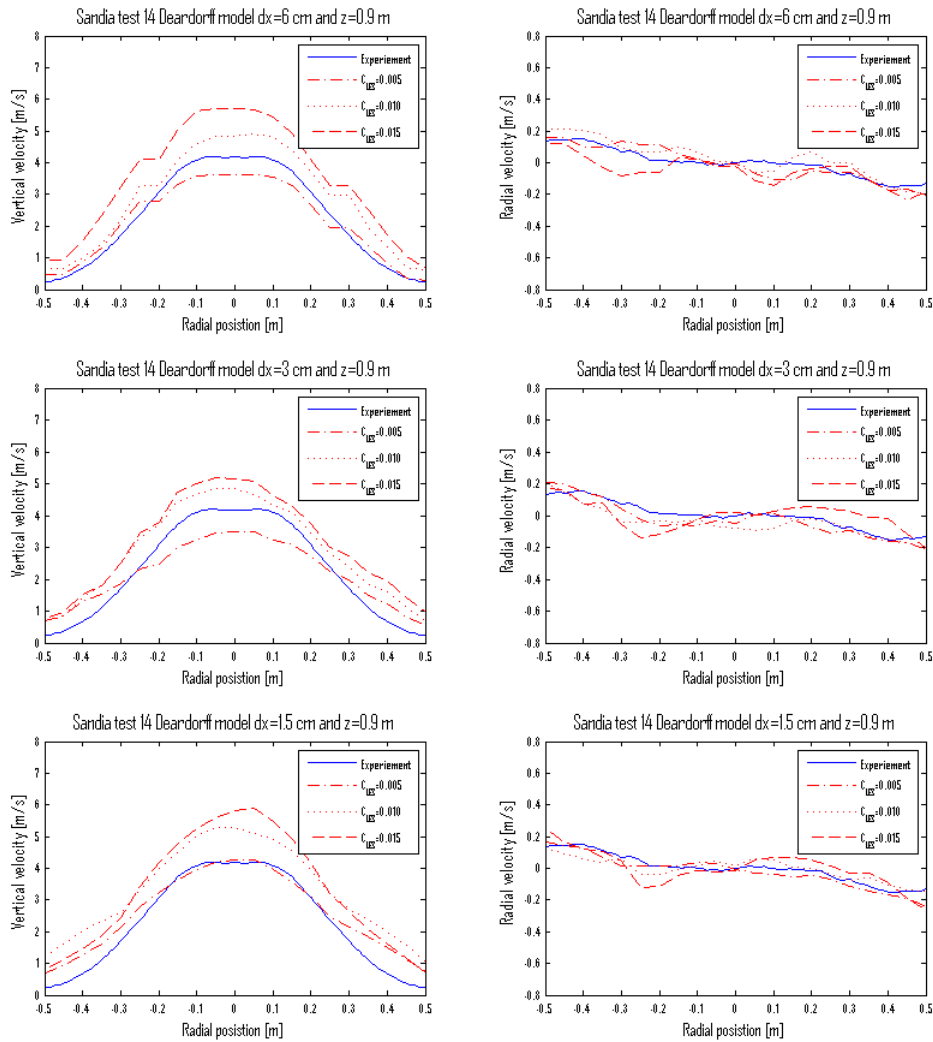


Figure 5.27: Sandia plume experiment test 14 with Smagosinsky turbulence model at $z = 0.9$ m. Vertical velocity to the left and radial velocity to the right. On the top the coarse grid $dx = 6$ cm, $dx = 3$ cm in the middle and $dx = 1.5$ cm at the bottom.

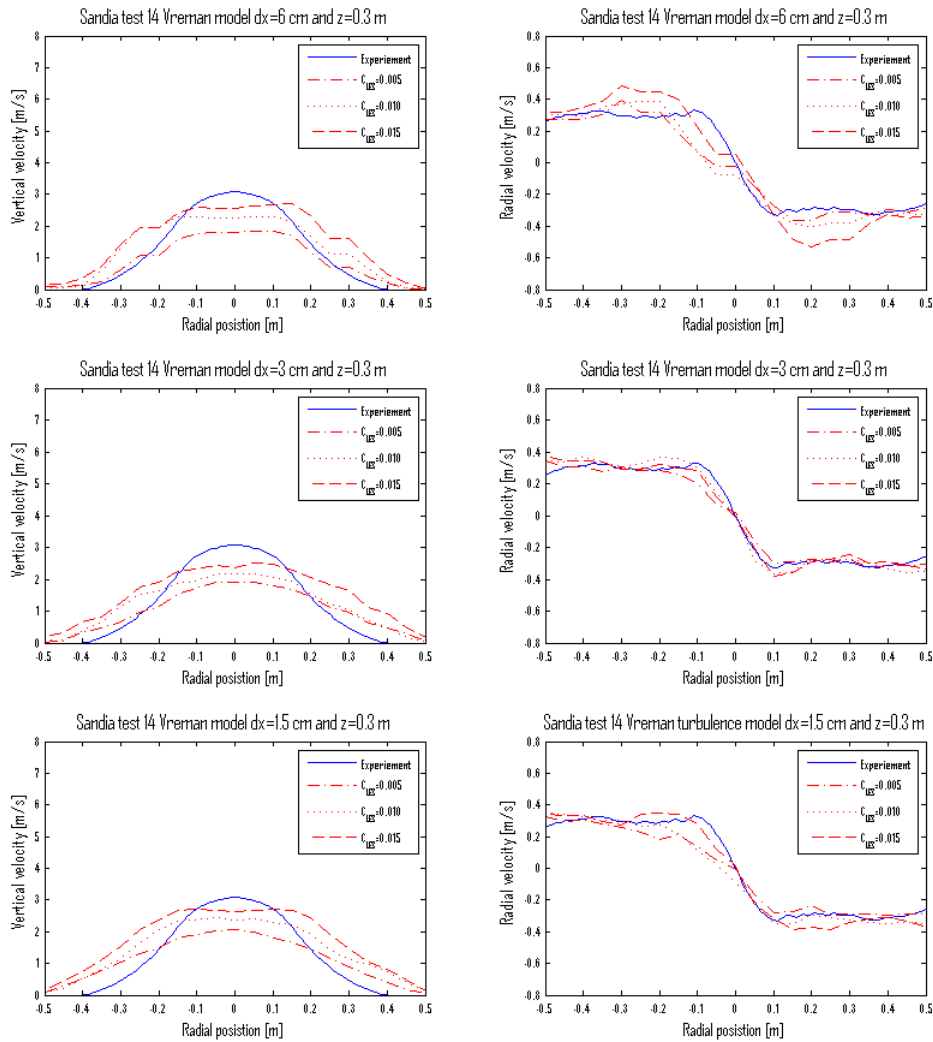


Figure 5.28: Sandia plume experiment test 14 with Vreman turbulence model at $z = 0.3$ m. Vertical velocity to the left and radial velocity to the right. On the top the coarse grid $dx = 6$ cm, $dx = 3$ cm in the middle and $dx = 1.5$ cm at the bottom.

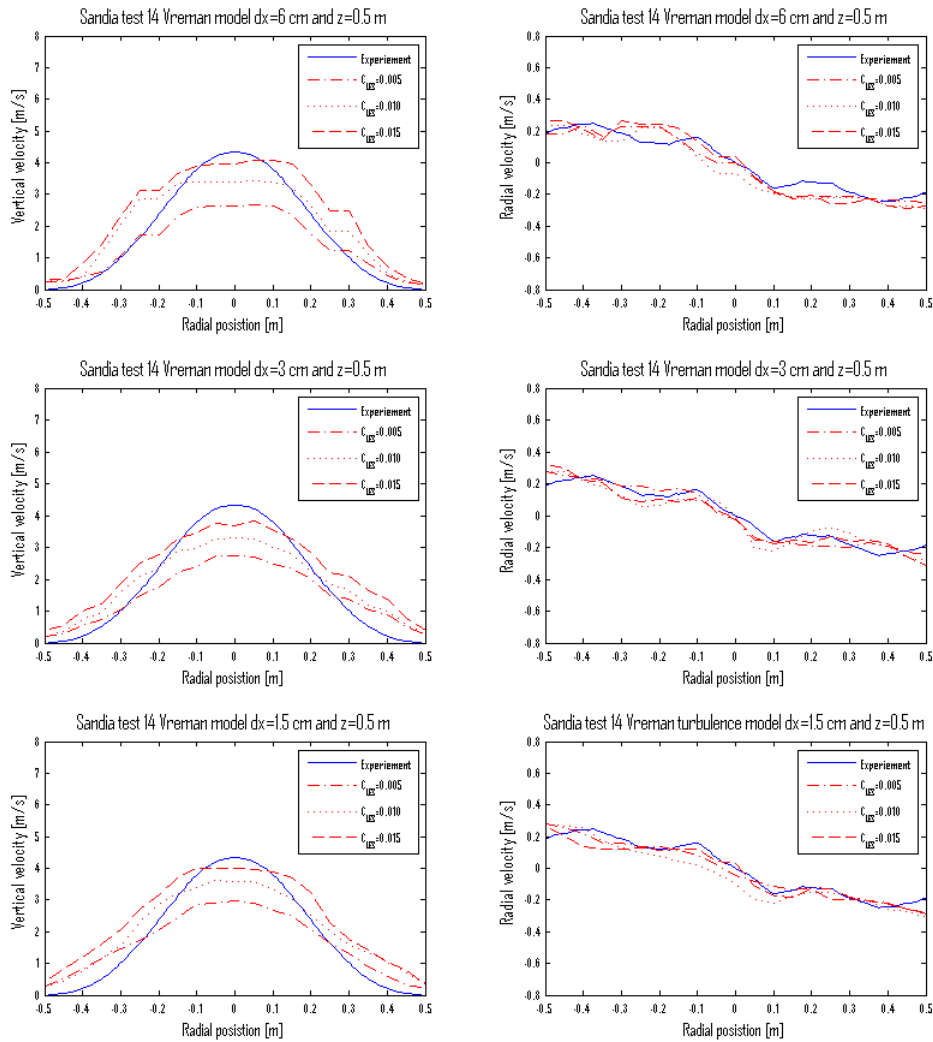


Figure 5.29: Sandia plume experiment test 14 with Vreman turbulence model at $z = 0.5$ m. Vertical velocity to the left and radial velocity to the right. On the top the coarse grid $dx = 6$ cm, $dx = 3$ cm in the middle and $dx = 1.5$ cm at the bottom.

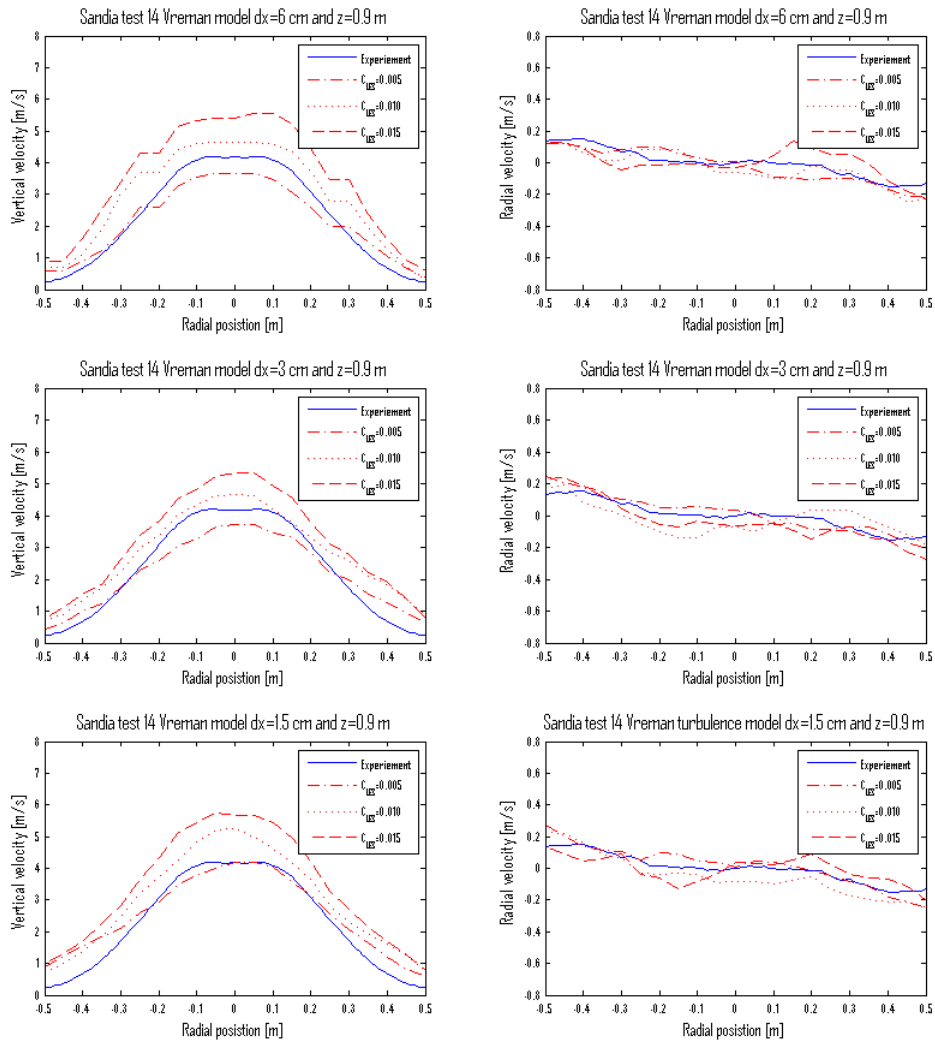


Figure 5.30: Sandia plume experiment test 14 with Vreman turbulence model at $z = 0.9$ m. Vertical velocity to the left and radial velocity to the right. On the top the coarse grid $dx = 6$ cm, $dx = 3$ cm in the middle and $dx = 1.5$ cm at the bottom.

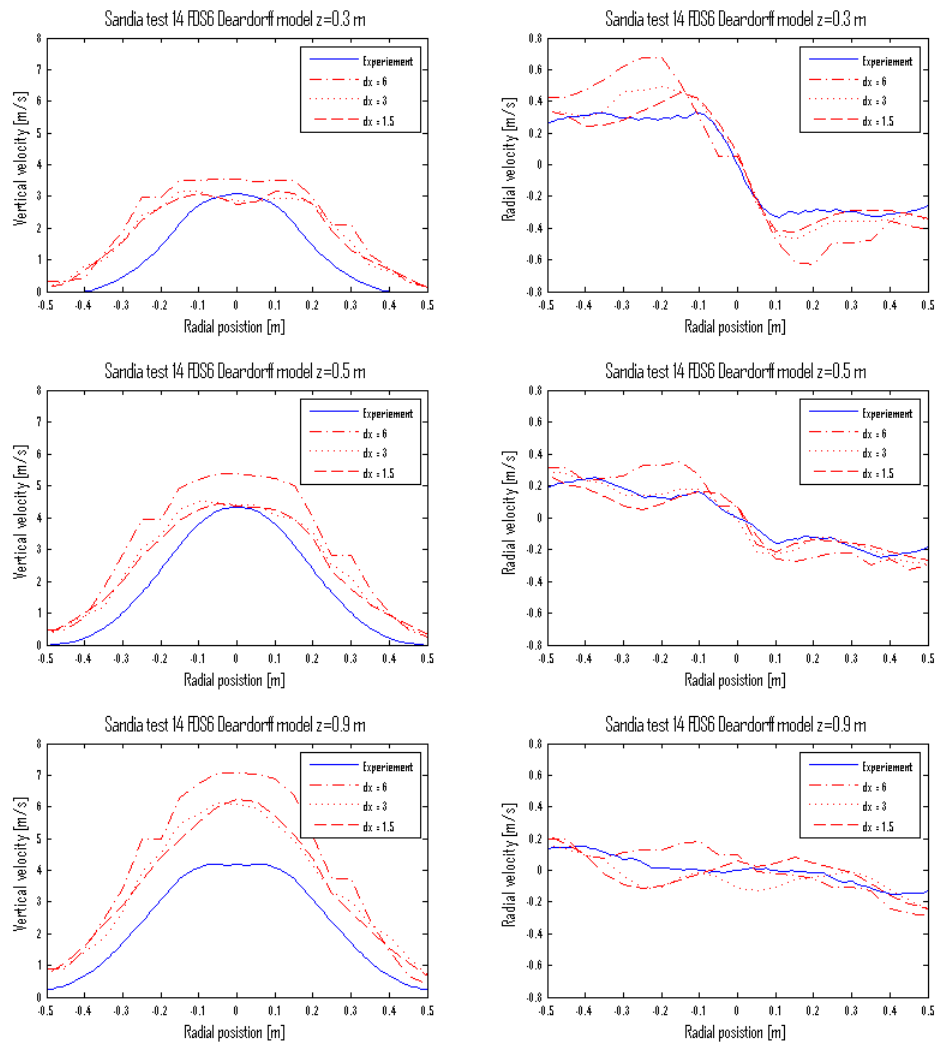


Figure 5.31: Sandia plume experiment test 14 with FDS6. Vertical velocity to the left and radial velocity to the right. On the top at $z = 0.3$ m, $z = 0.5$ m in the middle and $z = 0.9$ m at the bottom.

5.3.2 Methane Fire, Test 17

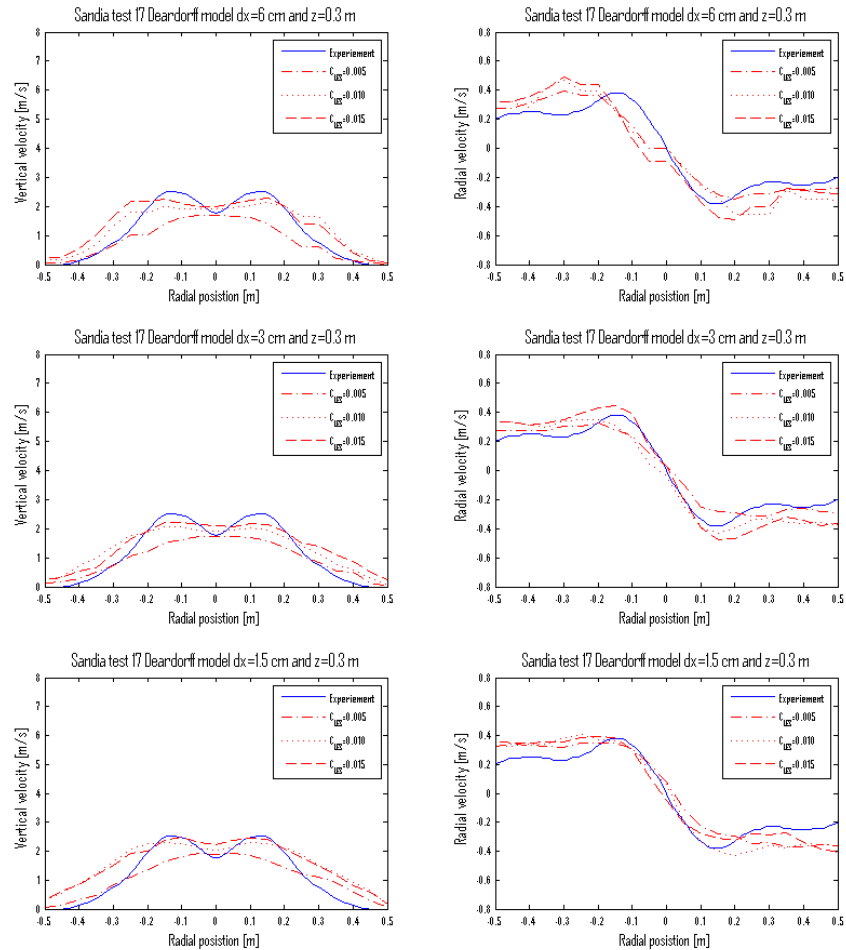


Figure 5.32: Sandia plume experiment test 17 with Deardorff turbulence model at $z = 0.3$ m. Vertical velocity to the left and radial velocity to the right. On the top the coarse grid $dx = 6$ cm, $dx = 3$ cm in the middle and $dx = 1.5$ cm at the bottom.

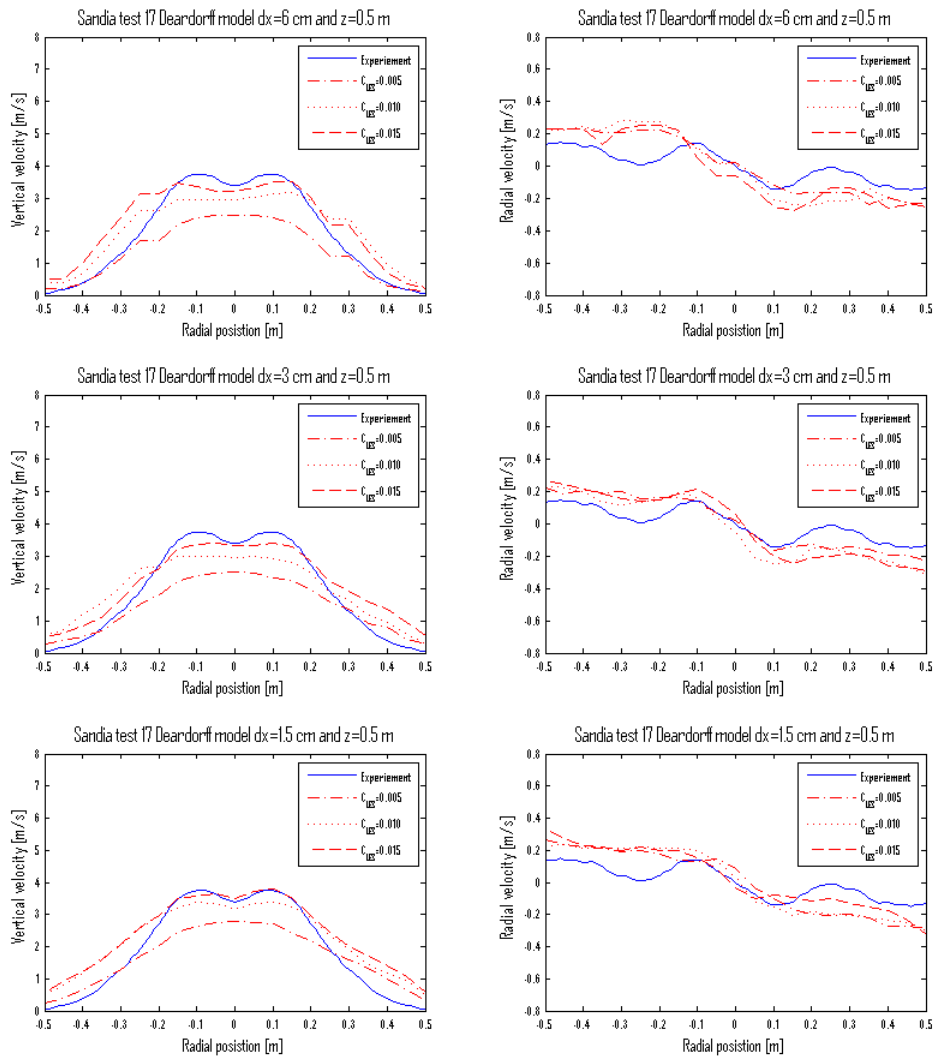


Figure 5.33: Sandia plume experiment test 17 with Deardorff turbulence model at $z = 0.5$ m. Vertical velocity to the left and radial velocity to the right. On the top the coarse grid $dx = 6$ cm, $dx = 3$ cm in the middle and $dx = 1.5$ cm at the bottom.

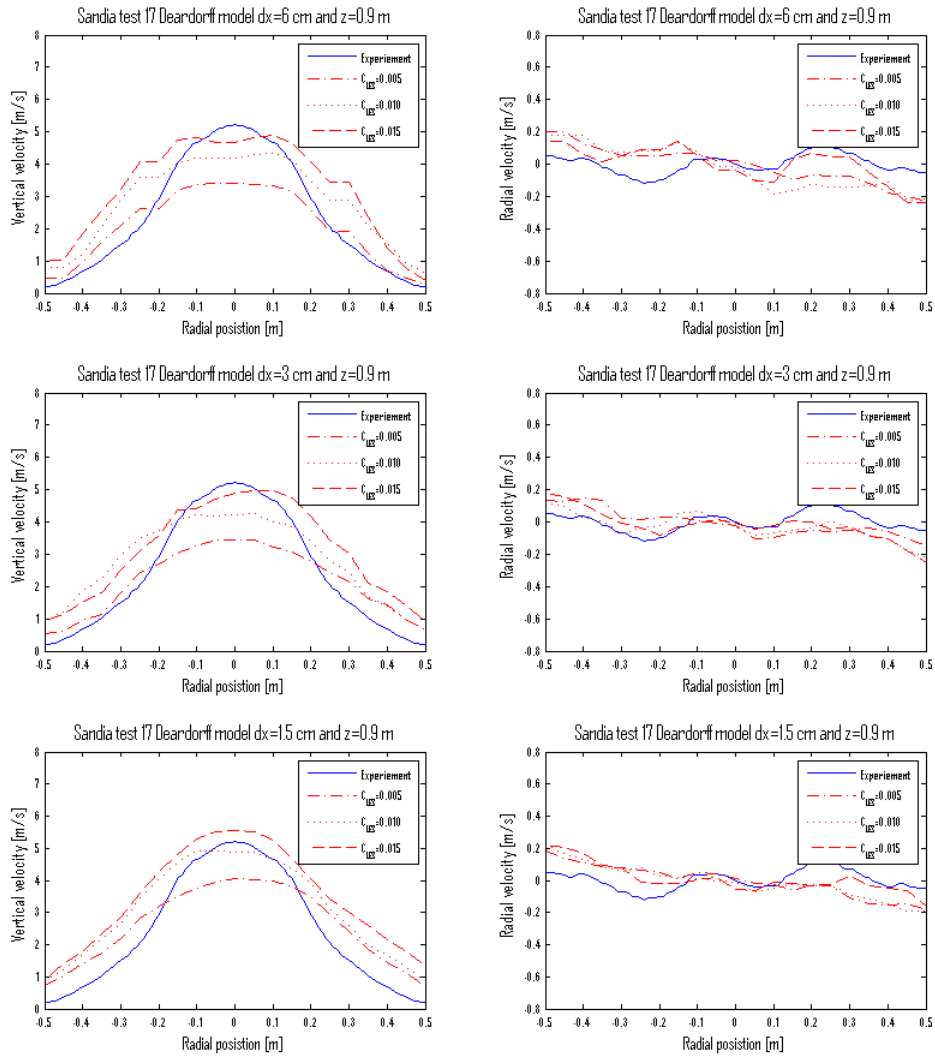


Figure 5.34: Sandia plume experiment test 17 with Deardorff turbulence model at $z = 0.9$ m. Vertical velocity to the left and radial velocity to the right. On the top the coarse grid $dx = 6$ cm, $dx = 3$ cm in the middle and $dx = 1.5$ cm at the bottom.

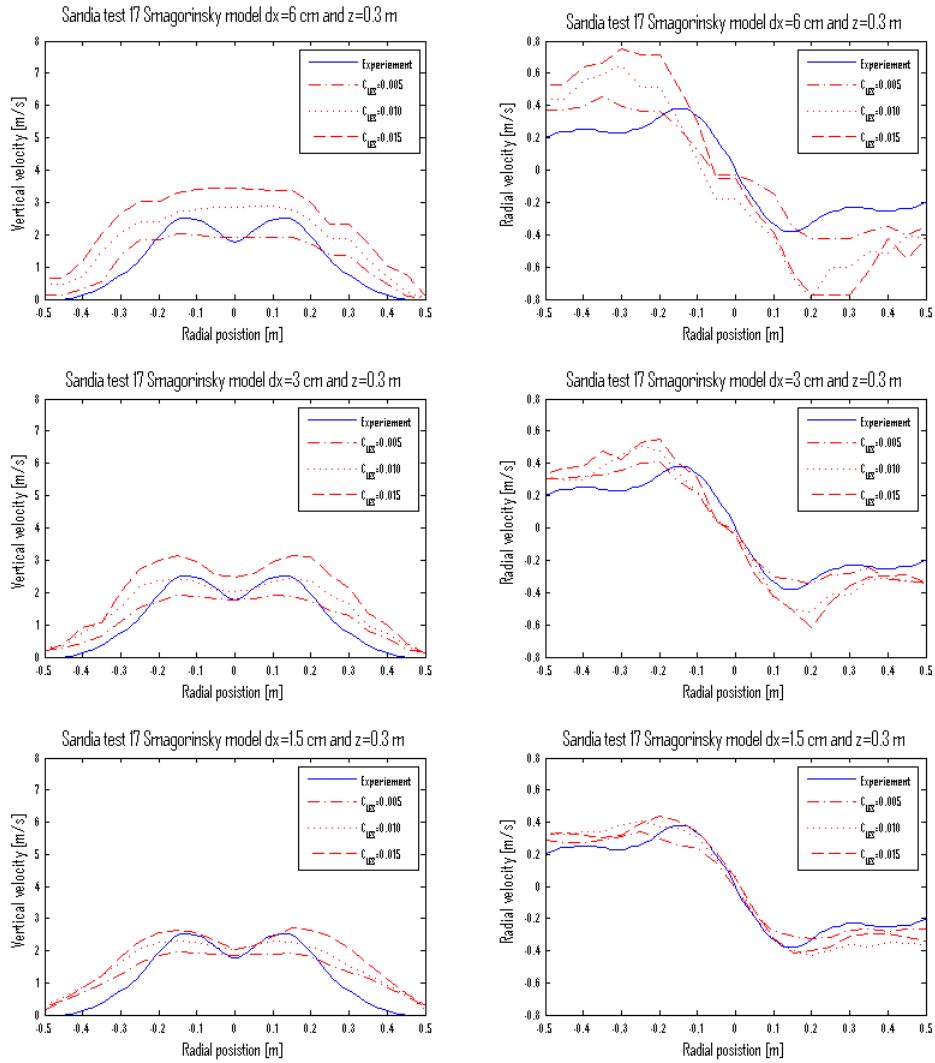


Figure 5.35: Sandia plume experiment test 17 with Smagosinsky turbulence model at $z = 0.3$ m. Vertical velocity to the left and radial velocity to the right. On the top the coarse grid $dx = 6$ cm, $dx = 3$ cm in the middle and $dx = 1.5$ cm at the bottom.

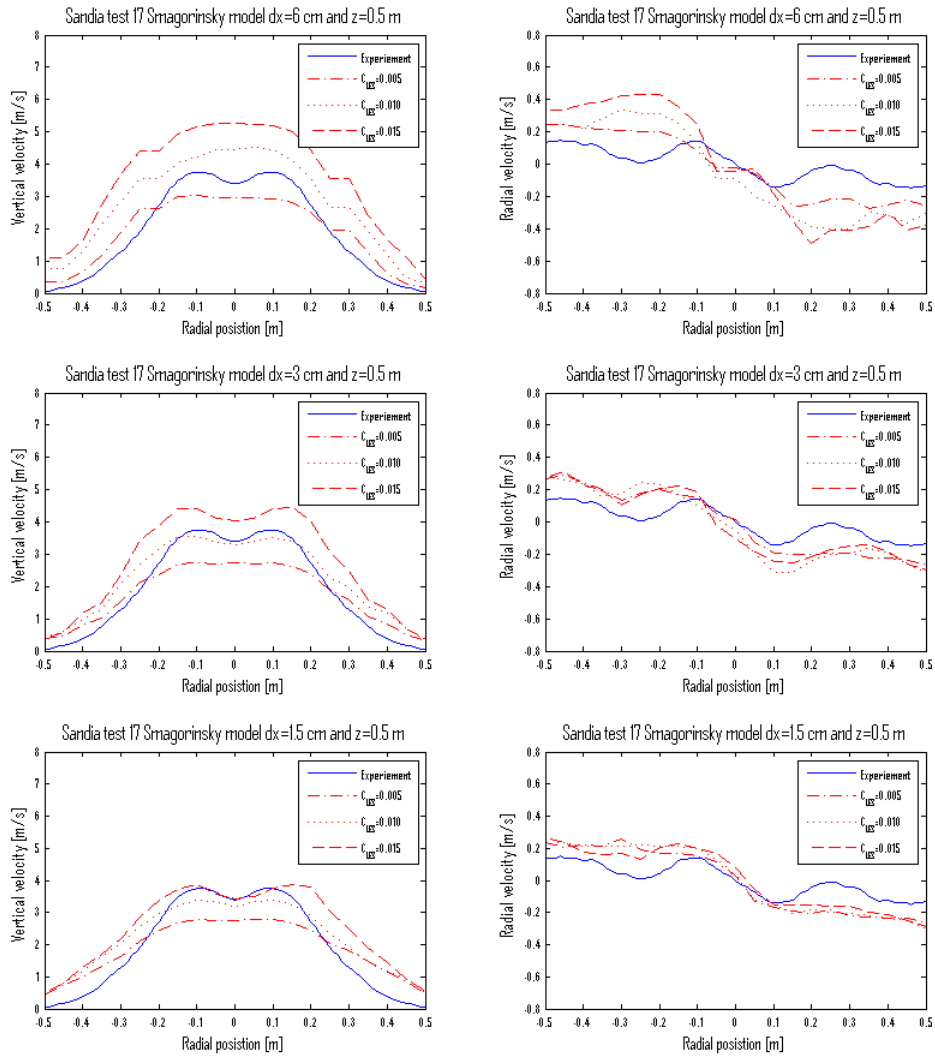


Figure 5.36: Sandia plume experiment test 17 with Smagorinsky turbulence model at $z = 0.5$ m. Vertical velocity to the left and radial velocity to the right. On the top the coarse grid $dx = 6$ cm, $dx = 3$ cm in the middle and $dx = 1.5$ cm at the bottom.

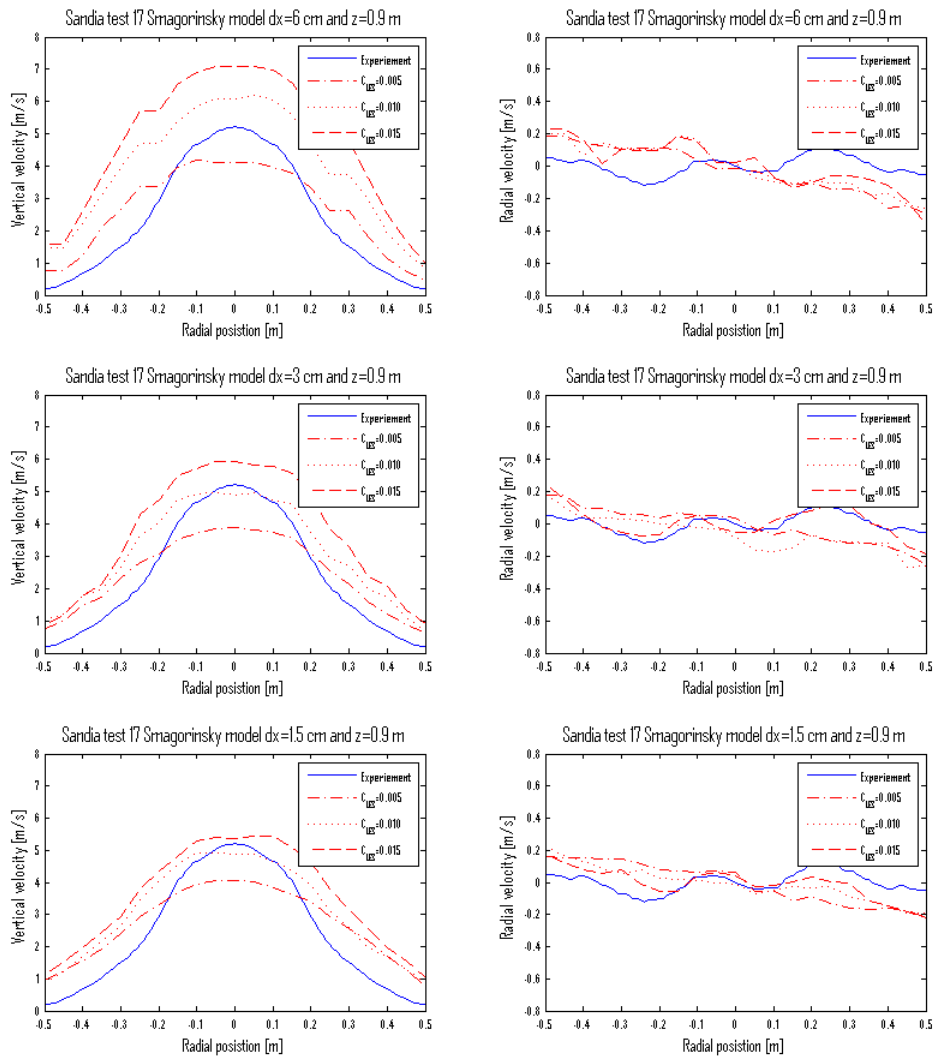


Figure 5.37: Sandia plume experiment test 17 with Smagorinsky turbulence model at $z = 0.9$ m. Vertical velocity to the left and radial velocity to the right. On the top the coarse grid $dx = 6$ cm, $dx = 3$ cm in the middle and $dx = 1.5$ cm at the bottom.

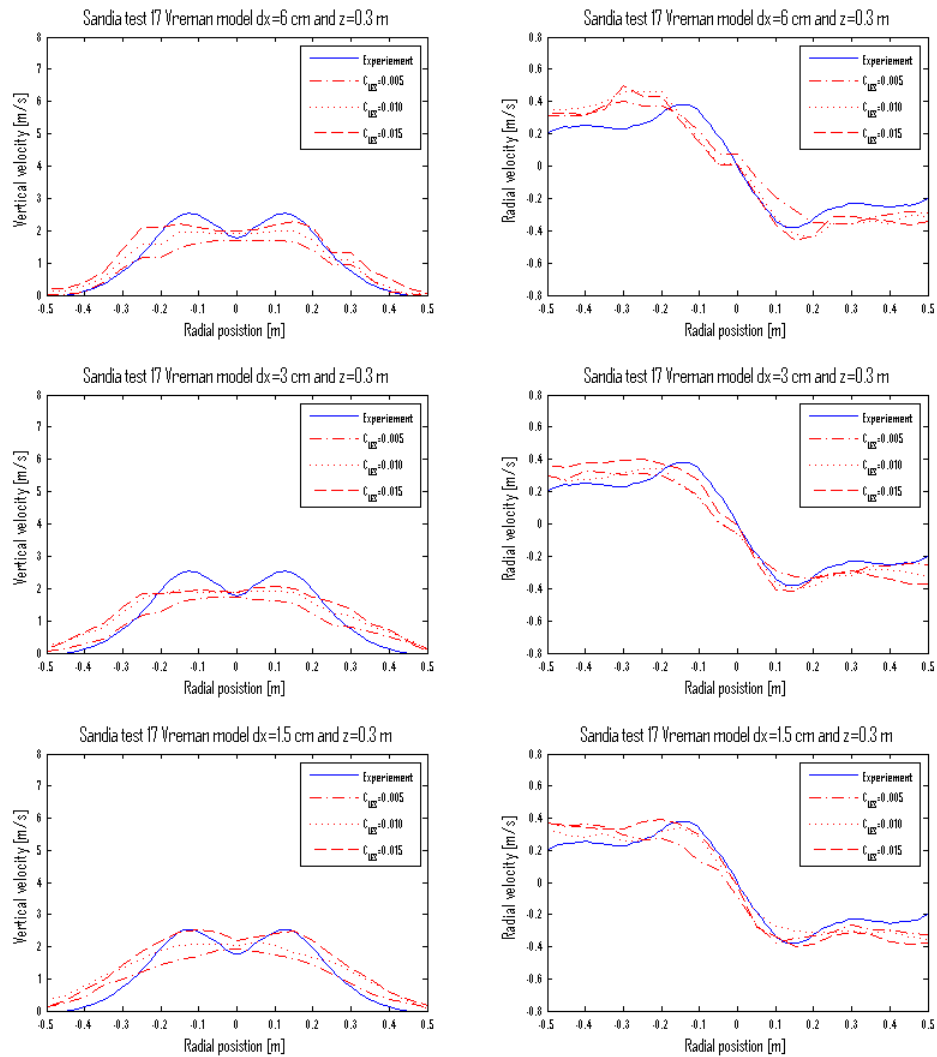


Figure 5.38: Sandia plume experiment test 17 with Vreman turbulence model at $z = 0.3$ m. Vertical velocity to the left and radial velocity to the right. On the top the coarse grid $dx = 6$ cm, $dx = 3$ cm in the middle and $dx = 1.5$ cm at the bottom.

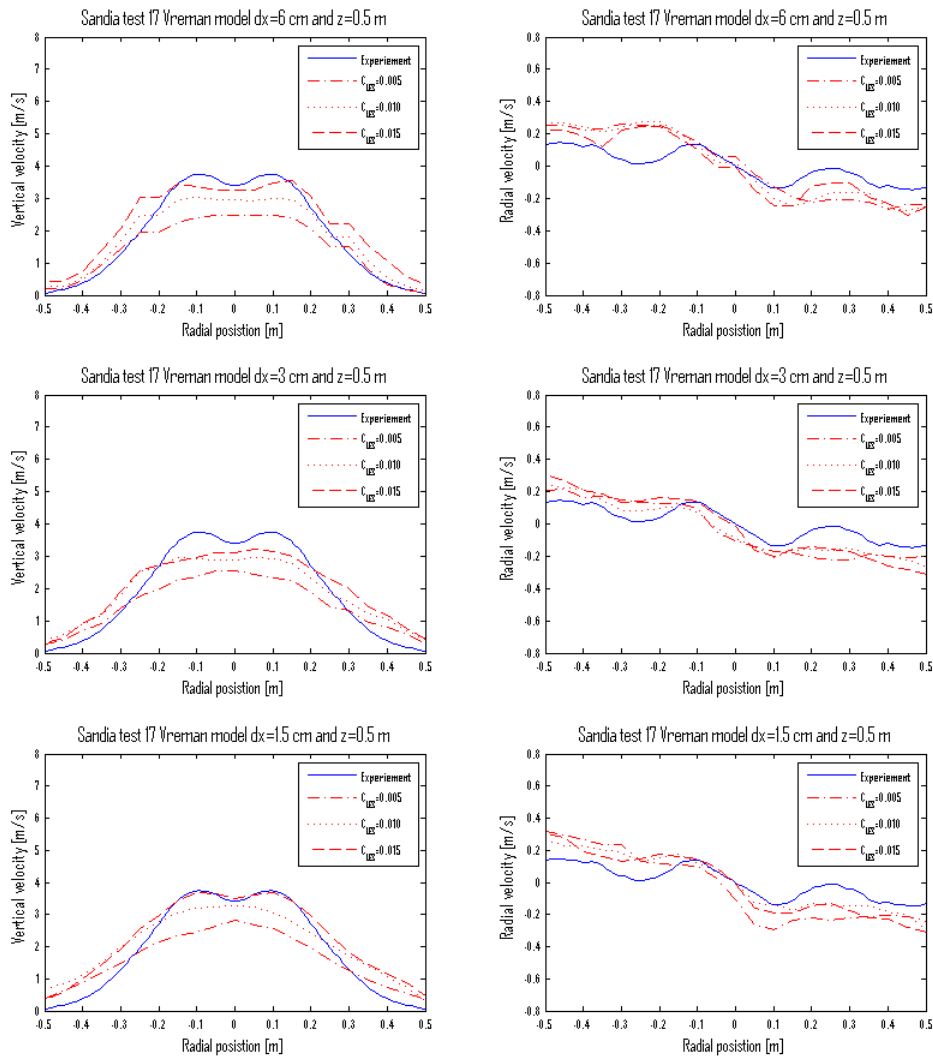


Figure 5.39: Sandia plume experiment test 17 with Vreman turbulence model at $z = 0.5$ m. Vertical velocity to the left and radial velocity to the right. On the top the coarse grid $dx = 6$ cm, $dx = 3$ cm in the middle and $dx = 1.5$ cm at the bottom.

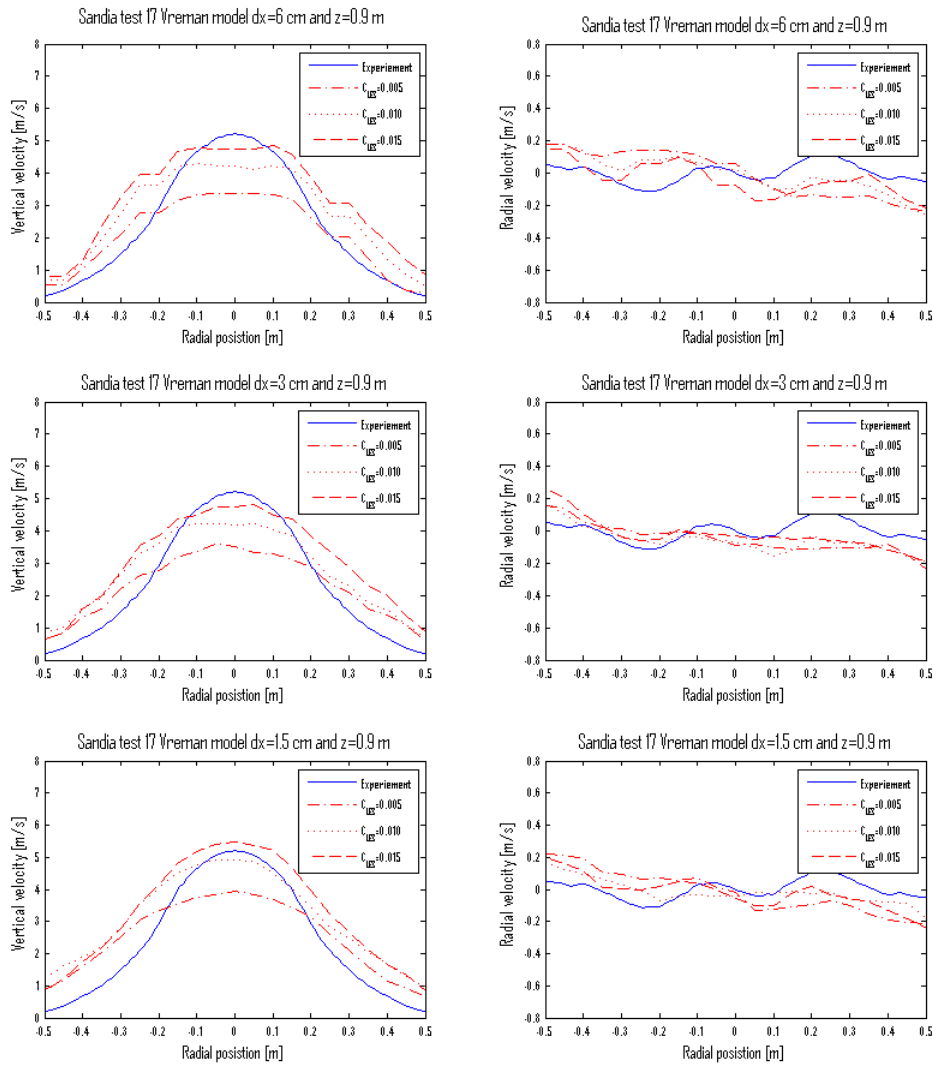


Figure 5.40: Sandia plume experiment test 17 with Vreman turbulence model at $z = 0.9$ m. Vertical velocity to the left and radial velocity to the right. On the top the coarse grid $dx = 6$ cm, $dx = 3$ cm in the middle and $dx = 1.5$ cm at the bottom.

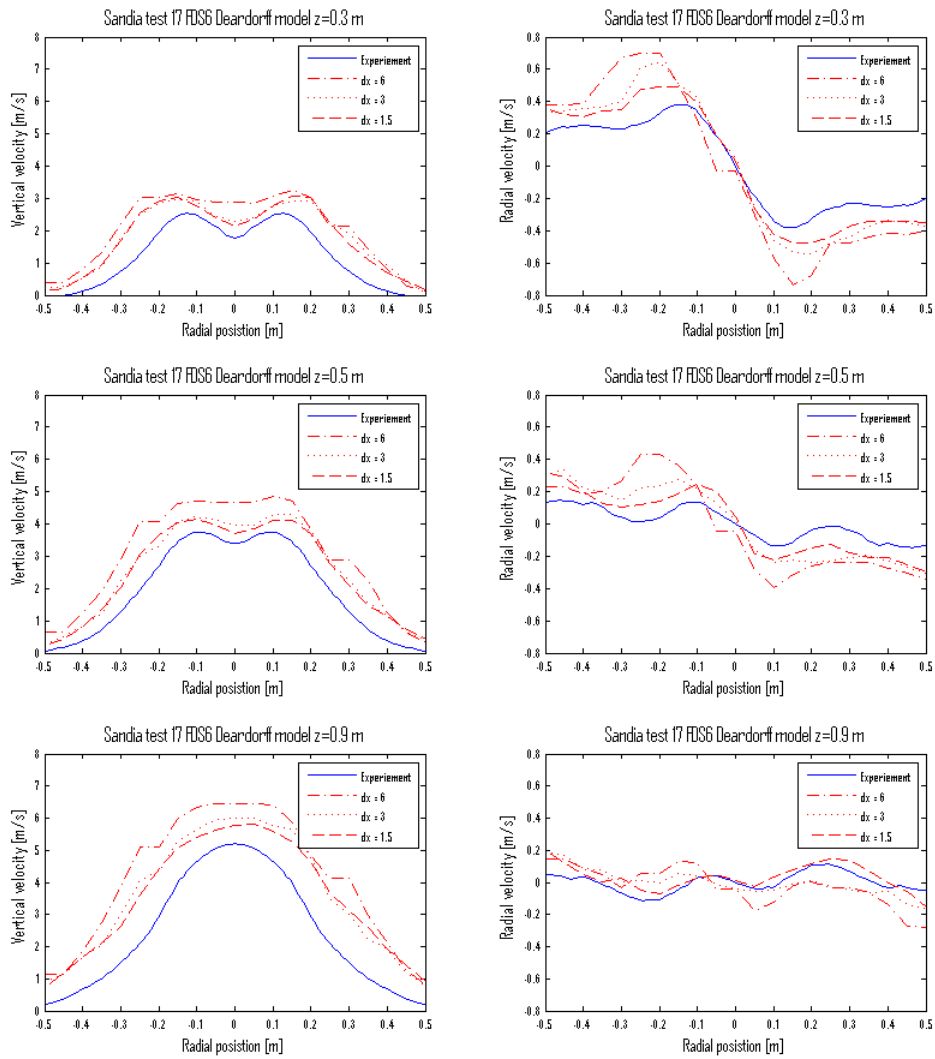


Figure 5.41: Sandia plume experiment test 17 with FDS6. Vertical velocity to the left and radial velocity to the right. On the top at $z = 0.3$ m, $z = 0.5$ m in the middle and $z = 0.9$ m at the bottom.

5.3.3 Methane Fire, Test 24

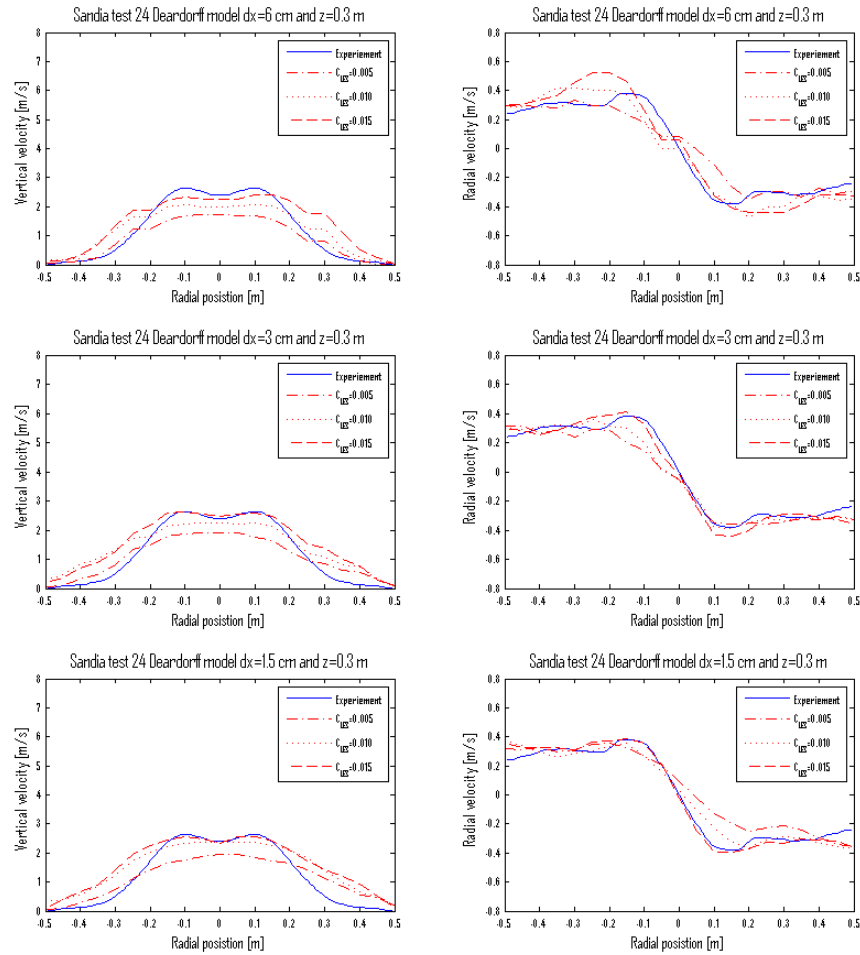


Figure 5.42: Sandia plume experiment test 24 with Deardorff turbulence model at $z = 0.3$ m. Vertical velocity to the left and radial velocity to the right. On the top the coarse grid $dx = 6$ cm, $dx = 3$ cm in the middle and $dx = 1.5$ cm at the bottom.

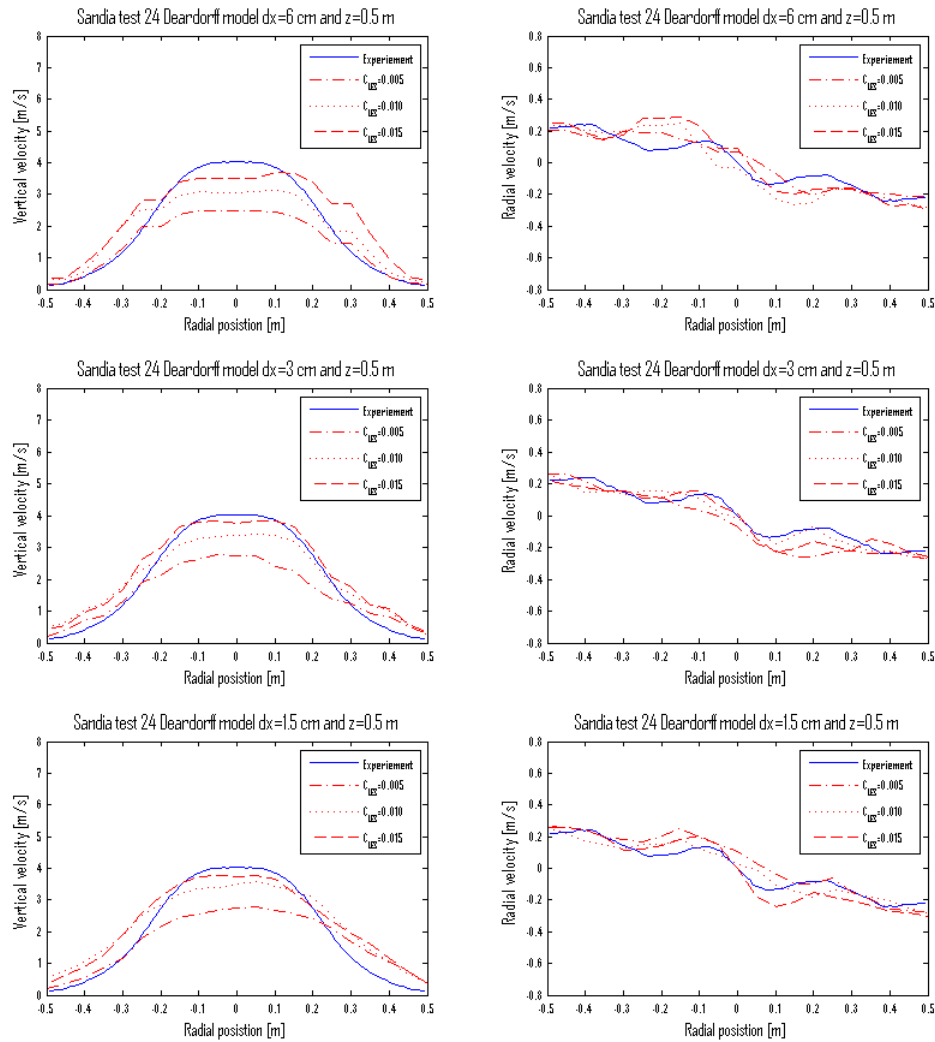


Figure 5.43: Sandia plume experiment test 24 with Deardorff turbulence model at $z = 0.5$ m. Vertical velocity to the left and radial velocity to the right. On the top the coarse grid $dx = 6$ cm, $dx = 3$ cm in the middle and $dx = 1.5$ cm at the bottom.

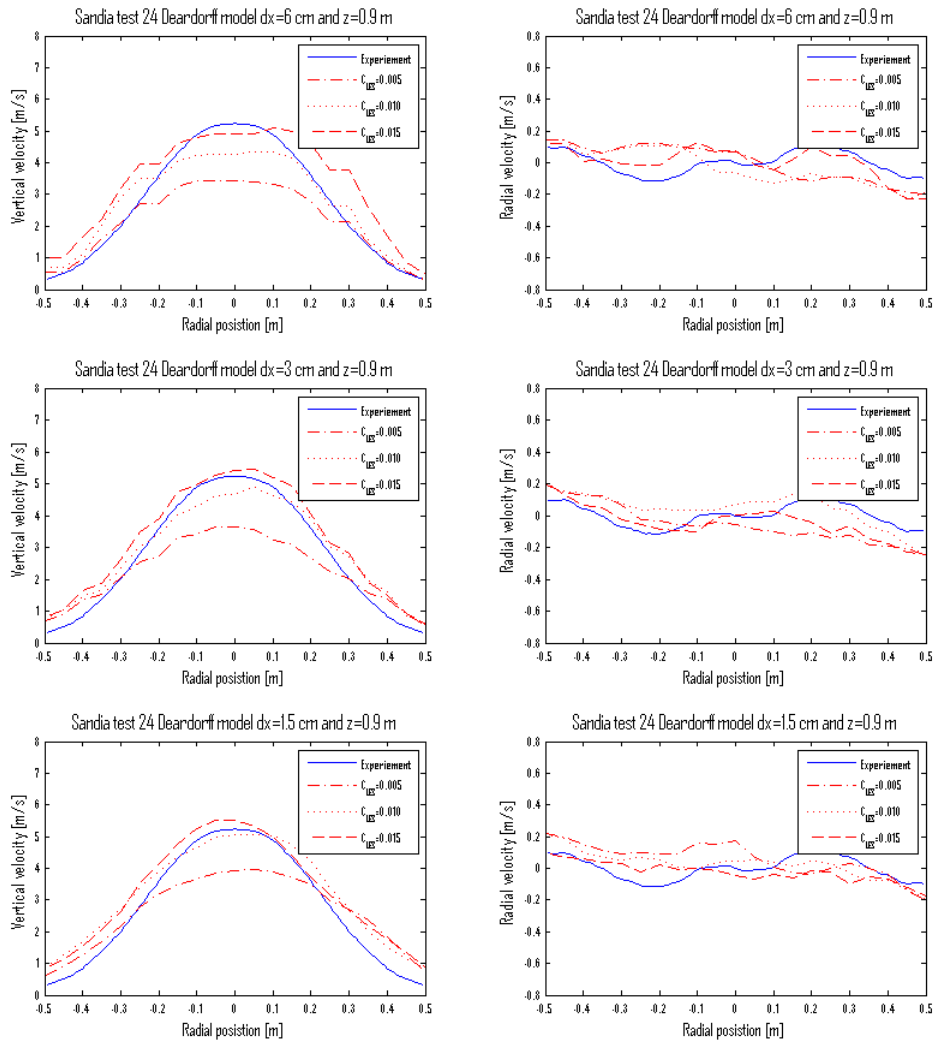


Figure 5.44: Sandia plume experiment test 24 with Deardorff turbulence model at $z = 0.9$ m. Vertical velocity to the left and radial velocity to the right. On the top the coarse grid $dx = 6$ cm, $dx = 3$ cm in the middle and $dx = 1.5$ cm at the bottom.

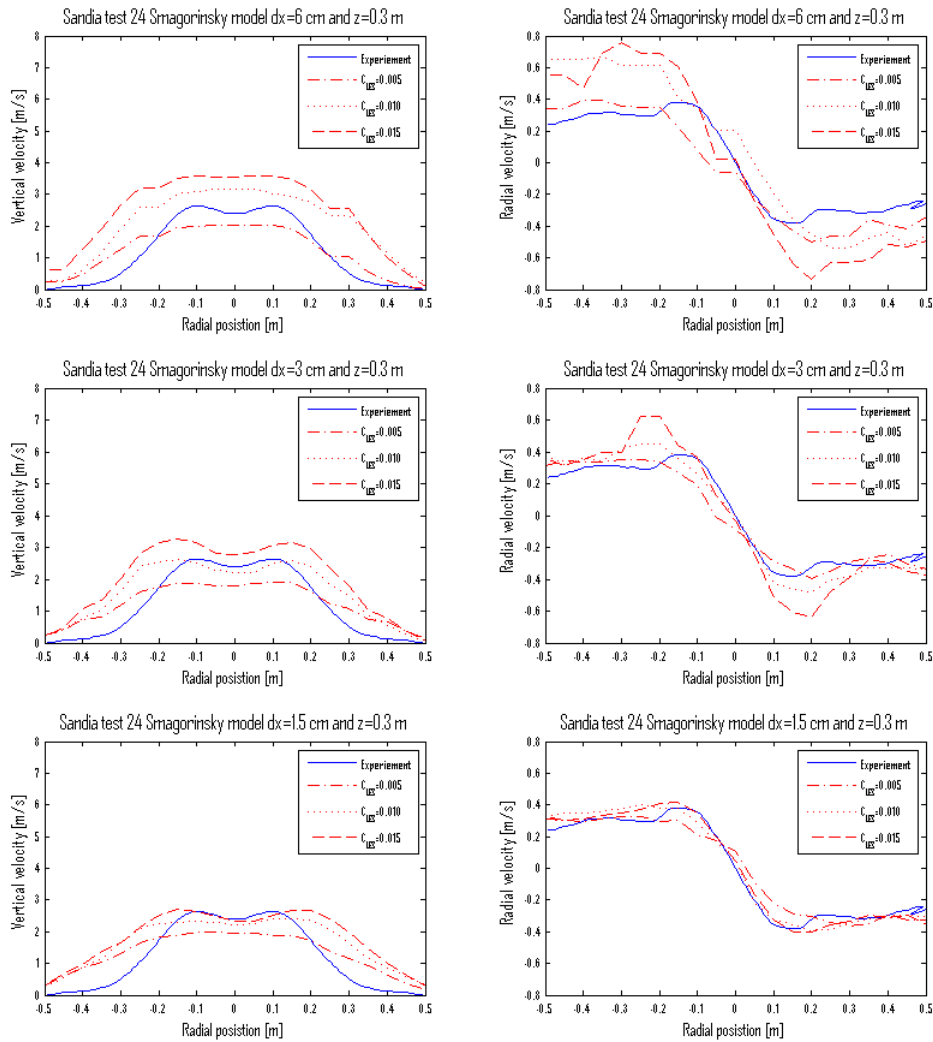


Figure 5.45: Sandia plume experiment test 24 with Smagosinsky turbulence model at $z = 0.3$ m. Vertical velocity to the left and radial velocity to the right. On the top the coarse grid $dx = 6$ cm, $dx = 3$ cm in the middle and $dx = 1.5$ cm at the bottom.

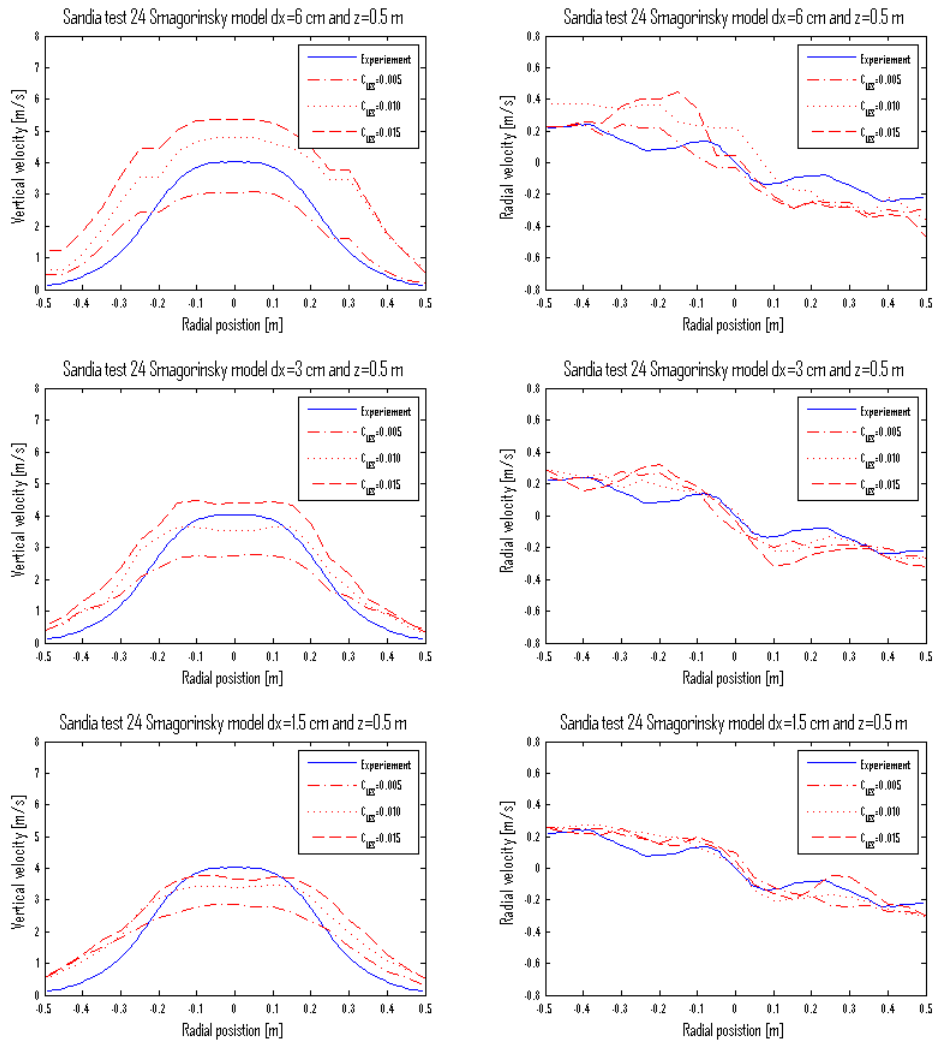


Figure 5.46: Sandia plume experiment test 24 with Smagosinsky turbulence model at $z = 0.5$ m. Vertical velocity to the left and radial velocity to the right. On the top the coarse grid $dx = 6$ cm, $dx = 3$ cm in the middle and $dx = 1.5$ cm at the bottom.

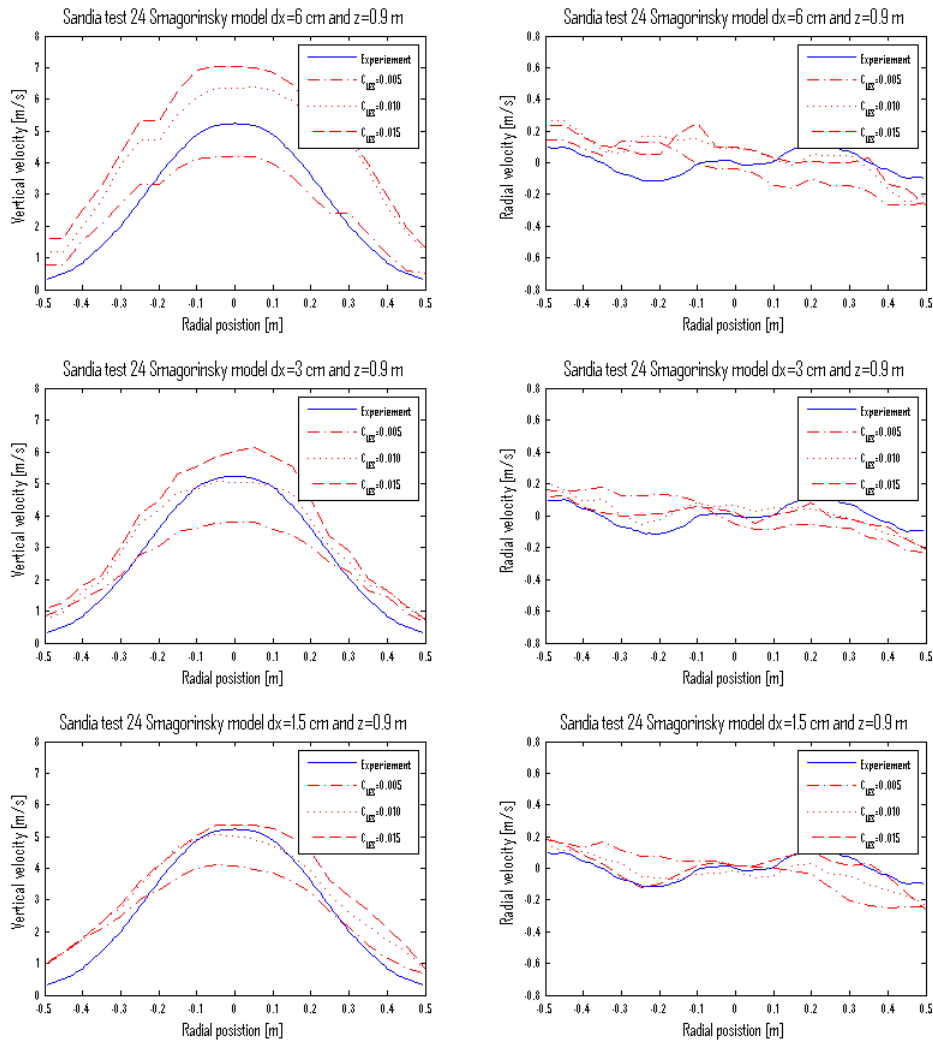


Figure 5.47: Sandia plume experiment test 24 with Smagosinsky turbulence model at $z = 0.9$ m. Vertical velocity to the left and radial velocity to the right. On the top the coarse grid $dx = 6$ cm, $dx = 3$ cm in the middle and $dx = 1.5$ cm at the bottom.

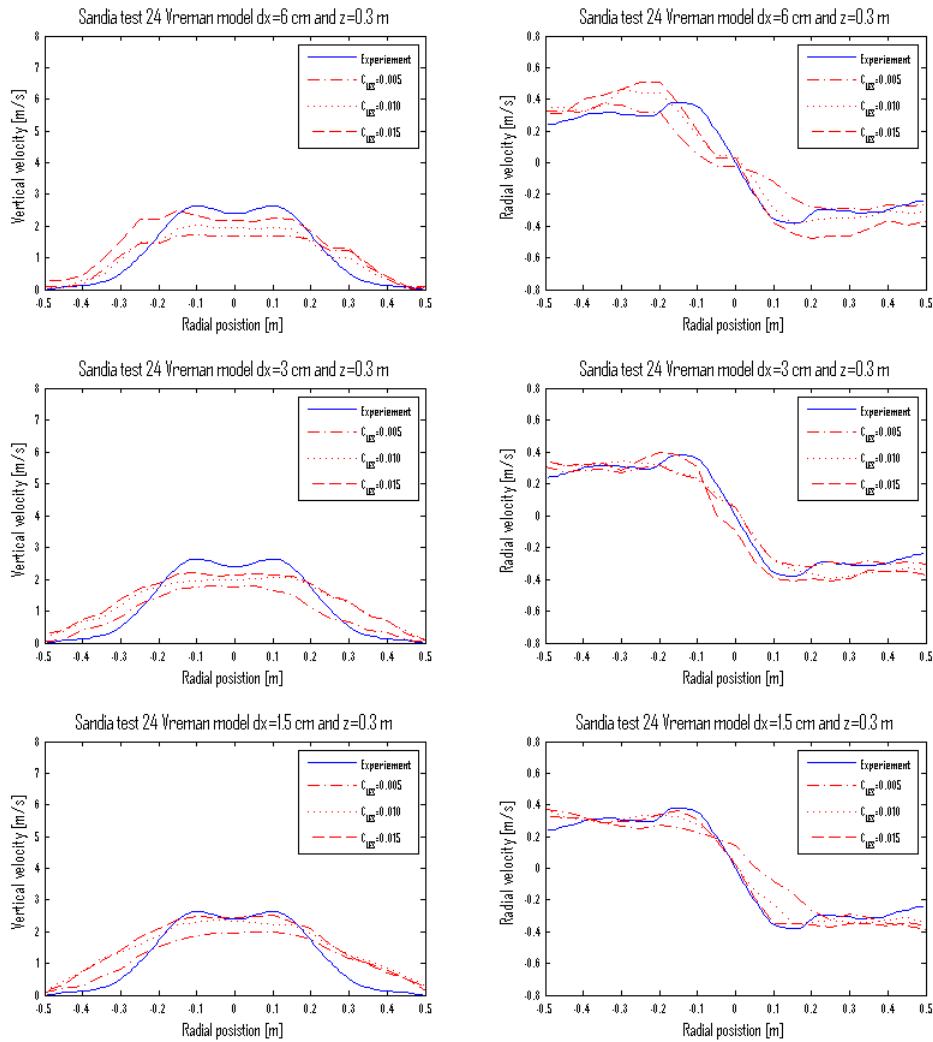


Figure 5.48: Sandia plume experiment test 24 with Vreman turbulence model at $z = 0.3$ m. Vertical velocity to the left and radial velocity to the right. On the top the coarse grid $dx = 6$ cm, $dx = 3$ cm in the middle and $dx = 1.5$ cm at the bottom.

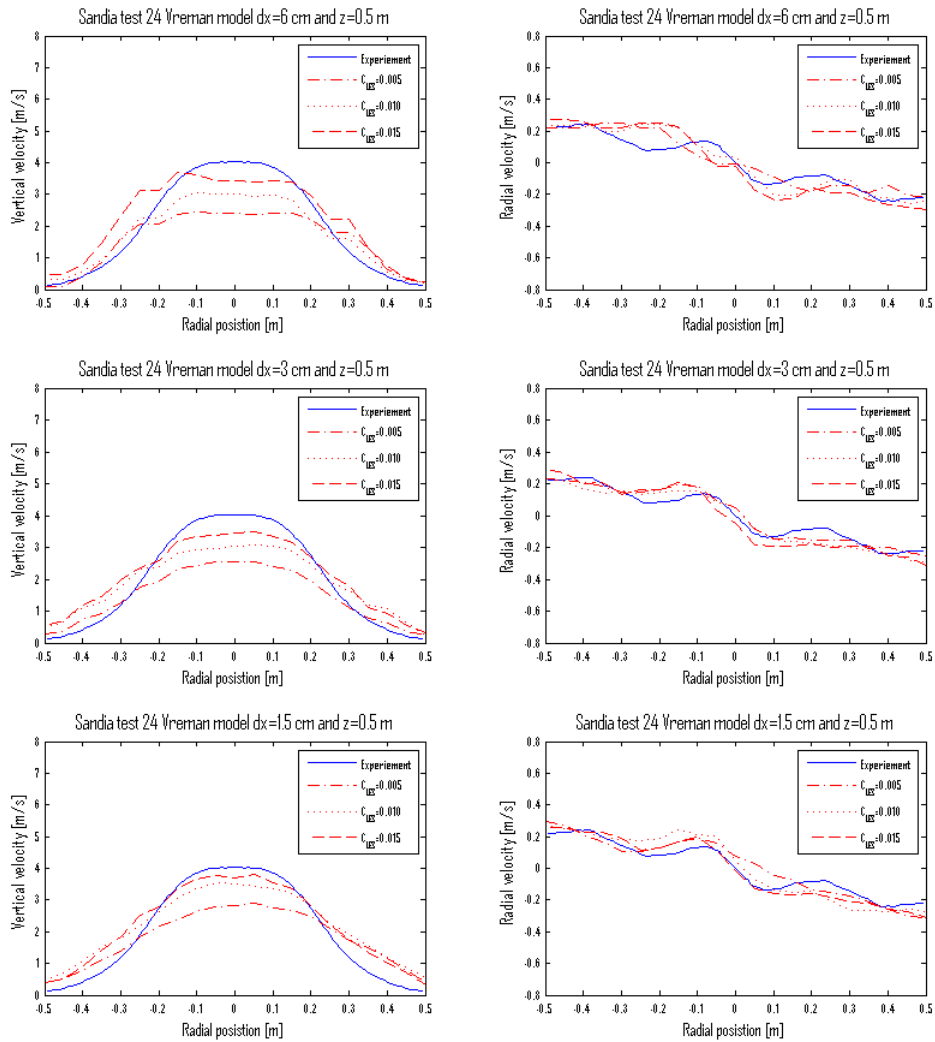


Figure 5.49: Sandia plume experiment test 24 with Vreman turbulence model at $z = 0.5$ m. Vertical velocity to the left and radial velocity to the right. On the top the coarse grid $dx = 6$ cm, $dx = 3$ cm in the middle and $dx = 1.5$ cm at the bottom.

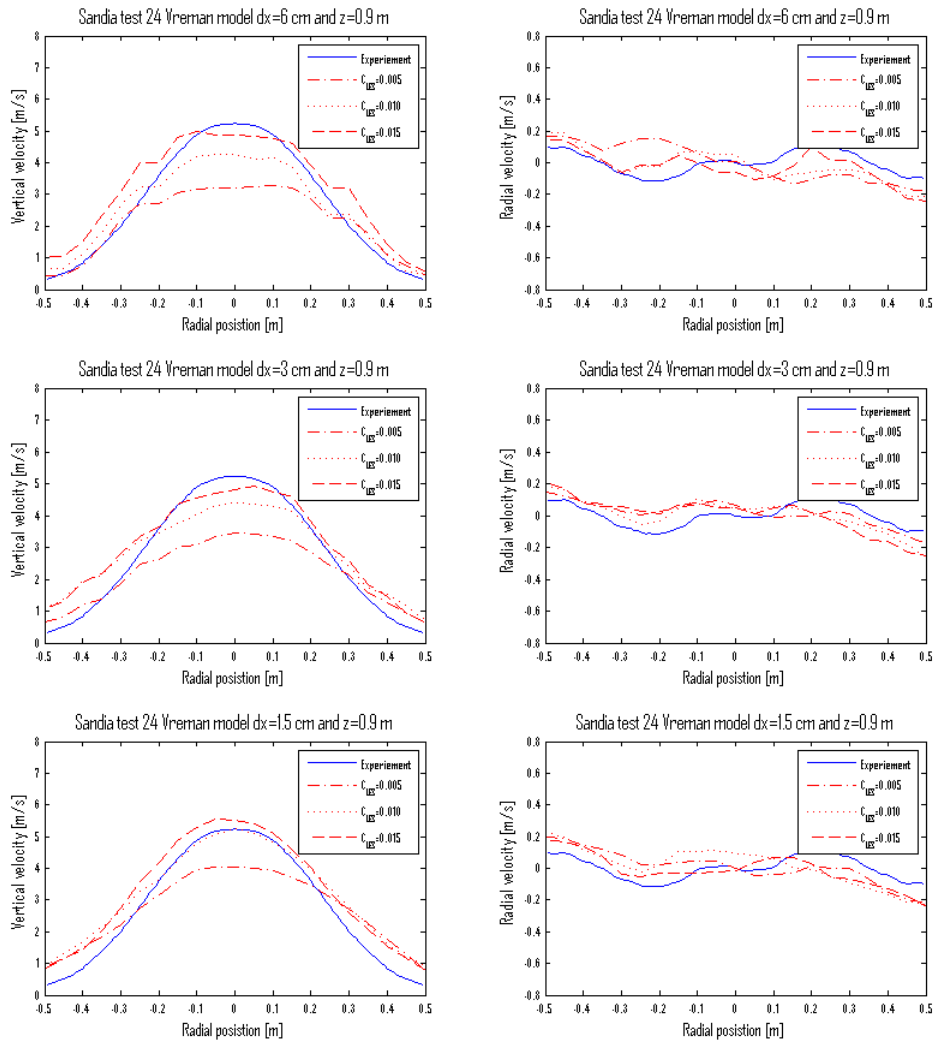


Figure 5.50: Sandia plume experiment test 24 with Vreman turbulence model at $z = 0.9$ m. Vertical velocity to the left and radial velocity to the right. On the top the coarse grid $dx = 6$ cm, $dx = 3$ cm in the middle and $dx = 1.5$ cm at the bottom.

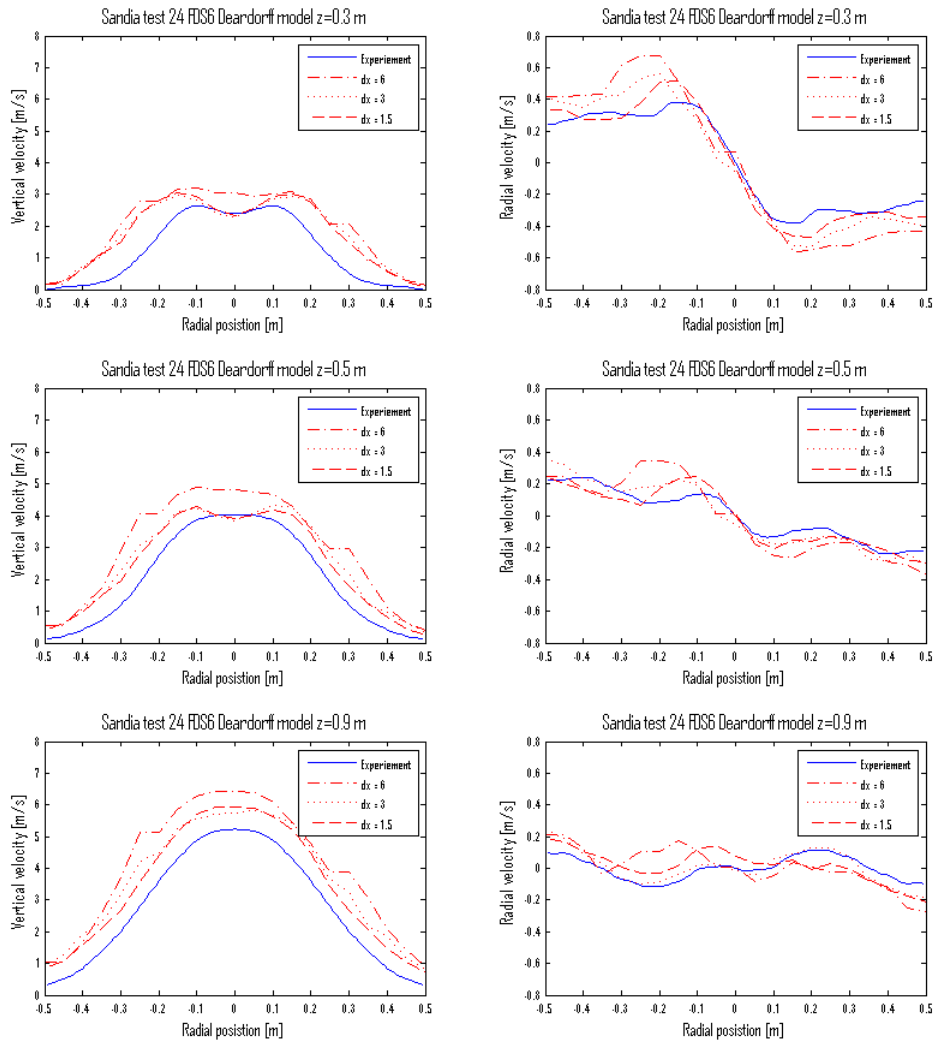


Figure 5.51: Sandia plume experiment test 24 with FDS6. Vertical velocity to the left and radial velocity to the right. On the top at $z = 0.3$ m, $z = 0.5$ m in the middle and $z = 0.9$ m at the bottom.

5.3.4 CPU clock time

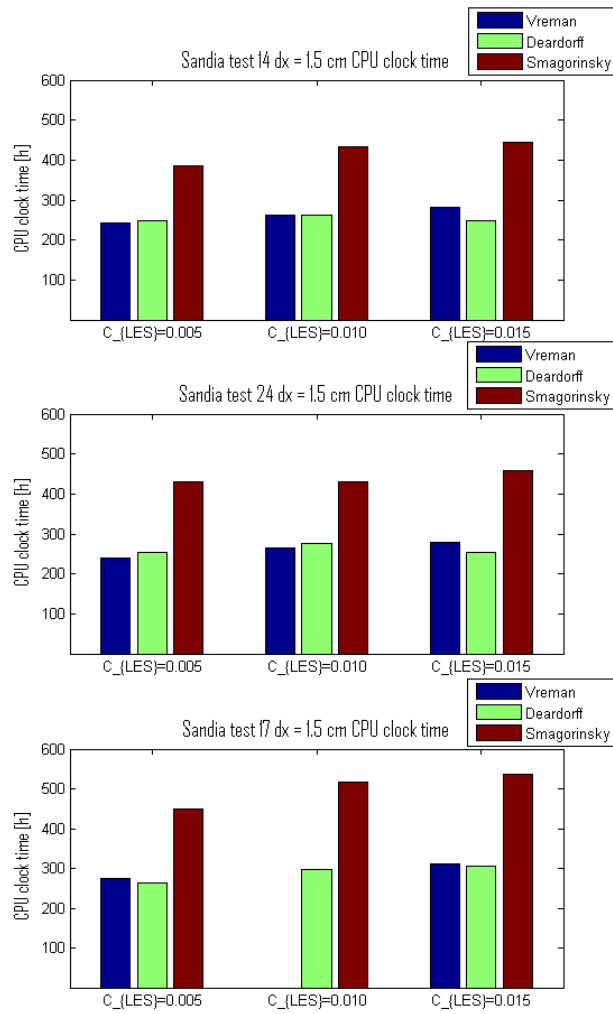


Figure 5.52: From top to bottom; CPU clock time for Sandia test 14, test 24 and test 17 with $dx = 1.5$ cm. Divided in groups of C_{LES} .

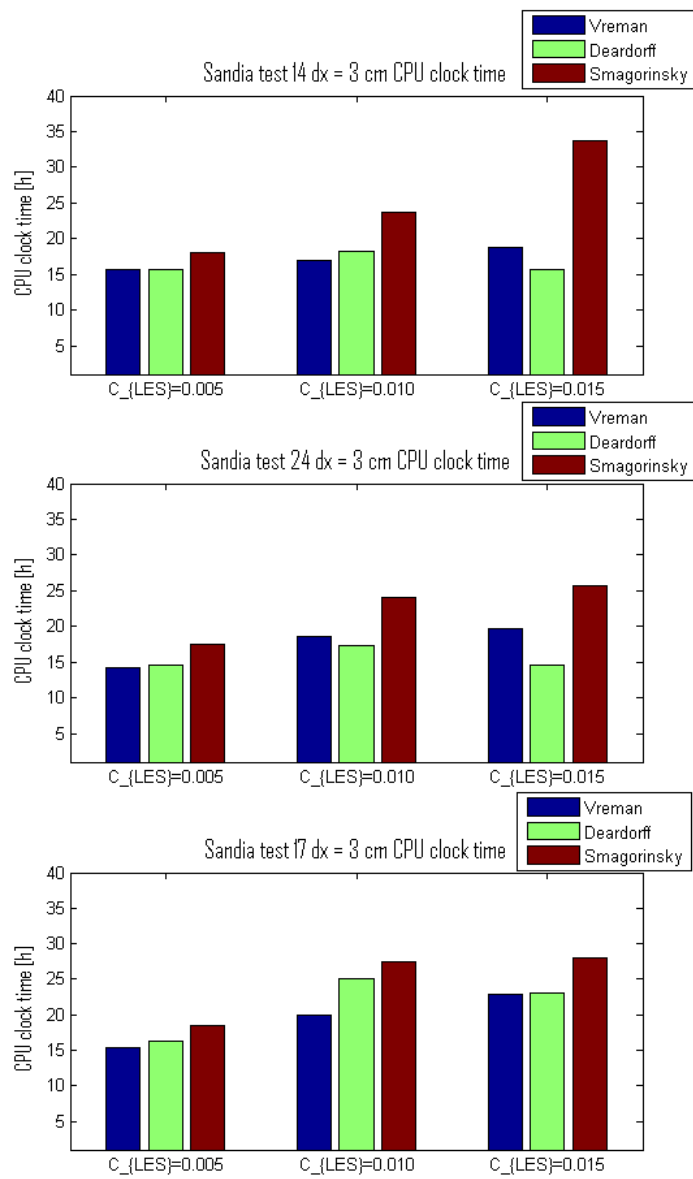


Figure 5.53: From top to bottom; CPU clock time for Sandia test 14, test 24 and test 17 with $dx = 3$ cm. Divided in groups of C_{LES} .

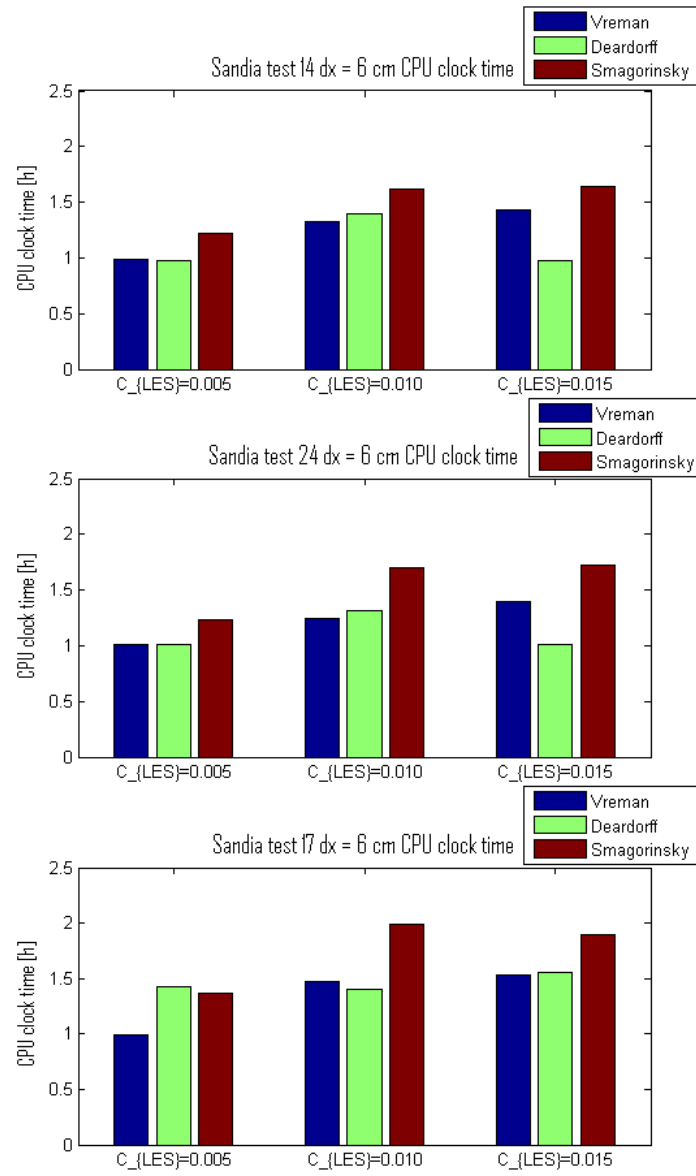


Figure 5.54: From top to bottom; CPU clock time for Sandia test 14, test 24 and test 17 with $dx = 6$ cm. Divided in groups of C_{LES} .

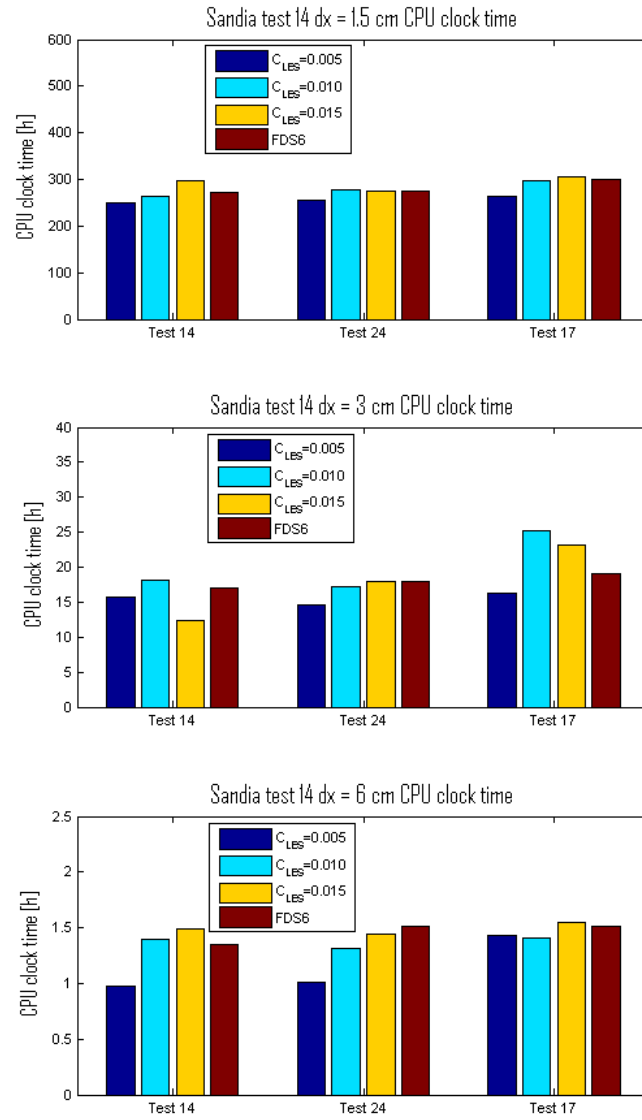


Figure 5.55: Comparison of CPU clock time between FDS6 and FDS-EDC for Sandia simulations. At the top $dx = 1.5$ cm, in the middle $dx = 3$ cm and $dx = 6$ cm at the bottom. Divided in groups of test 14, test 24 and test 17.

5.4 Discussion

5.4.1 McCaffery's Plume Correlation, Velocity and Temperature Profiles

In the McCaffery simulation the connection between centerline temperature and velocity are investigated when C_{LES} and grid resolutions are varied. With the fine grid the velocity profile is acceptably predicted with all turbulence models for all C_{LES} . The main difference is the peak value which is under estimated for $C_{LES} = 0.005$. However, the temperature is strongly under predicted just above the burner ($z < 1$) for $C_{LES} = 0.005$. The lower region right above the burner, approximately below 1 m where the velocity and temperature peak is located, is the most challenging area to model correctly. Particularly the peak temperature and its location. It is meaningless to quantify the error for the the temperature profile because of the steep slope. The error is large in this area, but the curves have the same shape and are just displaced. For all the turbulence models, the main difference in change of $C_{LES} = 0.01$ to $C_{LES} = 0.015$ is the maximum temperature.

Simulations with Deardorff turbulence model show that $C_{LES} = 0.005$ fits best for the velocity profile for 14 kW and 22 kW (5.1 and 5.2). As the HRR is increased $C_{LES} = 0.01$ and $C_{LES} = 0.015$ gives better results for the velocity even though the velocity peak is over estimated. With the finest grid, the temperature peaks are located too far away from the burner and becomes larger as the HRR is increased. This displacement is largest for $C_{LES} = 0.005$. For the other C_{LES} the error is about 50-70%. But for $C_{LES} = 0.015$ the peak value are strongly over predicted with up to 600°C (57 kW in Figure 5.5). Because of the over prediction, $C_{LES} = 0.01$ is the most correct constant for the Deardorff model in total.

The Smagorinsky turbulence model predicts the temperature profiles in McCaffery simulations better than Deardorff and Vreman. The temperature profile is in excellent agreement for $C_{LES} = 0.01$ with the finest grid. The under predictions of the velocity profiles are larger with the Smagorinsky model, particularly for the two highest HRR of 45 kW and 57 kW. However, the error in maximum temperatures for both $C_{LES} = 0.01$ and $C_{LES} = 0.015$ are not as over predicted as for the other models. The results for velocity is almost identical for the coarse grid when C_{LES} is changed.

The errors in maximum temperature for the Vreman turbulence model with $C_{LES} = 0.015$ are the smallest. With $C_{LES} = 0.01$ the errors are about the same as for the other models.

In Figures 5.16 and 5.17 the displacement of temperature peak value and the location for FDS6 may be seen. The maximum temperatures are not over estimated as much as for FDS-EDC with $C_{LES} = 0.015$ (Deardorff) for the three scenarios with largest HRR. The under estimation of velocity profiles is slightly larger for FDS6 than for FDS-EDC in contrast to the peak value, which more correctly predicted.

In Figure 5.56, Temperature and velocity contours for McCaffery 57 kW with Deardorff turbulence model is presented. This figure can be seen in connection with Figure 5.58 where the contour plot of HRRPUV is seen. Even though the fire size not equal the principle is the same. For the lowest $C_{LES} = 0.005$ the HRRPUV is under estimated

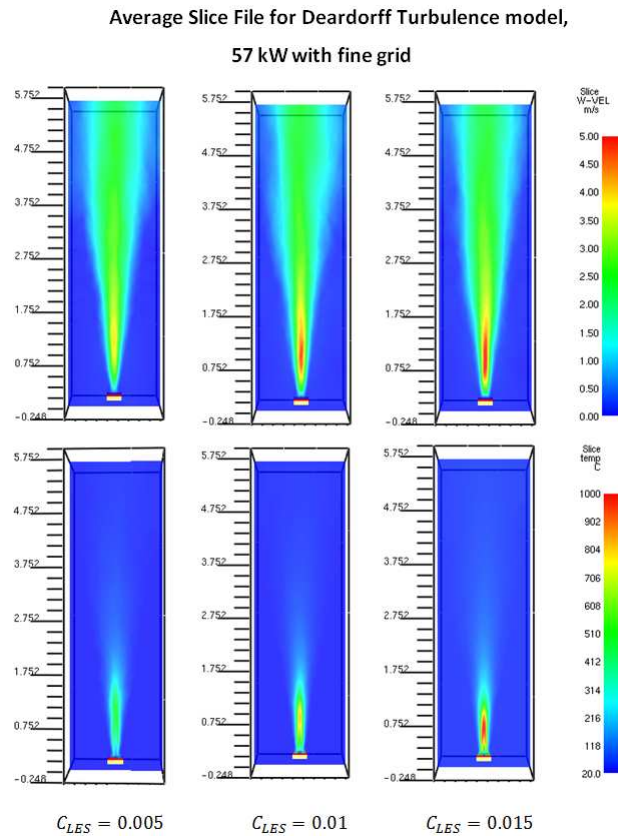


Figure 5.56: An example of temperature (bottom) and velocity (top) contour plot for McCaffery 57 kW with Deardorff turbulence model and the finest grid.

and smeared out over a longer travelled distance than the flame height. This leads to an under estimation of velocity and temperature. For the flame height $C_{LES} = 0.015$ is in best agreement with Heskestad correlation while the temperature and velocity profiles with $C_{LES} = 0.01$ is in best agreement with McCaffery correlation. I.e the same value of the constant do not necessarily has to fit for flame height, velocity and temperature profile, even for the same fire size.

5.4.2 Heskestad Flame Height Correlation

Figures 5.18-5.21 show that FDS-EDC for all turbulence models are strongly grid depended and are over predicting the flame height for coarse and medium grid resolution ($D^*/dx = 5$ and $D^*/dx = 10$). A constant can be established for all turbulence models to be in good agreement with the Heskestad correlation for large Q^* with the fine grid ($D^*/dx = 20$). Deardorff and Vreman turbulence model do not capture the slope for low Q^* as well as the Smagorinsky, especially not for the coarse grid. With the fine grid and

$C_{LES} = 0.015$, Vreman gives the worst results for $Q^* < 1$ with error ranging from -27% to 50% in contrast to Smagorinsky which captures the slope excellent. Except from the Smagorinsky model, the flame height is little influenced by the model constant for the coarse grid. However, the results are most sensitive to changes in C_{LES} for low Q^* .

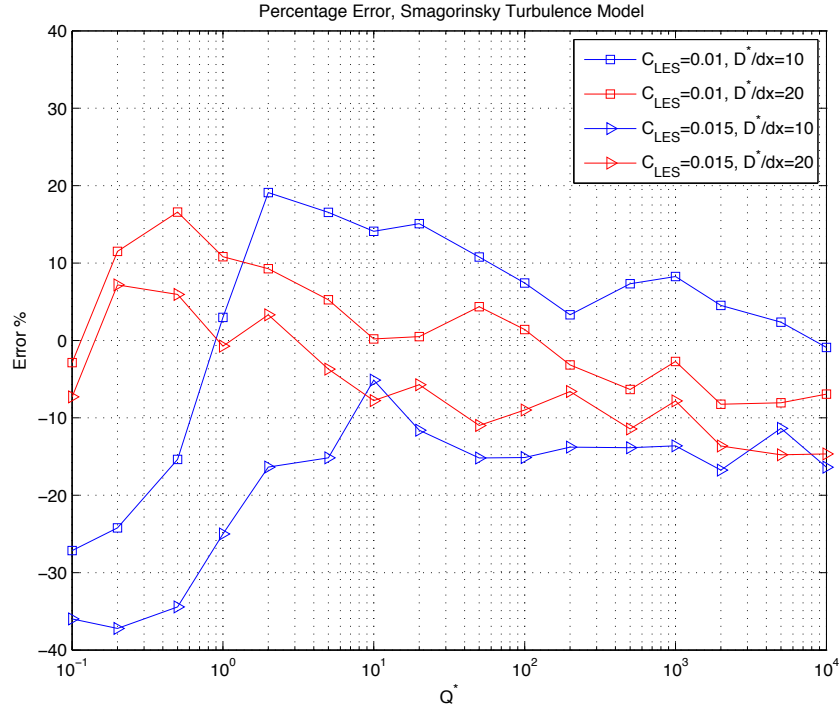


Figure 5.57: Comparison of percentages error in Heskestad flame height correlation with Smagorinsky turbulence model.

$C_{LES} = 0.015$ gives results in best agreement with the Heskestad flame height correlation for the Deardorff turbulence model (in Figure 5.18). With $D^*/dx = 20$ the maximum error is 27% for $Q^* < 1$ (except when $Q^* = 0.5$) else it is 12%, and for $D^*/dx = 10$ the maximum error is 25% in the whole range of Q^* .

It is more difficult to establish a constant for the Smagorinsky turbulence model with the fine grid in Figure 5.19. The Smagorinsky model is the model that is most sensitive to changes in the model constant with $D^*/dx = 5$ and $D^*/dx = 10$. By plotting the percentage error as in Figure 5.57, it can be seen that both $C_{LES} = 0.015$ and $C_{LES} = 0.01$ gives excellent results for $D^*/dx = 20$, even for low Q^* . With $C_{LES} = 0.015$ the absolute error is less than 14.7%. For medium grid resolution $D^*/dx = 10$, $C_{LES} = 0.01$ predicts the overall flame height slightly better than $C_{LES} = 0.015$, particularly for $2 > Q^*$. Both constants underestimate the flame height for the lowest Q^* with medium grid resolution.

With $C_{LES} = 0.015$ for the Vreman turbulence model (Figure 5.20), the flame height

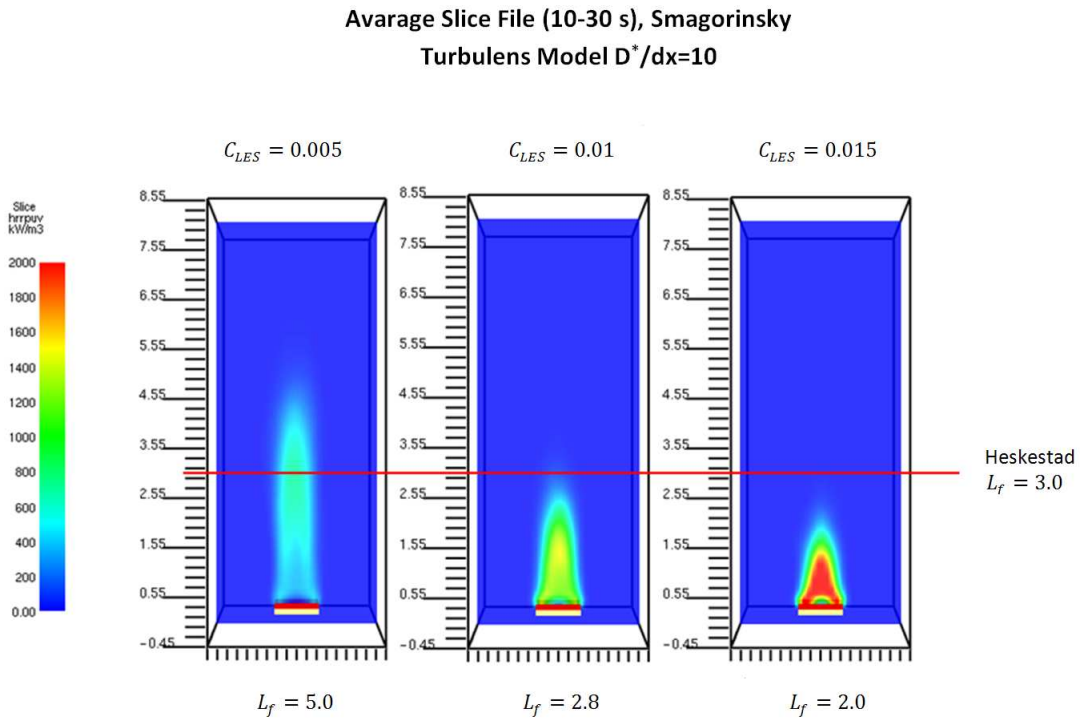


Figure 5.58: Slice file for heat release per unit volume (HRRPUV) versus flame height averaged from 10-30 seconds for Smagorinsky turbulence model, $D^*/dx = 10$.

deviates by -27% to +50% in the range $0.1 \leq Q^* \leq 2$ and up to 10% for $2 < Q^*$ with $D^*/dx = 20$. For the coarse grid, the flame height is over predicted by about 40%.

In Figure 5.21 FDS6 and FDS-EDC are compared with Heskestad flame height correlation for the Deardorff turbulence model. Surprisingly, FDS6 has also difficulties to capture the slope correctly in the interval $0.1 \geq Q^* \geq 1$. FDS6 is over predicting the flame height as FDS-EDC in this interval. In contrast to FDS-EDC, FDS6 is not as grid depended and gives satisfactory results for all grid resolutions. The explanation to this is that the mixing times are functions of the grid cell size, seen in eq. (3.4). The LES-EDC model could simply be made grid independent by establishing a dynamic model constant, C_{LES} , as a function of the grid cell size. For FDS6 the absolute error is less than 13.7% with $D^*/dx = 20$ if $2 < Q^*$, else it is up to 46%.

Actually, the absolute error is less for the coarser grids for low Q^* . With $D^*/dx = 10$ the 10.3% and 12.9% with $D^*/dx = 5$ except from $Q^* = 0.1$ (63% error).

Figure 5.58 is an example on how C_{LES} affects the flame height. Since the flame height is assumed to be where 99 % of fuel is consumed on average, a slice of heat release per unit volume (HRRPUV) is a good way to illustrate how C_{LES} affects the physics. When C_{LES} is increased, the local HRR also increase (right side of Figure 5.58). In case of under prediction of HRRPUV (small C_{LES}) too little fuel is consumed in the lower

flame region and allows more fuel to raise due to buoyancy forces. As a result, the fuel moves a longer distance before it is consumed, hence flame length is over estimated (left side of Figure 5.58).

5.4.3 Sandia Plume

It is obvious from the results that a time average of 10 seconds is too short. Since the boundary conditions are symmetric it is reasonable to expect symmetric behavior around the centerline of the flame. The consequence of too short time average may be seen in test 14 with the Smagorinsky turbulence model for the coarse grid in the lowest positions $z = 0.3$ m and $z = 0.5$ m (Figures 5.25 and 5.26) where the vertical peak velocity is displaced away from the center in radial position. This misplacement is generally not observed in such extent for simulations with finer grid. Radial velocities are also influenced by the too short time average period because the velocities in few cases are zero along the centerline.

The results show that the trend is the same for all the turbulence models. Not surprisingly, the velocity profiles are more difficult to model correctly as the position increase away from the fuel source. This can especially be seen for the lowest HRR in test 14 in $z = 0.9$ m, Figures 5.24, 5.27 and 5.30. It is difficult to establish a single C_{LES} that fits all the cases in all positions. The vertical velocity is overestimated in the edges of radial position in all heights even for the lowest C_{LES} of 0.005. However, an error of the vertical velocities in the edges or the radial velocity (in high z position) is not that crucial for the flame behavior. The reason is that in these places the velocities are low, and even though the percentage error is large the contribution to the over all upward mass rate in the flame is low. Actually, the velocity profiles should be considered in connection with densities to ensure correct upward mass transport. Experimental results could maybe reveal that the velocity is overestimated in place where the density is underestimated (i.e that underestimation of density compensate for overestimation of velocity) so that the mass transport is correctly modeled.

Deviation of the vertical velocity between the C_{LES} is largest in simulations with the coarse grid. The deviations are larger as the z -position increase. Velocities are over predicted with Smagorsinky turbulence model and FDS6 cases with the coarse grid which is in agreement with theory in Section 3.1 (over prediction of HRR if the grid is too coarse).

The radial velocity seems to be more difficult to model correctly than the vertical velocity. In Figures 5.25, 5.35 and 5.45 the radial velocity for the Smagorinsky turbulence model in $z = 0.3$ m appears almost to be random with the coarse grid. All over, Smagorinsky is the most grid dependent turbulence model. The error in the edges for the vertical velocities are slightly larger with Smagorsinsky compared with the other two turbulence models. In general, this error is less at the edges for all the models in $z = 0.5$ m and $z = 0.9$ m where the slope is steeper. In contrast to Vreman and Deardorff turbulence models, simulations with Smagorinsky and FDS6 are capturing the dip in the fuel rich area along the centerline of the flame in test 17. But for some reason the vertical velocity for all simulations, even for FDS6 (with the original combustion model),

Smokeview 5.6 - Oct 29 2010

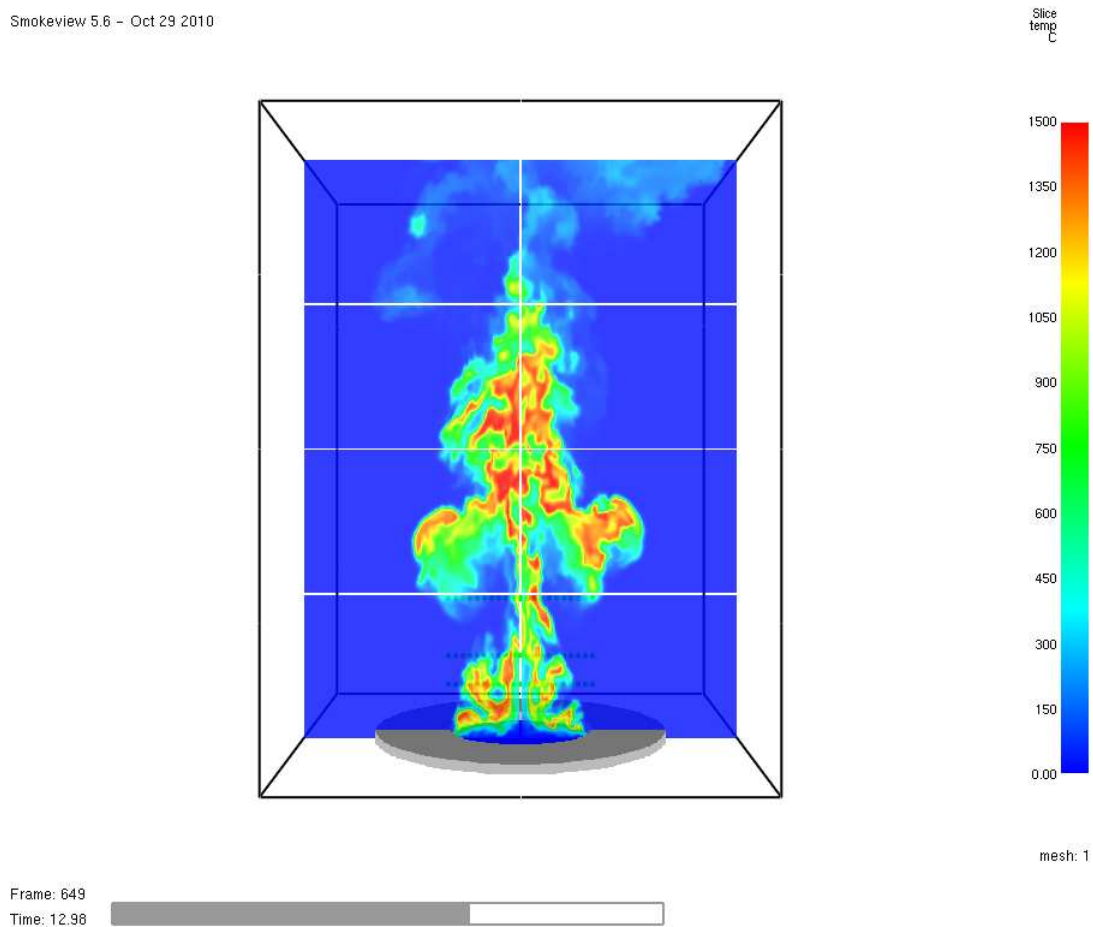


Figure 5.59: An example of temperature contours for FDS6 test 14 with $dx = 1.5$ cm at 13 second. Be aware that the screenshot represents instantaneous values and is not representative for the whole simulation time. The green dots is measuring points in heights of 0.3 m, 0.5 m and 0.9 m.

are remarkably over predicted 0.5 m and 0.9 m above the burner in test 14.

If FDS6 is used as acceptance criteria, all turbulence models for FDS-EDC with $C_{LES} = 0.015$ predicts the vertical velocity as well as FDS6 or even better with the finest grid. However, FDS6 is not as grid dependent as FDS-EDC. Other C_{LES} than 0.015 fits better in some cases with grids corresponds to $dx = 3$ cm and $dx = 6$ cm. But a constant should be establish for a fine grid ($dx = 1.5$ cm) and then in further work be modified to be grid independent. The deviation between $C_{LES} = 0.01$ and $C_{LES} = 0.015$ in the vertical velocity at $z = 0.3$ m is minimal in test 17 and 24 with all turbulence models. With $C_{LES} = 0.015$ the absolute maximum error of vertical velocities are approximately 15-20% while the radial velocity errors are some places up several hundred percent around the center .

Almost the same amount of code lines are added to the code as the amount of code lines which is commented out. Furthermore, one IF loop is commented out and one is added. If two similar cases is simulated with FDS6 and FDS-EDC contains the same amount of burning cells, then they should use the same CPU clock time in theory. Figure 5.55 confirms that this is almost correct. No systematic connection cannot be drawn whether CPU clock time for FDS6 simulations are larger than for FDS-EDC or the other way around. However, HRR release is related to the simulation time in most cases (see Table 5.2). Hence, test 17 takes longer time to simulate than test 24 and test 24 takes longer time to simulate than test 14. Figures 5.52 - 5.54 show that the Smagorinsky turbulence model is the most computational expensive. This is simply because the constant in the Smagorinsky model used in this thesis is dynamic and not static as for Deardorff and Vreman. The difference is much larger in percent if the grid is refined or the HRR increased. With the fine grid the difference is about 60%. Vreman and Deardorff turbulence models are roughly the same computational expensive.

Chapter 6

Flow Field Above Obstacle Inserted in Fire Plume

These experiments are inspired by experiments done by Lars Roar Skarsbøin a master's thesis delivered June 2011 at the University of Bergen [35]. Some improvements are done to make it closer to how it is modeled. In these experiments, square pipes are used instead of circular. The first reason is to generate more turbulence. Secondly, because a rectangular grid is used in simulations. Since only the combustion model is evaluated in this thesis and not the evaporation/pyrolysis and thermal radiation, liquid is replaced with gas to control the HRR. The burner size is decreased to be able to increase the flow velocity and also the degree of turbulence at lower HRR with less fuel.

The motivation for these experiments is to study the flow field above turbulence generating obstacles inserted in a fire. By systematically increase the HRR and height of the obstacles, a simple correlation between a turbulence property (TKE, turbulence intensity, velocity fluctuations, strain rate, etc.) and a dynamic constant C_{LES} may perhaps be established. It is also reasonable to believe that in such turbulent regime is where the largest difference between the sophisticated LES-EDC model and the already existing combustion model in FDS.

To finance the experiments, this study was linked up to the research program *Prediction and validation of pool fire developed in enclosures by means of CFD models for risk assessment of nuclear power plants*. During the planning, it turned out to be quite hard to find an institution that had the correct equipment and knowledge to operate Particle Image Velocimetry (PIV) to measure a velocity vector field. After some heavy delay, the experiments were performed at Lund University. Unfortunately, the outcome was no successful results. Hence, this study must be regarded as a pre-project for PIV measurements in the pool fire research programme and not a part of the validation of the combustion model.

6.1 Designing Experiments for CFD Validation

The philosophy of CFD model validation in matter of fire modeling may be separated in whether the fire is *specified* or *predicted* [32]. The choice is depended on the goal of validation. In this thesis the goal is to validate the combustion model, other models as evaporation, pyrolysis, soot, etc. is not of interest. Therefore, the fire should be *specified* rather than *predicted*. The road map for a CFD model in Figure 6.1 shows that the combustion is depended on other sub models in fire modeling. Sub models are only *models* consisting empirical correlations only valid in certain interval of physical values, and not necessarily physical formulas solving the actual physical problem. By specifying the fire the HRR is not influenced by quantities as radiation. Possible errors in sub models controlling the HRR are then eliminated. So in cases when single sub models are validated, it is preferable to involve a minimum of other sub models.

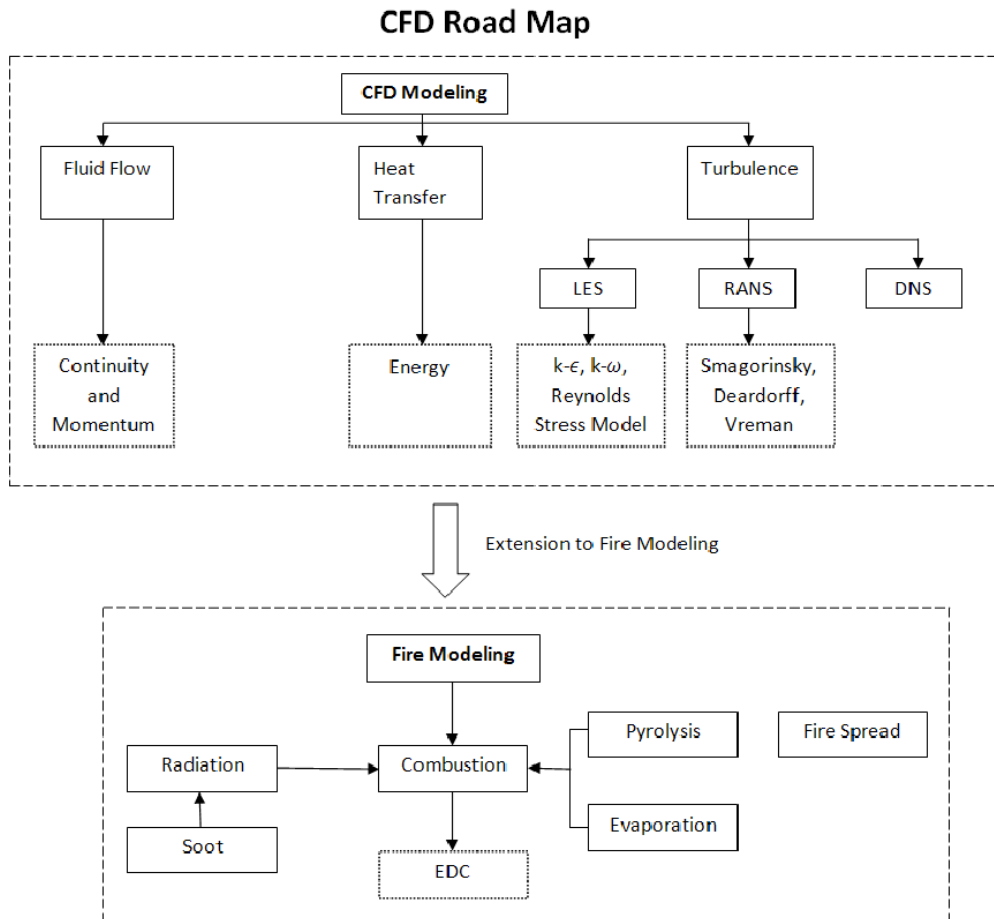


Figure 6.1: CFD road map; extension of CFD to fire modeling and overview of sub models.

In validations of CFD models, the experiments must be as close to the simulated scenario as possible. The HRR in the experiments must be controlled to be able to specify it in the input of simulations. A constant gas fire is therefore a good choice for validation of the combustion model. The HRR is then not influenced by the radiation which would be the case if a liquid fuel fire or a solid fuel fire is chosen. If a liquid fuel fire or a solid fuel fire is chosen, an error in the radiation modeling would influence the rate of pyrolysis or evaporation which further would lead to overestimation or underestimation of HRR.

Since uniform rectangular grid cells are applied in FDS, the geometrical shapes in the experimental set up should also be rectangular. So in these experiments, circular pipes used in Skarsbøs thesis were replaced with rectangular pipes. Additionally, geometrical dimensions smaller than the grid cell size should be avoided. However, most commercial CFD codes supports this by setting a porosity parameter in all faces of the grid cell.

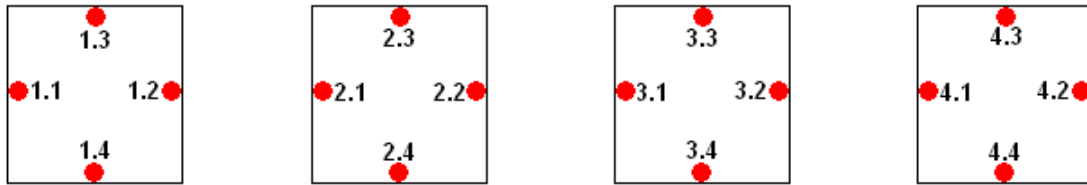


Figure 6.2: Numbering of thermal couples in the pipes.

Insertion of obstacles in flames leads to heat loss in the flame and affects the temperature, velocity, reaction rate, etc. Input in the simulations does not require inner temperature of the pipes, but it is an advantage to specify the temperature rather than predict it to eliminate a possible error in the heat transfer calculation. Therefore, 16 thermocouples were mounted in the pipes with improvised v-shaped wedges to find the steady state temperature. The placements of the thermocouples and numbering are seen in Figure 6.2.

6.2 Measurement Techniques

6.2.1 Particle Image Velocimetry (PIV)

Particle Image Velocimetry (PIV) is a sophisticated measuring technique for measurements of instantaneous velocity vectors in cross-section of a fluid flow. Wind tunnel velocity experiments, experimental verification of CFD models, measurements in pipe flows, spray and combustion research are examples of application areas of PIV [37]. Normally, low-mass particles are seeded in the flow, which is assumed to move free with the local flow velocity [36]. Two short time laser pulses illuminate a plane in the flow. Light is scattered by the seeded particles and are recorded by a synchronized camera. Through the post-processing, the two images are subdivided in *interrogation areas* and

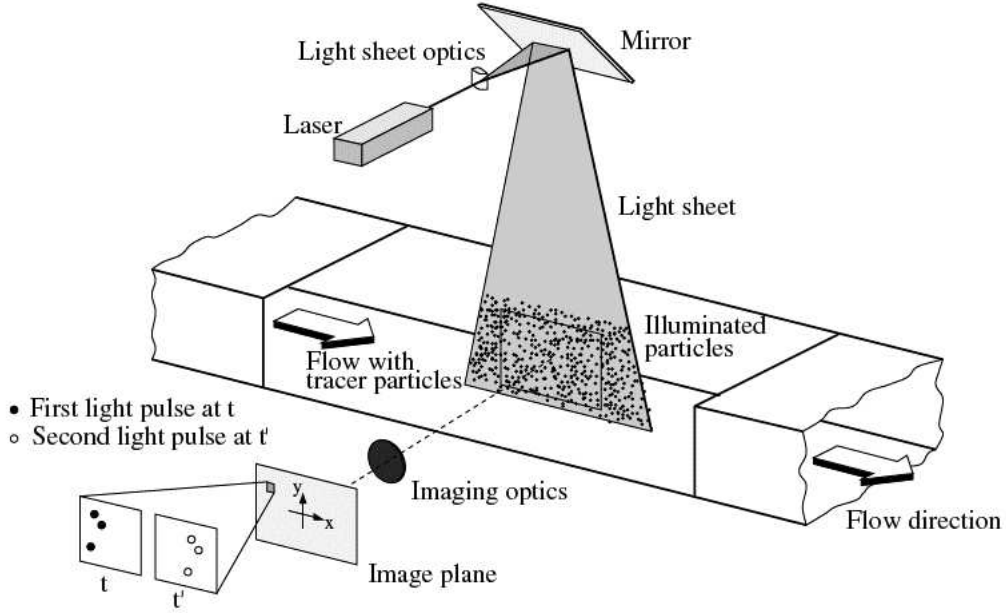


Figure 6.3: The principle of Particle Image Velocimetry (PIV) measuring technique [36].

the velocity vector is found from the movements of the particles. In order to obtain good signals, 10-25 particles should be recorded in each interrogation area [37].

6.2.2 Thermocouples

A thermocouple is a device for temperature measurements. Thermocouples can operate in a broad range of temperature and are inexpensive, durable and easy to apply. Two different conductors are coupled to a voltage logger, see Figure 6.4. The voltage produced by the conductors are proportional to the temperature. Temperature at the cold junction must be known and preferably kept constant to calculate the temperature at the hot junction. The temperature difference is given by

$$\Delta T = \sum_{n=0}^N a_n v^n \quad (6.1)$$

where v is the output voltage and a_n the a coefficient depending upon the metal. In some cases the temperature is found from a database. Databases are usually implemented in modern logging softwares on computers.

In the experiments in this thesis, thermocouples type K was used. For type K metal 1 is chromel (90 % nickel and 10 %chromium) and metal 2 amuel (95 % nickel, 2 % manganese, 2% aluminum and 1 % silicon). Thermocouples type K measures in the range -200 °C to 1350 °C.

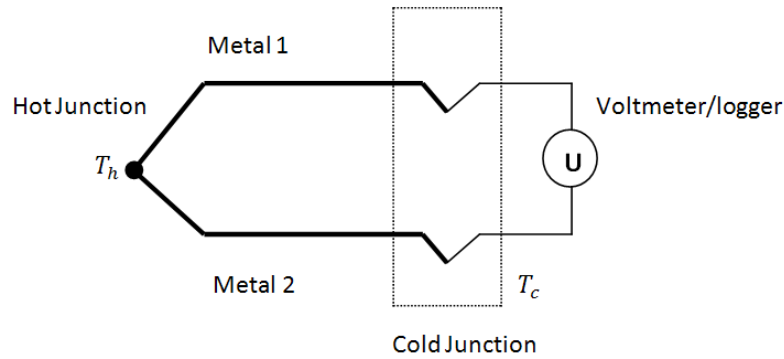


Figure 6.4: Thermocouple measurement circuit.

6.3 Experiments

Many possible scenarios were simulated before the experiments. The goal was to find an optimal set up with respect to fire size, HRR, cross-section pipe dimensions and the height of the pipes above the fire within limits of measurement range of equipments and other laboratory facilities. Another goal was to find in which combinations of the varied parameters that gave largest differences when comparing a fire plume with and without obstacles. Circular pipes, which were used in Skarsbøs experiments, were replaced with 60 mm x 60 mm (outer dimensions and thickness of 4 mm) square pipes. Unfortunately, only round-edged pipes were available in the area of Haugesund at moment the experiments were performed. However, a somewhat smaller dimension was preferable for an optimal turbulence intensity. But since a smaller dimension requires a finer resolution of the grid in simulations to capture the correct fluid flow between the pipes, 60 mm x 60 mm was an acceptable compromise.

Simulations showed that the pipes placed in the persistent flame region where the flow is accelerating (see Figure 2.7) gave highest rise in temperature and velocity. This is about equivalent to heights below 1/3 of the flame height. Furthermore, a distance of 60 mm between the pipes was used in the simulations. This distance was later changed to 40 mm after some test experiments revealed that the flow around and just above the obstacles got more stable.

In Table 6.1 the planned scenarios are given. The experiment set up is seen in Figure 6.5.

Table 6.1: Experimental scenarios.

Number	Fuel [-]	HRR [kW/m ²]	Heights of pipes [m]
1.1	Propane	500	0.15
1.2	Propane	500	0.30
1.3	Propane	500	0.45
2.1	Propane	1000	0.15
2.2	Propane	1000	0.30
2.3	Propane	1000	0.45
3.1	Propane	1500	0.15
3.2	Propane	1500	0.30
3.3	Propane	1500	0.45
4.1	Heptane	-	0.15
4.2	Heptane	-	0.30
4.3	Heptane	-	0.45

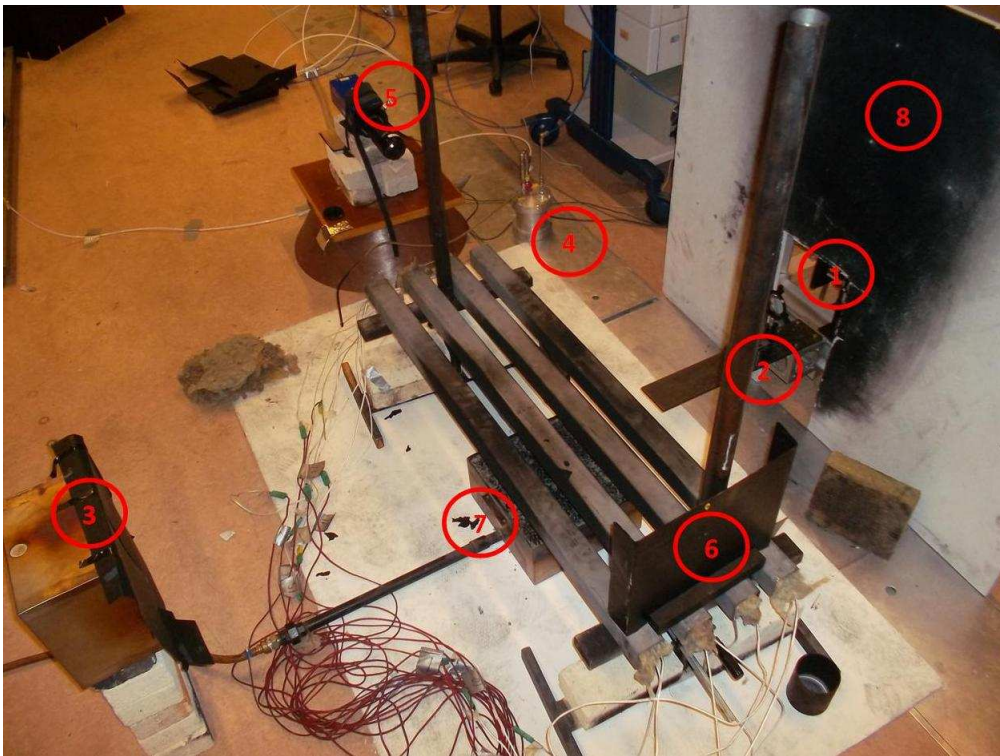


Figure 6.5: Experimental setup: (1) laser, (2) lens, (3) laser beam absorber, (4) seeding box, (5) camera, (6) anti-reflection shield, (7) gas burner and (8) wind shield.

6.3.1 Summary of the experiments

The laboratory that was booked for the experiments was not suited for fire experiments. It was used for enclosed bench scale flame experiments to study combustion processes in detail. Only four days were spent in the laboratory which turned out to be way too little time. Below, some limitations because of this and challenges during the experiments are described.

Scenarios

Initially, a series of 9 experiments was planned with a propane fire with HRR of 500 kW/m², 1000 kW/m² and 1500 kW/m², with pipes in heights of 0.15 m, 0.3 m and 0.45 m. Because the laboratory was loaded with a lot of expensive equipment and quite small relatively to the fire size, the plan was not achievable. Only experiments 500 kW/m² propane fire and 32 cm x 32 cm liquid methanol was performed.

Smoke hood and ventilation

The relative large fire size that was initially planned made it necessary to enlarged the smoke hood and set the ventilation on full power to prevent spread of smoke and hazardous seeding particles in the room. Another problem was then observed, the small fire got unstable because of the momentum from the ventilation and tilted in away from the laser. The problem was solved by placing a wind shield (number 8 in Figure 6.5) in front of the laser. However, this problem was not observed for larger fire (>500 kW/m²).

Calibration of the Laser and Camera

Calibration of laser and camera is the most time consuming part of the experiments. First, the camera must be focused on the measurement area, as seen in Figure 6.6. In these calibration experiments, the measurement area was set to 4 cm x 4 cm between the two pipes on the left side. Large measurement areas requires a strong laser to penetrate flame, especially for sooty flames. One of the uncertainties before doing the experiments was whether the laser used could penetrate such a sooty flame produced by propane. That is why methanol was chosen in the calibration experiments.

The camera does not necessarily has to be placed perpendicular to the laser sheet, since the distance between the dots on the calibration plate is known (in Figure 6.6). The correction was automatically fixed by the logging software that was used.

Since the seeding particles are traced as they are illuminated by the laser pulses, disturbing incoming light on the camera lens must be minimized. For this reason a black anti-reflection shield (number (6) in Figure 6.5) was placed behind the measurement area to absorb light in all wave lengths. Another uncertainty that arose regarding the disturbing light was the use of propane as fuel. Propane flames are sootier than for example methanol and are also therefore also emitting more thermal radiation.

The laser used was only able to operate on 4 Hz. This is not sufficient to capture turbulent motions. So the plan about studying turbulent characteristics was discarded

in the early stages. During the calibration, the shutter on the camera did only function sporadically. As a result, too much light was received on every second image making the tracing of particles impossible. From the experiments no conclusion could be drawn whether a propane flame is too sooty to measure a velocity vector field with the equipment available at Lund University.

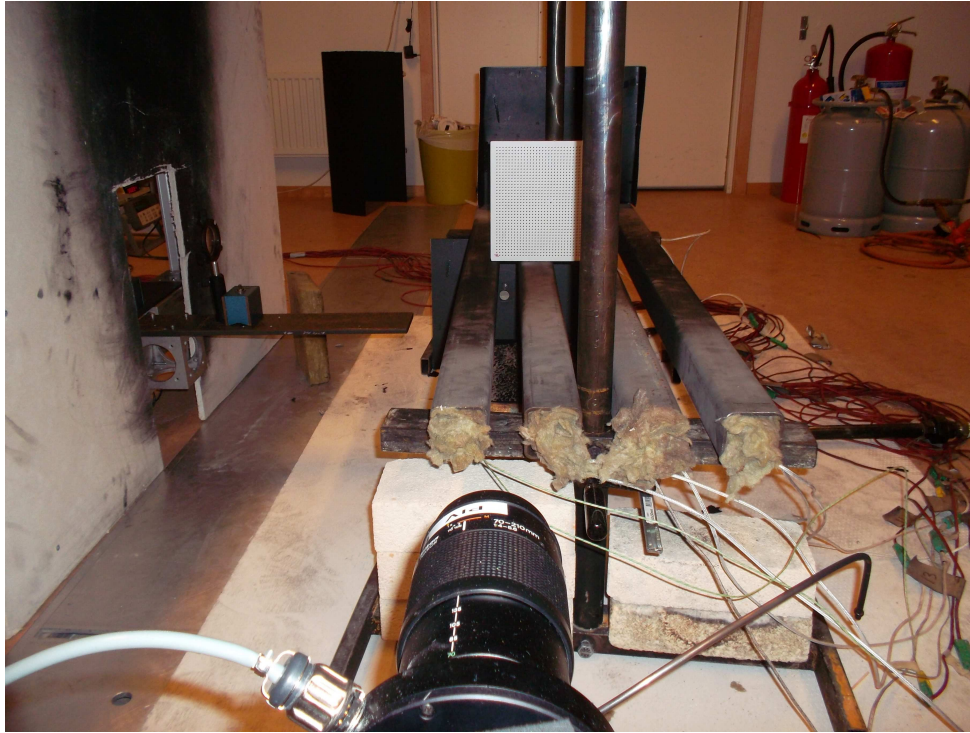


Figure 6.6: Calibration of the camera.

Seeding

Seeding of particles is the most challenging part of PIV measurements of flames. First of all, no universal method for seeding particles in flames exists. Secondly, the handling of seeding particles requires uttermost care due to hazards of inhaling it. Breathing masks and powerful ventilation are demanded. During these experiments, the flame was seeded in three different ways; by smoke sticks, smoke pellets and seeding of particles with pressurized air. All methods were some way unsuitable and the out coming results were of rather poor quality, primarily caused by the methods. Seeding with smoke was unsuitable because a stable concentration of smoke particles within measurable range was not achievable in the whole measurement area on a sufficient number of the images recorded. It was also attempted to seed the particles by pressurized in vertical direction, both upward and downward, and also horizontal direction faced in positive direction along the laser beam. When the particles were seeded upwards, a jet was clearly observed

in the results. It was obvious that the particles were strongly influenced by the release momentum and did not move free with the local flow velocity in the flame. In downward direction, seeding particles got stuck in burner. The measurement area was not provided with enough seeding when the seeding particles were supplied horizontally. Furthermore, the flame behavior was too much influenced when pressurized air method was applied for small fires.

Chapter 7

Conclusion

The PIV data from the experiments at Lund University were of rather poor quality and unsuitable for CFD validation. Too much light was received in the camera lens since the shutter on the camera only functioned sporadically on every second image. The seeding of particles turned out to be quite challenging and no successful method was found. Smoke pellets and smoke sticks did not provide enough seeding within measurable range in the desired area. The seeding particles did not move free with the local flow velocity when they were seeded by pressurized air, but were influenced by the release momentum. The flame behavior for small fires was also influenced by the pressurized air method

The validation of FDS-EDC revealed that the model is quite grid dependent. Except from the grid dependency the implemented code is in satisfactory agreement with the validation cases, and as good as the already existing or even better. Both models are about the same computational expensive. However, a single model constant, C_{LES} , gives not the most correct result for all the cases. An overall recommended C_{LES} of 0.015, as well as the already existing combustion model, over estimates the flame height for $Q^* \lesssim 1$. This over estimation of flame height is not observed with the Smagorinsky turbulence model. Furthermore, the maximum temperature is as much as 600°C with the Deardorff model for the McCaffery simulation of 57 kW. In addition, the temperature peak was located too far above the burner. The Smagorinsky model did not displace this peak in such extent as Deardorff and Vreman. For the McCaffery simulations, all turbulence models gave results in better agreement with $C_{LES} = 0.01$ than $C_{LES} = 0.015$. The Smagorinsky model, was the only turbulence model that captured the dip for the vertical velocity in the Sandia experiment test 17, but with the finest grid the CPU clock time was nearly 70% larger than the two other turbulence models.

Before LES-EDC can be applied in fire analysis the model must be modified to be grid independent. The model should also be validated in a wider range for temperature and velocity profiles in practical fire scale to establish a more accurate constant. A dynamic constant is not necessary for buoyancy-driven fires in the context of fire engineering, but could be a benefit for detailed investigation of flames.

7.1 Further Work

The author of this thesis and the participants of the experiments at Lund University discussed alternative ways to arrange experiments to achieve successful PIV measurements. Regarding the seeding, the most challenging part;

- the first step is to perform the experiments in a closed room where seeding particles are in no hazard to humans. Then it is possible to seed the flame with large amounts of particles.
- step two is to customize the burner and build in seeding point around the frame (maybe even in the middle of the burner too) and seed the particles with low-velocity controllable pressurized air.

The implemented code is validated against flame height in range $0.1 \leq Q^* \leq 10000$; radial and vertical (horizontal) velocity profiles in range $1.35 \leq Q^* \leq 2.2$; centerline velocity and temperature profiles in range $0.005 \leq Q^* \leq 0.02$. In further work, it could be interesting to investigate how the mentioned parameters interact with each other when C_{LES} is varied. The code should also be validated for temperature and velocity in the range of $0.1 \lesssim Q^* \lesssim 1.5$ where the FDS-EDC did not fit well for the flame height (except from Smagorinsky turbulence model). The flame height is varying significantly because of the unstable nature of fire [38]. This puff cycle could also be validated in further work [34]. At last the model has to be modified to be grid independent.

Bibliography

- [1] B.F.Magnussen. On the structure of turbulence and a generalized eddy dissipation concept for chemical reaction in turbulent flow. In *American Institute of Aeronautics and Astronautics, Aerospace Science Meeting*, number 19th, St. Louis, Missouri, USA, January 1981.
- [2] B.F. Magnussen and I.S. Ertesvåg. The eddy dissipation turbulence energy cascade model. *Combustion Science and Technology*, 159(1):213–235, Desember 2000.
- [3] B.F.Magnussen. The eddy dissipation concept a bridge between science and technology. In *ECCOMAS Thematic Conference on Computational Combustion*, Lisbon, June 2005.
- [4] K. McGrattan; R. McDermott; S. Hostikka and J. Floyd. *Fire Dynamics Fire Simulator (Version 5) User's Guide*. NIST, Washington, 2010.
- [5] K.E. Rian B. Panjwani, I.S.Ertesvåg and A. Gruber. Subgrid combustion modelling for large eddy simulations (les) of turbulent combustion using eddy dissipation concept (edc). pages 1–19, Lisbon, June 2010.
- [6] B. Panjwani. *Large Eddy Simulation of Turbulent Combustion With Chemical Kinetics: The Eddy Dissipation Concept as a Subgrid Combustion Model for Large Eddy Simulation: Theory and Validation*. PhD thesis, Norwegian University of Science and Technology, Trondheim, 2011.
- [7] L.X. Zhou L.Y. Hu and J.Zhang. Large-eddy simulation of a swirling diffusion flame using a som sgs combustion model. *Numerical Heat Transfer, Part B: Fundamentals: An International Journal of Computation and Methodology*, 50(1):41–58, 2006.
- [8] L.Y Hu L.X. Zhou and F. Wang. Large-eddy simulation of turbulent combustion using som and ebu sgs combustion models. pages 99–102, 2009.
- [9] J. D. Anderson Jr. *Computational Fluid Dynamics*. Number pp. 1-167. McGRAW-HILL, New York, 1th edition, 1995.
- [10] B. Karlsson and J.G. Quintiere. *Enclosure Fire Dynamics*. CRC press, Boca Raton, 1st edition, 1999.

- [11] S.R. Turns. *An Introduction to Combustion, Concepts and Applications*. McGraw-Hill, Boston, 2nd edition, 1999.
- [12] H. Tennekes and J.L. Lumley. *A First Course in Turbulence*. The MIT Press, Cambridge, 1972.
- [13] I.S. Ertesvåg. *Turbulent Strøyming og Forbrenning*. Tapir, Trondheim, 1st edition, 2000.
- [14] J. Warnatz; U. Mass and R.W. Dibble. *Combustion*. Number pp. 185-212. Springer, Germany, 4th edition, 2006.
- [15] G.H. Yeoh and K.K. Yuen. *Computational Fluid Dynamics in Fire Engineering*. Elsevier, Amsterdam, 1st edition, 2009.
- [16] B.E. Launder and D.B. Spalding. The numerical computation of turbulent flows. *Computer Methods in Applied Mechanics and Engineering*, 3(2):269–289, August 1974.
- [17] M. Germano; U. Piomelli; P. Moin and W. Cabot. A dynamic subgrid-scale eddy viscosity model. *Phys. Fluids A*, 3(7):1760–1765, November 1991.
- [18] Dennis Veynante Thierry Poinso. *Theoretical and Numerical Combustion*. Edwards, Philadelphia, 2nd edition, 2005.
- [19] A. W. Vreman. An eddy-viscosity subgrid-scale model for turbulent shear flow: Algebraic theory and applications. *Phys. Fluids*, 16(10):3670–3681, September 2004.
- [20] D. Drysdale. *An Introduction to Fire Dynamics*. Number pp. 1-29. John Wiley and Sons, Chichester, 2nd edition, 2007.
- [21] J. Chen S. McAllister and A.C. Fernandez-Pello. *Fundamentals of Combustion Processes*. Springer, April 2011.
- [22] R. Borghi and M. Destriau. *Combustion and Flames, Chemical and Physical Principles*. Éditions Technip, Paris, 1998.
- [23] G. Heskestad. *SFPE Handbook of Fire Protection Engineering, chapter Fire Plumes, Flame Height and Air Entrainment*. National Fire Protection Association (NFPA), 3rd edition, 2002.
- [24] B.J. MacCaffery. Purely buoyant diffusion flames: Some experimental results. (NB-SIR 79-1910), October 1979.
- [25] K. McGrattan; R. McDermott; S. Hostikka and J. Floyd. *Fire Dynamics Fire Simulator Technical Reference Guide, Volume 1: Mathematical Model*. NIST, Washington.

- [26] J.E. Floyd. *Multi-Parameter, Multiple Fuel Mixture Combustion Model for Fire Dynamics Simulator*. NIST, Baltimore, November 2008.
- [27] B. Husted J. Carlsson and U. Göransson. Fordele og faldgruber ved anvendelse af cfd til brandtekniske beregninger. *HVAC magasinet*, pages 44–47, July 2005.
- [28] E. Gissi. *An Introduction to Fire Simulation with FDS and Smokeview*, September 2009.
- [29] T. Yamamoto H. Aoki M. Yaga, H. Endo and T. Mirua. Modeling of eddy characteristic time in les for calculating tubrulent diffusion time. *International Journal of Heat and Mass Transfer*, 45(11):2343–2349, 2002.
- [30] American Society for Testing and Materials, West Conshohocken, West Conshohocken, Pennsylvania. ASTM E 1355-04. *Standard Guide for Evaluating the Predictive Capabilities of Deterministic Fire Models*, 1 edition, 2004. i.
- [31] K. McGrattan; R. McDermott; S. Hostikka and J. Floyd. *Fire Dynamics Simulator (Version 5) Technical Reference Guide, Volume 2: Verification*. NIST, Washington, 2010.
- [32] K. McGrattan; R. McDermott; S. Hostikka and J. Floyd. *Fire Dynamics Fire Simulator Technical Reference Guide, Volume 3: Validation*. NIST, Washington, 2010.
- [33] E. J. Weckman S. R. Tieszen, T. J. O’Hern and R. W. Schefer. Experimental study of the effect of fuel mass flux on a 1-m-diameter methane fire and comparison with a hydrogen fire. *Combustion and Flame*, 139(126-141), 2004.
- [34] R. W. Schefer E. J. Weckman S. R. Tieszen, T. J. O’Hern and T. K. Blanchat. Experimental study of the flow field in and around a one meter diameter methane fire. *Combustion and Flame*, 129:378–391, 2002.
- [35] Lars Roar Skarsbo. *An Experimental Study of Pool Fire and Validation of Different CFD Models*. PhD thesis, University of Bergen, June 2011.
- [36] S.T Wereley M. Raffel, C.E Willert and J. Kompenhans. *Particle Image Velocimetry: A Practical Guide*. Springer, Berlin, 2nd edition, 1998.
- [37] Particle image velocimetry (piv); www.dantecdynamics.com, March 2012.
- [38] Y. Xin; J.P. Gore; K.B. McGrattan; R.G. Rehm and H.R. Baum. Fire dynamics of a turbulent buoyant flame using mixture-fraction-based combustion model. *Combustion and Flame*, 141:329–335, 2005.

Appendix A

FDS input files

A.1 Sandia test 14

```
&HEAD CHID='Sandia_CH4_1m_Test14_dx1p5cm', TITLE='Sandia 1m low  
flow rate methane pool fire (Test 14), 1.5 cm resolution' /
```

```
&MULT ID='mesh array', DX=1.5,DY=1.5,DZ=1.0, I_UPPER=1,J_UPPER  
=1,K_UPPER=3 /  
&MESH IJK=96,96,64, XB=-1.5,0.0,-1.5,0.0,-.0625,0.9375, MULT_ID  
='mesh array' /
```

```
&TIME T_END=20. /  
&MISC TMPA=12.  
P_INF=80600.  
TURBULENCE_MODEL='VREMAN' /
```

```
&REAC FUEL='METHANE'  
HEAT_OF_COMBUSTION=50611.  
CRITICAL_FLAME_TEMPERATURE=1207 /
```

```
&RADI RADIATIVE_FRACTION=0.2 /  
&DUMP SIG_FIGS=4, SIG_FIGS_EXP=2 /  
&MATERIAL ID='STEEL', CONDUCTIVITY=54., SPECIFIC_HEAT=0.465,  
DENSITY=7850., EMISSIVITY=0.9 /  
&SURF ID='PLATE', COLOR='GRAY', DEFAULT=.TRUE., MATERIAL_ID='STEEL'  
, THICKNESS=0.025 /
```

```
&SURF ID='POOL', MASS_FLUX(1)=0.04, SPEC_ID(1)='METHANE',  
TMP_FRONT=11. /
```

```

&VENT XB= -0.5,0.5, -0.5,0.5, -.0625, -.0625,COLOR='BLUE',SURF_ID='
  POOL' /

&VENT XB= -1.5, -.5, -1.5,1.5, -.0625, -.0625,SURF_ID='OPEN' /
&VENT XB= .5,1.5, -1.5,1.5, -.0625, -.0625,SURF_ID='OPEN' /
&VENT XB= -1.5,1.5, -1.5, -.5, -.0625, -.0625,SURF_ID='OPEN' /
&VENT XB= -1.5,1.5, .5,1.5, -.0625, -.0625,SURF_ID='OPEN' /

&VENT MB='ZMAX',SURF_ID='OPEN' /
&VENT MB='YMIN',SURF_ID='OPEN' /
&VENT MB='YMAX',SURF_ID='OPEN' /
&VENT MB='XMIN',SURF_ID='OPEN' /
&VENT MB='XMAX',SURF_ID='OPEN' /

&SLCF PBY= -.0625, QUANTITY='VELOCITY', VECTOR=.TRUE. /
&SLCF PBY= -.0625, QUANTITY='DENSITY', CELL_CENTERED=.TRUE. /
&SLCF PBY= -.0625, QUANTITY='TEMPERATURE', CELL_CENTERED=.TRUE.
/
&SLCF PBY= -.0625, QUANTITY='HRRPUV', CELL_CENTERED=.TRUE. /
/&SLCF PBY= -.0625, QUANTITY='HRRPUA', CELL_CENTERED=.TRUE. /
&SLCF PBY= -.0625, QUANTITY='MASS FRACTION', SPEC_ID='METHANE',
  CELL_CENTERED=.TRUE. /
&SLCF PBY= -.0625, QUANTITY='C.SMAG', CELL_CENTERED=.TRUE. /
&SLCF PBY= -.0625, QUANTITY='TURBULENCE RESOLUTION',
  CELL_CENTERED=.TRUE. /
&SLCF PBY= -.0625, QUANTITY='WAVELET ERROR', QUANTITY2='MASS
  FRACTION', SPEC_ID='METHANE', CELL_CENTERED=.TRUE. /

&OBST XB= -0.70711,0.70711, -0.70711,0.70711, -0.0625,0 /
&OBST XB= -0.70711,0.70711, -0.70711,0.70711, -0.0625,0 /
&OBST XB= -0.69211,0.69211, -0.7218,0.7218, -0.0625,0 /
&OBST XB= -0.7218,0.7218, -0.69211,0.69211, -0.0625,0 /
&OBST XB= -0.67711,0.67711, -0.73588,0.73588, -0.0625,0 /
&OBST XB= -0.73588,0.73588, -0.67711,0.67711, -0.0625,0 /
&OBST XB= -0.66211,0.66211, -0.74941,0.74941, -0.0625,0 /
&OBST XB= -0.74941,0.74941, -0.66211,0.66211, -0.0625,0 /
&OBST XB= -0.64711,0.64711, -0.7624,0.7624, -0.0625,0 /
&OBST XB= -0.7624,0.7624, -0.64711,0.64711, -0.0625,0 /
&OBST XB= -0.63211,0.63211, -0.77488,0.77488, -0.0625,0 /
&OBST XB= -0.77488,0.77488, -0.63211,0.63211, -0.0625,0 /
&OBST XB= -0.61711,0.61711, -0.78688,0.78688, -0.0625,0 /
&OBST XB= -0.78688,0.78688, -0.61711,0.61711, -0.0625,0 /
&OBST XB= -0.60211,0.60211, -0.79842,0.79842, -0.0625,0 /

```

```
&OBST XB= -0.79842 ,0.79842 , -0.60211 ,0.60211 , -0.0625 ,0 /
&OBST XB= -0.58711 ,0.58711 , -0.80951 ,0.80951 , -0.0625 ,0 /
&OBST XB= -0.80951 ,0.80951 , -0.58711 ,0.58711 , -0.0625 ,0 /
&OBST XB= -0.57211 ,0.57211 , -0.82018 ,0.82018 , -0.0625 ,0 /
&OBST XB= -0.82018 ,0.82018 , -0.57211 ,0.57211 , -0.0625 ,0 /
&OBST XB= -0.55711 ,0.55711 , -0.83044 ,0.83044 , -0.0625 ,0 /
&OBST XB= -0.83044 ,0.83044 , -0.55711 ,0.55711 , -0.0625 ,0 /
&OBST XB= -0.54211 ,0.54211 , -0.84031 ,0.84031 , -0.0625 ,0 /
&OBST XB= -0.84031 ,0.84031 , -0.54211 ,0.54211 , -0.0625 ,0 /
&OBST XB= -0.52711 ,0.52711 , -0.8498 ,0.8498 , -0.0625 ,0 /
&OBST XB= -0.8498 ,0.8498 , -0.52711 ,0.52711 , -0.0625 ,0 /
&OBST XB= -0.51211 ,0.51211 , -0.85892 ,0.85892 , -0.0625 ,0 /
&OBST XB= -0.85892 ,0.85892 , -0.51211 ,0.51211 , -0.0625 ,0 /
&OBST XB= -0.49711 ,0.49711 , -0.86769 ,0.86769 , -0.0625 ,0 /
&OBST XB= -0.86769 ,0.86769 , -0.49711 ,0.49711 , -0.0625 ,0 /
&OBST XB= -0.48211 ,0.48211 , -0.87611 ,0.87611 , -0.0625 ,0 /
&OBST XB= -0.87611 ,0.87611 , -0.48211 ,0.48211 , -0.0625 ,0 /
&OBST XB= -0.46711 ,0.46711 , -0.8842 ,0.8842 , -0.0625 ,0 /
&OBST XB= -0.8842 ,0.8842 , -0.46711 ,0.46711 , -0.0625 ,0 /
&OBST XB= -0.45211 ,0.45211 , -0.89196 ,0.89196 , -0.0625 ,0 /
&OBST XB= -0.89196 ,0.89196 , -0.45211 ,0.45211 , -0.0625 ,0 /
&OBST XB= -0.43711 ,0.43711 , -0.89941 ,0.89941 , -0.0625 ,0 /
&OBST XB= -0.89941 ,0.89941 , -0.43711 ,0.43711 , -0.0625 ,0 /
&OBST XB= -0.42211 ,0.42211 , -0.90655 ,0.90655 , -0.0625 ,0 /
&OBST XB= -0.90655 ,0.90655 , -0.42211 ,0.42211 , -0.0625 ,0 /
&OBST XB= -0.40711 ,0.40711 , -0.91338 ,0.91338 , -0.0625 ,0 /
&OBST XB= -0.91338 ,0.91338 , -0.40711 ,0.40711 , -0.0625 ,0 /
&OBST XB= -0.39211 ,0.39211 , -0.91992 ,0.91992 , -0.0625 ,0 /
&OBST XB= -0.91992 ,0.91992 , -0.39211 ,0.39211 , -0.0625 ,0 /
&OBST XB= -0.37711 ,0.37711 , -0.92617 ,0.92617 , -0.0625 ,0 /
&OBST XB= -0.92617 ,0.92617 , -0.37711 ,0.37711 , -0.0625 ,0 /
&OBST XB= -0.36211 ,0.36211 , -0.93214 ,0.93214 , -0.0625 ,0 /
&OBST XB= -0.93214 ,0.93214 , -0.36211 ,0.36211 , -0.0625 ,0 /
&OBST XB= -0.34711 ,0.34711 , -0.93783 ,0.93783 , -0.0625 ,0 /
&OBST XB= -0.93783 ,0.93783 , -0.34711 ,0.34711 , -0.0625 ,0 /
&OBST XB= -0.33211 ,0.33211 , -0.94324 ,0.94324 , -0.0625 ,0 /
&OBST XB= -0.94324 ,0.94324 , -0.33211 ,0.33211 , -0.0625 ,0 /
&OBST XB= -0.31711 ,0.31711 , -0.94839 ,0.94839 , -0.0625 ,0 /
&OBST XB= -0.94839 ,0.94839 , -0.31711 ,0.31711 , -0.0625 ,0 /
&OBST XB= -0.30211 ,0.30211 , -0.95327 ,0.95327 , -0.0625 ,0 /
&OBST XB= -0.95327 ,0.95327 , -0.30211 ,0.30211 , -0.0625 ,0 /
&OBST XB= -0.28711 ,0.28711 , -0.9579 ,0.9579 , -0.0625 ,0 /
&OBST XB= -0.9579 ,0.9579 , -0.28711 ,0.28711 , -0.0625 ,0 /
```

```

&OBST XB= -0.27211,0.27211,-0.96227,0.96227,-0.0625,0 /
&OBST XB= -0.96227,0.96227,-0.27211,0.27211,-0.0625,0 /
&OBST XB= -0.25711,0.25711,-0.96638,0.96638,-0.0625,0 /
&OBST XB= -0.96638,0.96638,-0.25711,0.25711,-0.0625,0 /
&OBST XB= -0.24211,0.24211,-0.97025,0.97025,-0.0625,0 /
&OBST XB= -0.97025,0.97025,-0.24211,0.24211,-0.0625,0 /
&OBST XB= -0.22711,0.22711,-0.97387,0.97387,-0.0625,0 /
&OBST XB= -0.97387,0.97387,-0.22711,0.22711,-0.0625,0 /
&OBST XB= -0.21211,0.21211,-0.97725,0.97725,-0.0625,0 /
&OBST XB= -0.97725,0.97725,-0.21211,0.21211,-0.0625,0 /
&OBST XB= -0.19711,0.19711,-0.98038,0.98038,-0.0625,0 /
&OBST XB= -0.98038,0.98038,-0.19711,0.19711,-0.0625,0 /
&OBST XB= -0.18211,0.18211,-0.98328,0.98328,-0.0625,0 /
&OBST XB= -0.98328,0.98328,-0.18211,0.18211,-0.0625,0 /
&OBST XB= -0.16711,0.16711,-0.98594,0.98594,-0.0625,0 /
&OBST XB= -0.98594,0.98594,-0.16711,0.16711,-0.0625,0 /
&OBST XB= -0.15211,0.15211,-0.98836,0.98836,-0.0625,0 /
&OBST XB= -0.98836,0.98836,-0.15211,0.15211,-0.0625,0 /
&OBST XB= -0.13711,0.13711,-0.99056,0.99056,-0.0625,0 /
&OBST XB= -0.99056,0.99056,-0.13711,0.13711,-0.0625,0 /
&OBST XB= -0.12211,0.12211,-0.99252,0.99252,-0.0625,0 /
&OBST XB= -0.99252,0.99252,-0.12211,0.12211,-0.0625,0 /
&OBST XB= -0.10711,0.10711,-0.99425,0.99425,-0.0625,0 /
&OBST XB= -0.99425,0.99425,-0.10711,0.10711,-0.0625,0 /
&OBST XB= -0.092107,0.092107,-0.99575,0.99575,-0.0625,0 /
&OBST XB= -0.99575,0.99575,-0.092107,0.092107,-0.0625,0 /
&OBST XB= -0.077107,0.077107,-0.99702,0.99702,-0.0625,0 /
&OBST XB= -0.99702,0.99702,-0.077107,0.077107,-0.0625,0 /
&OBST XB= -0.062107,0.062107,-0.99807,0.99807,-0.0625,0 /
&OBST XB= -0.99807,0.99807,-0.062107,0.062107,-0.0625,0 /
&OBST XB= -0.047107,0.047107,-0.99889,0.99889,-0.0625,0 /
&OBST XB= -0.99889,0.99889,-0.047107,0.047107,-0.0625,0 /
&OBST XB= -0.032107,0.032107,-0.99948,0.99948,-0.0625,0 /
&OBST XB= -0.99948,0.99948,-0.032107,0.032107,-0.0625,0 /
&OBST XB= -0.017107,0.017107,-0.99985,0.99985,-0.0625,0 /
&OBST XB= -0.99985,0.99985,-0.017107,0.017107,-0.0625,0 /
&OBST XB= -0.0021068,0.0021068,-1,1,-0.0625,0 /
&OBST XB= -1,1,-0.0021068,0.0021068,-0.0625,0 /

&HOLE XB= -0.35355,0.35355,-0.35355,0.35355,-.125,.1/
&HOLE XB= -0.35355,0.35355,-0.35355,0.35355,-.125,.1/
&HOLE XB= -0.33755,0.33755,-0.36886,0.36886,-.125,.1/
&HOLE XB= -0.36886,0.36886,-0.33755,0.33755,-.125,.1/

```


&HOLE XB= -0.32155,0.32155,-0.38289,0.38289,-.125,.1/
&HOLE XB= -0.38289,0.38289,-0.32155,0.32155,-.125,.1/
&HOLE XB= -0.30555,0.30555,-0.39577,0.39577,-.125,.1/
&HOLE XB= -0.39577,0.39577,-0.30555,0.30555,-.125,.1/
&HOLE XB= -0.28955,0.28955,-0.40763,0.40763,-.125,.1/
&HOLE XB= -0.40763,0.40763,-0.28955,0.28955,-.125,.1/
&HOLE XB= -0.27355,0.27355,-0.41853,0.41853,-.125,.1/
&HOLE XB= -0.41853,0.41853,-0.27355,0.27355,-.125,.1/
&HOLE XB= -0.25755,0.25755,-0.42856,0.42856,-.125,.1/
&HOLE XB= -0.42856,0.42856,-0.25755,0.25755,-.125,.1/
&HOLE XB= -0.24155,0.24155,-0.43778,0.43778,-.125,.1/
&HOLE XB= -0.43778,0.43778,-0.24155,0.24155,-.125,.1/
&HOLE XB= -0.22555,0.22555,-0.44623,0.44623,-.125,.1/
&HOLE XB= -0.44623,0.44623,-0.22555,0.22555,-.125,.1/
&HOLE XB= -0.20955,0.20955,-0.45397,0.45397,-.125,.1/
&HOLE XB= -0.45397,0.45397,-0.20955,0.20955,-.125,.1/
&HOLE XB= -0.19355,0.19355,-0.46102,0.46102,-.125,.1/
&HOLE XB= -0.46102,0.46102,-0.19355,0.19355,-.125,.1/
&HOLE XB= -0.17755,0.17755,-0.46741,0.46741,-.125,.1/
&HOLE XB= -0.46741,0.46741,-0.17755,0.17755,-.125,.1/
&HOLE XB= -0.16155,0.16155,-0.47318,0.47318,-.125,.1/
&HOLE XB= -0.47318,0.47318,-0.16155,0.16155,-.125,.1/
&HOLE XB= -0.14555,0.14555,-0.47835,0.47835,-.125,.1/
&HOLE XB= -0.47835,0.47835,-0.14555,0.14555,-.125,.1/
&HOLE XB= -0.12955,0.12955,-0.48292,0.48292,-.125,.1/
&HOLE XB= -0.48292,0.48292,-0.12955,0.12955,-.125,.1/
&HOLE XB= -0.11355,0.11355,-0.48693,0.48693,-.125,.1/
&HOLE XB= -0.48693,0.48693,-0.11355,0.11355,-.125,.1/
&HOLE XB= -0.097553,0.097553,-0.49039,0.49039,-.125,.1/
&HOLE XB= -0.49039,0.49039,-0.097553,0.097553,-.125,.1/
&HOLE XB= -0.081553,0.081553,-0.4933,0.4933,-.125,.1/
&HOLE XB= -0.4933,0.4933,-0.081553,0.081553,-.125,.1/
&HOLE XB= -0.065553,0.065553,-0.49568,0.49568,-.125,.1/
&HOLE XB= -0.49568,0.49568,-0.065553,0.065553,-.125,.1/
&HOLE XB= -0.049553,0.049553,-0.49754,0.49754,-.125,.1/
&HOLE XB= -0.49754,0.49754,-0.049553,0.049553,-.125,.1/
&HOLE XB= -0.033553,0.033553,-0.49887,0.49887,-.125,.1/
&HOLE XB= -0.49887,0.49887,-0.033553,0.033553,-.125,.1/
&HOLE XB= -0.017553,0.017553,-0.49969,0.49969,-.125,.1/
&HOLE XB= -0.49969,0.49969,-0.017553,0.017553,-.125,.1/
&HOLE XB= -0.0015534,0.0015534,-0.5,0.5,-.125,.1/
&HOLE XB= -0.5,0.5,-0.0015534,0.0015534,-.125,.1/

Radial profiles of velocity and mass fraction

```
&DEVC XB= -0.50,0.50,0.0,0.0,0.3,0.3, QUANTITY='W-VELOCITY', ID
      ='Wp3', POINTS=21, X_ID='x' /
```

```
&DEVC XB= -0.50,0.50,0.0,0.0,0.5,0.5, QUANTITY='W-VELOCITY', ID
      ='Wp5', POINTS=21, HIDE_COORDINATES=.TRUE. /
```

```
&DEVC XB= -0.50,0.50,0.0,0.0,0.9,0.9, QUANTITY='W-VELOCITY', ID
      ='Wp9', POINTS=21, HIDE_COORDINATES=.TRUE. /
```

```
&DEVC XB= -0.50,0.50,0.0,0.0,0.3,0.3, QUANTITY='U-VELOCITY', ID
      ='Up3', POINTS=21, HIDE_COORDINATES=.TRUE. /
```

```
&DEVC XB= -0.50,0.50,0.0,0.0,0.5,0.5, QUANTITY='U-VELOCITY', ID
      ='Up5', POINTS=21, HIDE_COORDINATES=.TRUE. /
```

```
&DEVC XB= -0.50,0.50,0.0,0.0,0.9,0.9, QUANTITY='U-VELOCITY', ID
      ='Up9', POINTS=21, HIDE_COORDINATES=.TRUE. /
```

```
&DEVC XB= -0.50,0.50,0.0,0.0,0.3,0.3, QUANTITY='W-VELOCITY', ID
      ='Wp3_rms', STATISTICS='RMS', POINTS=21, HIDE_COORDINATES=.
      TRUE. /
```

```
&DEVC XB= -0.50,0.50,0.0,0.0,0.5,0.5, QUANTITY='W-VELOCITY', ID
      ='Wp5_rms', STATISTICS='RMS', POINTS=21, HIDE_COORDINATES=.
      TRUE. /
```

```
&DEVC XB= -0.50,0.50,0.0,0.0,0.9,0.9, QUANTITY='W-VELOCITY', ID
      ='Wp9_rms', STATISTICS='RMS', POINTS=21, HIDE_COORDINATES=.
      TRUE. /
```

```
&DEVC XB= -0.50,0.50,0.0,0.0,0.3,0.3, QUANTITY='U-VELOCITY', ID
      ='Up3_rms', STATISTICS='RMS', POINTS=21, HIDE_COORDINATES=.
      TRUE. /
```

```
&DEVC XB= -0.50,0.50,0.0,0.0,0.5,0.5, QUANTITY='U-VELOCITY', ID
      ='Up5_rms', STATISTICS='RMS', POINTS=21, HIDE_COORDINATES=.
      TRUE. /
```

```
&DEVC XB= -0.50,0.50,0.0,0.0,0.9,0.9, QUANTITY='U-VELOCITY', ID
      ='Up9_rms', STATISTICS='RMS', POINTS=21, HIDE_COORDINATES=.
      TRUE. /
```

```
&TAIL /
```

A.2 Sandia test 17

```
&HEAD CHID='Sandia_CH4_1m_Test17_dx1p5cm', TITLE='Sandia 1m
      high flow rate methane pool fire (Test 17), 1.5 cm
      resolution' /
```

```

&MULT ID='mesh array' , DX=1.5,DY=1.5,DZ=1.0, I_UPPER=1,J_UPPER
  =1,K_UPPER=3 /
&MESH IJK=96,96,64, XB=-1.5,0.0,-1.5,0.0,-.0625,0.9375, MULT_ID
  ='mesh array' /

&TIME T_END=20. /
&MISC TMPA=5.
      P_INF=81100.
      TURBULENCE_MODEL='VREMAN' /

&REAC FUEL='METHANE'
      HEAT_OF_COMBUSTION=50350.
      CRITICAL_FLAME_TEMPERATURE=1207 /

&RADI RADIATIVE_FRACTION=0.2 /
&DUMP SIG_FIGS=4, SIG_FIGS_EXP=2 /
&MATERIAL ID='STEEL', CONDUCTIVITY=54., SPECIFIC_HEAT=0.465,
      DENSITY=7850., EMISSIVITY=0.9 /
&SURF ID='PLATE', COLOR='GRAY', DEFAULT=.TRUE., MATERIAL_ID='STEEL'
      , THICKNESS=0.025 /

&SURF ID='POOL', MASS_FLUX(1)=0.066, SPEC_ID(1)='METHANE',
      TMP_FRONT=1. /

&VENT XB=-0.5,0.5,-0.5,0.5,-.0625,-.0625,COLOR='BLUE', SURF_ID='
  POOL' /

&VENT XB=-1.5,-.5,-1.5,1.5,-.0625,-.0625,SURF_ID='OPEN' /
&VENT XB=.5,1.5,-1.5,1.5,-.0625,-.0625,SURF_ID='OPEN' /
&VENT XB=-1.5,1.5,-1.5,-.5,-.0625,-.0625,SURF_ID='OPEN' /
&VENT XB=-1.5,1.5,.5,1.5,-.0625,-.0625,SURF_ID='OPEN' /

&VENT MB='ZMAX', SURF_ID='OPEN' /
&VENT MB='YMIN', SURF_ID='OPEN' /
&VENT MB='YMAX', SURF_ID='OPEN' /
&VENT MB='XMIN', SURF_ID='OPEN' /
&VENT MB='XMAX', SURF_ID='OPEN' /

&SLCF PBX=-.0625, QUANTITY='VELOCITY', VECTOR=.TRUE. /
&SLCF PBX=-.0625, QUANTITY='DENSITY', CELL_CENTERED=.TRUE. /
&SLCF PBX=-.0625, QUANTITY='TEMPERATURE', CELL_CENTERED=.TRUE.
  /

```

```

&SLCF PBY=-.0625, QUANTITY='HRRPUV', CELL_CENTERED=.TRUE. /
/&SLCF PBY=-.0625, QUANTITY='HRRPUA', CELL_CENTERED=.TRUE. /
&SLCF PBY=-.0625, QUANTITY='MASS FRACTION', SPEC_ID='METHANE',
  CELL_CENTERED=.TRUE. /
&SLCF PBY=-.0625, QUANTITY='C.SMAG', CELL_CENTERED=.TRUE. /
&SLCF PBY=-.0625, QUANTITY='TURBULENCE RESOLUTION',
  CELL_CENTERED=.TRUE. /
&SLCF PBY=-.0625, QUANTITY='WAVELET ERROR', QUANTITY2='MASS
  FRACTION', SPEC_ID='METHANE', CELL_CENTERED=.TRUE. /

&OBST XB=-0.70711,0.70711,-0.70711,0.70711,-0.0625,0 /
&OBST XB=-0.70711,0.70711,-0.70711,0.70711,-0.0625,0 /
&OBST XB=-0.69211,0.69211,-0.7218,0.7218,-0.0625,0 /
&OBST XB=-0.7218,0.7218,-0.69211,0.69211,-0.0625,0 /
&OBST XB=-0.67711,0.67711,-0.73588,0.73588,-0.0625,0 /
&OBST XB=-0.73588,0.73588,-0.67711,0.67711,-0.0625,0 /
&OBST XB=-0.66211,0.66211,-0.74941,0.74941,-0.0625,0 /
&OBST XB=-0.74941,0.74941,-0.66211,0.66211,-0.0625,0 /
&OBST XB=-0.64711,0.64711,-0.7624,0.7624,-0.0625,0 /
&OBST XB=-0.7624,0.7624,-0.64711,0.64711,-0.0625,0 /
&OBST XB=-0.63211,0.63211,-0.77488,0.77488,-0.0625,0 /
&OBST XB=-0.77488,0.77488,-0.63211,0.63211,-0.0625,0 /
&OBST XB=-0.61711,0.61711,-0.78688,0.78688,-0.0625,0 /
&OBST XB=-0.78688,0.78688,-0.61711,0.61711,-0.0625,0 /
&OBST XB=-0.60211,0.60211,-0.79842,0.79842,-0.0625,0 /
&OBST XB=-0.79842,0.79842,-0.60211,0.60211,-0.0625,0 /
&OBST XB=-0.58711,0.58711,-0.80951,0.80951,-0.0625,0 /
&OBST XB=-0.80951,0.80951,-0.58711,0.58711,-0.0625,0 /
&OBST XB=-0.57211,0.57211,-0.82018,0.82018,-0.0625,0 /
&OBST XB=-0.82018,0.82018,-0.57211,0.57211,-0.0625,0 /
&OBST XB=-0.55711,0.55711,-0.83044,0.83044,-0.0625,0 /
&OBST XB=-0.83044,0.83044,-0.55711,0.55711,-0.0625,0 /
&OBST XB=-0.54211,0.54211,-0.84031,0.84031,-0.0625,0 /
&OBST XB=-0.84031,0.84031,-0.54211,0.54211,-0.0625,0 /
&OBST XB=-0.52711,0.52711,-0.8498,0.8498,-0.0625,0 /
&OBST XB=-0.8498,0.8498,-0.52711,0.52711,-0.0625,0 /
&OBST XB=-0.51211,0.51211,-0.85892,0.85892,-0.0625,0 /
&OBST XB=-0.85892,0.85892,-0.51211,0.51211,-0.0625,0 /
&OBST XB=-0.49711,0.49711,-0.86769,0.86769,-0.0625,0 /
&OBST XB=-0.86769,0.86769,-0.49711,0.49711,-0.0625,0 /
&OBST XB=-0.48211,0.48211,-0.87611,0.87611,-0.0625,0 /
&OBST XB=-0.87611,0.87611,-0.48211,0.48211,-0.0625,0 /
&OBST XB=-0.46711,0.46711,-0.8842,0.8842,-0.0625,0 /

```

```
&OBST XB= -0.8842 ,0.8842 , -0.46711 ,0.46711 , -0.0625 ,0 /
&OBST XB= -0.45211 ,0.45211 , -0.89196 ,0.89196 , -0.0625 ,0 /
&OBST XB= -0.89196 ,0.89196 , -0.45211 ,0.45211 , -0.0625 ,0 /
&OBST XB= -0.43711 ,0.43711 , -0.89941 ,0.89941 , -0.0625 ,0 /
&OBST XB= -0.89941 ,0.89941 , -0.43711 ,0.43711 , -0.0625 ,0 /
&OBST XB= -0.42211 ,0.42211 , -0.90655 ,0.90655 , -0.0625 ,0 /
&OBST XB= -0.90655 ,0.90655 , -0.42211 ,0.42211 , -0.0625 ,0 /
&OBST XB= -0.40711 ,0.40711 , -0.91338 ,0.91338 , -0.0625 ,0 /
&OBST XB= -0.91338 ,0.91338 , -0.40711 ,0.40711 , -0.0625 ,0 /
&OBST XB= -0.39211 ,0.39211 , -0.91992 ,0.91992 , -0.0625 ,0 /
&OBST XB= -0.91992 ,0.91992 , -0.39211 ,0.39211 , -0.0625 ,0 /
&OBST XB= -0.37711 ,0.37711 , -0.92617 ,0.92617 , -0.0625 ,0 /
&OBST XB= -0.92617 ,0.92617 , -0.37711 ,0.37711 , -0.0625 ,0 /
&OBST XB= -0.36211 ,0.36211 , -0.93214 ,0.93214 , -0.0625 ,0 /
&OBST XB= -0.93214 ,0.93214 , -0.36211 ,0.36211 , -0.0625 ,0 /
&OBST XB= -0.34711 ,0.34711 , -0.93783 ,0.93783 , -0.0625 ,0 /
&OBST XB= -0.93783 ,0.93783 , -0.34711 ,0.34711 , -0.0625 ,0 /
&OBST XB= -0.33211 ,0.33211 , -0.94324 ,0.94324 , -0.0625 ,0 /
&OBST XB= -0.94324 ,0.94324 , -0.33211 ,0.33211 , -0.0625 ,0 /
&OBST XB= -0.31711 ,0.31711 , -0.94839 ,0.94839 , -0.0625 ,0 /
&OBST XB= -0.94839 ,0.94839 , -0.31711 ,0.31711 , -0.0625 ,0 /
&OBST XB= -0.30211 ,0.30211 , -0.95327 ,0.95327 , -0.0625 ,0 /
&OBST XB= -0.95327 ,0.95327 , -0.30211 ,0.30211 , -0.0625 ,0 /
&OBST XB= -0.28711 ,0.28711 , -0.9579 ,0.9579 , -0.0625 ,0 /
&OBST XB= -0.9579 ,0.9579 , -0.28711 ,0.28711 , -0.0625 ,0 /
&OBST XB= -0.27211 ,0.27211 , -0.96227 ,0.96227 , -0.0625 ,0 /
&OBST XB= -0.96227 ,0.96227 , -0.27211 ,0.27211 , -0.0625 ,0 /
&OBST XB= -0.25711 ,0.25711 , -0.96638 ,0.96638 , -0.0625 ,0 /
&OBST XB= -0.96638 ,0.96638 , -0.25711 ,0.25711 , -0.0625 ,0 /
&OBST XB= -0.24211 ,0.24211 , -0.97025 ,0.97025 , -0.0625 ,0 /
&OBST XB= -0.97025 ,0.97025 , -0.24211 ,0.24211 , -0.0625 ,0 /
&OBST XB= -0.22711 ,0.22711 , -0.97387 ,0.97387 , -0.0625 ,0 /
&OBST XB= -0.97387 ,0.97387 , -0.22711 ,0.22711 , -0.0625 ,0 /
&OBST XB= -0.21211 ,0.21211 , -0.97725 ,0.97725 , -0.0625 ,0 /
&OBST XB= -0.97725 ,0.97725 , -0.21211 ,0.21211 , -0.0625 ,0 /
&OBST XB= -0.19711 ,0.19711 , -0.98038 ,0.98038 , -0.0625 ,0 /
&OBST XB= -0.98038 ,0.98038 , -0.19711 ,0.19711 , -0.0625 ,0 /
&OBST XB= -0.18211 ,0.18211 , -0.98328 ,0.98328 , -0.0625 ,0 /
&OBST XB= -0.98328 ,0.98328 , -0.18211 ,0.18211 , -0.0625 ,0 /
&OBST XB= -0.16711 ,0.16711 , -0.98594 ,0.98594 , -0.0625 ,0 /
&OBST XB= -0.98594 ,0.98594 , -0.16711 ,0.16711 , -0.0625 ,0 /
&OBST XB= -0.15211 ,0.15211 , -0.98836 ,0.98836 , -0.0625 ,0 /
&OBST XB= -0.98836 ,0.98836 , -0.15211 ,0.15211 , -0.0625 ,0 /
```

```

&OBST XB= -0.13711,0.13711,-0.99056,0.99056,-0.0625,0 /
&OBST XB= -0.99056,0.99056,-0.13711,0.13711,-0.0625,0 /
&OBST XB= -0.12211,0.12211,-0.99252,0.99252,-0.0625,0 /
&OBST XB= -0.99252,0.99252,-0.12211,0.12211,-0.0625,0 /
&OBST XB= -0.10711,0.10711,-0.99425,0.99425,-0.0625,0 /
&OBST XB= -0.99425,0.99425,-0.10711,0.10711,-0.0625,0 /
&OBST XB= -0.092107,0.092107,-0.99575,0.99575,-0.0625,0 /
&OBST XB= -0.99575,0.99575,-0.092107,0.092107,-0.0625,0 /
&OBST XB= -0.077107,0.077107,-0.99702,0.99702,-0.0625,0 /
&OBST XB= -0.99702,0.99702,-0.077107,0.077107,-0.0625,0 /
&OBST XB= -0.062107,0.062107,-0.99807,0.99807,-0.0625,0 /
&OBST XB= -0.99807,0.99807,-0.062107,0.062107,-0.0625,0 /
&OBST XB= -0.047107,0.047107,-0.99889,0.99889,-0.0625,0 /
&OBST XB= -0.99889,0.99889,-0.047107,0.047107,-0.0625,0 /
&OBST XB= -0.032107,0.032107,-0.99948,0.99948,-0.0625,0 /
&OBST XB= -0.99948,0.99948,-0.032107,0.032107,-0.0625,0 /
&OBST XB= -0.017107,0.017107,-0.99985,0.99985,-0.0625,0 /
&OBST XB= -0.99985,0.99985,-0.017107,0.017107,-0.0625,0 /
&OBST XB= -0.0021068,0.0021068,-1,1,-0.0625,0 /
&OBST XB= -1,1,-0.0021068,0.0021068,-0.0625,0 /

&HOLE XB= -0.35355,0.35355,-0.35355,0.35355,-.125,.1/
&HOLE XB= -0.35355,0.35355,-0.35355,0.35355,-.125,.1/
&HOLE XB= -0.33755,0.33755,-0.36886,0.36886,-.125,.1/
&HOLE XB= -0.36886,0.36886,-0.33755,0.33755,-.125,.1/
&HOLE XB= -0.32155,0.32155,-0.38289,0.38289,-.125,.1/
&HOLE XB= -0.38289,0.38289,-0.32155,0.32155,-.125,.1/
&HOLE XB= -0.30555,0.30555,-0.39577,0.39577,-.125,.1/
&HOLE XB= -0.39577,0.39577,-0.30555,0.30555,-.125,.1/
&HOLE XB= -0.28955,0.28955,-0.40763,0.40763,-.125,.1/
&HOLE XB= -0.40763,0.40763,-0.28955,0.28955,-.125,.1/
&HOLE XB= -0.27355,0.27355,-0.41853,0.41853,-.125,.1/
&HOLE XB= -0.41853,0.41853,-0.27355,0.27355,-.125,.1/
&HOLE XB= -0.25755,0.25755,-0.42856,0.42856,-.125,.1/
&HOLE XB= -0.42856,0.42856,-0.25755,0.25755,-.125,.1/
&HOLE XB= -0.24155,0.24155,-0.43778,0.43778,-.125,.1/
&HOLE XB= -0.43778,0.43778,-0.24155,0.24155,-.125,.1/
&HOLE XB= -0.22555,0.22555,-0.44623,0.44623,-.125,.1/
&HOLE XB= -0.44623,0.44623,-0.22555,0.22555,-.125,.1/
&HOLE XB= -0.20955,0.20955,-0.45397,0.45397,-.125,.1/
&HOLE XB= -0.45397,0.45397,-0.20955,0.20955,-.125,.1/
&HOLE XB= -0.19355,0.19355,-0.46102,0.46102,-.125,.1/
&HOLE XB= -0.46102,0.46102,-0.19355,0.19355,-.125,.1/

```

```

&HOLE XB= -0.17755,0.17755,-0.46741,0.46741,-.125,.1/
&HOLE XB= -0.46741,0.46741,-0.17755,0.17755,-.125,.1/
&HOLE XB= -0.16155,0.16155,-0.47318,0.47318,-.125,.1/
&HOLE XB= -0.47318,0.47318,-0.16155,0.16155,-.125,.1/
&HOLE XB= -0.14555,0.14555,-0.47835,0.47835,-.125,.1/
&HOLE XB= -0.47835,0.47835,-0.14555,0.14555,-.125,.1/
&HOLE XB= -0.12955,0.12955,-0.48292,0.48292,-.125,.1/
&HOLE XB= -0.48292,0.48292,-0.12955,0.12955,-.125,.1/
&HOLE XB= -0.11355,0.11355,-0.48693,0.48693,-.125,.1/
&HOLE XB= -0.48693,0.48693,-0.11355,0.11355,-.125,.1/
&HOLE XB= -0.097553,0.097553,-0.49039,0.49039,-.125,.1/
&HOLE XB= -0.49039,0.49039,-0.097553,0.097553,-.125,.1/
&HOLE XB= -0.081553,0.081553,-0.4933,0.4933,-.125,.1/
&HOLE XB= -0.4933,0.4933,-0.081553,0.081553,-.125,.1/
&HOLE XB= -0.065553,0.065553,-0.49568,0.49568,-.125,.1/
&HOLE XB= -0.49568,0.49568,-0.065553,0.065553,-.125,.1/
&HOLE XB= -0.049553,0.049553,-0.49754,0.49754,-.125,.1/
&HOLE XB= -0.49754,0.49754,-0.049553,0.049553,-.125,.1/
&HOLE XB= -0.033553,0.033553,-0.49887,0.49887,-.125,.1/
&HOLE XB= -0.49887,0.49887,-0.033553,0.033553,-.125,.1/
&HOLE XB= -0.017553,0.017553,-0.49969,0.49969,-.125,.1/
&HOLE XB= -0.49969,0.49969,-0.017553,0.017553,-.125,.1/
&HOLE XB= -0.0015534,0.0015534,-0.5,0.5,-.125,.1/
&HOLE XB= -0.5,0.5,-0.0015534,0.0015534,-.125,.1/

```

Radial profiles of velocity and mass fraction

```

&DEVC XB= -0.50,0.50,0.0,0.0,0.3,0.3, QUANTITY='W-VELOCITY', ID
= 'Wp3', POINTS=21, X_ID='x' /
&DEVC XB= -0.50,0.50,0.0,0.0,0.5,0.5, QUANTITY='W-VELOCITY', ID
= 'Wp5', POINTS=21, HIDE_COORDINATES=.TRUE. /
&DEVC XB= -0.50,0.50,0.0,0.0,0.9,0.9, QUANTITY='W-VELOCITY', ID
= 'Wp9', POINTS=21, HIDE_COORDINATES=.TRUE. /

&DEVC XB= -0.50,0.50,0.0,0.0,0.3,0.3, QUANTITY='U-VELOCITY', ID
= 'Up3', POINTS=21, HIDE_COORDINATES=.TRUE. /
&DEVC XB= -0.50,0.50,0.0,0.0,0.5,0.5, QUANTITY='U-VELOCITY', ID
= 'Up5', POINTS=21, HIDE_COORDINATES=.TRUE. /
&DEVC XB= -0.50,0.50,0.0,0.0,0.9,0.9, QUANTITY='U-VELOCITY', ID
= 'Up9', POINTS=21, HIDE_COORDINATES=.TRUE. /

&DEVC XB= -0.50,0.50,0.0,0.0,0.3,0.3, QUANTITY='W-VELOCITY', ID
= 'Wp3_rms', STATISTICS='RMS', POINTS=21, HIDE_COORDINATES=.

```

```

TRUE. /
&DEVC XB= -0.50,0.50,0.0,0.0,0.5,0.5, QUANTITY='W-VELOCITY', ID
  ='Wp5_rms', STATISTICS='RMS', POINTS=21, HIDE_COORDINATES=.
TRUE. /
&DEVC XB= -0.50,0.50,0.0,0.0,0.9,0.9, QUANTITY='W-VELOCITY', ID
  ='Wp9_rms', STATISTICS='RMS', POINTS=21, HIDE_COORDINATES=.
TRUE. /

&DEVC XB= -0.50,0.50,0.0,0.0,0.3,0.3, QUANTITY='U-VELOCITY', ID
  ='Up3_rms', STATISTICS='RMS', POINTS=21, HIDE_COORDINATES=.
TRUE. /
&DEVC XB= -0.50,0.50,0.0,0.0,0.5,0.5, QUANTITY='U-VELOCITY', ID
  ='Up5_rms', STATISTICS='RMS', POINTS=21, HIDE_COORDINATES=.
TRUE. /
&DEVC XB= -0.50,0.50,0.0,0.0,0.9,0.9, QUANTITY='U-VELOCITY', ID
  ='Up9_rms', STATISTICS='RMS', POINTS=21, HIDE_COORDINATES=.
TRUE. /

&TAIL /

```

A.3 Sandia test 24

```

&HEAD CHID='Sandia_CH4_1m_Test24_dx1p5cm', TITLE='Sandia 1m med
  flow rate methane pool fire (Test 24), 1.5 cm resolution' /

&MULT ID='mesh array', DX=1.5,DY=1.5,DZ=1.0, LUPPER=1,J_UPPER
  =1,K_UPPER=3 /
&MESH IJK=96,96,64, XB= -1.5,0.0, -1.5,0.0, -.0625,0.9375, MULT_ID
  ='mesh array' /

&TIME T_END=20. /
&MISC TMPA=17.
  P_INF=81300.
  TURBULENCE_MODEL='VREMAN' /

&REAC FUEL='METHANE'
  HEAT_OF_COMBUSTION=49728.
  CRITICAL_FLAME_TEMPERATURE=1207 /

&RADI RADIATIVE_FRACTION=0.2 /
&DUMP SIG_FIGS=4, SIG_FIGS_EXP=2 /
&MAIL ID='STEEL', CONDUCTIVITY=54., SPECIFIC_HEAT=0.465,
  DENSITY=7850., EMISSIVITY=0.9 /

```



```

&SURF ID='PLATE' , COLOR='GRAY' , DEFAULT=.TRUE. , MATL_ID='STEEL
  ' , THICKNESS=0.025 /

&SURF ID='POOL' , MASS_FLUX(1)=0.053 , SPEC_ID(1)='METHANE' ,
  TMP_FRONT=15. /

&VENT XB=-0.5,0.5,-0.5,0.5,-.0625,-.0625 , COLOR='BLUE' , SURF_ID='
  POOL' /

&VENT XB=-1.5,-.5,-1.5,1.5,-.0625,-.0625 , SURF_ID='OPEN' /
&VENT XB=.5,1.5,-1.5,1.5,-.0625,-.0625 , SURF_ID='OPEN' /
&VENT XB=-1.5,1.5,-1.5,-.5,-.0625,-.0625 , SURF_ID='OPEN' /
&VENT XB=-1.5,1.5,.5,1.5,-.0625,-.0625 , SURF_ID='OPEN' /

&VENT MB='ZMAX' , SURF_ID='OPEN' /
&VENT MB='YMIN' , SURF_ID='OPEN' /
&VENT MB='YMAX' , SURF_ID='OPEN' /
&VENT MB='XMIN' , SURF_ID='OPEN' /
&VENT MB='XMAX' , SURF_ID='OPEN' /

&SLCF PBY=-.0625 , QUANTITY='VELOCITY' , VECTOR=.TRUE. /
&SLCF PBY=-.0625 , QUANTITY='DENSITY' , CELL_CENTERED=.TRUE. /
&SLCF PBY=-.0625 , QUANTITY='TEMPERATURE' , CELL_CENTERED=.TRUE.
  /
&SLCF PBY=-.0625 , QUANTITY='HRRPUV' , CELL_CENTERED=.TRUE. /
/&SLCF PBY=-.0625 , QUANTITY='HRRPUA' , CELL_CENTERED=.TRUE. /
&SLCF PBY=-.0625 , QUANTITY='MASS FRACTION' , SPEC_ID='METHANE' ,
  CELL_CENTERED=.TRUE. /
&SLCF PBY=-.0625 , QUANTITY='C_SMAG' , CELL_CENTERED=.TRUE. /
&SLCF PBY=-.0625 , QUANTITY='TURBULENCE RESOLUTION' ,
  CELL_CENTERED=.TRUE. /
&SLCF PBY=-.0625 , QUANTITY='WAVELET ERROR' , QUANTITY2='MASS
  FRACTION' , SPEC_ID='METHANE' , CELL_CENTERED=.TRUE. /

&OBST XB=-0.70711,0.70711,-0.70711,0.70711,-0.0625,0 /
&OBST XB=-0.70711,0.70711,-0.70711,0.70711,-0.0625,0 /
&OBST XB=-0.69211,0.69211,-0.7218,0.7218,-0.0625,0 /
&OBST XB=-0.7218,0.7218,-0.69211,0.69211,-0.0625,0 /
&OBST XB=-0.67711,0.67711,-0.73588,0.73588,-0.0625,0 /
&OBST XB=-0.73588,0.73588,-0.67711,0.67711,-0.0625,0 /
&OBST XB=-0.66211,0.66211,-0.74941,0.74941,-0.0625,0 /
&OBST XB=-0.74941,0.74941,-0.66211,0.66211,-0.0625,0 /
&OBST XB=-0.64711,0.64711,-0.7624,0.7624,-0.0625,0 /

```

```
&OBST XB= -0.7624,0.7624,-0.64711,0.64711,-0.0625,0 /
&OBST XB= -0.63211,0.63211,-0.77488,0.77488,-0.0625,0 /
&OBST XB= -0.77488,0.77488,-0.63211,0.63211,-0.0625,0 /
&OBST XB= -0.61711,0.61711,-0.78688,0.78688,-0.0625,0 /
&OBST XB= -0.78688,0.78688,-0.61711,0.61711,-0.0625,0 /
&OBST XB= -0.60211,0.60211,-0.79842,0.79842,-0.0625,0 /
&OBST XB= -0.79842,0.79842,-0.60211,0.60211,-0.0625,0 /
&OBST XB= -0.58711,0.58711,-0.80951,0.80951,-0.0625,0 /
&OBST XB= -0.80951,0.80951,-0.58711,0.58711,-0.0625,0 /
&OBST XB= -0.57211,0.57211,-0.82018,0.82018,-0.0625,0 /
&OBST XB= -0.82018,0.82018,-0.57211,0.57211,-0.0625,0 /
&OBST XB= -0.55711,0.55711,-0.83044,0.83044,-0.0625,0 /
&OBST XB= -0.83044,0.83044,-0.55711,0.55711,-0.0625,0 /
&OBST XB= -0.54211,0.54211,-0.84031,0.84031,-0.0625,0 /
&OBST XB= -0.84031,0.84031,-0.54211,0.54211,-0.0625,0 /
&OBST XB= -0.52711,0.52711,-0.8498,0.8498,-0.0625,0 /
&OBST XB= -0.8498,0.8498,-0.52711,0.52711,-0.0625,0 /
&OBST XB= -0.51211,0.51211,-0.85892,0.85892,-0.0625,0 /
&OBST XB= -0.85892,0.85892,-0.51211,0.51211,-0.0625,0 /
&OBST XB= -0.49711,0.49711,-0.86769,0.86769,-0.0625,0 /
&OBST XB= -0.86769,0.86769,-0.49711,0.49711,-0.0625,0 /
&OBST XB= -0.48211,0.48211,-0.87611,0.87611,-0.0625,0 /
&OBST XB= -0.87611,0.87611,-0.48211,0.48211,-0.0625,0 /
&OBST XB= -0.46711,0.46711,-0.8842,0.8842,-0.0625,0 /
&OBST XB= -0.8842,0.8842,-0.46711,0.46711,-0.0625,0 /
&OBST XB= -0.45211,0.45211,-0.89196,0.89196,-0.0625,0 /
&OBST XB= -0.89196,0.89196,-0.45211,0.45211,-0.0625,0 /
&OBST XB= -0.43711,0.43711,-0.89941,0.89941,-0.0625,0 /
&OBST XB= -0.89941,0.89941,-0.43711,0.43711,-0.0625,0 /
&OBST XB= -0.42211,0.42211,-0.90655,0.90655,-0.0625,0 /
&OBST XB= -0.90655,0.90655,-0.42211,0.42211,-0.0625,0 /
&OBST XB= -0.40711,0.40711,-0.91338,0.91338,-0.0625,0 /
&OBST XB= -0.91338,0.91338,-0.40711,0.40711,-0.0625,0 /
&OBST XB= -0.39211,0.39211,-0.91992,0.91992,-0.0625,0 /
&OBST XB= -0.91992,0.91992,-0.39211,0.39211,-0.0625,0 /
&OBST XB= -0.37711,0.37711,-0.92617,0.92617,-0.0625,0 /
&OBST XB= -0.92617,0.92617,-0.37711,0.37711,-0.0625,0 /
&OBST XB= -0.36211,0.36211,-0.93214,0.93214,-0.0625,0 /
&OBST XB= -0.93214,0.93214,-0.36211,0.36211,-0.0625,0 /
&OBST XB= -0.34711,0.34711,-0.93783,0.93783,-0.0625,0 /
&OBST XB= -0.93783,0.93783,-0.34711,0.34711,-0.0625,0 /
&OBST XB= -0.33211,0.33211,-0.94324,0.94324,-0.0625,0 /
&OBST XB= -0.94324,0.94324,-0.33211,0.33211,-0.0625,0 /
```

```
&OBST XB= -0.31711,0.31711,-0.94839,0.94839,-0.0625,0 /
&OBST XB= -0.94839,0.94839,-0.31711,0.31711,-0.0625,0 /
&OBST XB= -0.30211,0.30211,-0.95327,0.95327,-0.0625,0 /
&OBST XB= -0.95327,0.95327,-0.30211,0.30211,-0.0625,0 /
&OBST XB= -0.28711,0.28711,-0.9579,0.9579,-0.0625,0 /
&OBST XB= -0.9579,0.9579,-0.28711,0.28711,-0.0625,0 /
&OBST XB= -0.27211,0.27211,-0.96227,0.96227,-0.0625,0 /
&OBST XB= -0.96227,0.96227,-0.27211,0.27211,-0.0625,0 /
&OBST XB= -0.25711,0.25711,-0.96638,0.96638,-0.0625,0 /
&OBST XB= -0.96638,0.96638,-0.25711,0.25711,-0.0625,0 /
&OBST XB= -0.24211,0.24211,-0.97025,0.97025,-0.0625,0 /
&OBST XB= -0.97025,0.97025,-0.24211,0.24211,-0.0625,0 /
&OBST XB= -0.22711,0.22711,-0.97387,0.97387,-0.0625,0 /
&OBST XB= -0.97387,0.97387,-0.22711,0.22711,-0.0625,0 /
&OBST XB= -0.21211,0.21211,-0.97725,0.97725,-0.0625,0 /
&OBST XB= -0.97725,0.97725,-0.21211,0.21211,-0.0625,0 /
&OBST XB= -0.19711,0.19711,-0.98038,0.98038,-0.0625,0 /
&OBST XB= -0.98038,0.98038,-0.19711,0.19711,-0.0625,0 /
&OBST XB= -0.18211,0.18211,-0.98328,0.98328,-0.0625,0 /
&OBST XB= -0.98328,0.98328,-0.18211,0.18211,-0.0625,0 /
&OBST XB= -0.16711,0.16711,-0.98594,0.98594,-0.0625,0 /
&OBST XB= -0.98594,0.98594,-0.16711,0.16711,-0.0625,0 /
&OBST XB= -0.15211,0.15211,-0.98836,0.98836,-0.0625,0 /
&OBST XB= -0.98836,0.98836,-0.15211,0.15211,-0.0625,0 /
&OBST XB= -0.13711,0.13711,-0.99056,0.99056,-0.0625,0 /
&OBST XB= -0.99056,0.99056,-0.13711,0.13711,-0.0625,0 /
&OBST XB= -0.12211,0.12211,-0.99252,0.99252,-0.0625,0 /
&OBST XB= -0.99252,0.99252,-0.12211,0.12211,-0.0625,0 /
&OBST XB= -0.10711,0.10711,-0.99425,0.99425,-0.0625,0 /
&OBST XB= -0.99425,0.99425,-0.10711,0.10711,-0.0625,0 /
&OBST XB= -0.092107,0.092107,-0.99575,0.99575,-0.0625,0 /
&OBST XB= -0.99575,0.99575,-0.092107,0.092107,-0.0625,0 /
&OBST XB= -0.077107,0.077107,-0.99702,0.99702,-0.0625,0 /
&OBST XB= -0.99702,0.99702,-0.077107,0.077107,-0.0625,0 /
&OBST XB= -0.062107,0.062107,-0.99807,0.99807,-0.0625,0 /
&OBST XB= -0.99807,0.99807,-0.062107,0.062107,-0.0625,0 /
&OBST XB= -0.047107,0.047107,-0.99889,0.99889,-0.0625,0 /
&OBST XB= -0.99889,0.99889,-0.047107,0.047107,-0.0625,0 /
&OBST XB= -0.032107,0.032107,-0.99948,0.99948,-0.0625,0 /
&OBST XB= -0.99948,0.99948,-0.032107,0.032107,-0.0625,0 /
&OBST XB= -0.017107,0.017107,-0.99985,0.99985,-0.0625,0 /
&OBST XB= -0.99985,0.99985,-0.017107,0.017107,-0.0625,0 /
&OBST XB= -0.0021068,0.0021068,-1,1,-0.0625,0 /
```

```
&OBST XB= -1,1,-0.0021068,0.0021068,-0.0625,0 /

&HOLE XB= -0.35355,0.35355,-0.35355,0.35355,-.125,.1/
&HOLE XB= -0.35355,0.35355,-0.35355,0.35355,-.125,.1/
&HOLE XB= -0.33755,0.33755,-0.36886,0.36886,-.125,.1/
&HOLE XB= -0.36886,0.36886,-0.33755,0.33755,-.125,.1/
&HOLE XB= -0.32155,0.32155,-0.38289,0.38289,-.125,.1/
&HOLE XB= -0.38289,0.38289,-0.32155,0.32155,-.125,.1/
&HOLE XB= -0.30555,0.30555,-0.39577,0.39577,-.125,.1/
&HOLE XB= -0.39577,0.39577,-0.30555,0.30555,-.125,.1/
&HOLE XB= -0.28955,0.28955,-0.40763,0.40763,-.125,.1/
&HOLE XB= -0.40763,0.40763,-0.28955,0.28955,-.125,.1/
&HOLE XB= -0.27355,0.27355,-0.41853,0.41853,-.125,.1/
&HOLE XB= -0.41853,0.41853,-0.27355,0.27355,-.125,.1/
&HOLE XB= -0.25755,0.25755,-0.42856,0.42856,-.125,.1/
&HOLE XB= -0.42856,0.42856,-0.25755,0.25755,-.125,.1/
&HOLE XB= -0.24155,0.24155,-0.43778,0.43778,-.125,.1/
&HOLE XB= -0.43778,0.43778,-0.24155,0.24155,-.125,.1/
&HOLE XB= -0.22555,0.22555,-0.44623,0.44623,-.125,.1/
&HOLE XB= -0.44623,0.44623,-0.22555,0.22555,-.125,.1/
&HOLE XB= -0.20955,0.20955,-0.45397,0.45397,-.125,.1/
&HOLE XB= -0.45397,0.45397,-0.20955,0.20955,-.125,.1/
&HOLE XB= -0.19355,0.19355,-0.46102,0.46102,-.125,.1/
&HOLE XB= -0.46102,0.46102,-0.19355,0.19355,-.125,.1/
&HOLE XB= -0.17755,0.17755,-0.46741,0.46741,-.125,.1/
&HOLE XB= -0.46741,0.46741,-0.17755,0.17755,-.125,.1/
&HOLE XB= -0.16155,0.16155,-0.47318,0.47318,-.125,.1/
&HOLE XB= -0.47318,0.47318,-0.16155,0.16155,-.125,.1/
&HOLE XB= -0.14555,0.14555,-0.47835,0.47835,-.125,.1/
&HOLE XB= -0.47835,0.47835,-0.14555,0.14555,-.125,.1/
&HOLE XB= -0.12955,0.12955,-0.48292,0.48292,-.125,.1/
&HOLE XB= -0.48292,0.48292,-0.12955,0.12955,-.125,.1/
&HOLE XB= -0.11355,0.11355,-0.48693,0.48693,-.125,.1/
&HOLE XB= -0.48693,0.48693,-0.11355,0.11355,-.125,.1/
&HOLE XB= -0.097553,0.097553,-0.49039,0.49039,-.125,.1/
&HOLE XB= -0.49039,0.49039,-0.097553,0.097553,-.125,.1/
&HOLE XB= -0.081553,0.081553,-0.4933,0.4933,-.125,.1/
&HOLE XB= -0.4933,0.4933,-0.081553,0.081553,-.125,.1/
&HOLE XB= -0.065553,0.065553,-0.49568,0.49568,-.125,.1/
&HOLE XB= -0.49568,0.49568,-0.065553,0.065553,-.125,.1/
&HOLE XB= -0.049553,0.049553,-0.49754,0.49754,-.125,.1/
&HOLE XB= -0.49754,0.49754,-0.049553,0.049553,-.125,.1/
&HOLE XB= -0.033553,0.033553,-0.49887,0.49887,-.125,.1/
```

```

&HOLE XB= -0.49887,0.49887,-0.033553,0.033553,-.125,.1/
&HOLE XB= -0.017553,0.017553,-0.49969,0.49969,-.125,.1/
&HOLE XB= -0.49969,0.49969,-0.017553,0.017553,-.125,.1/
&HOLE XB= -0.0015534,0.0015534,-0.5,0.5,-.125,.1/
&HOLE XB= -0.5,0.5,-0.0015534,0.0015534,-.125,.1/

```

Radial profiles of velocity and mass fraction

```

&DEVC XB= -0.50,0.50,0.0,0.0,0.3,0.3, QUANTITY='W-VELOCITY', ID
  ='Wp3', POINTS=21, X_ID='x' /
&DEVC XB= -0.50,0.50,0.0,0.0,0.5,0.5, QUANTITY='W-VELOCITY', ID
  ='Wp5', POINTS=21, HIDE_COORDINATES=.TRUE. /
&DEVC XB= -0.50,0.50,0.0,0.0,0.9,0.9, QUANTITY='W-VELOCITY', ID
  ='Wp9', POINTS=21, HIDE_COORDINATES=.TRUE. /

&DEVC XB= -0.50,0.50,0.0,0.0,0.3,0.3, QUANTITY='U-VELOCITY', ID
  ='Up3', POINTS=21, HIDE_COORDINATES=.TRUE. /
&DEVC XB= -0.50,0.50,0.0,0.0,0.5,0.5, QUANTITY='U-VELOCITY', ID
  ='Up5', POINTS=21, HIDE_COORDINATES=.TRUE. /
&DEVC XB= -0.50,0.50,0.0,0.0,0.9,0.9, QUANTITY='U-VELOCITY', ID
  ='Up9', POINTS=21, HIDE_COORDINATES=.TRUE. /

&DEVC XB= -0.50,0.50,0.0,0.0,0.3,0.3, QUANTITY='W-VELOCITY', ID
  ='Wp3_rms', STATISTICS='RMS', POINTS=21, HIDE_COORDINATES=.
  TRUE. /
&DEVC XB= -0.50,0.50,0.0,0.0,0.5,0.5, QUANTITY='W-VELOCITY', ID
  ='Wp5_rms', STATISTICS='RMS', POINTS=21, HIDE_COORDINATES=.
  TRUE. /
&DEVC XB= -0.50,0.50,0.0,0.0,0.9,0.9, QUANTITY='W-VELOCITY', ID
  ='Wp9_rms', STATISTICS='RMS', POINTS=21, HIDE_COORDINATES=.
  TRUE. /

&DEVC XB= -0.50,0.50,0.0,0.0,0.3,0.3, QUANTITY='U-VELOCITY', ID
  ='Up3_rms', STATISTICS='RMS', POINTS=21, HIDE_COORDINATES=.
  TRUE. /
&DEVC XB= -0.50,0.50,0.0,0.0,0.5,0.5, QUANTITY='U-VELOCITY', ID
  ='Up5_rms', STATISTICS='RMS', POINTS=21, HIDE_COORDINATES=.
  TRUE. /
&DEVC XB= -0.50,0.50,0.0,0.0,0.9,0.9, QUANTITY='U-VELOCITY', ID
  ='Up9_rms', STATISTICS='RMS', POINTS=21, HIDE_COORDINATES=.
  TRUE. /

&TAIL /

```

A.4 Heskestad

```

&HEAD CHID='Qs=10000_RI=20', TITLE='Flame Height Test , Q
      *=10000' /
&MESH IJK=65,65,160, XB=-72.0,72.0,-72.0,72.0,-18.0,342. /
&MISC TURBULENCE_MODEL='VREMAN' /
&TIME T_END=200. /

&REAC FUEL='PROPANE', C=3., H=8., SOOT_YIELD=0.015 /
&SURF ID='burner', HRRPUA=15127250., COLOR='RED' /
&OBST XB=-0.5,0.5,-0.5,0.5,-5.0,0.0, SURF_IDS='burner', 'INERT
      ', 'INERT', THICKEN=.TRUE. /

&VENT MB='XMIN', SURF_ID='OPEN' /
&VENT MB='XMAX', SURF_ID='OPEN' /
&VENT MB='YMIN', SURF_ID='OPEN' /
&VENT MB='YMAX', SURF_ID='OPEN' /
&VENT MB='ZMIN', SURF_ID='OPEN' /
&VENT MB='ZMAX', SURF_ID='OPEN' /

&SLCF PBY=0., QUANTITY='TEMPERATURE', VECTOR=.TRUE. /
&SLCF PBY=0., QUANTITY='HRRPUV' /
&SLCF PBY=0., QUANTITY='MIXING TIME' /
&DEVC XB=0.0,0.0,0.0,0.0,1.12,340.77, QUANTITY='HRRPUL', POINTS
      =152, Z_ID='Height', ID='HRRPUL' /
&TAIL /

```

A.5 McCaffery

```

&HEAD CHID='McCaffrey_57_kW_fine', TITLE='McCaffrey, NBSIR
      79-1910, 57 kW Natural Gas' /
&MISC TURBULENCE_MODEL='VREMAN' /
&MULT ID='mesh', DX=0.62, DY=0.62, DZ=1.55, L_UPPER=2, J_UPPER
      =2, K_UPPER=3 /
&MESH IJK=40,40,100, XB=-0.93,-0.31,-0.93,-0.31,-0.248,1.302,
      MULT_ID='mesh' /

&TIME T_END=30. /

&SURF ID='burner', HRRPUA=639., TMP_FRONT=100., COLOR='RED' /
&OBST XB=-.15,0.15,-.15,0.15,-.10,0.00, SURF_IDS='burner', 'INERT
      ', 'INERT' /

```

```

&REAC FUEL='METHANE'
      C=1.
      H=4.
      CO_YIELD=0.0
      SOOT_YIELD=0.0 /

&RADI RADIATIVEFRACTION=0.20 /

&VENT MB='XMIN' , SURF_ID='OPEN' /
&VENT MB='XMAX' , SURF_ID='OPEN' /
&VENT MB='YMIN' , SURF_ID='OPEN' /
&VENT MB='YMAX' , SURF_ID='OPEN' /
&VENT MB='ZMAX' , SURF_ID='OPEN' /
&VENT MB='ZMIN' , SURF_ID='OPEN' /

&DEVC ID='temp20' , XB=0.00,0.00,0.00,0.00,0.0155,5.9365 , POINTS
      =192, QUANTITY='TEMPERATURE' , Z_ID='Height' /
&DEVC ID='velo20' , XB=0.00,0.00,0.00,0.00,0.0155,5.9365 , POINTS
      =192, QUANTITY='W-VELOCITY' , HIDE_COORDINATES=.TRUE. /

&DEVC XYZ=0,0,0.3 , QUANTITY='W-VELOCITY' /

&SLCF PBY=0.0 , QUANTITY='WAVELET ERROR' , QUANTITY2='MASS
      FRACTION' , SPEC_ID='METHANE' /
&SLCF PBY=0.0 , QUANTITY='WAVELET ERROR' , QUANTITY2='HRRPUV' /
&SLCF PBY=0.0 , QUANTITY='WAVELET ERROR' , QUANTITY2='TEMPERATURE
      ' /
&SLCF PBY=0.0 , QUANTITY='TURBULENCE RESOLUTION' /

&SLCF PBY=0.0,QUANTITY='TEMPERATURE' ,VECTOR=.TRUE. /
&SLCF PBY=0.0,QUANTITY='HRRPUV' /

&TAIL /

```

Appendix B

Implemented code

B.1 fire.f90

```
1 MODULE FIRE
2
3 ! Compute combustion
4
5 USE PRECISION_PARAMETERS
6 USE GLOBAL_CONSTANTS
7 USE MESH_POINTERS
8 USE COMP_FUNCTIONS, ONLY: SECOND
9
10 IMPLICIT NONE
11 PRIVATE
12 CHARACTER(255), PARAMETER :: fireid='$Id:_fire.f90_10216_
    2012-03-08_16:22:22Z_craigweinschenk_$'
13 CHARACTER(255), PARAMETER :: firerev='$Revision:_10216_$'
14 CHARACTER(255), PARAMETER :: firedate='$Date:_2012-03-08_
    17:22:22_+0100_(to,_08_mar_2012)__$'
15
16 TYPE(REACTION_TYPE), POINTER :: RN=>NULL()
17 REAL(EB) :: Q_UPPER
18
19 PUBLIC COMBUSTION, GET_REV_fire
20
21 CONTAINS
22
23
24 SUBROUTINE COMBUSTION(NM)
25
26 INTEGER, INTENT(IN) :: NM
```



```

27 REAL(EB) :: TNOW
28
29 IF (EVACUATION_ONLY(NM)) RETURN
30
31 TNOW=SECOND()
32
33 IF (INIT_HRRPUV) RETURN
34
35 CALL POINT_TO_MESH(NM)
36
37 !CALL COMPUTE_STRAIN_RATE(NM)
38
39 ! Upper bounds on local HRR per unit volume
40
41 Q_UPPER = HRRPUA_SHEET/CELL_SIZE + HRRPUV_AVERAGE
42
43 ! Call combustion ODE solver
44 CALL COMBUSTION_GENERAL
45
46 TUSED(10,NM)=TUSED(10,NM)+SECOND()-TNOW
47
48 END SUBROUTINE COMBUSTION
49
50
51 SUBROUTINE COMBUSTION_GENERAL
52
53 ! Generic combustion routine for multi step reactions with
54 ! kinetics either mixing controlled, finite rate,
55 ! or a temperature threshold mixed approach
56 USE PHYSICAL_FUNCTIONS, ONLY: GET_SPECIFIC_GAS_CONSTANT,
57     GET_MASS_FRACTION_ALL, GET_SPECIFIC_HEAT, GET_MOLECULAR_WEIGHT
58     , &
59     GET_SENSIBLE_ENTHALPY_DIFF,
60     GET_MASS_FRACTION !ADDED
61 INTEGER :: I, J, K, NS, NR, II, JJ, KK, IIG, JJG, KKG, IW, N
62 REAL(EB) :: ZZ_GET(0:N_TRACKED_SPECIES), ZZ_MIN=1.E-10_EB, DZZ(0:
63     N_TRACKED_SPECIES), CP, HDIFF, Y_O2, Y_FUEL, Y_PRODUCT !ADDED
64 LOGICAL :: DO_REACTION, REACTANTS_PRESENT, Q_EXISTS
65 TYPE (REACTION_TYPE), POINTER :: RN
66 TYPE (SPECIES_MIXTURE_TYPE), POINTER :: SM, SM0
67
68 Q = 0. _EB

```

```

65 D_REACTION = 0._EB
66 Q_EXISTS = .FALSE.
67 SMO => SPECIES_MIXTURE(0)
68
69 DO K=1,KBAR
70   DO J=1,JBAR
71     ILOOP: DO I=1,IBAR
72       !Check to see if a reaction is possible
73       IF (SOLID(CELL_INDEX(I,J,K))) CYCLE ILOOP
74       ZZ_GET(1:N_TRACKED_SPECIES) = ZZ(I,J,K,1:
       N_TRACKED_SPECIES)
75       ZZ_GET(0) = 1._EB - MIN(1._EB,SUM(ZZ_GET(1:
       N_TRACKED_SPECIES)))
76       DO_REACTION = .FALSE.
77       DO NR=1,N_REACTIONS
78         RN=>REACTION(NR)
79         REACTANTS_PRESENT = .TRUE.
80         DO NS=0,N_TRACKED_SPECIES
81           IF (RN%NU(NS)<0._EB .AND. ZZ_GET(NS) < ZZ_MIN)
82             THEN
83               REACTANTS_PRESENT = .FALSE.
84               EXIT
85             ENDDIF
86           END DO
87           IF (.NOT. DO_REACTION) DO_REACTION =
88             REACTANTS_PRESENT
89         END DO
90         IF (.NOT. DO_REACTION) CYCLE ILOOP
91         DZZ(1:N_TRACKED_SPECIES) = ZZ_GET(1:N_TRACKED_SPECIES)
92         ! store old ZZ for divergence term
93         ! Easily allow for user selected ODE solver
94         SELECT CASE (COMBUSTION_ODE)
95         CASE(SINGLE_EXACT)
96           !CALL ODE_EXACT(I,J,K,ZZ_GET,Q(I,J,K))
97           CALL ODE_EXPLICIT_EULER(I,J,K,ZZ_GET,Q(I,J,K))
98         CASE(EXPLICIT_EULER)
99           CALL ODE_EXPLICIT_EULER(I,J,K,ZZ_GET,Q(I,J,K))
100        CASE(RUNGE_KUTTA_2)
101          CALL ODE_RUNGE_KUTTA_2(I,J,K,ZZ_GET,Q(I,J,K))
102        CASE(RK2_RICHARDSON)
103          CALL ODE_RK2_RICHARDSON(I,J,K,ZZ_GET,Q(I,J,K))
104        END SELECT

```

```

103      ! Update RSUM and ZZ
104      IF (ABS(Q(I , J ,K)) > ZERO_P) THEN
105          Q_EXISTS = .TRUE.
106          CALL GET_SPECIFIC_GAS_CONSTANT(ZZ_GET ,RSUM(I , J ,K) )
107          TMP(I , J ,K) = PBAR(K,PRESSURE_ZONE(I , J ,K) )/(RSUM(I , J
108              ,K)*RHO(I , J ,K) )
109          ZZ(I , J ,K,1:N_TRACKED_SPECIES) = ZZ_GET(1:
110              N_TRACKED_SPECIES)
111          ! Divergence term
112          DZZ(1:N_TRACKED_SPECIES) = ZZ_GET(1:
113              N_TRACKED_SPECIES) - DZZ(1:N_TRACKED_SPECIES)
114          CALL GET_SPECIFIC_HEAT(ZZ_GET ,CP ,TMP(I , J ,K) )
115          DO N=1,N_TRACKED_SPECIES
116              SM => SPECIES_MIXTURE(N)
117              CALL GET_SENSIBLE_ENTHALPY_DIFF(N,TMP(I , J ,K) ,
118                  HDIFF)
119              D_REACTION(I , J ,K) = D_REACTION(I , J ,K) + ( (SM%
120                  RCON-SM0%RCON) /RSUM(I , J ,K) - &
121
122
123
124
125
126
127
128
129
130
131
132
133
134
135
136
137
138
139
140
141
142
143
144
145
146
147
148
149
150
151
152
153
154
155
156
157
158
159
160
161
162
163
164
165
166
167
168
169
170
171
172
173
174
175
176
177
178
179
180
181
182
183
184
185
186
187
188
189
190
191
192
193
194
195
196
197
198
199
200
201
202
203
204
205
206
207
208
209
210
211
212
213
214
215
216
217
218
219
220
221
222
223
224
225
226
227
228
229
230
231
232
233
234
235
236
237
238
239
240
241
242
243
244
245
246
247
248
249
250
251
252
253
254
255
256
257
258
259
260
261
262
263
264
265
266
267
268
269
270
271
272
273
274
275
276
277
278
279
280
281
282
283
284
285
286
287
288
289
290
291
292
293
294
295
296
297
298
299
300
301
302
303
304
305
306
307
308
309
310
311
312
313
314
315
316
317
318
319
320
321
322
323
324
325
326
327
328
329
330
331
332
333
334
335
336
337
338
339
340
341
342
343
344
345
346
347
348
349
350
351
352
353
354
355
356
357
358
359
360
361
362
363
364
365
366
367
368
369
370
371
372
373
374
375
376
377
378
379
380
381
382
383
384
385
386
387
388
389
390
391
392
393
394
395
396
397
398
399
400
401
402
403
404
405
406
407
408
409
410
411
412
413
414
415
416
417
418
419
420
421
422
423
424
425
426
427
428
429
430
431
432
433
434
435
436
437
438
439
440
441
442
443
444
445
446
447
448
449
450
451
452
453
454
455
456
457
458
459
460
461
462
463
464
465
466
467
468
469
470
471
472
473
474
475
476
477
478
479
480
481
482
483
484
485
486
487
488
489
490
491
492
493
494
495
496
497
498
499
500
501
502
503
504
505
506
507
508
509
510
511
512
513
514
515
516
517
518
519
520
521
522
523
524
525
526
527
528
529
530
531
532
533
534
535
536
537
538
539
540
541
542
543
544
545
546
547
548
549
550
551
552
553
554
555
556
557
558
559
560
561
562
563
564
565
566
567
568
569
570
571
572
573
574
575
576
577
578
579
580
581
582
583
584
585
586
587
588
589
590
591
592
593
594
595
596
597
598
599
600
601
602
603
604
605
606
607
608
609
610
611
612
613
614
615
616
617
618
619
620
621
622
623
624
625
626
627
628
629
630
631
632
633
634
635
636
637
638
639
640
641
642
643
644
645
646
647
648
649
650
651
652
653
654
655
656
657
658
659
660
661
662
663
664
665
666
667
668
669
670
671
672
673
674
675
676
677
678
679
680
681
682
683
684
685
686
687
688
689
690
691
692
693
694
695
696
697
698
699
700
701
702
703
704
705
706
707
708
709
710
711
712
713
714
715
716
717
718
719
720
721
722
723
724
725
726
727
728
729
730
731
732
733
734
735
736
737
738
739
740
741
742
743
744
745
746
747
748
749
750
751
752
753
754
755
756
757
758
759
760
761
762
763
764
765
766
767
768
769
770
771
772
773
774
775
776
777
778
779
780
781
782
783
784
785
786
787
788
789
790
791
792
793
794
795
796
797
798
799
800
801
802
803
804
805
806
807
808
809
810
811
812
813
814
815
816
817
818
819
820
821
822
823
824
825
826
827
828
829
830
831
832
833
834
835
836
837
838
839
840
841
842
843
844
845
846
847
848
849
850
851
852
853
854
855
856
857
858
859
860
861
862
863
864
865
866
867
868
869
870
871
872
873
874
875
876
877
878
879
880
881
882
883
884
885
886
887
888
889
890
891
892
893
894
895
896
897
898
899
900
901
902
903
904
905
906
907
908
909
910
911
912
913
914
915
916
917
918
919
920
921
922
923
924
925
926
927
928
929
930
931
932
933
934
935
936
937
938
939
940
941
942
943
944
945
946
947
948
949
950
951
952
953
954
955
956
957
958
959
960
961
962
963
964
965
966
967
968
969
970
971
972
973
974
975
976
977
978
979
980
981
982
983
984
985
986
987
988
989
990
991
992
993
994
995
996
997
998
999
1000

```

```

130     JJ = WALL(IW)%ONE_D%JJ
131     KK = WALL(IW)%ONE_D%KK
132     IIG = WALL(IW)%ONE_D%IIG
133     JJG = WALL(IW)%ONE_D%JJG
134     KKG = WALL(IW)%ONE_D%KKG
135     Q( II , JJ ,KK) = Q( IIG , JJG ,KKG)
136 ENDDO
137
138 END SUBROUTINE COMBUSTION_GENERAL
139
140 SUBROUTINE ODEEXACT( I , J ,K , ZZ_GET , Q_NEW)
141 INTEGER,INTENT(IN) :: I , J ,K
142 REAL(EB) ,INTENT(OUT) :: Q_NEW
143 REAL(EB) ,INTENT(INOUT) :: ZZ_GET (0:N_TRACKED_SPECIES)
144 REAL(EB) :: DZF , Q_BOUND_1 , Q_BOUND_2 , RATE_CONSTANT , Z_LIMITER ,
      REACTANT_MIN , DT2
145 LOGICAL :: MIN_FOUND
146 INTEGER :: NS
147 TYPE(REACTION_TYPE) ,POINTER :: RN=>NULL()
148
149 Q_NEW = 0._EB
150 RN=>REACTION(1)
151 CALL COMPUTE_RATE_CONSTANT(1 , RN%MODE , 1 , 0._EB , RATE_CONSTANT ,
      ZZ_GET , I , J ,K)
152
153 IF (RATE_CONSTANT < ZERO_P) RETURN
154
155 Z_LIMITER = RATE_CONSTANT*MIX_TIME(I , J ,K)
156
157 DZF = -1._EB
158 !Check for reactant (i.e. fuel or oxidizer) limited combustion
159 MIN_FOUND = .FALSE.
160 REACTANT_MIN=1._EB
161 DO NS=0,N_TRACKED_SPECIES
162     IF (RN%NU(NS) < -ZERO_P) &
163         REACTANT_MIN = MIN( REACTANT_MIN , -ZZ_GET(NS) *
            SPECIES_MIXTURE (RN%FUEL_SMIX_INDEX)%MW / (
            SPECIES_MIXTURE (NS)%MW * RN%NU(NS) ) )
164     IF (ABS(Z_LIMITER - REACTANT_MIN) <= SPACING(Z_LIMITER))
        THEN
165         MIN_FOUND = .TRUE.
166         DZF = REACTANT_MIN * (1._EB - EXP(-DT/MIX_TIME(I , J ,K)))
167     EXIT

```

```

168     ENDIF
169 ENDDO
170
171 !For product limited combsiton find time of switch from product
172 limited to reactant limited (if it occurs)
173 !and do two step exact solution
173 IF (.NOT. MIN_FOUND) THEN
174     DT2 = MIX_TIME(I , J ,K) *LOG((Z_LIMITER+REACTANT_MIN) / (2. _EB*
175         Z_LIMITER))
175     IF (DT2 < DT) THEN
176         DZF = ZZ_GET(RN%FUEL_SMIX_INDEX) - Z_LIMITER*(EXP(DT2/
177             MIX_TIME(I , J ,K)) - 1._EB)
177         REACTANT_MIN = REACTANT_MIN - DZF
178         DZF = DZF + REACTANT_MIN*(1. _EB-EXP(-(DT-DT2)/MIX_TIME(I ,
179             J ,K)))
179     ELSE
180         DZF = ZZ_GET(RN%FUEL_SMIX_INDEX) - Z_LIMITER*(EXP(DT/
181             MIX_TIME(I , J ,K)) - 1._EB)
181     ENDIF
182 ENDIF
183
184 DZF = MIN(DZF, ZZ_GET(RN%FUEL_SMIX_INDEX))
185
186 !***** TEMP OVERRIDE TO ENSURE SAME RESULTS AS PREVIOUS
187 *****
187 !DZF = Z_LIMITER*(1. _EB-EXP(-DT/MIX_TIME(I , J ,K)))
188 !
189 *****
189
190 Q_BOUND_1 = DZF*RHO(I , J ,K) *RN%HEAT_OF_COMBUSTION/DT
191 Q_BOUND_2 = Q_UPPER
192 Q_NEW = MIN(Q_BOUND_1, Q_BOUND_2)
193 DZF = Q_NEW*DT / (RHO(I , J ,K) *RN%HEAT_OF_COMBUSTION)
194
195 ZZ_GET = ZZ_GET + DZF*RN%NU*SPECIES_MIXTURE%MW/SPECIES_MIXTURE(
196     RN%FUEL_SMIX_INDEX)%MW
196
197 END SUBROUTINE ODE_EXACT
198
199
200 SUBROUTINE ODE_EXPLICIT_EULER(I , J ,K, ZZ_GET , Q_OUT)
201 INTEGER,INTENT(IN) :: I , J ,K

```

```

202 REAL(EB) ,INTENT(OUT) :: Q_OUT
203 REAL(EB) ,INTENT(INOUT) :: ZZ_GET(0:N_TRACKED_SPECIES)
204 REAL(EB) :: ZZ_0(0:N_TRACKED_SPECIES) , ZZ_I(0:N_TRACKED_SPECIES)
      , ZZ_N(0:N_TRACKED_SPECIES) , DZZDT(0:N_TRACKED_SPECIES) , &
205      DT_ODE, DT_NEW, RATE_CONSTANT(1:N_REACTIONS) , Q_NR(1:
      N_REACTIONS) , Q_SUM, DT_SUM
206 INTEGER :: NR, I_TS , NS
207 INTEGER, PARAMETER :: NODETS=20
208 TYPE(REACTION_TYPE) , POINTER :: RN=>NULL()
209
210 Q_OUT = 0._EB
211 ZZ_0 = MAX(0._EB , ZZ_GET)
212 ZZ_I = ZZ_0
213 DT_ODE = DT/REAL(NODETS,EB)
214 DT_NEW = DT_ODE
215 DT_SUM = 0._EB
216 I_TS = 1
217 ODELOOP: DO WHILE (DT_SUM < DT)
218     DZZDT = 0._EB
219     RATE_CONSTANT = 0._EB
220     Q_NR = 0._EB
221     REACTIONLOOP: DO NR = 1 , N_REACTIONS
222         RN => REACTION(NR)
223         CALL COMPUTE_RATE_CONSTANT(NR, RN%MODE, I_TS , Q_OUT,
      RATE_CONSTANT(NR) , ZZ_I , I , J , K)
224         IF (RATE_CONSTANT(NR) < ZERO_P) CYCLE REACTIONLOOP
225         Q_NR(NR) = RATE_CONSTANT(NR) * RN%HEAT_OF_COMBUSTION * RHO(I ,
      J , K)
226         DZZDT = DZZDT + RN%NU * SPECIES_MIXTURE%MW /
      SPECIES_MIXTURE(RN%FUEL_SMIX_INDEX)%MW * RATE_CONSTANT(
      NR)
227     END DO REACTIONLOOP
228     IF (ALL(DZZDT < ZERO_P)) EXIT ODELOOP
229     ZZ_N = ZZ_I + DZZDT * DT_NEW
230
231     IF (ANY(ZZ_N < 0._EB)) THEN
232         DO NS=0, N_TRACKED_SPECIES
233             IF (ZZ_N(NS) < 0._EB .AND. ABS(DZZDT(NS)) > ZERO_P)
      DT_NEW = MIN(DT_NEW, -ZZ_I(NS) / DZZDT(NS))
234         ENDDO
235     ENDIF
236
237     Q_SUM = SUM(Q_NR)

```

```

238   IF (Q_OUT + Q_SUM*DT_NEW > Q_UPPER * DT) THEN
239     DT_NEW = MAX(0._EB, (Q_UPPER * DT - Q_OUT)) / Q_SUM
240     Q_OUT = Q_OUT + Q_SUM * DT_NEW
241     ZZ_I = ZZ_I + DZZDT * DT_NEW
242     EXIT ODELOOP
243   ENDIF
244   Q_OUT = Q_OUT + Q_SUM * DT_NEW
245   ZZ_I = ZZ_I + DZZDT * DT_NEW
246   DT_SUM = DT_SUM + DT_NEW
247   IF (DT_NEW < DT_ODE) DT_NEW = DT_ODE
248   IF (DT_NEW + DT_SUM > DT) DT_NEW = DT - DT_SUM
249   I_TS = I_TS + 1
250 ENDDO ODELOOP
251
252 ZZ_GET = ZZ_GET + ZZ_I - ZZ_0
253 Q_OUT = Q_OUT / DT
254
255 RETURN
256
257 END SUBROUTINE ODE_EXPLICIT_EULER
258
259
260 SUBROUTINE ODE_RUNGE_KUTTA_2(I, J, K, ZZ_GET, Q_OUT)
261 INTEGER, INTENT(IN) :: I, J, K
262 REAL(EB), INTENT(OUT) :: Q_OUT
263 REAL(EB), INTENT(INOUT) :: ZZ_GET(0:N_TRACKED_SPECIES)
264 REAL(EB) :: ZZ_0(0:N_TRACKED_SPECIES), ZZ_I(0:N_TRACKED_SPECIES)
265           , ZZ_N(0:N_TRACKED_SPECIES), &
266           DZZDT(0:N_TRACKED_SPECIES), DZZDT2(0:
267           N_TRACKED_SPECIES), &
268           DT_ODE, DT_NEW, RATE_CONSTANT(1:N_REACTIONS), Q_NR(1:
269           N_REACTIONS), Q_NR2(1:N_REACTIONS), Q_SUM, DT_SUM
270
271 INTEGER :: NR, I_TS, NS
272 INTEGER, PARAMETER :: NODETS=20
273 TYPE(REACTION_TYPE), POINTER :: RN=>NULL()
274
275 Q_OUT = 0._EB
276 ZZ_0 = MAX(0._EB, ZZ_GET)
277 ZZ_I = ZZ_0
278 DT_ODE = DT / REAL(NODETS, EB)
279 DT_NEW = DT_ODE
280 DT_SUM = 0._EB

```

```

278 I_TS = 1
279 ODELOOP: DO WHILE (DT_SUM < DT)
280     DZZDT = 0._EB
281     DZZDT2 = 0._EB
282     Q_NR = 0._EB
283     Q_NR2 = 0._EB
284     RATECONSTANT = 0._EB
285     REACTIONLOOP: DO NR = 1, N_REACTIONS
286         RN => REACTION(NR)
287         CALL COMPUTERATECONSTANT(NR,RN%MODE,I_TS,Q_OUT,
            RATECONSTANT(NR),ZZ_I,I,J,K)
288         IF (RATECONSTANT(NR) < ZERO_P) CYCLE REACTIONLOOP
289         Q_NR(NR) = RATECONSTANT(NR)*RN%HEAT_OF_COMBUSTION*RHO(I,
            J,K)
290         DZZDT = DZZDT + RN%NU * SPECIES_MIXTURE%MW/
            SPECIES_MIXTURE(RN%FUEL_SMIX_INDEX)%MW*RATECONSTANT(
            NR)
291     END DO REACTIONLOOP
292     IF (ALL(DZZDT < ZERO_P)) EXIT ODELOOP
293     ZZ_N = ZZ_I + DZZDT * DT_NEW
294
295     IF (ANY(ZZ_N < 0._EB)) THEN
296         DO NS=0,N_TRACKED_SPECIES
297             IF (ZZ_N(NS) < 0._EB .AND. ABS(DZZDT(NS))>ZERO_P)
                DT_NEW = MIN(DT_NEW,-ZZ_I(NS)/DZZDT(NS))
298         ENDDO
299     ENDIF
300
301     ZZ_N = ZZ_I + DZZDT * DT_NEW
302
303     REACTIONLOOP2: DO NR = 1, N_REACTIONS
304         RN => REACTION(NR)
305         CALL COMPUTERATECONSTANT(NR,RN%MODE,I_TS,Q_OUT,
            RATECONSTANT(NR),ZZ_N,I,J,K)
306         IF (RATECONSTANT(NR) < ZERO_P) CYCLE REACTIONLOOP2
307         Q_NR2(NR) = RATECONSTANT(NR)*RN%HEAT_OF_COMBUSTION*RHO(I
            ,J,K)
308         DZZDT2 = DZZDT2 + RN%NU * SPECIES_MIXTURE%MW/
            SPECIES_MIXTURE(RN%FUEL_SMIX_INDEX)%MW*RATECONSTANT(
            NR)
309     END DO REACTIONLOOP2
310     IF (ALL(DZZDT2 < ZERO_P)) EXIT ODELOOP
311     ZZ_N = ZZ_I + 0.5._EB*(DZZDT+DZZDT2)*DT_NEW

```



```

312
313   IF (ANY(ZZ_N < 0._EB)) THEN
314     DO NS=0,N_TRACKED_SPECIES
315       IF (ZZ_N(NS) < 0._EB .AND. ABS(DZZDT(NS)+DZZDT2(NS))>
          ZERO_P) DT_NEW = MIN(DT_NEW, -2._EB*ZZ_I(NS)/(DZZDT
          (NS)+DZZDT2(NS)))
316     ENDDO
317   ENDIF
318
319   Q_SUM = SUM(0.5 _EB*(Q_NR+Q_NR2))
320
321   IF (Q_OUT + Q_SUM*DT_NEW > Q_UPPER * DT) THEN
322     DT_NEW = MAX(0._EB, (Q_UPPER * DT - Q_OUT))/Q_SUM
323     Q_OUT = Q_OUT+Q_SUM*DT_NEW
324     ZZ_I = ZZ_I + 0.5 _EB*(DZZDT+DZZDT2)*DT_NEW
325     EXIT ODELOOP
326   ENDIF
327
328   ZZ_I = ZZ_I + 0.5 _EB*(DZZDT+DZZDT2)*DT_NEW
329
330   Q_OUT = Q_OUT+Q_SUM*DT_NEW
331
332   DT_SUM = DT_SUM + DT_NEW
333   IF (DT_NEW < DT_ODE) DT_NEW = DT_ODE
334   IF (DT_NEW + DT_SUM > DT) DT_NEW = DT - DT_SUM
335   I_TS = I_TS + 1
336 ENDDO ODELOOP
337
338 ZZ_GET = ZZ_GET + ZZ_I - ZZ_0
339 Q_OUT = Q_OUT / DT
340
341 RETURN
342
343 END SUBROUTINE ODE_RUNGEKUTTA_2
344
345 SUBROUTINE ODE_RK2_RICHARDSON(I, J, K, ZZ_GET, Q_OUT)
346 INTEGER, INTENT(IN) :: I, J, K
347 REAL(EB), INTENT(OUT) :: Q_OUT
348 REAL(EB), INTENT(INOUT) :: ZZ_GET(0:N_TRACKED_SPECIES)
349 REAL(EB) :: ZZ_0(0:N_TRACKED_SPECIES), DZZDT(0:N_TRACKED_SPECIES
    ), DZZDT2(0:N_TRACKED_SPECIES), RATE_CONSTANT(1:N_REACTIONS), &
350     ERR_EST, TOL_INT_VECTOR(1:N_REACTIONS), ERR_TOL,
    Q_NR_1(1:N_REACTIONS), Q_NR2_1(1:N_REACTIONS),

```

```

351      Q_NR_2(1:N_REACTIONS), &
      Q_NR2_2(1:N_REACTIONS), Q_NR_4(1:N_REACTIONS),
352      Q_NR2_4(1:N_REACTIONS), Q_SUM_1, Q_SUM_2, Q_SUM_4, &
      A1(0:N_TRACKED_SPECIES), A2(0:N_TRACKED_SPECIES), A4
      (0:N_TRACKED_SPECIES), DT_SUB, DT_SUB_NEW, DT_ITER
      , &
353      DT_A1, DT_A2, DT_A4, ZZ_STORE(0:N_TRACKED_SPECIES, 0:3)
      , TV(0:2), ZZ_DIFF(0:2), Q1, Q2, Q4, Q_OUT2
354 INTEGER :: I_TS, NR, NS, NSS, ITER, TVI, RICH_ITER
355 INTEGER, PARAMETER :: NODETS=20, SUB_DT1=1, SUB_DT2=2, SUB_DT4=4,
      TV_ITER_MIN=5, Q_ITER_MAX=10, RICH_ITER_MAX=100
356 TYPE(REACTION_TYPE), POINTER :: RN=>NULL()
357
358 Q_OUT = 0._EB
359 Q_OUT2 = 0._EB
360 RICH_ITER=0
361 ITER=0
362 DT_ITER = 0._EB
363 I_TS = 1
364 DT_SUB = DT
365 DT_SUB_NEW = DT_SUB
366
367 ! Setting up tolerance vector from inputs
368 DO NR = 1, N_REACTIONS
369     RN => REACTION(NR)
370     TOLINT_VECTOR(NR)=RN%TOLINT
371 ENDDO
372 ERR_TOL = MINVAL(ABS(TOLINT_VECTOR))
373
374 INTEGRATION_LOOP: DO WHILE (DT_ITER < DT)
375     ERR_EST = 10._EB*ERR_TOL
376     RICH_EX_LOOP: DO WHILE (ERR_EST > ERR_TOL)
377         DT_SUB = DT_SUB_NEW
378         IF (DT_ITER + DT_SUB > DT) THEN
379             DT_SUB = DT - DT_ITER
380         ENDIF
381
382         !-----
383         ! Calculate A1 term
384         ! Time step = DT_SUB
385         !-----
386         ZZ_0 = MAX(0._EB, ZZ_GET)
387         Q1 = Q_OUT2

```

```

388     ODE_LOOP1: DO NS = 1, SUB_DT1
389         DZZDT = 0._EB
390         DZZDT2 = 0._EB
391         RATE_CONSTANT = 0._EB
392
393     REACTION_LOOP: DO NR = 1, N_REACTIONS
394         RN => REACTION(NR)
395         CALL COMPUTE_RATE_CONSTANT(NR, RN%MODE, I_TS, Q_OUT2,
396             RATE_CONSTANT(NR), ZZ_0, I, J, K)
397         IF (RATE_CONSTANT(NR) <= 0.0_EB) CYCLE
398             REACTION_LOOP
399         DZZDT = DZZDT + RN%NU*SPECIES_MIXTURE%MW/
400             SPECIES_MIXTURE(RN%FUEL_SMIX_INDEX)%MW*
401             RATE_CONSTANT(NR)
402         Q_NR_1(NR) = RATE_CONSTANT(NR)*RN%
403             HEAT_OF_COMBUSTION*RHO(I, J, K)
404     END DO REACTION_LOOP
405     IF (ALL(DZZDT < 0._EB)) EXIT INTEGRATION_LOOP
406     A1 = ZZ_0 + DZZDT*DT_SUB
407     IF (ANY(A1 < 0._EB)) THEN
408         DO NSS=0, N_TRACKED_SPECIES
409             IF (A1(NSS) < 0._EB .AND. ABS(DZZDT(NSS))>ZERO_P
410                 ) THEN
411                 DT_SUB = MIN(DT_SUB, -ZZ_0(NSS)/DZZDT(NSS))
412             ENDIF
413         ENDDO
414         A1 = ZZ_0 + DZZDT*DT_SUB
415     ENDIF
416
417     REACTION_LOOP2: DO NR = 1, N_REACTIONS
418         RN => REACTION(NR)
419         CALL COMPUTE_RATE_CONSTANT(NR, RN%MODE, I_TS, Q_OUT2,
420             RATE_CONSTANT(NR), A1, I, J, K)
421         IF (RATE_CONSTANT(NR) <= 0.0_EB) CYCLE
422             REACTION_LOOP2
423         DZZDT2 = DZZDT2 + RN%NU*SPECIES_MIXTURE%MW/
424             SPECIES_MIXTURE(RN%FUEL_SMIX_INDEX)%MW*
425             RATE_CONSTANT(NR)
426         Q_NR2_1(NR) = RATE_CONSTANT(NR)*RN%
427             HEAT_OF_COMBUSTION*RHO(I, J, K)
428     END DO REACTION_LOOP2
429     IF (ALL(DZZDT2 < 0._EB)) EXIT INTEGRATION_LOOP
430     A1 = ZZ_0 + 0.5_EB*(DZZDT+DZZDT2)*DT_SUB

```

```

420     IF (ANY(A1 < 0._EB)) THEN
421         DO NSS=0,N_TRACKED_SPECIES
422             IF (A1(NSS) < 0._EB .AND. ABS(DZZDT(NSS)+DZZDT2(
                     NSS))>ZERO_P) THEN
423                 DT_SUB = MIN(DT_SUB, -2._EB*ZZ_0(NSS)/(DZZDT(
                     NSS)+DZZDT2(NSS)))
424             ENDIF
425         ENDDO
426         A1 = ZZ_0 + 0.5_EB*(DZZDT+DZZDT2)*DT_SUB
427     ENDIF
428
429     Q_SUM_1 = SUM(0.5_EB*(Q_NR_1+Q_NR2_1))
430     IF (Q1 + Q_SUM_1*DT_SUB > Q_UPPER * DT) THEN
431         DT_SUB_NEW = MAX(0.0_EB, (Q_UPPER * DT-Q1)/Q_SUM_1)
432         Q1 = Q1+Q_SUM_1*DT_SUB_NEW
433         A1 = ZZ_0 + 0.5_EB*(DZZDT+DZZDT2)*DT_SUB_NEW
434         EXIT ODELOOP1
435     ENDIF
436     Q1 = Q1+Q_SUM_1*DT_SUB
437     I_TS = I_TS + 1
438 ENDDO ODELOOP1
439 DT_A1 = DT_SUB
440
441     !-----
442     ! Calculate A2 term
443     ! Time step = DT.SUB/2
444     !-----
445     ZZ_0 = MAX(0._EB, ZZ_GET)
446     Q2 = Q_OUT2
447 ODE_LOOP2: DO NS = 1, SUB_DT2
448     DZZDT = 0._EB
449     DZZDT2 = 0._EB
450     RATE_CONSTANT = 0._EB
451
452     REACTION_LOOP2: DO NR = 1, N_REACTIONS
453         RN => REACTION(NR)
454         CALL COMPUTE_RATE_CONSTANT(NR, RN%MODE, I_TS, Q_OUT2,
                     RATE_CONSTANT(NR), ZZ_0, I, J, K)
455         IF (RATE_CONSTANT(NR) <= 0.0_EB) CYCLE
                     REACTION_LOOP2
456         DZZDT = DZZDT + RN%NU*SPECIES_MIXTURE%MW/
                     SPECIES_MIXTURE(RN%FUEL_SMIX_INDEX)%MW*
                     RATE_CONSTANT(NR)

```

```

457         Q_NR_2(NR) = RATE_CONSTANT(NR)*RN%
              HEAT_OF_COMBUSTION*RHO(I , J ,K)
458     END DO REACTION_LOOP_2
459     A2 = ZZ_0 + DZZDT*(DT_SUB/REAL(SUB_DT2,EB))
460     IF (ANY(A2 < 0._EB)) THEN
461         DO NSS=0,N_TRACKED_SPECIES
462             IF (A2(NSS) < 0._EB .AND. ABS(DZZDT(NSS))>ZERO_P
              ) THEN
463                 DT_SUB = MIN(DT_SUB, -ZZ_0(NSS) /DZZDT(NSS))
464             ENDIF
465         ENDDO
466         A2 = ZZ_0 + DZZDT*(DT_SUB/REAL(SUB_DT2,EB))
467     ENDIF
468
469     REACTION_LOOP2.2: DO NR = 1, N_REACTIONS
470         RN => REACTION(NR)
471         CALL COMPUTE_RATE_CONSTANT(NR,RN%MODE, I_TS , Q_OUT2,
              RATE_CONSTANT(NR) ,A2, I , J ,K)
472         IF (RATE_CONSTANT(NR) <= 0.0_EB) CYCLE
              REACTION_LOOP2.2
473         DZZDT2 = DZZDT2 + RN%NU*SPECIES_MIXTURE%MW/
              SPECIES_MIXTURE(RN%FUEL_SMIX_INDEX)%MW*
              RATE_CONSTANT(NR)
474         Q_NR2.2(NR) = RATE_CONSTANT(NR)*RN%
              HEAT_OF_COMBUSTION*RHO(I , J ,K)
475     END DO REACTION_LOOP2.2
476     A2 = ZZ_0 + 0.5_EB*(DZZDT+DZZDT2)*(DT_SUB/REAL(SUB_DT2
              ,EB))
477     IF (ANY(A2 < 0._EB)) THEN
478         DO NSS=0,N_TRACKED_SPECIES
479             IF (A2(NSS) < 0._EB .AND. ABS(DZZDT(NSS)+DZZDT2(
              NSS))>ZERO_P) THEN
480                 DT_SUB = MIN(DT_SUB, -2._EB*ZZ_0(NSS) / (DZZDT(
              NSS)+DZZDT2(NSS)))
481             ENDIF
482         ENDDO
483         A2 = ZZ_0 + 0.5_EB*(DZZDT+DZZDT2)*(DT_SUB/REAL(
              SUB_DT2,EB))
484     ENDIF
485
486     Q_SUM_2 = SUM(0.5_EB*(Q_NR_2+Q_NR2.2))
487     IF (Q2+Q_SUM_2*(DT_SUB/REAL(SUB_DT2,EB)) > Q_UPPER *
              DT) THEN

```

```

488         DT_SUB_NEW = MAX(0.0_EB, (Q_UPPER * DT - Q2) / Q_SUM_2)
489         Q2 = Q2 + Q_SUM_2 * (DT_SUB_NEW)
490         A2 = ZZ_0 + 0.5_EB * (DZZDT + DZZDT2) * (DT_SUB_NEW)
491         EXIT ODE_LOOP2
492     ENDF
493     Q2 = Q2 + Q_SUM_2 * (DT_SUB / REAL(SUB_DT2, EB))
494     I_TS = I_TS + 1
495     ZZ_0 = A2
496 ENDDO ODE_LOOP2
497 DT_A2 = DT_SUB
498 IF (DT_A2 < DT_A1) THEN
499     DT_SUB_NEW = DT_A2
500     CYCLE RICH_EX_LOOP
501 ENDF
502
503     !-----
504     ! Calculate A4 term
505     ! Time step = DT_SUB/4
506     !-----
507     ZZ_0 = MAX(0. _EB, ZZ_GET)
508     Q4 = Q_OUT2
509     ODE_LOOP4: DO NS = 1, SUB_DT4
510         DZZDT = 0. _EB
511         DZZDT2 = 0. _EB
512         RATE_CONSTANT = 0. _EB
513
514         REACTION_LOOP4: DO NR = 1, N_REACTIONS
515             RN => REACTION(NR)
516             CALL COMPUTE_RATE_CONSTANT(NR, RN%MODE, I_TS, Q_OUT2,
517                 RATE_CONSTANT(NR), ZZ_0, I, J, K)
518             IF (RATE_CONSTANT(NR) <= 0.0_EB) CYCLE
519                 REACTION_LOOP4
520             DZZDT = DZZDT + RN%NU * SPECIES_MIXTURE%MW /
521                 SPECIES_MIXTURE(RN%FUEL_SMIX_INDEX)%MW *
522                 RATE_CONSTANT(NR)
523             Q_NR_4(NR) = RATE_CONSTANT(NR) * RN%
524                 HEAT_OF_COMBUSTION * RHO(I, J, K)
525         END DO REACTION_LOOP4
526     A4 = ZZ_0 + DZZDT * (DT_SUB / REAL(SUB_DT4, EB))
527     IF (ANY(A4 < 0. _EB)) THEN
528         DO NSS = 0, N_TRACKED_SPECIES
529             IF (A4(NSS) < 0. _EB .AND. ABS(DZZDT(NSS)) > ZERO_P
530                 ) THEN

```

```

525             DT_SUB = MIN(DT_SUB, -ZZ_0(NSS) / DZZDT(NSS))
526             ENDIF
527             ENDDO
528             A4 = ZZ_0 + DZZDT*(DT_SUB/REAL(SUB_DT4,EB))
529             ENDIF
530
531             REACTION_LOOP2_4: DO NR = 1, N_REACTIONS
532                 RN => REACTION(NR)
533                 CALL COMPUTE_RATE_CONSTANT(NR, RN%MODE, I_TS, Q_OUT2,
                    RATE_CONSTANT(NR), A4, I, J, K)
534                 IF (RATE_CONSTANT(NR) <= 0.0_EB) CYCLE
                    REACTION_LOOP2_4
535                 DZZDT2 = DZZDT2 + RN%NU*SPECIES_MIXTURE%MW/
                    SPECIES_MIXTURE(RN%FUEL_SMIX_INDEX)%MW*
                    RATE_CONSTANT(NR)
536                 Q_NR2_4(NR) = RATE_CONSTANT(NR)*RN%
                    HEAT_OF_COMBUSTION*RHO(I, J, K)
537             END DO REACTION_LOOP2_4
538             A4 = ZZ_0 + 0.5_EB*(DZZDT+DZZDT2)*(DT_SUB/REAL(SUB_DT4
                    ,EB))
539             IF (ANY(A4 < 0._EB)) THEN
540                 DO NSS=0, N_TRACKED_SPECIES
541                     IF (A4(NSS) < 0._EB .AND. ABS(DZZDT(NSS)+DZZDT2(
                        NSS))>ZERO_P) THEN
542                         DT_SUB = MIN(DT_SUB, -2._EB*ZZ_0(NSS) / (DZZDT(
                            NSS)+DZZDT2(NSS)))
543                     ENDIF
544                 ENDDO
545                 A4 = ZZ_0 + 0.5_EB*(DZZDT+DZZDT2)*(DT_SUB/REAL(
                    SUB_DT4,EB))
546             ENDIF
547
548             Q_SUM_4 = SUM(0.5_EB*(Q_NR_4+Q_NR2_4))
549             IF (ABS(Q4+Q_SUM_4*(DT_SUB/REAL(SUB_DT4,EB))) >
                    Q_UPPER*DT) THEN
550                 DT_SUB_NEW = MAX(0.0_EB, (Q_UPPER*DT-Q4)/Q_SUM_4)
551                 Q4 = Q4+Q_SUM_4*(DT_SUB_NEW)
552                 A4 = ZZ_0 + 0.5_EB*(DZZDT+DZZDT2)*(DT_SUB_NEW)
553                 IF (ITER >= Q_ITER_MAX) THEN
554                     Q_OUT = Q4/DT
555                     ZZ_GET = A4
556                 EXIT INTEGRATION_LOOP
557             ENDIF

```

```

558         EXIT ODELOOP4
559     ENDF
560     Q4 = Q4+Q_SUM.4*(DT.SUB/REAL(SUB_DT4,EB))
561     I_TS = I_TS + 1
562     ZZ_0 = A4
563 ENDDO ODELOOP4
564 DT_A4 = DT.SUB
565 IF (DT_A4 < DT_A2) THEN
566     DT.SUB_NEW = DT_A4
567     CYCLE RICH_EX_LOOP
568 ENDF
569
570     ! Species Error Analysis
571     ERR_EST = MAXVAL(ABS((4._EB*A4-A2) - (4._EB*A2-A1)))/45.
572     _EB ! Estimate Error
573 IF (ERR_EST <= 0.0 _EB) THEN
574     DT.SUB_NEW = DT
575 ELSE
576     DT.SUB_NEW =DT.SUB*(ERR_TOL/(ERR_EST))**(0.25 _EB) !
577     Determine New Time Step
578 ENDF
579
580     RICH_ITER = RICH_ITER+1
581     IF (RICH_ITER >= RICH_ITER_MAX) EXIT RICH_EX_LOOP
582 ENDDO RICH_EX_LOOP
583
584 DT_ITER = DT_ITER + DT.SUB
585 ITER = ITER + 1
586 MAX_CHEM_SUBIT = MAX(MAX_CHEM_SUBIT,ITER)
587 ZZ_GET = (4._EB*A4-A2)/3._EB
588 Q_OUT = (4._EB*Q4-Q2)/3._EB/DT
589 Q_OUT2 = (4._EB*Q4-Q2)/3._EB
590
591     ! Total Variation Scheme
592 DO NS = 0,N_TRACKED_SPECIES
593     DO TVI = 0,2
594         ZZ_STORE(NS,TVI)=ZZ_STORE(NS,TVI+1)
595     ENDDO
596     ZZ_STORE(NS,3) = (4._EB*A4(NS)-A2(NS))/3._EB
597 ENDDO
598
599 REACTION_LOOP_TV: DO NR = 1, N_REACTIONS
600     RN => REACTION(NR)

```



```

599     IF (.NOT. RN%REVERSIBLE) CYCLE REACTIONLOOP_TV
600     DO TVI = 0,2
601         TV(TVI) = ABS(ZZ_STORE(RN%FUEL_SMIX_INDEX, TVI+1)-
        ZZ_STORE(RN%FUEL_SMIX_INDEX, TVI))
602         ZZ_DIFF(TVI) = ZZ_STORE(RN%FUEL_SMIX_INDEX, TVI+1)-
        ZZ_STORE(RN%FUEL_SMIX_INDEX, TVI)
603     ENDDO
604     IF (SUM(TV) > 0.0_EB .AND. SUM(TV) >= ABS(2.5_EB*SUM(
        ZZ_DIFF)) .AND. ITER >= TV_ITER_MIN) EXIT
        INTEGRATIONLOOP
605     ENDDO REACTIONLOOP_TV
606
607 ENDDO INTEGRATIONLOOP
608
609 RETURN
610
611 END SUBROUTINE ODE_RK2_RICHARDSON
612
613 RECURSIVE SUBROUTINE COMPUTE_RATE_CONSTANT(NR,MODE, I_TS, Q_IN,
        RATE_CONSTANT, ZZ_GET, I, J, K)
614 USE PHYSICAL_FUNCTIONS, ONLY : GET_MASS_FRACTION_ALL,
        GET_MASS_FRACTION, GET_VISCOSITY
615 REAL(EB), INTENT(IN) :: ZZ_GET(0:N_TRACKED_SPECIES), Q_IN
616 INTEGER, INTENT(IN) :: NR, I_TS, MODE, I, J, K
617 REAL(EB), INTENT(INOUT) :: RATE_CONSTANT
618 REAL(EB) :: YY_PRIMITIVE(1:N_SPECIES), Y_F_MIN=1.E-15_EB, ZZ_MIN
        =1.E-10_EB, YY_F_LIM, ZZ_REACTANT, ZZ_PRODUCT, &
619         TAU_D, TAU_G, TAU_U, DELTA, RATE_CONSTANT_ED,
        RATE_CONSTANT_FR, GAMMA_LAMBDA, NU, Y_FUEL, Y_O2,
        Y_PRODUCT, S, &
620         CHI_1, CHI_2, CHI_3, CHI, C_LES !ADDED
621 INTEGER :: NS
622 TYPE(REACTION_TYPE), POINTER :: RN=>NULL()
623
624 RN => REACTION(NR)
625
626 SELECT CASE (MODE)
627     CASE(MIXED)
628         IF (Q_IN > 0._EB .AND. RN%THRESHOLD_TEMP >= TMP(I, J, K))
        THEN
629             CALL COMPUTE_RATE_CONSTANT(NR, EDDY_DISSIPATION, I_TS,
        Q_IN, RATE_CONSTANT, ZZ_GET, I, J, K)
630         ELSE

```

```

631      CALL COMPUTE_RATE_CONSTANT(NR, FINITE_RATE, I_TS, Q_IN,
        RATE_CONSTANT, ZZ_GET, I, J, K)
632      ENDIF
633      CASE(EDDY DISSIPATION)
634      IF_SUPPRESSION: IF (SUPPRESSION) THEN
635          ! Evaluate empirical extinction criteria
636          IF (I_TS==1) THEN
637              IF (EXTINCTION(I, J, K, ZZ_GET)) THEN
638                  RATE_CONSTANT = 0._EB
639                  RETURN
640              ENDIF
641          !ELSE
642          ! IF (RATE_CONSTANT <= ZERO_P) RETURN
643          ENDIF
644      ENDIF IF_SUPPRESSION
645
646      FIXED_TIME: IF (FIXED_MIX_TIME > 0._EB) THEN
647          MIX_TIME(I, J, K) = FIXED_MIX_TIME
648
649      ELSE FIXED_TIME
650          IF (TWO_D) THEN
651              DELTA = MAX(DX(I), DZ(K))
652          ELSE
653              DELTA = MAX(DX(I), DY(J), DZ(K))
654          ENDIF
655
656          !LES_IF: IF (LES) THEN
657
658              !TAU_D = D_Z(MIN(4999, NINT(TMP(I, J, K))), RN%
        FUEL_SMIX_INDEX)
659              !TAU_D = DELTA**2/TAU_D ! diffusive time scale
660
661              !IF (TURB_MODEL==DEARDORFF) THEN
662                  !TAU_U = 0.1_EB*SC*RHO(I, J, K)*DELTA**2/MU(I, J
        ,K) ! turbulent mixing time scale
663              !ELSE
664                  !TAU_U = DELTA/SQRT(2._EB*KSGS(I, J, K)+1.E-10
        _EB) ! advective time scale
665              !ENDIF
666
667              !TAU_G = SQRT(2._EB*DELTA/(GRAV+1.E-10_EB)) !
        acceleration time scale
668

```

```

669          !MIX_TIME(I,J,K)=MAX(TAU_CHEM,MIN(TAU_D,TAU_U,
        TAU_G,TAU_FLAME)) ! Eq. 7, McDermott,
        McGrattan, Floyd
670
671          !ELSE LES_IF
672
673          !TAU_D = D_Z(MIN(4999,NINT(TMP(I,J,K))),RN%
        FUEL_SMIX_INDEX)
674          !TAU_D = DELTA**2/TAU_D
675          !MIX_TIME(I,J,K)=TAU_D
676
677          !ENDIF LES_IF
678          MIX_TIME(I,J,K) = 1._EB/ABS(STRAIN_RATE(I,J,K)) !
        ADDED
679      ENDIF FIXED_TIME
680
681      YY_F_LIM=1.E15_EB
682      IF (N_REACTIONS > 1) THEN
683          DO NS=0,N_TRACKED_SPECIES
684              IF (RN%NU(NS) < -ZERO_P) THEN
685                  IF (ZZ_GET(NS) < ZZ_MIN) THEN
686                      RATE_CONSTANT = 0._EB
687                      RETURN
688                  ENDIF
689                  YY_F_LIM = MIN(YY_F_LIM,&
690                      ZZ_GET(NS)*SPECIES_MIXTURE(RN%
        FUEL_SMIX_INDEX)%MW/(ABS(RN
        %NU(NS))*SPECIES_MIXTURE(NS
        )%MW))
691              ENDIF
692          ENDDO
693      ELSE
694          ZZ_REACTANT = 0._EB
695          ZZ_PRODUCT = 0._EB
696          DO NS=0,N_TRACKED_SPECIES
697              IF (RN%NU(NS) < -ZERO_P) THEN
698                  IF (ZZ_GET(NS) < ZZ_MIN) THEN
699                      RATE_CONSTANT = 0._EB
700                      RETURN
701                  ENDIF
702                  ZZ_REACTANT = ZZ_REACTANT - RN%NU(NS)*
        SPECIES_MIXTURE(NS)%MW
703                  YY_F_LIM = MIN(YY_F_LIM,&

```

```

704          ZZ_GET(NS)*SPECIES_MIXTURE(RN%
          FUEL_SMIX_INDEX)%MW/(ABS(RN
          %NU(NS))*SPECIES_MIXTURE(NS
          )%MW))
705          ELSEIF(RN%NU(NS)>ZERO_P ) THEN
706              ZZ_PRODUCT = ZZ_PRODUCT + ZZ_GET(NS)
707          ENDIF
708      ENDDO
709      ZZ_PRODUCT = BETA_EDC*MAX(ZZ_PRODUCT*
          SPECIES_MIXTURE(RN%FUEL_SMIX_INDEX)%MW/
          ZZ_REACTANT, Y_P_MIN_EDC)
710      YY_F_LIM = MIN(YY_F_LIM, ZZ_PRODUCT)
711  ENDIF
712  YY_F_LIM = MAX(YY_F_LIM, Y_F_MIN)
713  !RATE_CONSTANT = YY_F_LIM/MIX_TIME(I, J, K)
714
715  !The Eddy Dissipation Consept (EDC) Combustion Model (
          by Hjertager and Magnussen) for LES proposed by
          Balram et al.
716  NU = MU(I, J, K)/RHO(I, J, K)
717  C_LES = 0.10_EB
718  !IF(SELECT_TURB == DEARDORFF) THEN
719  !    C_LES =
720  !ELSEIF(SELECT_TURB == DYNMAG)THEN
721  !    C_LES =
722  !ELSEIF(SELECT_TURB == VREMAN)THEN
723  !    C_LES =
724  !ELSE
725  !    WRITE(*,*) 'The chosen turbulence model is not
          supported by the combustion model'
726  !END
727
728  GAMMALAMBDA = C_LES*(NU/NU_EDDY(I, J, K))**0.25_EB
729  IF(GAMMALAMBDA > 1._EB)THEN
730      GAMMALAMBDA = 1._EB
731  END IF
732
733  CALL GET_MASS_FRACTION(ZZ_GET, FUEL_INDEX, Y_FUEL) !
          ADDED
734  CALL GET_MASS_FRACTION(ZZ_GET, O2_INDEX, Y_O2) !ADDED
735  Y_PRODUCT = 1._EB - (Y_FUEL + Y_O2)
736

```

```

737      S = SPECIES(FUEL_INDEX)%MW/(RN%NU_O2*SPECIES(O2_INDEX)
          %MW)
738      Y_O2 = Y_O2/S
739      Y_PRODUCT = Y_PRODUCT/(1._EB + S)
740      CHI_1 = ((YY_F_LIM + Y_PRODUCT)**2)/((Y_FUEL +
          Y_PRODUCT)*(Y_O2 + Y_PRODUCT))
741      CHI_2 = MIN(Y_PRODUCT/(GAMMALAMBDA*(YY_F_LIM +
          Y_PRODUCT)), 1._EB)
742      CHI_3 = MIN(GAMMALAMBDA*(YY_F_LIM + Y_PRODUCT)/
          YY_F_LIM, 1._EB)
743      CHI = CHI_1*CHI_2*CHI_3
744
745      RATE_CONSTANT = YY_F_LIM*CHI/(MIX_TIME(I, J, K) * (1._EB -
          CHI*GAMMALAMBDA**2))
746      !RATE_CONSTANT = YY_F_LIM*CHI*GAMMALAMBDA**2/(
          MIX_TIME(I, J, K) * (1._EB - CHI*GAMMALAMBDA**2))
747
748
749      CASE(FINITE_RATE)
750          RATE_CONSTANT = 0._EB
751          CALL GET_MASS_FRACTION_ALL(ZZ_GET, YY_PRIMITIVE)
752          RATE_CONSTANT = RN%A*RHO(I, J, K)**RN%/RHO.EXPONENT*EXP(-RN%/
          E/(R0*TMP(I, J, K)))*TMP(I, J, K)**RN%/N_T
753          IF (ALL(RN%N_S < -998._EB)) THEN
754              DO NS=0, N_TRACKED_SPECIES
755                  IF (RN%NU(NS) < 0._EB .AND. ZZ_GET(NS) < ZZ_MIN) THEN
756                      RATE_CONSTANT = 0._EB
757                      RETURN
758                  ENDIF
759              ENDDO
760          ELSE
761              DO NS=1, N_SPECIES
762                  IF (ABS(RN%N_S(NS)) <= ZERO_P) CYCLE
763                  IF (RN%N_S(NS) >= -998._EB) THEN
764                      IF (YY_PRIMITIVE(NS) < ZZ_MIN) THEN
765                          RATE_CONSTANT = 0._EB
766                      ELSE
767                          RATE_CONSTANT = YY_PRIMITIVE(NS)**RN%N_S(NS)*
                              RATE_CONSTANT
768                      ENDIF
769                  ENDIF
770              ENDDO
771          ENDIF

```

```

772
773     CASE(EDDY DISSIPATION CONCEPT)
774         CALL COMPUTE_RATE_CONSTANT(NR, EDDY DISSIPATION, I_TS, Q_IN,
              RATE_CONSTANT, ZZ_GET, I, J, K)
775         RATE_CONSTANT_ED=RATE_CONSTANT
776         CALL COMPUTE_RATE_CONSTANT(NR, FINITE_RATE, I_TS, Q_IN,
              RATE_CONSTANT, ZZ_GET, I, J, K)
777         RATE_CONSTANT_FR=RATE_CONSTANT
778         IF (ABS(RATE_CONSTANT_ED) < ZERO_P .AND. ABS(
              RATE_CONSTANT_FR) < ZERO_P) THEN
779             RATE_CONSTANT=0.0_EB
780         ELSE
781             RATE_CONSTANT = (RATE_CONSTANT_ED*RATE_CONSTANT_FR) / (
              RATE_CONSTANT_ED+RATE_CONSTANT_FR)
782         ENDF
783     END SELECT
784
785     RETURN
786
787     CONTAINS
788
789     LOGICAL FUNCTION EXTINCTION(I, J, K, ZZ_IN)
790     !This routine determines if local extinction occurs for a
791     !mixing controlled reaction.
792     !This is determined as follows:
793     !1) Determine how much fuel can burn (DZ_FUEL) by finding the
794     !limiting reactant and expressing it in terms of fuel mass
795     !2) Remove that amount of fuel from the local mixture,
796     !everything else is "air"
797     ! (i.e. if we are fuel rich, excess fuel acts as a diluent)
798     !3) Search to find the minimum reactant other than fuel.
799     ! Using the reaction stoichiometry, determine how much "air"
800     !(DZ_AIR) is needed to burn the fuel.
801     !4) GET_AVERAGE_SPECIFIC_HEAT for the fuel and the "air" at the
802     !current temp and the critical flame temp
803     !5) Check to see if the heat released from burning DZ_FUEL can
804     !raise the current temperature of DZ_FUEL and DZ_AIR
805     ! above the critical flame temp.
806     USE PHYSICAL_FUNCTIONS, ONLY: GET_AVERAGE_SPECIFIC_HEAT
807     REAL(EB), INTENT(IN) :: ZZ_IN (0:N_TRACKED_SPECIES)
808     REAL(EB) :: DZ_AIR, DZ_FUEL, CPBAR_F_0, CPBAR_F_N, CPBAR_G_0,
809     CPBAR_G_N, ZZ_GET (0:N_TRACKED_SPECIES)
810     INTEGER, INTENT(IN) :: I, J, K

```

```

804 INTEGER :: NS
805
806 EXTINCTION = .FALSE.
807 IF (TMP(I,J,K) < RN%AUTO_IGNITION_TEMPERATURE) THEN
808     EXTINCTION = .TRUE.
809 ELSE
810     DZ_FUEL = 1._EB
811     DZ_AIR = 0._EB
812     !Search reactants to find limiting reactant and express it
      as fuel mass. This is the amount of fuel
813     !that can burn
814     DO NS = 0,N_TRACKED_SPECIES
815         IF (RN%NU(NS)<=-ZERO_P) &
816             DZ_FUEL = MIN(DZ_FUEL,-ZZ_IN(NS)*SPECIES_MIXTURE(RN%
                FUEL_SMIX_INDEX)%MW/(RN%NU(NS)*SPECIES_MIXTURE(NS)%
                MW))
817     ENDDO
818     !Get the specific heat for the fuel at the current and
      critical flame temperatures
819     ZZ_GET = 0._EB
820     ZZ_GET(RN%FUEL_SMIX_INDEX) = 1._EB
821     CALL GET_AVERAGE_SPECIFIC_HEAT(ZZ_GET,CPBAR_F_0,TMP(I,J,K))
822     CALL GET_AVERAGE_SPECIFIC_HEAT(ZZ_GET,CPBAR_F_N,RN%
        CRIT_FLAME_TMP)
823     ZZ_GET = ZZ_IN
824     !Remove the burnable fuel from the local mixture and
      renormalize. The remainder is "air"
825     ZZ_GET(RN%FUEL_SMIX_INDEX) = ZZ_GET(RN%FUEL_SMIX_INDEX) -
        DZ_FUEL
826     ZZ_GET = ZZ_GET/SUM(ZZ_GET)
827     !Get the specific heat for the "air"
828     CALL GET_AVERAGE_SPECIFIC_HEAT(ZZ_GET,CPBAR_G_0,TMP(I,J,K))
829     CALL GET_AVERAGE_SPECIFIC_HEAT(ZZ_GET,CPBAR_G_N,RN%
        CRIT_FLAME_TMP)
830     !Loop over non-fuel reactants and find the minimum.
      Determine how much "air" is needed to provide the limiting
      reactant
831     DO NS = 0,N_TRACKED_SPECIES
832         IF (RN%NU(NS)<=-ZERO_P .AND. NS/=RN%FUEL_SMIX_INDEX)
            &
833             DZ_AIR = MAX(DZ_AIR, -DZ_FUEL*RN%NU(NS)*
                SPECIES_MIXTURE(NS)%MW/SPECIES_MIXTURE(RN%
                FUEL_SMIX_INDEX)%MW/ZZ_GET(NS))

```

```

834  ENDDO
835  !See if enough energy is released to raise the fuel and
      required "air" temperatures above the critical flame temp
836  IF ( (DZ_FUEL*CPBAR_F_0 + DZ_AIR*CPBAR_G_0)*TMP(I,J,K) +
      DZ_FUEL*RN%HEAT_OF_COMBUSTION < &
837      (DZ_FUEL*CPBAR_F_N + DZ_AIR*CPBAR_G_N)*RN%
      CRIT_FLAME_TMP) EXTINCTION = .TRUE.
838  ENDIF
839
840  END FUNCTION EXTINCTION
841
842
843  REAL(EB) FUNCTION KSGS(I,J,K)
844  INTEGER, INTENT(IN) :: I,J,K
845  REAL(EB) :: EPSK
846
847  ! ke dissipation rate, assumes production=dissipation
848
849  EPSK = MU(I,J,K)*STRAIN_RATE(I,J,K)**2/RHO(I,J,K)
850
851  KSGS = 2.25_EB*(EPSK*DELTA/PI)**TWIH ! estimate of subgrid ke,
      from Kolmogorov spectrum
852
853  END FUNCTION KSGS
854
855  END SUBROUTINE COMPUTE_RATE_CONSTANT
856
857
858  SUBROUTINE GET_REV_fire(MODULE_REV,MODULE_DATE)
859  INTEGER,INTENT(INOUT) :: MODULE_REV
860  CHARACTER(255),INTENT(INOUT) :: MODULE_DATE
861
862  WRITE(MODULE_DATE,'(A)') firerev(INDEX(firerev,':')+2:LEN_TRIM(
      firerev)-2)
863  READ (MODULE_DATE,'(I5)') MODULE_REV
864  WRITE(MODULE_DATE,'(A)') firedate
865
866  END SUBROUTINE GET_REV_fire
867
868  END MODULE FIRE

```


B.2 velo.f90

Modified subroutine in velo.f90:

```

1  SUBROUTINE COMPUTE_VISCOSITY(NM)
2
3  USE PHYSICAL_FUNCTIONS, ONLY: GET_VISCOSITY
4  USE TURBULENCE, ONLY: VARDEN_DYNMAG, TEST_FILTER, EX2G3D
5  INTEGER, INTENT(IN) :: NM
6  REAL(EB) :: ZZ_GET(0:N_TRACKED_SPECIES), DELTA, NU_G, GRAD_RHO(3),
      U2, V2, W2, AA, A_IJ(3,3), BB, B_IJ(3,3), &
7      DUDX, DUDY, DUDZ, DVDX, DVDY, DVDZ, DWDX, DWDY, DWDZ, MU_DNS
      , KSGS !, NU_EDDY(1:IBAR, 1:JBAR, 1:KBAR)
8  INTEGER :: I, J, K, IIG, JJG, KKG, II, JJ, KK, IW, TURB_MODEL_TMP, IOR
9  REAL(EB), POINTER, DIMENSION(:,:,:) :: RHOP=>NULL(), UP=>NULL(),
      VP=>NULL(), WP=>NULL(), &
10      UP_HAT=>NULL(), VP_HAT=>
      NULL(), WP_HAT=>NULL()
      , &
11      UU=>NULL(), VV=>NULL(), WW
      =>NULL()
12 REAL(EB), POINTER, DIMENSION(:,:,:) :: ZZP=>NULL()
13 TYPE(WALLTYPE), POINTER :: WG=>NULL()
14
15 CALL POINT_TO_MESH(NM)
16
17 IF (PREDICTOR) THEN
18   RHOP => RHO
19   UU   => U
20   VV   => V
21   WW   => W
22   IF (N_TRACKED_SPECIES > 0) ZZP => ZZ
23 ELSE
24   RHOP => RHOS
25   UU   => US
26   VV   => VS
27   WW   => WS
28   IF (N_TRACKED_SPECIES > 0 .AND. .NOT.EVACUATION_ONLY(NM))
      ZZP => ZZS
29 ENDIF
30
31 ! Compute viscosity for DNS using primitive species/mixture
      fraction
32

```

```

33 !$OMP PARALLEL DEFAULT(NONE) &
34 !$OMP SHARED(N_TRACKED_SPECIES, EVACUATION_ONLY, KBAR, JBAR, IBAR,
      SOLID, CELL_INDEX, ZZP, MU, TMP, &
35 !$OMP      LES, NM, C_SMAGORINSKY, TWO_D, DX, DY, DZ, RDX, RDY, RDZ, UU
      , VV, WW, RHOP, CSD2, &
36 !$OMP      N_EXTERNAL_WALL_CELLS, N_INTERNAL_WALL_CELLS, KRES,
      &
37 !$OMP      IBP1, JBP1, KBP1, TURB_MODEL_TMP, TURB_MODEL, PREDICTOR
      , STRAIN_RATE, UP, VP, WP, WORK1, WORK2, WORK3, WC, WALL, U_GHOST,
      V_GHOST, &
38 !$OMP      W_GHOST, UP_HAT, VP_HAT, WP_HAT, WORK4, WORK5, WORK6,
      DELTA, KSGS, NU_EDDY, C_DEARDORFF, DUDX, DVDY, DWDZ, DUDY, DUDZ, DVDX
      , DVDZ, &
39 !$OMP      DWDX, DWDY, II, JJ, KK, A_IJ, AA, B_IJ, BB, C_VREMAN,
      GRAV_VISC, GRAD_RHO, NU_G, C_G, GVEC, IOR, MU_DNS) &
40 !$OMP PRIVATE(ZZ_GET)
41
42 IF (N_TRACKED_SPECIES>0 .AND. EVACUATION_ONLY(NM)) ZZ_GET(1:
      N_TRACKED_SPECIES) = 0._EB
43
44 !$OMP DO COLLAPSE(3) SCHEDULE(STATIC) &
45 !$OMP PRIVATE(K, J, I)
46 DO K=1, KBAR
47   DO J=1, JBAR
48     DO I=1, IBAR
49       IF (SOLID(CELL_INDEX(I, J, K))) CYCLE
50       IF (N_TRACKED_SPECIES>0 .AND. .NOT.EVACUATION_ONLY(NM)
          ) ZZ_GET(1:N_TRACKED_SPECIES) = ZZP(I, J, K, 1:
          N_TRACKED_SPECIES)
51       CALL GET_VISCOSITY(ZZ_GET, MU(I, J, K), TMP(I, J, K))
52     ENDDO
53   ENDDO
54 ENDDO
55 !$OMP END DO
56
57
58 TURB_MODEL_TMP = TURB_MODEL
59 IF (EVACUATION_ONLY(NM)) TURB_MODEL_TMP = CONSMAG
60
61 SELECT_TURB: SELECT CASE (TURB_MODEL_TMP)
62
63   CASE (CONSMAG, DYNMAG) SELECT_TURB ! Smagorinsky (1963) eddy
      viscosity

```

```

64
65     CALL COMPUTE_STRAIN_RATE(NM)
66
67     IF (PREDICTOR .AND. TURB_MODEL_TMP==DYNMAG) CALL
        VARDEN_DYNMAG(NM) ! dynamic procedure, Moin et al.
        (1991)
68
69     !$OMP DO COLLAPSE(3) SCHEDULE(STATIC) &
70     !$OMP PRIVATE(K, J, I)
71     DO K=1,KBAR
72         DO J=1,JBAR
73             DO I=1,IBAR
74                 IF (SOLID(CELL_INDEX(I, J, K))) CYCLE
75                 MU(I, J, K) = MU(I, J, K) + RHOP(I, J, K)*CSD2(I, J, K)*
                    STRAIN_RATE(I, J, K)
76                 !NU_EDDY = MU(I, J, K)/RHO(I, J, K)
77                 NU_EDDY(I, J, K) = MU(I, J, K)/RHO(I, J, K)
78             ENDDO
79         ENDDO
80     ENDDO
81     !$OMP END DO
82
83     CASE (DEARDORFF) SELECT_TURB ! Deardorff (1980) eddy
        viscosity model (current default)
84
85     ! Velocities relative to the p-cell center
86
87     !!!     CALL COMPUTE_STRAIN_RATE(NM) ! til forbrenningsmodell
88
89     UP => WORK1
90     VP => WORK2
91     WP => WORK3
92     UP=0._EB
93     VP=0._EB
94     WP=0._EB
95
96     DO K=1,KBAR
97         DO J=1,JBAR
98             DO I=1,IBAR
99                 UP(I, J, K) = 0.5_EB*(UU(I, J, K) + UU(I-1, J, K))
100                VP(I, J, K) = 0.5_EB*(VV(I, J, K) + VV(I, J-1, K))
101                WP(I, J, K) = 0.5_EB*(WW(I, J, K) + WW(I, J, K-1))
102            ENDDO

```

```

103         ENDDO
104     ENDDO
105
106         ! extrapolate to ghost cells
107
108     CALL EX2G3D(UP, -1.E10_EB, 1.E10_EB)
109     CALL EX2G3D(VP, -1.E10_EB, 1.E10_EB)
110     CALL EX2G3D(WP, -1.E10_EB, 1.E10_EB)
111
112     DO IW=1,N_EXTERNAL_WALL_CELLS
113         WC=>WALL(IW)
114         IF (WC%BOUNDARY_TYPE/=INTERPOLATED_BOUNDARY) CYCLE
115         II = WC%II
116         JJ = WC%JJ
117         KK = WC%KK
118         UP( II , JJ ,KK) = U_GHOST(IW)
119         VP( II , JJ ,KK) = V_GHOST(IW)
120         WP( II , JJ ,KK) = W_GHOST(IW)
121     ENDDO
122
123     UP_HAT => WORK4
124     VP_HAT => WORK5
125     WP_HAT => WORK6
126     UP_HAT=0._EB
127     VP_HAT=0._EB
128     WP_HAT=0._EB
129
130     CALL TEST_FILTER(UP_HAT,UP, -1.E10_EB, 1.E10_EB)
131     CALL TEST_FILTER(VP_HAT,VP, -1.E10_EB, 1.E10_EB)
132     CALL TEST_FILTER(WP_HAT,WP, -1.E10_EB, 1.E10_EB)
133
134     DO K=1,KBAR
135         DO J=1,JBAR
136             DO I=1,IBAR
137                 IF (SOLID(CELL_INDEX(I, J, K))) CYCLE
138                 IF (TWO_D) THEN
139                     DELTA = MAX(DX(I), DZ(K))
140                 ELSE
141                     DELTA = MAX(DX(I), DY(J), DZ(K))
142                 ENDIF
143
144                 KSGS = 0.5_EB*( (UP(I, J, K)-UP_HAT(I, J, K))**2 + (
                    VP(I, J, K)-VP_HAT(I, J, K))**2 + (WP(I, J, K)-

```

```

145      WP_HAT(I , J ,K) )**2 )
      !KSGS(I , J ,K) = 0.5_EB*( (UP(I , J ,K)-UP_HAT(I , J ,K)
      )**2 + (VP(I , J ,K)-VP_HAT(I , J ,K))**2 + (WP(I , J
      ,K)-WP_HAT(I , J ,K))**2 )
146      !NU_EDDY(I , J ,K) = C_DEARDORFF*DELTA*SQRT(KSGS)
147      NU_EDDY(I , J ,K) = C_DEARDORFF*DELTA*SQRT(KSGS)
148
149      MU(I , J ,K) = MU(I , J ,K) + RHOP(I , J ,K)*NU_EDDY(I , J ,
      K)
150      ENDDO
151      ENDDO
152      ENDDO
153
154      CASE (VREMAN) SELECT_TURB ! Vreman (2004) eddy viscosity
      model (experimental)
155
156      ! A. W. Vreman. An eddy-viscosity subgrid-scale model for
      turbulent shear flow: Algebraic theory and
      applications .
157      ! Phys. Fluids , 16(10):3670-3681, 2004.
158
159      DO K=1,KBAR
160          DO J=1,JBAR
161              DO I=1,IBAR
162                  IF (SOLID(CELL_INDEX(I , J ,K))) CYCLE
163                  DUDX = RDX(I) *(UU(I , J ,K)-UU(I-1,J ,K))
164                  DVDY = RDY(J) *(VV(I , J ,K)-VV(I , J-1,K))
165                  DWDZ = RDZ(K) *(WW(I , J ,K)-WW(I , J ,K-1))
166                  DUDY = 0.25_EB*RDY(J) *(UU(I , J+1,K)-UU(I , J-1,K)+
                  UU(I-1,J+1,K)-UU(I-1,J-1,K))
167                  DUDZ = 0.25_EB*RDZ(K) *(UU(I , J ,K+1)-UU(I , J ,K-1)+
                  UU(I-1,J ,K+1)-UU(I-1,J ,K-1))
168                  DVDX = 0.25_EB*RDX(I) *(VV(I+1,J ,K)-VV(I-1,J ,K)+
                  VV(I+1,J-1,K)-VV(I-1,J-1,K))
169                  DVDZ = 0.25_EB*RDZ(K) *(VV(I , J ,K+1)-VV(I , J ,K-1)+
                  VV(I , J-1,K+1)-VV(I , J-1,K-1))
170                  DWDX = 0.25_EB*RDX(I) *(WW(I+1,J ,K)-WW(I-1,J ,K)+
                  WW(I+1,J ,K-1)-WW(I-1,J ,K-1))
171                  DWDY = 0.25_EB*RDY(J) *(WW(I , J+1,K)-WW(I , J-1,K)+
                  WW(I , J+1,K-1)-WW(I , J-1,K-1))
172
173                  ! Vreman, Eq. (6)
174                  A_IJ(1 ,1)=DUDX; A_IJ(2 ,1)=DUDY; A_IJ(3 ,1)=DUDZ

```

```

175      A_IJ(1,2)=DVDX; A_IJ(2,2)=DVDY; A_IJ(3,2)=DVDZ
176      A_IJ(1,3)=DWDX; A_IJ(2,3)=DWDY; A_IJ(3,3)=DWDZ
177
178      AA=0._EB
179      DO JJ=1,3
180          DO II=1,3
181              AA = AA + A_IJ(II ,JJ)*A_IJ(II ,JJ)
182          ENDDO
183      ENDDO
184
185      ! Vreman, Eq. (7)
186      B_IJ(1,1)=(DX(I)*A_IJ(1,1))**2 + (DY(J)*A_IJ
187          (2,1))**2 + (DZ(K)*A_IJ(3,1))**2
188      B_IJ(2,2)=(DX(I)*A_IJ(1,2))**2 + (DY(J)*A_IJ
189          (2,2))**2 + (DZ(K)*A_IJ(3,2))**2
190      B_IJ(3,3)=(DX(I)*A_IJ(1,3))**2 + (DY(J)*A_IJ
191          (2,3))**2 + (DZ(K)*A_IJ(3,3))**2
192
193      B_IJ(1,2)=DX(I)**2*A_IJ(1,1)*A_IJ(1,2) + DY(J)
194          **2*A_IJ(2,1)*A_IJ(2,2) + DZ(K)**2*A_IJ(3,1)*
195          A_IJ(3,2)
196      B_IJ(1,3)=DX(I)**2*A_IJ(1,1)*A_IJ(1,3) + DY(J)
197          **2*A_IJ(2,1)*A_IJ(2,3) + DZ(K)**2*A_IJ(3,1)*
198          A_IJ(3,3)
199      B_IJ(2,3)=DX(I)**2*A_IJ(1,2)*A_IJ(1,3) + DY(J)
200          **2*A_IJ(2,2)*A_IJ(2,3) + DZ(K)**2*A_IJ(3,2)*
201          A_IJ(3,3)
202
203      BB = B_IJ(1,1)*B_IJ(2,2) - B_IJ(1,2)**2 &
204          + B_IJ(1,1)*B_IJ(3,3) - B_IJ(1,3)**2 &
205          + B_IJ(2,2)*B_IJ(3,3) - B_IJ(2,3)**2      !
206          Vreman, Eq. (8)
207
208      IF (ABS(AA)>ZERO.P) THEN
209          NUEDDY(I , J,K) = C_VREMAN*SQRT(BB/AA)      !
210          Vreman, Eq. (5)
211      ELSE
212          NUEDDY(I , J,K)=0._EB
213      ENDIF
214
215      MU(I , J,K) = MU(I , J,K) + RHOP(I , J,K)*NUEDDY(I , J ,
216          K)

```

```

206         ENDDO
207     ENDDO
208 ENDDO
209
210 END SELECT SELECT_TURB
211
212 ! Add viscosity for stably stratified flows (experimental)
213
214 GRAVITY_IF: IF (LES .AND. GRAV_VISC) THEN
215
216     DO K=1,KBAR
217         DO J=1,JBAR
218             DO I=1,IBAR
219                 IF (SOLID(CELL_INDEX(I , J ,K))) CYCLE
220                 IF (TWO_D) THEN
221                     DELTA = MAX(DX(I) ,DZ(K) )
222                 ELSE
223                     DELTA = MAX(DX(I) ,DY(J) ,DZ(K) )
224                 ENDIF
225
226                 GRAD_RHO(1) = 0.5 _EB *RDX(I) *(RHOP(I+1,J,K)-RHOP(I
227                     -1,J,K))
228                 GRAD_RHO(2) = 0.5 _EB *RDY(J) *(RHOP(I , J+1,K)-RHOP(I , J
229                     -1,K))
230                 GRAD_RHO(3) = 0.5 _EB *RDZ(K) *(RHOP(I , J ,K+1)-RHOP(I , J
231                     ,K-1))
232
233                 NU_G = C_G *DELTA**2 *SQRT(MAX(ZERO_P ,DOT_PRODUCT(
234                     GRAD_RHO,GVEC) ) /RHOP(I , J ,K) )
235
236                 MU(I , J ,K) = MAX(MU(I , J ,K) ,RHOP(I , J ,K) *NU_G)
237             ENDDO
238         ENDDO
239     ENDDO
240
241 ! Compute resolved kinetic energy per unit mass
242
243 !$OMP DO COLLAPSE(3) SCHEDULE(STATIC) PRIVATE(K, J, I, U2, V2, W2)
244 DO K=1,KBAR
245     DO J=1,JBAR
246         DO I=1,IBAR

```

```

245         U2 = 0.25_EB*(UU(I-1,J,K)+UU(I,J,K))**2
246         V2 = 0.25_EB*(VV(I,J-1,K)+VV(I,J,K))**2
247         W2 = 0.25_EB*(WW(I,J,K-1)+WW(I,J,K))**2
248         KRES(I,J,K) = 0.5_EB*(U2+V2+W2)
249     ENDDO
250 ENDDO
251 ENDDO
252 !$OMP END DO NOWAIT
253
254 ! Mirror viscosity into solids and exterior boundary cells
255
256 !$OMP DO SCHEDULE(STATIC) &
257 !$OMP PRIVATE(IW, II, JJ, KK, IIG, JJG, KKG)
258 WALLLOOP: DO IW=1,N_EXTERNAL_WALL_CELLS+N_INTERNAL_WALL_CELLS
259     WC=>WALL(IW)
260     IF (WC%BOUNDARY_TYPE/=NULLBOUNDARY) CYCLE WALLLOOP
261     II = WC%II
262     JJ = WC%JJ
263     KK = WC%KK
264     IOR = WC%IOR
265     IIG = WC%IIG
266     JJG = WC%JJG
267     KKG = WC%KKG
268
269     SELECT CASE(WC%BOUNDARY_TYPE)
270     CASE(SOLIDBOUNDARY)
271         IF (LES) THEN
272             IF (N_TRACKED_SPECIES>0 .AND. .NOT.EVACUATION_ONLY(
273                 NM)) &
274                 ZZ_GET(1:N_TRACKED_SPECIES) = ZZP(IIG, JJG, KKG, 1:
275                     N_TRACKED_SPECIES)
276             CALL GET_VISCOSITY(ZZ_GET, MU_DNS, TMP(IIG, JJG, KKG))
277             SELECT CASE (IOR)
278             CASE ( 1); MU(IIG, JJG, KKG) = MAX(MU_DNS, ONTH*MU(
279                 IIG+1, JJG, KKG))
280             CASE (-1); MU(IIG, JJG, KKG) = MAX(MU_DNS, ONTH*MU(
281                 IIG-1, JJG, KKG))
282             CASE ( 2); MU(IIG, JJG, KKG) = MAX(MU_DNS, ONTH*MU(
283                 IIG, JJG+1, KKG))
284             CASE (-2); MU(IIG, JJG, KKG) = MAX(MU_DNS, ONTH*MU(
285                 IIG, JJG-1, KKG))
286             CASE ( 3); MU(IIG, JJG, KKG) = MAX(MU_DNS, ONTH*MU(
287                 IIG, JJG, KKG+1))

```



```

281          CASE (-3); MU(IIG ,JJG ,KKG) = MAX(MU_DNS,ONTH*MU(
                IIG ,JJG ,KKG-1))
282          END SELECT
283          ENDIF
284          IF (SOLID(CELLINDEX( II , JJ ,KK))) MU( II , JJ ,KK) = MU(IIG
                ,JJG ,KKG)
285          CASE(OPEN_BOUNDARY,MIRROR_BOUNDARY)
286          MU( II , JJ ,KK) = MU(IIG ,JJG ,KKG)
287          KRES( II , JJ ,KK) = KRES(IIG ,JJG ,KKG)
288          END SELECT
289 ENDDO WALLLOOP
290 !$OMP END DO
291
292 !$OMP WORKSHARE
293 MU( 0 ,0:JBP1, 0) = MU( 1 ,0:JBP1,1)
294 MU( IBP1 ,0:JBP1, 0) = MU( IBAR ,0:JBP1,1)
295 MU( IBP1 ,0:JBP1,KBP1) = MU( IBAR ,0:JBP1,KBAR)
296 MU( 0 ,0:JBP1,KBP1) = MU( 1 ,0:JBP1,KBAR)
297 MU(0:IBP1 , 0, 0) = MU(0:IBP1 , 1,1)
298 MU(0:IBP1 ,JBP1,0) = MU(0:IBP1 ,JBAR,1)
299 MU(0:IBP1 ,JBP1,KBP1) = MU(0:IBP1 ,JBAR,KBAR)
300 MU(0:IBP1 ,0 ,KBP1) = MU(0:IBP1 , 1 ,KBAR)
301 MU(0 , 0 ,0:KBP1) = MU( 1 , 1 ,0:KBP1)
302 MU( IBP1 ,0 ,0:KBP1) = MU( IBAR , 1 ,0:KBP1)
303 MU( IBP1 ,JBP1 ,0:KBP1) = MU( IBAR ,JBAR ,0:KBP1)
304 MU(0 ,JBP1 ,0:KBP1) = MU( 1 ,JBAR ,0:KBP1)
305 !$OMP END WORKSHARE
306 !$OMP END PARALLEL
307
308 END SUBROUTINE COMPUTE_VISCOSITY

```

B.3 mesh.f90

Modified subroutine in mesh.f90:

```

1 MODULE MESH_VARIABLES
2
3 ! Data structure for mesh-dependent variables
4
5 USE PRECISION_PARAMETERS
6 USE TYPES
7 IMPLICIT NONE
8
9 CHARACTER(255), PARAMETER :: meshid=' $Id: mesh.f90_10087_
    2012-02-15_21:06:17Z_randy.mcdermott_$ '
10 CHARACTER(255), PARAMETER :: meshrev=' $Revision: 10087_$ '
11 CHARACTER(255), PARAMETER :: meshdate=' $Date: 2012-02-15_
    22:06:17_+0100_(on, 15_feb_2012)__$ '
12
13 TYPE MESH_TYPE
14
15 REAL(EB), POINTER, DIMENSION(:,:,:) :: &
16     U, V, W, US, VS, WS, DDDT, D, DS, H, HS, KRES, FVX, FVY, FVZ, RHO,
    RHOS, &
17     MU, TMP, Q, FRHO, KAPPA, QR, QR_W, UII, RSUM, D_LAGRANGIAN,
    D_REACTION, &
18     CSD2, MIX_TIME, STRAIN_RATE, KFST4, RHO_H_S_OVER_PBAR,
    D_RHSOP_DT, D_RHSOP_DT_S, NU_EDDY !ADDED
19
20 REAL(EB), POINTER, DIMENSION(:,:,:) :: ZZ, ZZS,
    DEL_RHO_D_DEL_Z
21 REAL(EB), POINTER, DIMENSION(:,:,:) :: AVG_DROP_DEN,
    AVG_DROP_TMP, AVG_DROP_RAD, AVG_DROP_AREA
22 REAL(EB), POINTER, DIMENSION(:,:,:) :: AVG_DROP_DEN_ALL
23 REAL(EB), POINTER, DIMENSION(:,:) :: UVW_GHOST
24
25 REAL(EB) :: POIS_PTB, POIS_ERR
26 REAL(EB), POINTER, DIMENSION(:) :: SAVE1, SAVE2, WORK
27 REAL(EB), POINTER, DIMENSION(:,:,:) :: PRHS
28 REAL(EB), POINTER, DIMENSION(:,:) :: BXS, BXF, BYS, BYF, BZS, BZF
    , BXST, BXFT, BYST, BYFT, BZST, BZFT
29 INTEGER :: LSAVE, LWORK, LBC, MBC, NBC, ITRN, JTRN, KTRN, IPS
30 REAL(EB), POINTER, DIMENSION(:) :: P_0, RHO_0, TMP_0, D_PBAR_DT
    , D_PBAR_S_DT, U_LEAK, U_DUCT
31 REAL(EB), POINTER, DIMENSION(:,:) :: PBAR, PBAR_S, R_PBAR

```

```

32  INTEGER, POINTER, DIMENSION(: , : , : ) :: PRESSURE_ZONE
33  INTEGER, POINTER, DIMENSION(:) :: PRESSURE_BC_INDEX
34  REAL(EB) , POINTER, DIMENSION(: , : , : ) :: WORK1,WORK2,WORK3,
    WORK4,WORK5,WORK6,WORK7,WORK8
35
36  REAL(EB) , POINTER, DIMENSION(: , : , : ) :: TURB_WORK1,TURB_WORK2
    ,TURB_WORK3,TURB_WORK4
37  REAL(EB) , POINTER, DIMENSION(: , : , : ) :: TURB_WORK5,TURB_WORK6
    ,TURB_WORK7,TURB_WORK8
38  REAL(EB) , POINTER, DIMENSION(: , : , : ) :: TURB_WORK9,
    TURB_WORK10
39  REAL(EB) , POINTER, DIMENSION(:) :: TURB_WORK11,TURB_WORK12
40
41  REAL(EB) , POINTER, DIMENSION(: , : , : ) :: IBM_SAVE1 ,IBM_SAVE2 ,
    IBM_SAVE3 ,IBM_SAVE4 ,IBM_SAVE5 ,IBM_SAVE6
42  INTEGER, POINTER, DIMENSION(: , : , : ) :: U_MASK, V_MASK, W_MASK,
    P_MASK
43
44  REAL(EB) , POINTER, DIMENSION(:) :: WALL_WORK1,WALL_WORK2
45  REAL(FB) , POINTER, DIMENSION(: , : , : , : ) :: QQ
46  REAL(FB) , POINTER, DIMENSION(: , : ) :: PP,PPN
47  INTEGER, POINTER, DIMENSION(: , : ) :: IBK
48  INTEGER, POINTER, DIMENSION(: , : , : ) :: IBLK
49
50  REAL(EB) :: DT,DT_PREV,DT_NEXT,DT_INIT
51  REAL(EB) :: CFL,DIVMX,DIVMN,VN,RESMAX,PART_CFL
52  INTEGER :: ICFL ,JCFL,KCFL,IMX,JMX,KMX,IMN,JMN,KMN, I_VN ,
    J_VN ,K_VN ,IRM ,JRM,KRM
53
54  INTEGER :: N_EDGES
55  INTEGER, POINTER, DIMENSION(: , : ) :: IJKE ,EDGE_INDEX
56  REAL(EB) , POINTER, DIMENSION(: , : ) :: TAU_E,OME_E
57  INTEGER, POINTER, DIMENSION(: , : ) :: EDGE_TYPE
58
59  INTEGER :: MESHLEVEL
60  INTEGER :: IBAR ,JBAR ,KBAR ,IBM1 ,JBM1 ,KBM1 ,IBP1 ,JBP1 ,KBP1
61  INTEGER, POINTER, DIMENSION(:) :: RGB
62  REAL(EB) :: DXI,DETA,DZETA,RDXI,RDETA,RDZETA, &
63  DXMIN,DXMAX,DYMIN,DYMAX,DZMIN,DZMAX, &
64  XS,XF,YS,YF,ZS,ZF,RDXINT,RDYINT,RDZINT,CELL_SIZE
65  REAL(EB) , POINTER, DIMENSION(:) :: R,RC,X,Y,Z,XC,YC,ZC,HX,HY
    ,HZ, &
66  DX,RDX,DXN,RDXN,DY,RDY,DYN,RDYN,DZ,RDZ,DZN,RDZN, &

```

```

67         CELLSI, CELLSJ, CELLSK, RRN
68     REAL(FB) , POINTER, DIMENSION(:) :: XPLT, YPLT, ZPLT
69
70     INTEGER :: N_OBST
71     TYPE(OBSTRUCTION_TYPE) , POINTER, DIMENSION(:) :: OBSTRUCTION
72
73     INTEGER :: N_VENT
74     TYPE(VENTS_TYPE) , POINTER, DIMENSION(:) :: VENTS
75
76     INTEGER, POINTER, DIMENSION(:,:,:) :: CELL_INDEX
77     INTEGER, POINTER, DIMENSION(:) :: I_CELL, J_CELL, K_CELL,
78         OBST_INDEX_C
79     INTEGER, POINTER, DIMENSION(:,:) :: WALL_INDEX
80     LOGICAL, POINTER, DIMENSION(:) :: SOLID, EXTERIOR
81
82     INTEGER :: N_INTERNAL_WALL_CELLS, N_EXTERNAL_WALL_CELLS,
83         N_VIRTUAL_WALL_CELLS, N_GHOST_WALL_CELLS, &
84         CELL_COUNT, WALL_COUNTER
85     REAL(EB) :: BC_CLOCK
86     REAL(EB) , POINTER, DIMENSION(:,:) ::
87         EDGE_INTERPOLATION_FACTOR, AWMLAEROSOL
88     REAL(EB) , POINTER, DIMENSION(:) :: DUWDT, &
89         D_CORR, DS_CORR, UVW_SAVE, U_GHOST, V_GHOST, W_GHOST
90     TYPE(WALL_TYPE) , POINTER, DIMENSION(:) :: WALL
91     TYPE(OMESH_TYPE) , POINTER, DIMENSION(:) :: OMESH
92     TYPE(LAGRANGIAN_PARTICLE_TYPE) , POINTER, DIMENSION(:) ::
93         LAGRANGIAN_PARTICLE
94
95     INTEGER :: NLP, NLPDIM
96     TYPE(HUMAN_TYPE) , POINTER, DIMENSION(:) :: HUMAN
97     INTEGER :: N_HUMANS, N_HUMANS_DIM
98     TYPE(HUMAN_GRID_TYPE) , POINTER, DIMENSION(:,:) :: HUMAN_GRID
99
100
101     INTEGER :: N_SLCF
102     TYPE(SLICE_TYPE) , POINTER, DIMENSION(:) :: SLICE
103
104     INTEGER, POINTER, DIMENSION(:,:) :: INC
105     INTEGER :: NPATCH
106
107     REAL(EB) , POINTER, DIMENSION(:,:,:,) :: UIID
108     INTEGER :: RAD_CALL_COUNTER, ANGLE_INC_COUNTER
109
110     INTEGER, POINTER, DIMENSION(:,:,:) :: INTERPOLATED_MESH

```

```

106  CHARACTER(80) , POINTER, DIMENSION(:) :: STRING
107  INTEGER :: N_STRINGS,N_STRINGS_MAX
108
109  !rm ->
110  ! REAL(EB) , POINTER, DIMENSION(:,:,:,) :: DMPVDT,FM,VEG
111  INTEGER, POINTER, DIMENSION(:,:,:) :: K_AGL_SLICE
112  REAL(EB) ,POINTER, DIMENSION(:,:) :: LS,Z_TERRAIN,VEG_DRAG
113  INTEGER :: N_TERRAIN_SLCF
114  REAL(EB) :: VEG_CLOCK_BC !surf veg
115  !rm <-
116
117  END TYPE MESH_TYPE
118
119  TYPE (MESH_TYPE) , SAVE, DIMENSION(:) , ALLOCATABLE, TARGET ::
    MESHES
120
121  END MODULE MESH_VARIABLES
122
123
124  MODULE MESH_POINTERS
125
126  USE PRECISION_PARAMETERS
127  USE MESH_VARIABLES
128  IMPLICIT NONE
129
130  REAL(EB) , POINTER, DIMENSION(:,:,:) :: &
131      U,V,W,US,VS,WS,DDDT,D,DS,H,HS,KRES,FVX,FVY,FVZ,RHO,
        RHOS, &
132      MU,TMP,Q,FRHO,KAPPA,QR,QR_W,UH,RSUM,D_LAGRANGIAN,
        D_REACTION, &
133      CSD2,MTR,MSR,WEM,MIX_TIME,STRAIN_RATE,KFST4,
        RHO_H_S_OVER_PBAR,D_RHSOP_DT,D_RHSOP_DT_S,NU_EDDY
        !ADDED
134  REAL(EB) , POINTER, DIMENSION(:,:,:,) :: ZZ,ZZS,DEL_RHO,D_DEL_Z
135  REAL(EB) , POINTER, DIMENSION(:,:,:,) :: AVG_DROP_DEN,
        AVG_DROP_TMP,AVG_DROP_RAD,AVG_DROP_AREA
136  REAL(EB) , POINTER, DIMENSION(:,:,:) :: AVG_DROP_DEN_ALL
137  REAL(EB) , POINTER, DIMENSION(:,:) :: UVW_GHOST
138  REAL(EB) , POINTER :: POIS_PTB,POIS_ERR
139  REAL(EB) , POINTER, DIMENSION(:) :: SAVE1,SAVE2,WORK
140  REAL(EB) , POINTER, DIMENSION(:,:,:) :: PRHS
141  REAL(EB) , POINTER, DIMENSION(:,:) :: BXS,BXF,BYS,BYF,BZS,BZF,
        BXST,BXFT,BYST,BYFT,BZST,BZFT

```

142 **INTEGER, POINTER** :: LSAVE,LWORK,LBC,MBC,NBC,ITRN,JTRN,KTRN,IPS
 143 **REAL(EB), POINTER, DIMENSION(:)** :: P_0,RHO_0,TMP_0,D_PBAR_DT,
 D_PBAR_S_DT,U_LEAK,U_DUCT
 144 **REAL(EB), POINTER, DIMENSION(:,:)** :: PBAR,PBAR_S,R_PBAR
 145 **INTEGER, POINTER, DIMENSION(:,:,:) ::** PRESSURE_ZONE
 146 **INTEGER, POINTER, DIMENSION(:)** :: PRESSURE_BC_INDEX
 147 **REAL(EB), POINTER, DIMENSION(:,:,:) ::** WORK1,WORK2,WORK3,WORK4,
 WORK5,WORK6,WORK7,WORK8
 148
 149 **REAL(EB), POINTER, DIMENSION(:,:,:) ::** TURB_WORK1,TURB_WORK2,
 TURB_WORK3,TURB_WORK4
 150 **REAL(EB), POINTER, DIMENSION(:,:,:) ::** TURB_WORK5,TURB_WORK6,
 TURB_WORK7,TURB_WORK8
 151 **REAL(EB), POINTER, DIMENSION(:,:,:) ::** TURB_WORK9,TURB_WORK10
 152 **REAL(EB), POINTER, DIMENSION(:)** :: TURB_WORK11,TURB_WORK12
 153
 154 **REAL(EB), POINTER, DIMENSION(:,:,:) ::** IBM_SAVE1,IBM_SAVE2,
 IBM_SAVE3,IBM_SAVE4,IBM_SAVE5,IBM_SAVE6
 155 **INTEGER, POINTER, DIMENSION(:,:,:) ::** U_MASK,V_MASK,W_MASK,
 P_MASK
 156
 157 **REAL(EB), POINTER, DIMENSION(:)** :: WALLWORK1,WALLWORK2
 158 **REAL(FB), POINTER, DIMENSION(:,:,:) ::** QQ
 159 **REAL(FB), POINTER, DIMENSION(:,:)** :: PP,PPN
 160 **INTEGER, POINTER, DIMENSION(:,:)** :: IBK
 161 **INTEGER, POINTER, DIMENSION(:,:,:) ::** IBLK
 162 **REAL(EB), POINTER** :: DT,DT_PREV,DT_NEXT,DT_INIT
 163 **REAL(EB), POINTER** :: CFL,DIVMX,DIVMN,VN,RESMAX,PART_CFL
 164 **INTEGER, POINTER** :: ICFL,JCFL,KCFL,IMX,JMX,KMX,IMN,JMN,KMN,I_VN
 ,J_VN,K_VN,IRM,JRM,KRM
 165 **INTEGER, POINTER** :: N_EDGES
 166 **INTEGER, POINTER, DIMENSION(:,:)** :: IJKE,EDGE_INDEX
 167 **REAL(EB), POINTER, DIMENSION(:,:)** :: TAU_E,OME_E
 168 **INTEGER, POINTER, DIMENSION(:,:)** :: EDGE_TYPE
 169
 170 **INTEGER, POINTER** :: MESHLEVEL
 171 **INTEGER, POINTER** :: IBAR,JBAR,KBAR,IBM1,JBM1,KBM1,IBP1,JBP1,
 KBP1
 172 **INTEGER, POINTER, DIMENSION(:)** :: RGB
 173 **REAL(EB), POINTER** :: DXI,DETA,DZETA,RDXI,RDETA,RDZETA, &
 174 DXMIN,DXMAX,DYMIN,DYMAX,DZMIN,DZMAX, &
 175 XS,XF,YS,YF,ZS,ZF,RDXINT,RDYINT,RDZINT,CELL_SIZE

```

176 REAL(EB) , POINTER, DIMENSION(:) :: R,RC,X,Y,Z,XC,YC,ZC,HX,HY,HZ
    , &
177     DX,RDX,DXN,RDXN,DY,RDY,DYN,RDYN,DZ,RDZ,DZN,RDZN, &
178     CELLSI,CELLSJ,CELLSK,RRN
179 REAL(FB) , POINTER, DIMENSION(:) :: XPLT,YPLT,ZPLT
180 INTEGER, POINTER :: N_OBST
181 TYPE(OBSTRUCTION_TYPE) , POINTER, DIMENSION(:) :: OBSTRUCTION
182 INTEGER, POINTER :: N_VENT
183 TYPE(VENTS_TYPE) , POINTER, DIMENSION(:) :: VENTS
184 INTEGER, POINTER, DIMENSION(:,:,:) :: CELL_INDEX
185 INTEGER, POINTER, DIMENSION(:) :: I_CELL,J_CELL,K_CELL,
    OBST_INDEX_C
186 INTEGER, POINTER, DIMENSION(:,:) :: WALL_INDEX
187 LOGICAL, POINTER, DIMENSION(:) :: SOLID,EXTERIOR
188 INTEGER, POINTER :: N_INTERNAL_WALL_CELLS,N_EXTERNAL_WALL_CELLS
    ,N_VIRTUAL_WALL_CELLS,N_GHOST_WALL_CELLS, &
189     CELL_COUNT,WALL_COUNTER
190 REAL(EB) ,POINTER :: BC_CLOCK
191 REAL(EB) , POINTER, DIMENSION(:,:) :: EDGE_INTERPOLATION_FACTOR,
    AWMLAEROSOL
192 REAL(EB) , POINTER, DIMENSION(:) :: DUWDT, &
193     D_CORR,DS_CORR,UVW_SAVE,U_GHOST,V_GHOST,W_GHOST
194 TYPE(WALL_TYPE) , POINTER, DIMENSION(:) :: WALL
195 TYPE(OMESH_TYPE) , POINTER, DIMENSION(:) :: OMESH
196 TYPE(LAGRANGIAN_PARTICLE_TYPE) , POINTER, DIMENSION(:) ::
    LAGRANGIAN_PARTICLE
197 INTEGER, POINTER :: NLP,NLPDIM
198 TYPE(HUMAN_TYPE) , POINTER, DIMENSION(:) :: HUMAN
199 INTEGER, POINTER :: N_HUMANS,N_HUMANS_DIM
200 TYPE(HUMAN_GRID_TYPE) , POINTER, DIMENSION(:,:) :: HUMAN_GRID
201 INTEGER, POINTER :: N_SLCF
202 TYPE(SLICE_TYPE) , POINTER, DIMENSION(:) :: SLICE
203 INTEGER, POINTER, DIMENSION(:,:) :: INC
204 INTEGER, POINTER :: NPATCH
205 REAL(EB) , POINTER, DIMENSION(:,:,:,) :: UIID
206 INTEGER, POINTER :: RAD_CALL_COUNTER,ANGLE_INC_COUNTER
207 INTEGER, POINTER, DIMENSION(:,:,:) :: INTERPOLATED_MESH
208 CHARACTER(80) , POINTER, DIMENSION(:) :: STRING
209 INTEGER, POINTER :: N_STRINGS,N_STRINGS_MAX
210 !rm ->
211 !REAL(EB) , POINTER, DIMENSION(:,:,:,) :: DMPVDT_FM_VEG
212 INTEGER, POINTER, DIMENSION(:,:,:) :: K_AGL_SLICE
213 REAL(EB) , POINTER,DIMENSION(:,:) :: LS_Z_TERRAIN,VEG_DRAG

```

```
214 INTEGER, POINTER :: N_TERRAIN_SLCF
215 REAL(EB), POINTER :: VEG_CLOCK_BC !surf veg
216 !rm <-
217
218 CONTAINS
```


B.4 init.f90

Modified subroutine in init.f90:

```

1  SUBROUTINE INITIALIZE_MESH_VARIABLES(NM)
2
3  USE PHYSICAL_FUNCTIONS, ONLY: GET_VISCOSITY,
      GET_SPECIFIC_GAS_CONSTANT, GET_SPECIFIC_HEAT
4  USE GEOMETRY_FUNCTIONS, ONLY: ASSIGN_PRESSURE_ZONE
5  USE RADCONS, ONLY: UIIDIM
6  USE CONTROL_VARIABLES
7  INTEGER :: N, I, J, K, II, JJ, KK, IPTS, JPTS, KPTS, N_EDGES_DIM,
      N_TOTAL_WALL_CELLS, IW, IWE, IWG, IC, SURF_INDEX, IOR, IOPZ, &
8      IERR, IB, JB, KB, IPZ
9  INTEGER, INTENT(IN) :: NM
10 REAL(EB) :: MU_N, ZZ_GET(0:N_TRACKED_SPECIES), VC, RTRM, CP, CS,
      DELTA
11 INTEGER, POINTER :: IBP1, JBP1, KBP1, IBAR, JBAR, KBAR, N_EDGES
12 REAL(EB), POINTER :: XS, XF, YS, YF, ZS, ZF
13 TYPE (INITIALIZATION_TYPE), POINTER :: IN
14 TYPE (P_ZONE_TYPE), POINTER :: PZ
15 TYPE (DEVICE_TYPE), POINTER :: DV
16 TYPE (VENTS_TYPE), POINTER :: VT
17
18 IERR = 0
19 M => MESHES(NM)
20 IBP1 =>M%IBP1
21 JBP1 =>M%JBP1
22 KBP1 =>M%KBP1
23 IBAR =>M%IBAR
24 JBAR =>M%JBAR
25 KBAR =>M%KBAR
26 N_EDGES=>M%N_EDGES
27 XS=>M%XS
28 YS=>M%YS
29 ZS=>M%ZS
30 XF=>M%XF
31 YF=>M%YF
32 ZF=>M%ZF
33 ALLOCATE(M%RHO(0:IBP1,0:JBP1,0:KBP1),STAT=IZERO)
34 CALL ChkMemErr('INIT', 'RHO', IZERO)
35 ALLOCATE(M%RHOS(0:IBP1,0:JBP1,0:KBP1),STAT=IZERO)
36 CALL ChkMemErr('INIT', 'RHOS', IZERO)
37 M%RHOS = RHOA

```

```

38 ALLOCATE(M%TMP(0:IBP1,0:JBP1,0:KBP1),STAT=IZERO)
39 CALL ChkMemErr('INIT','TMP',IZERO)
40 ALLOCATE(M%FRHO(0:IBP1,0:JBP1,0:KBP1),STAT=IZERO)
41 CALL ChkMemErr('INIT','FRHO',IZERO)
42 ALLOCATE(M%U(0:IBP1,0:JBP1,0:KBP1),STAT=IZERO)
43 CALL ChkMemErr('INIT','U',IZERO)
44 ALLOCATE(M%V(0:IBP1,0:JBP1,0:KBP1),STAT=IZERO)
45 CALL ChkMemErr('INIT','V',IZERO)
46 ALLOCATE(M%W(0:IBP1,0:JBP1,0:KBP1),STAT=IZERO)
47 CALL ChkMemErr('INIT','W',IZERO)
48 ALLOCATE(M%US(0:IBP1,0:JBP1,0:KBP1),STAT=IZERO)
49 CALL ChkMemErr('INIT','US',IZERO)
50 ALLOCATE(M%VS(0:IBP1,0:JBP1,0:KBP1),STAT=IZERO)
51 CALL ChkMemErr('INIT','VS',IZERO)
52 ALLOCATE(M%WS(0:IBP1,0:JBP1,0:KBP1),STAT=IZERO)
53 CALL ChkMemErr('INIT','WS',IZERO)
54 ALLOCATE(M%FVX(0:IBP1,0:JBP1,0:KBP1),STAT=IZERO)
55 CALL ChkMemErr('INIT','FVX',IZERO)
56 ALLOCATE(M%FVY(0:IBP1,0:JBP1,0:KBP1),STAT=IZERO)
57 CALL ChkMemErr('INIT','FVY',IZERO)
58 ALLOCATE(M%FVZ(0:IBP1,0:JBP1,0:KBP1),STAT=IZERO)
59 CALL ChkMemErr('INIT','FVZ',IZERO)
60 ALLOCATE(M%H(0:IBP1,0:JBP1,0:KBP1),STAT=IZERO)
61 CALL ChkMemErr('INIT','H',IZERO)
62 ALLOCATE(M%HS(0:IBP1,0:JBP1,0:KBP1),STAT=IZERO)
63 CALL ChkMemErr('INIT','HS',IZERO)
64 ALLOCATE(M%KRES(0:IBP1,0:JBP1,0:KBP1),STAT=IZERO)
65 CALL ChkMemErr('INIT','KRES',IZERO)
66 ALLOCATE(M%DDDT(0:IBP1,0:JBP1,0:KBP1),STAT=IZERO)
67 CALL ChkMemErr('INIT','DDDT',IZERO)
68 ALLOCATE(M%D(0:IBP1,0:JBP1,0:KBP1),STAT=IZERO)
69 CALL ChkMemErr('INIT','D',IZERO)
70 ALLOCATE(M%DS(0:IBP1,0:JBP1,0:KBP1),STAT=IZERO)
71 CALL ChkMemErr('INIT','DS',IZERO)
72 ALLOCATE(M%MU(0:IBP1,0:JBP1,0:KBP1),STAT=IZERO)
73 CALL ChkMemErr('INIT','MU',IZERO)
74 ALLOCATE(M%STRAIN_RATE(0:IBP1,0:JBP1,0:KBP1),STAT=IZERO)
75 CALL ChkMemErr('INIT','STRAIN_RATE',IZERO)
76 ALLOCATE(M%NU_EDDY(0:IBP1,0:JBP1,0:KBP1),STAT=IZERO) !ADDED
77 CALL ChkMemErr('INIT','NU_EDDY',IZERO) !ADDED
78 ALLOCATE(M%CS2(0:IBP1,0:JBP1,0:KBP1),STAT=IZERO)
79 CALL ChkMemErr('INIT','CS',IZERO)
80

```

```

81 IF (.NOT.EVACUATION_ONLY(NM)) THEN
82   ALLOCATE(M%Q(0:IBP1,0:JBP1,0:KBP1),STAT=IZERO)
83   CALL ChkMemErr('INIT','Q',IZERO)
84 ENDIF
85
86 ALLOCATE(M%MIX_TIME(0:IBP1,0:JBP1,0:KBP1),STAT=IZERO)
87 CALL ChkMemErr('INIT','MIX.TIME',IZERO)
88 M%MIX_TIME=M%DT
89
90 ! Background pressure, temperature, density as a function of
    height (Z coordinate)
91
92 ALLOCATE(M%PBAR(0:KBP1,0:N_ZONE),STAT=IZERO)
93 CALL ChkMemErr('INIT','PBAR',IZERO)
94 ALLOCATE(M%PBAR_S(0:KBP1,0:N_ZONE),STAT=IZERO)
95 CALL ChkMemErr('INIT','PBAR_S',IZERO)
96 ALLOCATE(M%R_PBAR(0:KBP1,0:N_ZONE),STAT=IZERO)
97 CALL ChkMemErr('INIT','R_PBAR',IZERO)
98 ALLOCATE(M%D_PBAR_DT(0:N_ZONE),STAT=IZERO)
99 CALL ChkMemErr('INIT','D_PBAR_DT',IZERO)
100 ALLOCATE(M%D_PBAR_S_DT(0:N_ZONE),STAT=IZERO)
101 CALL ChkMemErr('INIT','D_PBAR_S_DT',IZERO)
102 ALLOCATE(M%P_0(0:KBP1),STAT=IZERO)
103 CALL ChkMemErr('INIT','P_0',IZERO)
104 ALLOCATE(M%TMP_0(0:KBP1),STAT=IZERO)
105 CALL ChkMemErr('INIT','TMP_0',IZERO)
106 ALLOCATE(M%RHO_0(0:KBP1),STAT=IZERO)
107 CALL ChkMemErr('INIT','RHO_0',IZERO)
108
109 ! Leaks
110
111 ALLOCATE(M%U_LEAK(0:N_ZONE),STAT=IZERO)
112 CALL ChkMemErr('INIT','U_LEAK',IZERO)
113 M%U_LEAK = 0._EB
114
115 ! Allocate species arrays
116
117 IF (N_TRACKED_SPECIES>0 .AND. .NOT.EVACUATION_ONLY(NM)) THEN
118   ALLOCATE(M%ZZ(0:IBP1,0:JBP1,0:KBP1,N_TRACKED_SPECIES),STAT=
    IZERO)
119   CALL ChkMemErr('INIT','ZZ',IZERO)
120   M%ZZ = 0._EB

```

```

121   ALLOCATE(M%ZZS(0:IBP1,0:JBP1,0:KBP1,N_TRACKED_SPECIES),STAT=
      IZERO)
122   CALL ChkMemErr('INIT','ZZS',IZERO)
123   M%ZZS = 0._EB
124   ALLOCATE(M%DEL_RHO_D_DEL_Z(0:IBP1,0:JBP1,0:KBP1,
      N_TRACKED_SPECIES),STAT=IZERO)
125   CALL ChkMemErr('INIT','DEL_RHO_D_DEL_Z',IZERO)
126   M%DEL_RHO_D_DEL_Z = 0._EB
127   ENDF
128
129   ALLOCATE(M%RSUM(0:IBP1,0:JBP1,0:KBP1),STAT=IZERO)
130   CALL ChkMemErr('INIT','RSUM',IZERO)
131   M%RSUM = RSUM0
132
133   ! Allocate reaction divergence
134
135   IF (N_REACTIONS > 0) THEN
136     ALLOCATE(M%D_REACTION(0:IBP1,0:JBP1,0:KBP1),STAT=IZERO)
137     CALL ChkMemErr('INIT','D_REACTION',IZERO)
138     M%D_REACTION = 0._EB
139   ENDF
140
141   ! Enthalpy arrays (experimental)
142
143   IF (ENTHALPY_TRANSPORT) THEN
144     ALLOCATE(M%RHO_H_S_OVER_PBAR(0:IBP1,0:JBP1,0:KBP1),STAT=
      IZERO)
145     CALL ChkMemErr('INIT','RHO_H_S_OVER_PBAR',IZERO)
146     M%RHO_H_S_OVER_PBAR = 0._EB ! initialized in DENSITY
147     ALLOCATE(M%D_RHSOP_DT(0:IBP1,0:JBP1,0:KBP1),STAT=IZERO)
148     CALL ChkMemErr('INIT','D_RHSOP_DT',IZERO)
149     M%D_RHSOP_DT = 0._EB
150     ALLOCATE(M%D_RHSOP_DT_S(0:IBP1,0:JBP1,0:KBP1),STAT=IZERO)
151     CALL ChkMemErr('INIT','D_RHSOP_DT_S',IZERO)
152     M%D_RHSOP_DT_S = 0._EB
153   ENDF
154
155   ! Allocate water mass arrays if sprinklers are present
156
157   IF (PARTICLE_FILE) PARTICLE_TAG = NM
158
159   IF (N_LAGRANGIAN_CLASSES > 0 .AND. .NOT. EVACUATION_ONLY(NM))
      THEN

```

```

160     ALLOCATE(M%AVG_DROP_DEN_ALL(0:IBP1,0:JBP1,0:KBP1),STAT=IZERO
      )
161     CALL ChkMemErr('INIT','AVG_DROP_DEN_ALL',IZERO)
162     M%AVG_DROP_DEN_ALL=0._EB
163 ENDIF
164
165 IF (N_LP_ARRAY_INDICES>0 .AND. .NOT.EVACUATION_ONLY(NM)) THEN
166     ALLOCATE(M%QR_W(0:IBP1,0:JBP1,0:KBP1),STAT=IZERO)
167     CALL ChkMemErr('INIT','QR_W',IZERO)
168     M%QR_W = 0._EB
169     ALLOCATE(M%AVG_DROP_DEN(0:IBP1,0:JBP1,0:KBP1,
      N_LP_ARRAY_INDICES),STAT=IZERO)
170     CALL ChkMemErr('INIT','AVG_DROP_DEN',IZERO)
171     M%AVG_DROP_DEN=0._EB
172     ALLOCATE(M%AVG_DROP_AREA(0:IBP1,0:JBP1,0:KBP1,
      N_LP_ARRAY_INDICES),STAT=IZERO)
173     CALL ChkMemErr('INIT','AVG_DROP_AREA',IZERO)
174     M%AVG_DROP_AREA=0._EB
175     ALLOCATE(M%AVG_DROP_TMP(0:IBP1,0:JBP1,0:KBP1,
      N_LP_ARRAY_INDICES),STAT=IZERO)
176     CALL ChkMemErr('INIT','AVG_DROP_TMP',IZERO)
177     M%AVG_DROP_TMP=TMPM
178     ALLOCATE(M%AVG_DROP_RAD(0:IBP1,0:JBP1,0:KBP1,
      N_LP_ARRAY_INDICES),STAT=IZERO)
179     CALL ChkMemErr('INIT','AVG_DROP_RAD',IZERO)
180     M%AVG_DROP_RAD=0._EB
181     ALLOCATE(M%D_LAGRANGIAN(0:IBP1,0:JBP1,0:KBP1),STAT=IZERO)
182     CALL ChkMemErr('INIT','D_LAGRANGIAN',IZERO)
183     M%D_LAGRANGIAN = 0._EB
184 ENDIF
185
186 ! If radiation absorption desired allocate arrays
187
188 IF (.NOT.EVACUATION_ONLY(NM)) THEN
189     ALLOCATE(M%QR(0:IBP1,0:JBP1,0:KBP1),STAT=IZERO)
190     CALL ChkMemErr('INIT','QR',IZERO)
191     M%QR = 0._EB
192     ALLOCATE(M%KAPPA(0:IBP1,0:JBP1,0:KBP1),STAT=IZERO)
193     CALL ChkMemErr('INIT','KAPPA',IZERO)
194     M%KAPPA = KAPPA0
195     ALLOCATE(M%UII(0:IBP1,0:JBP1,0:KBP1),STAT=IZERO)
196     CALL ChkMemErr('INIT','UII',IZERO)
197     M%UII = 0._EB

```

```

198     ALLOCATE(M%KFST4(0:IBP1,0:JBP1,0:KBP1),STAT=IZERO)
199     CALL ChkMemErr('INIT','KFST4',IZERO)
200     M%KFST4 = 0._EB
201 ELSE
202     ALLOCATE(M%QR(0:IBP1,0:JBP1,0:KBP1),STAT=IZERO)
203     CALL ChkMemErr('INIT','QR',IZERO)
204     M%QR = 0._EB
205 ENDIF
206
207 ! Work arrays
208
209 ALLOCATE(M%WORK1(0:IBP1,0:JBP1,0:KBP1),STAT=IZERO)
210 CALL ChkMemErr('INIT','WORK1',IZERO)
211 ALLOCATE(M%WORK2(0:IBP1,0:JBP1,0:KBP1),STAT=IZERO)
212 CALL ChkMemErr('INIT','WORK2',IZERO)
213 ALLOCATE(M%WORK3(0:IBP1,0:JBP1,0:KBP1),STAT=IZERO)
214 CALL ChkMemErr('INIT','WORK3',IZERO)
215 ALLOCATE(M%WORK4(0:IBP1,0:JBP1,0:KBP1),STAT=IZERO)
216 CALL ChkMemErr('INIT','WORK4',IZERO)
217 ALLOCATE(M%WORK5(0:IBP1,0:JBP1,0:KBP1),STAT=IZERO)
218 CALL ChkMemErr('INIT','WORK5',IZERO)
219 ALLOCATE(M%WORK6(0:IBP1,0:JBP1,0:KBP1),STAT=IZERO)
220 CALL ChkMemErr('INIT','WORK6',IZERO)
221 ALLOCATE(M%WORK7(0:IBP1,0:JBP1,0:KBP1),STAT=IZERO)
222 CALL ChkMemErr('INIT','WORK7',IZERO)
223 ALLOCATE(M%WORK8(0:IBP1,0:JBP1,0:KBP1),STAT=IZERO)
224 CALL ChkMemErr('INIT','WORK8',IZERO)
225
226 IF (IMMERSED_BOUNDARY_METHOD==2) THEN
227     ALLOCATE(M%IBM_SAVE1(0:IBP1,0:JBP1,0:KBP1),STAT=IZERO)
228     CALL ChkMemErr('INIT','IBM_SAVE1',IZERO)
229     ALLOCATE(M%IBM_SAVE2(0:IBP1,0:JBP1,0:KBP1),STAT=IZERO)
230     CALL ChkMemErr('INIT','IBM_SAVE2',IZERO)
231     ALLOCATE(M%IBM_SAVE3(0:IBP1,0:JBP1,0:KBP1),STAT=IZERO)
232     CALL ChkMemErr('INIT','IBM_SAVE3',IZERO)
233     ALLOCATE(M%IBM_SAVE4(0:IBP1,0:JBP1,0:KBP1),STAT=IZERO)
234     CALL ChkMemErr('INIT','IBM_SAVE4',IZERO)
235     ALLOCATE(M%IBM_SAVE5(0:IBP1,0:JBP1,0:KBP1),STAT=IZERO)
236     CALL ChkMemErr('INIT','IBM_SAVE5',IZERO)
237     ALLOCATE(M%IBM_SAVE6(0:IBP1,0:JBP1,0:KBP1),STAT=IZERO)
238     CALL ChkMemErr('INIT','IBM_SAVE6',IZERO)
239 ENDIF
240

```

```

241 ! Boundary file patch counter
242
243 ALLOCATE(M%INC( -3:3,0:M%N_OBST) ,STAT=IZERO)
244 CALL ChkMemErr( 'INIT' , 'INC' , IZERO)
245
246 ! Initialize background pressure , temperature and density
247
248 M%D_PBAR_DT = 0._EB
249 M%D_PBAR_S_DT = 0._EB
250
251 IF (STRATIFICATION .AND. .NOT.EVACUATION_ONLY(NM)) THEN
252   DO K=0,M%KBP1
253     M%TMP_0(K) = TMPA + LAPSE_RATE*(M%ZC(K)-GROUND_LEVEL)
254     IF (ABS(LAPSE_RATE)>ZERO_P) THEN
255       M%P_0(K) = P_INF*(M%TMP_0(K)/M%TMP_0(0))**(GVEC(3)/
        RSUM0/LAPSE_RATE)
256     ELSE
257       M%P_0(K) = P_INF*EXP(GVEC(3)*(M%ZC(K)-GROUND_LEVEL)/(
        RSUM0*TMPA))
258     ENDIF
259   ENDDO
260 ELSE
261   M%TMP_0(:) = TMPA
262   M%P_0(:) = P_INF
263 ENDIF
264 DO K=0,M%KBP1
265   M%PBAR(K,:) = M%P_0(K)
266   M%PBAR_S(K,:) = M%P_0(K)
267   M%RHO_0(K) = M%P_0(K)/(M%TMP_0(K)*RSUM0)
268 ENDDO
269
270 ! Initialize various time step variables
271
272 M%DT_PREV = M%DT
273 M%DT_NEXT = M%DT
274 M%DT_INIT = M%DT
275
276 ! Initialize major arrays
277
278 DO K=0,M%KBP1
279   M%RHO(:, :, K) = M%RHO_0(K)
280   M%TMP(:, :, K) = M%TMP_0(K)
281 ENDDO

```

```

282 IF (.NOT.EVACUATION_ONLY(NM)) M%FRHO = 0._EB
283 M%U = U0
284 M%V = V0
285 M%W = W0
286 M%US = U0
287 M%VS = V0
288 M%WS = W0
289 M%FVX = 0._EB
290 M%FVY = 0._EB
291 M%FVZ = 0._EB
292 M%H = H0
293 M%HS = H0
294 M%KRES = 0._EB
295
296 M%DDDT = 0._EB
297 M%D = 0._EB
298 M%DS = 0._EB
299 IF (.NOT.EVACUATION_ONLY(NM)) THEN
300     M%Q = 0._EB
301 ENDIF
302 IF (EVACUATION_ONLY(NM)) THEN
303     M%U = 0._EB
304     M%V = 0._EB
305     M%W = 0._EB
306     M%US = 0._EB
307     M%VS = 0._EB
308     M%WS = 0._EB
309     M%H = 0._EB
310     M%HS = 0._EB
311 ENDIF
312 IF (N_TRACKED_SPECIES > 0 .AND. .NOT.EVACUATION_ONLY(NM)) M%
    DEL_RHO_D_DEL_Z = 0._EB
313
314 ! Viscosity
315
316 IF (N_TRACKED_SPECIES>0) ZZ_GET(1:N_TRACKED_SPECIES) =
    SPECIES_MIXTURE(1:N_TRACKED_SPECIES)%ZZ0
317 CALL GET_VISCOSITY(ZZ_GET, MU_N, TMPA)
318 M%MU = MU_N
319
320 CS = C_SMAGORINSKY
321 IF (EVACUATION_ONLY(NM)) CS=0.9._EB
322 DO K=0,KBP1

```



```

323     DO J=0,JBP1
324         DO I=0,IBP1
325             IF (TWO_D) THEN
326                 DELTA = MAX(M%DX(I) ,M%DZ(K) )
327             ELSE
328                 DELTA = MAX(M%DX(I) ,M%DY(J) ,M%DZ(K) )
329             ENDIF
330             M%CSD2(I , J ,K) = (CS*DELTA)**2
331         ENDDO
332     ENDDO
333 ENDDO
334
335 ! Initialize mass fraction arrays
336
337 IF (N_TRACKED_SPECIES > 0 .AND. .NOT.EVACUATION_ONLY(NM) ) THEN
338     DO N=1,N_TRACKED_SPECIES
339         M%ZZ (: , : , : ,N) = SPECIES_MIXTURE(N)%ZZ0
340         M%ZS (: , : , : ,N) = SPECIES_MIXTURE(N)%ZZ0
341     ENDDO
342 ENDIF
343
344 ! Initialize pressure ZONES
345
346 ALLOCATE(M%PRESSURE_ZONE(0:IBP1 , 0:JBP1 , 0:KBP1) ,STAT=IZERO)
347 CALL ChkMemErr( 'INIT' , 'PRESSURE_ZONE' , IZERO)
348 M%PRESSURE_ZONE = 0
349 ZONELOOP: DO N=1,N_ZONE
350     IF (EVACUATION_ONLY(NM) ) CYCLE ZONELOOP
351     PZ => P_ZONE(N)
352     DO K=0,KBP1
353         DO J=0,JBP1
354             DO I=0,IBP1
355                 IF (M%PRESSURE_ZONE(I , J ,K)==N) CYCLE
356                 IF (M%X(I) > PZ%X1 .AND. M%X(I) < PZ%X2 .AND. &
357                     M%Y(J) > PZ%Y1 .AND. M%Y(J) < PZ%Y2 .AND. &
358                     M%Z(K) > PZ%Z1 .AND. M%Z(K) < PZ%Z2) THEN
359                     M%PRESSURE_ZONE(I , J ,K) = N
360                 DO IOPZ=0,N_ZONE
361                     IF (PZ%LEAK_AREA(IOPZ) > 0._EB)
362                         ACTUALLEAK_AREA(N,IOPZ) = PZ%LEAK_AREA(

```

```

                                IOPZ)
363      ENDDO
364      IF (.NOT.M%$SOLID(M%$CELL_INDEX(I , J,K))) CALL
                                ASSIGN_PRESSURE_ZONE(NM,M%$XC(I) ,M%$YC(J) ,M%$ZC
                                (K) ,N)
365      ENDDIF
366      ENDDO
367      ENDDO
368      ENDDO
369 ENDDO ZONE_LOOP
370
371
372 ! Over-ride default ambient conditions with user-prescribed
    ! INITIALizations
373
374 DO N=1,N_INIT
375   IF (EVACUATION_ONLY(NM)) CYCLE
376   IN => INITIALIZATION(N)
377   DO K=0,KBP1
378     DO J=0,JBP1
379       DO I=0,IBP1
380         IF (M%$XC(I) > IN%$X1 .AND. M%$XC(I) < IN%$X2 .AND. &
381             M%$YC(J) > IN%$Y1 .AND. M%$YC(J) < IN%$Y2 .AND. &
382             M%$ZC(K) > IN%$Z1 .AND. M%$ZC(K) < IN%$Z2) THEN
383           M%$IMP(I , J,K)           = IN%$TEMPERATURE
384           M%$RHO(I , J,K)           = IN%$DENSITY
385           IF (N_TRACKED_SPECIES>0) M%$ZZ(I , J ,K, 1:
                                N_TRACKED_SPECIES) = IN%$MASS_FRACTION(1:
                                N_TRACKED_SPECIES)
386           IF (IN%$ADJUST_DENSITY)   M%$RHO(I , J ,K) = M%$RHO(
                                I , J ,K) *M%$P_0(K) /P_INF
387           IF (IN%$ADJUST_TEMPERATURE) M%$IMP(I , J ,K) = M%$IMP(
                                I , J ,K) *M%$P_0(K) /P_INF
388           M%$Q(I , J ,K) = IN%$HRRPUV
389       ENDDIF
390     ENDDO
391   ENDDO
392 ENDDO
393 ENDDO
394
395 ! Compute molecular weight term RSUM=R0*SUM(Y_i/M_i)
396
397 IF (N_TRACKED_SPECIES>0 .AND. .NOT.EVACUATION_ONLY(NM)) THEN

```

```

398     DO K=1,KBAR
399         DO J=1,JBAR
400             DO I=1,IBAR
401                 ZZ_GET(1:N_TRACKED_SPECIES) = M%ZZ(I,J,K,1:
                     N_TRACKED_SPECIES)
402                 CALL GET_SPECIFIC_GAS_CONSTANT(ZZ_GET,M%RSUM(I,J,K)
                     )
403             ENDDO
404         ENDDO
405     ENDDO
406 ENDIF
407
408 ! Allocate and Initialize Mesh-Dependent Radiation Arrays
409
410 M%QR = 0._EB
411 IF (.NOT.EVACUATION_ONLY(NM)) THEN
412     M%KAPPA = KAPPA0
413     M%UII = 4._EB*SIGMA*TMPA4
414 ENDIF
415 M%ANGLE_INC_COUNTER = 0
416 M%RAD_CALL_COUNTER = 0
417 IF (RADIATION .AND. .NOT.EVACUATION_ONLY(NM)) THEN
418     ALLOCATE(M%UIID(0:M%IBP1,0:M%JBP1,0:M%KBP1,1:UIIDIM),STAT=
         IZERO)
419     CALL ChkMemErr('INIT', 'UIID', IZERO)
420     M%UIID = 0.
421 ENDIF
422
423 ! General work arrays
424
425 M%WORK1 = 0._EB
426 M%WORK2 = 0._EB
427 M%WORK3 = 0._EB
428 M%WORK4 = 0._EB
429 M%WORK5 = 0._EB
430 M%WORK6 = 0._EB
431 IF (.NOT.EVACUATION_ONLY(NM)) M%WORK7 = 0._EB
432
433 ! Immersed Boundary Method
434
435 IF (IMMERSED_BOUNDARY_METHOD==2) THEN
436     M%IBM_SAVE1 = 0._EB
437     M%IBM_SAVE2 = 0._EB

```

```

438     M%IBM_SAVE3 = 0._EB
439     M%IBM_SAVE4 = 0._EB
440     M%IBM_SAVE5 = 0._EB
441     M%IBM_SAVE6 = 0._EB
442 ENDIF
443
444 IF (IMMERSED_BOUNDARY_METHOD >= 0) THEN
445     ALLOCATE(M%U_MASK(0:M%IBP1,0:M%JBP1,0:M%KBP1),STAT=IZERO)
446     CALL ChkMemErr('INIT_IBM','U_MASK',IZERO)
447     ALLOCATE(M%V_MASK(0:M%IBP1,0:M%JBP1,0:M%KBP1),STAT=IZERO)
448     CALL ChkMemErr('INIT_IBM','V_MASK',IZERO)
449     ALLOCATE(M%W_MASK(0:M%IBP1,0:M%JBP1,0:M%KBP1),STAT=IZERO)
450     CALL ChkMemErr('INIT_IBM','W_MASK',IZERO)
451     ALLOCATE(M%P_MASK(0:M%IBP1,0:M%JBP1,0:M%KBP1),STAT=IZERO)
452     CALL ChkMemErr('INIT_IBM','P_MASK',IZERO)
453     M%U_MASK=1
454     M%V_MASK=1
455     M%W_MASK=1
456     M%P_MASK=1
457 ENDIF
458
459 ! Determine the total number of wall cells to allocate
460
461 M%N_INTERNAL_WALL_CELLS = 0
462
463 OBST_LOOP_1: DO N=1,M%N_OBST
464     OB=>M%OBSTRUCTION(N)
465     IF (OB%CONSUMABLE .AND. .NOT.EVACUATION_ONLY(NM)) THEN
466         IB = OB%I2-OB%I1
467         JB = OB%J2-OB%J1
468         KB = OB%K2-OB%K1
469         M%N_INTERNAL_WALL_CELLS = M%N_INTERNAL_WALL_CELLS + 2*(
            MAX(1,IB)*JB*KB + MAX(1,JB)*IB*KB + MAX(1,KB)*IB*JB)
470     ELSE
471         DO K=OB%K1+1,OB%K2
472             DO J=OB%J1+1,OB%J2
473                 IC = M%CELL_INDEX(OB%I1,J,K)
474                 IF (.NOT.M%SOLID(IC).OR.M%OBSTRUCTION(M%
                    OBST_INDEX_C(IC))%REMOVABLE) M%
                    N_INTERNAL_WALL_CELLS = M%N_INTERNAL_WALL_CELLS
                    +1
475                 IC = M%CELL_INDEX(OB%I2+1,J,K)

```

```

476         IF ( .NOT.M%SOLID(IC) .OR.M%OBSTRUCTION(M%
              OBST_INDEX_C(IC))%REMOVABLE) M%
              N_INTERNAL_WALL_CELLS = M%N_INTERNAL_WALL_CELLS
              +1
477         ENDDO
478     ENDDO
479     DO K=OB%K1+1,OB%K2
480         DO I=OB%I1+1,OB%I2
481             IC = M%CELL_INDEX(I,OB%J1,K)
482             IF ( .NOT.M%SOLID(IC) .OR.M%OBSTRUCTION(M%
                  OBST_INDEX_C(IC))%REMOVABLE) M%
                  N_INTERNAL_WALL_CELLS = M%N_INTERNAL_WALL_CELLS
                  +1
483             IC = M%CELL_INDEX(I,OB%J2+1,K)
484             IF ( .NOT.M%SOLID(IC) .OR.M%OBSTRUCTION(M%
                  OBST_INDEX_C(IC))%REMOVABLE) M%
                  N_INTERNAL_WALL_CELLS = M%N_INTERNAL_WALL_CELLS
                  +1
485         ENDDO
486     ENDDO
487     DO J=OB%J1+1,OB%J2
488         DO I=OB%I1+1,OB%I2
489             IC = M%CELL_INDEX(I,J,OB%K1)
490             IF ( .NOT.M%SOLID(IC) .OR.M%OBSTRUCTION(M%
                  OBST_INDEX_C(IC))%REMOVABLE) M%
                  N_INTERNAL_WALL_CELLS = M%N_INTERNAL_WALL_CELLS
                  +1
491             IC = M%CELL_INDEX(I,J,OB%K2+1)
492             IF ( .NOT.M%SOLID(IC) .OR.M%OBSTRUCTION(M%
                  OBST_INDEX_C(IC))%REMOVABLE) M%
                  N_INTERNAL_WALL_CELLS = M%N_INTERNAL_WALL_CELLS
                  +1
493         ENDDO
494     ENDDO
495     ENDF
496 ENDDO OBST_LOOP_1
497
498 ! Add wall cells for VIRTUAL devices
499
500 M%N_VIRTUAL_WALL_CELLS = 0
501
502 DO N=1,N_DEVC
503     DV => DEVICE(N)

```

```

504     IF (DV%MESH/=NM) CYCLE
505     IF (EVACUATION_ONLY(NM)) CYCLE
506     IF (DV%QUANTITY/= 'CABLE_TEMPERATURE') CYCLE
507     M%N_VIRTUAL_WALL_CELLS = M%N_VIRTUAL_WALL_CELLS + 1
508 ENDDO
509
510 ! Compute the number of ghost wall cells (external wall cells
      outside the computational domain)
511
512 M%N_GHOST_WALL_CELLS = 8*(IBP1+JBP1+KBP1)
513
514 ! Allocate arrays indexed by wall cells (IW). Note the order of
      the cells in the overall array.
515
516 N_TOTAL_WALL_CELLS = M%N_EXTERNAL_WALL_CELLS + M%
      N_INTERNAL_WALL_CELLS + M%N_VIRTUAL_WALL_CELLS + M%
      N_GHOST_WALL_CELLS
517
518 ALLOCATE(M%WALL(0:N_TOTAL_WALL_CELLS) ,STAT=IZERO)
519 CALL ChkMemErr( 'INIT' , 'WALL' , IZERO)
520 M%WALL%RHO_F = RHOA
521 M%WALL%ONE_D%EMISSIVITY = 1._EB
522 M%WALL%U_TAU = 0._EB
523
524 NOT_EVAC_IF_1: IF (.NOT.EVACUATION_ONLY(NM)) THEN
525
526     M%WALL%TMP_F = TMPA
527     M%WALL%TMP_B = TMPA
528     DO IW=1,N_TOTAL_WALL_CELLS
529         ALLOCATE(M%WALL(IW)%ZZ_F(N_TRACKED_SPECIES) ,STAT=IZERO)
530         CALL ChkMemErr( 'INIT' , 'WALL(IW)%ZZ_F' , IZERO)
531         M%WALL(IW)%ZZ_F(1:N_TRACKED_SPECIES) = SPECIES_MIXTURE(1:
            N_TRACKED_SPECIES)%ZZ0
532     ENDDO
533     M%WALL%ONE_D%QRADIN = SIGMA*TMPA4
534     M%WALL%ONE_D%QRADOUT = SIGMA*TMPA4
535     M%WALL%ONE_D%QCONF = 0._EB
536     M%WALL%ONE_D%HEAT_TRANS_COEF = 0._EB
537
538     ALLOCATE(M%D_CORR(M%N_EXTERNAL_WALL_CELLS) ,STAT=IZERO)
539     CALL ChkMemErr( 'INIT' , 'D.CORR' , IZERO)
540     ALLOCATE(M%DS_CORR(M%N_EXTERNAL_WALL_CELLS) ,STAT=IZERO)
541     CALL ChkMemErr( 'INIT' , 'DS.CORR' , IZERO)

```

```

542     M%D_CORR = 0._EB
543     M%DS_CORR = 0._EB
544     ALLOCATE(M%UVW_SAVE(M%N_EXTERNAL_WALL_CELLS) ,STAT=IZERO)
545     CALL ChkMemErr ( 'INIT' , 'UVW_SAVE' , IZERO)
546     M%UVW_SAVE = 0._EB
547
548     ALLOCATE(M%U_GHOST(M%N_EXTERNAL_WALL_CELLS) ,STAT=IZERO)
549     CALL ChkMemErr ( 'INIT' , 'U_GHOST' , IZERO)
550     ALLOCATE(M%V_GHOST(M%N_EXTERNAL_WALL_CELLS) ,STAT=IZERO)
551     CALL ChkMemErr ( 'INIT' , 'V_GHOST' , IZERO)
552     ALLOCATE(M%W_GHOST(M%N_EXTERNAL_WALL_CELLS) ,STAT=IZERO)
553     CALL ChkMemErr ( 'INIT' , 'W_GHOST' , IZERO)
554     M%U_GHOST = 0._EB
555     M%V_GHOST = 0._EB
556     M%W_GHOST = 0._EB
557
558 ENDIF NOT_EVAC_IF_1
559
560 ! Allocate arrays for turbulent inflow boundary conditions (
      experimental)
561
562 VENT_LOOP: DO N=1,M%N_VENT
563     VT => M%VENTS(N)
564     EDDY_IF: IF (VT%N_EDDY>0) THEN
565         SELECT CASE(ABS(VT%IOR))
566             CASE(1)
567                 ALLOCATE(VT%U_EDDY(VT%J1+1:VT%J2 ,VT%K1+1:VT%K2) ,
                          STAT=IZERO)
568                 CALL ChkMemErr ( 'READ_VENT' , 'U_EDDY' , IZERO)
569                 ALLOCATE(VT%V_EDDY(VT%J1+1:VT%J2 ,VT%K1+1:VT%K2) ,
                          STAT=IZERO)
570                 CALL ChkMemErr ( 'READ_VENT' , 'V_EDDY' , IZERO)
571                 ALLOCATE(VT%W_EDDY(VT%J1+1:VT%J2 ,VT%K1+1:VT%K2) ,
                          STAT=IZERO)
572                 CALL ChkMemErr ( 'READ_VENT' , 'W_EDDY' , IZERO)
573             CASE(2)
574                 ALLOCATE(VT%U_EDDY(VT%I1+1:VT%I2 ,VT%K1+1:VT%K2) ,
                          STAT=IZERO)
575                 CALL ChkMemErr ( 'READ_VENT' , 'U_EDDY' , IZERO)
576                 ALLOCATE(VT%V_EDDY(VT%I1+1:VT%I2 ,VT%K1+1:VT%K2) ,
                          STAT=IZERO)
577                 CALL ChkMemErr ( 'READ_VENT' , 'V_EDDY' , IZERO)

```

```

578      ALLOCATE(VT%W_EDDY(VT%I1+1:VT%I2,VT%K1+1:VT%K2),
              STAT=IZERO)
579      CALL ChkMemErr('READ_VENT', 'W_EDDY', IZERO)
580      CASE(3)
581      ALLOCATE(VT%U_EDDY(VT%I1+1:VT%I2,VT%J1+1:VT%J2),
              STAT=IZERO)
582      CALL ChkMemErr('READ_VENT', 'U_EDDY', IZERO)
583      ALLOCATE(VT%V_EDDY(VT%I1+1:VT%I2,VT%J1+1:VT%J2),
              STAT=IZERO)
584      CALL ChkMemErr('READ_VENT', 'V_EDDY', IZERO)
585      ALLOCATE(VT%W_EDDY(VT%I1+1:VT%I2,VT%J1+1:VT%J2),
              STAT=IZERO)
586      CALL ChkMemErr('READ_VENT', 'W_EDDY', IZERO)
587      END SELECT
588      ALLOCATE(VT%X_EDDY(VT%N_EDDY),STAT=IZERO)
589      CALL ChkMemErr('READ_VENT', 'X_EDDY', IZERO)
590      ALLOCATE(VT%Y_EDDY(VT%N_EDDY),STAT=IZERO)
591      CALL ChkMemErr('READ_VENT', 'Y_EDDY', IZERO)
592      ALLOCATE(VT%Z_EDDY(VT%N_EDDY),STAT=IZERO)
593      CALL ChkMemErr('READ_VENT', 'Z_EDDY', IZERO)
594      ALLOCATE(VT%CU_EDDY(VT%N_EDDY),STAT=IZERO)
595      CALL ChkMemErr('READ_VENT', 'CU_EDDY', IZERO)
596      ALLOCATE(VT%CV_EDDY(VT%N_EDDY),STAT=IZERO)
597      CALL ChkMemErr('READ_VENT', 'CV_EDDY', IZERO)
598      ALLOCATE(VT%CW_EDDY(VT%N_EDDY),STAT=IZERO)
599      CALL ChkMemErr('READ_VENT', 'CW_EDDY', IZERO)
600      VT%U_EDDY=0._EB
601      VT%V_EDDY=0._EB
602      VT%W_EDDY=0._EB
603      VT%X_EDDY=0._EB
604      VT%Y_EDDY=0._EB
605      VT%Z_EDDY=0._EB
606      VT%CU_EDDY=0._EB
607      VT%CV_EDDY=0._EB
608      VT%CW_EDDY=0._EB
609      ENDIF EDDY_IF
610      ENDDO VENT_LOOP
611
612      M%WALL%IW = T_BEGIN
613
614      NOT_EVAC_IF_2: IF (.NOT.EVACUATION_ONLY(NM)) THEN
615          M%WALL%EW = 0._EB
616          M%WALL%KW = 0._EB

```



```

617 DO IW=1,N_TOTAL_WALL_CELLS
618 ALLOCATE(M%WALL(IW)%RHODW(N_TRACKED_SPECIES),STAT=IZERO)
619 CALL ChkMemErr('INIT','WALL(IW)%RHODW',IZERO)
620 M%WALL(IW)%RHODW = 0.1_EB ! Do not initialize to zero to
        avoid divide by zero in the first time step
621 ENDDO
622 M%WALL%AREA_ADJUST = 1._EB
623 DO IW=1,N_TOTAL_WALL_CELLS
624 ALLOCATE(M%WALL(IW)%ONE_D%MASSFLUX(0:N_TRACKED_SPECIES),
        STAT=IZERO)
625 CALL ChkMemErr('INIT','WALL(IW)%ONE_D%MASSFLUX',IZERO)
626 M%WALL(IW)%ONE_D%MASSFLUX = 0._EB
627 ALLOCATE(M%WALL(IW)%ONE_D%MASSFLUX_ACTUAL(0:
        N_TRACKED_SPECIES),STAT=IZERO)
628 CALL ChkMemErr('INIT','WALL(IW)%ONE_D%MASSFLUX_ACTUAL',
        IZERO)
629 M%WALL(IW)%ONE_D%MASSFLUX_ACTUAL = 0._EB
630 ENDDO
631 M%WALL%NPPCW = 1
632 M%WALL%BACK_INDEX = 0
633 M%WALL%AW = 0._EB
634 M%WALL%RAW = 0._EB
635 ENDIF NOT_EVAC_IF_2
636
637 M%WALL%RDN = 1._EB
638 M%WALL%UW0 = 0._EB
639 M%WALL%UW = 0._EB
640 M%WALL%UWS = 0._EB
641 M%WALL%OBST_INDEX = 0
642 M%WALL%VENT_INDEX = 0
643 ALLOCATE(M%DUWDT(N_TOTAL_WALL_CELLS),STAT=IZERO)
644 CALL ChkMemErr('INIT','DUWDT',IZERO)
645 M%DUWDT = 0._EB
646 ALLOCATE(M%PRESSURE_BC_INDEX(0:M%N_EXTERNAL_WALL_CELLS),STAT=
        IZERO)
647 CALL ChkMemErr('INIT','PRESSURE_BC_INDEX_',IZERO)
648 M%PRESSURE_BC_INDEX = NEUMANN
649 M%WALL%PRESSURE_BC_INDEX = NEUMANN
650 M%WALL%SURF_INDEX_ORIG = 0
651 M%WALL%BOUNDARY_TYPE = NULLBOUNDARY
652 ALLOCATE(M%WALL_INDEX(0:M%CELL_COUNT,-3:3),STAT=IZERO)
653 CALL ChkMemErr('INIT','WALL_INDEX',IZERO)
654 M%WALL_INDEX = 0

```

```

655 ALLOCATE(M%EDGE_INDEX(0:M%CELL_COUNT,1:12),STAT=IZERO)
656 CALL ChkMemErr('INIT','EDGE_INDEX',IZERO)
657 M%EDGE_INDEX = 0
658 ALLOCATE(M%UVW_GHOST(0:M%CELL_COUNT,3),STAT=IZERO)
659 CALL ChkMemErr('INIT','UVW_GHOST',IZERO)
660 M%UVW_GHOST = 0
661
662 ! Surface soot array
663
664 IF (N_SURFACE_DENSITY_SPECIES > 0 .AND. .NOT.EVACUATION_ONLY(NM
    )) THEN
665     ALLOCATE(M%AWMAEROSOL(N_TOTAL_WALL_CELLS,
        N_SURFACE_DENSITY_SPECIES),STAT=IZERO)
666     CALL ChkMemErr('INIT','AWMAEROSOL',IZERO)
667     M%AWMAEROSOL = 0._EB
668     DO IW=1,N_TOTAL_WALL_CELLS
669         ALLOCATE(M%WALL(IW)%AWMAEROSOL(N_SURFACE_DENSITY_SPECIES
            ),STAT=IZERO)
670         CALL ChkMemErr('INIT','WALL(IW)%AWMAEROSOL',IZERO)
671         M%WALL(IW)%AWMAEROSOL = 0._EB
672     ENDDO
673 ENDIF
674
675 ! Surface water arrays
676
677 IF (ACCUMULATE_WATER .AND. .NOT.EVACUATION_ONLY(NM)) THEN
678     DO IW = 1,N_TOTAL_WALL_CELLS
679         ALLOCATE(M%WALL(IW)%A_LP_MPUA(N_LP_ARRAY_INDICES),STAT=
            IZERO)
680         CALL ChkMemErr('INIT','WALL(IW)%A_LP_MPUA',IZERO)
681         M%WALL(IW)%A_LP_MPUA = 0._EB
682     ENDDO
683 ENDIF
684
685 IF (.NOT.EVACUATION_ONLY(NM)) THEN
686
687     DO IW = 1,N_TOTAL_WALL_CELLS
688         ALLOCATE(M%WALL(IW)%LP_MPUA(N_LP_ARRAY_INDICES),STAT=
            IZERO)
689         CALL ChkMemErr('INIT','WALL(IW)%LP_MPUA',IZERO)
690         M%WALL(IW)%LP_MPUA = 0._EB
691         ALLOCATE(M%WALL(IW)%LP_CPUA(N_LP_ARRAY_INDICES),STAT=
            IZERO)

```

```

692     CALL ChkMemErr( 'INIT' , 'WALL(IW)%LP_CPUA' , IZERO)
693     M%WALL(IW)%LP_CPUA = 0. _EB
694     ENDDO
695 ENDIF
696
697 ! Surface work arrays
698 ALLOCATE(M%WALLWORK1(N_TOTAL_WALL_CELLS) ,STAT=IZERO)
699 CALL ChkMemErr( 'INIT' , 'WALLWORK1' , IZERO)
700 ALLOCATE(M%WALLWORK2(N_TOTAL_WALL_CELLS) ,STAT=IZERO)
701 CALL ChkMemErr( 'INIT' , 'WALLWORK2' , IZERO)
702
703 ! Vegetation surface drag
704
705 ALLOCATE(M%VEG_DRAG(0:IBP1 , 0:JBP1) ,STAT=IZERO)
706 CALL ChkMemErr( 'INIT' , 'VEG_DRAG' , IZERO)
707 M%VEG_DRAG = 0. _EB
708
709 ! Set up boundary arrays for external boundaries of the current
       mesh
710
711 IWE = 0
712 IWG = M%N_EXTERNAL_WALL_CELLS + M%N_INTERNAL_WALL_CELLS + M%
       N_VIRTUAL_WALL_CELLS
713
714 DO K=0,KBP1
715     DO J=0,JBP1
716         I = 0
717         SURF_INDEX = DEFAULT_SURF_INDEX
718         IOR = 1
719         IF (J==0 .OR. J==JBP1 .OR. K==0 .OR. K==KBP1) THEN
720             IWG = IWG + 1
721             IW = IWG
722         ELSE
723             IWE = IWE + 1
724             IW = IWE
725         ENDIF
726         CALL INIT_WALL_CELL(NM, I , J , K, 0 , IW, IOR, SURF_INDEX, IERR)
727         IF (IERR.>0) RETURN
728     ENDDO
729 ENDDO
730 DO K=0,KBP1
731     DO J=0,JBP1
732         I = IBP1

```

```

733     SURF_INDEX = DEFAULT_SURF_INDEX
734     IOR = -1
735     IF (J==0 .OR. J==JBP1 .OR. K==0 .OR. K==KBP1) THEN
736         IWG = IWG + 1
737         IW = IWG
738     ELSE
739         IWE = IWE + 1
740         IW = IWE
741     ENDIF
742     CALL INIT_WALL_CELL(NM, I , J , K, 0 , IW, IOR, SURF_INDEX, IERR)
743     IF (IERR>0) RETURN
744 ENDDO
745 ENDDO
746
747 DO K=0,KBP1
748     DO I=0,IBP1
749         J = 0
750         SURF_INDEX = DEFAULT_SURF_INDEX
751         IOR = 2
752         IF (I==0 .OR. I==IBP1 .OR. K==0 .OR. K==KBP1) THEN
753             IWG = IWG + 1
754             IW = IWG
755         ELSE
756             IWE = IWE + 1
757             IW = IWE
758         ENDIF
759         CALL INIT_WALL_CELL(NM, I , J , K, 0 , IW, IOR, SURF_INDEX, IERR)
760         IF (IERR>0) RETURN
761     ENDDO
762 ENDDO
763 DO K=0,KBP1
764     DO I=0,IBP1
765         J = JBP1
766         SURF_INDEX = DEFAULT_SURF_INDEX
767         IOR = -2
768         IF (I==0 .OR. I==IBP1 .OR. K==0 .OR. K==KBP1) THEN
769             IWG = IWG + 1
770             IW = IWG
771         ELSE
772             IWE = IWE + 1
773             IW = IWE
774         ENDIF
775         CALL INIT_WALL_CELL(NM, I , J , K, 0 , IW, IOR, SURF_INDEX, IERR)

```

```

776         IF (IERR>0) RETURN
777     ENDDO
778 ENDDO
779
780 IF (.NOT.EVACUATION_ONLY(NM)) THEN
781 DO J=0,JBP1
782     DO I=0,IBP1
783         K = 0
784         SURF_INDEX = DEFAULT_SURF_INDEX
785         IOR = 3
786         IF (I==0 .OR. I==IBP1 .OR. J==0 .OR. J==JBP1) THEN
787             IWG = IWG + 1
788             IW = IWG
789         ELSE
790             IWE = IWE + 1
791             IW = IWE
792         ENDIF
793         CALL INIT_WALL_CELL(NM,I,J,K,0,IW,IOR,SURF_INDEX,IERR)
794         IF (IERR>0) RETURN
795     ENDDO
796 ENDDO
797 DO J=0,JBP1
798     DO I=0,IBP1
799         K = KBP1
800         SURF_INDEX = DEFAULT_SURF_INDEX
801         IOR = -3
802         IF (I==0 .OR. I==IBP1 .OR. J==0 .OR. J==JBP1) THEN
803             IWG = IWG + 1
804             IW = IWG
805         ELSE
806             IWE = IWE + 1
807             IW = IWE
808         ENDIF
809         CALL INIT_WALL_CELL(NM,I,J,K,0,IW,IOR,SURF_INDEX,IERR)
810         IF (IERR>0) RETURN
811     ENDDO
812 ENDDO
813 ENDIF
814
815 ! Go through all obstructions and decide which cell faces ought
      to be given a wall cell index and initialized
816
817 M%N_INTERNAL_WALL_CELLS = 0

```

```

818
819 OBST_LOOP_2: DO N=1,M%N_OBST
820     OB=>M%OBSTRUCTION(N)
821
822     DO K=OB%K1+1,OB%K2
823         DO J=OB%J1+1,OB%J2
824             I = OB%I1+1
825             IF (I==1) CYCLE ! Don't assign wall cell index to
                ! obstruction face pointing out of the computational
                ! domain
826             IC = M%CELL_INDEX(I-1,J,K)
827             IF (M%SOLID(IC) .AND. .NOT.M%OBSTRUCTION(M%
                ! Permanently
                ! covered face
                OBST_INDEX_C(IC))%REMOVABLE) CYCLE
828             IOR = -1
829             SURF_INDEX = OB%SURF_INDEX(IOR)
830             IW = M%WALL_INDEX(IC,-IOR)
831             IF (IW==0) THEN
832                 M%N_INTERNAL_WALL_CELLS = M%N_INTERNAL_WALL_CELLS +
                    1
833                 IW = M%N_EXTERNAL_WALL_CELLS + M%
                    N_INTERNAL_WALL_CELLS
834             ENDIF
835             CALL INIT_WALL_CELL(NM,I,J,K,N,IW,IOR,SURF_INDEX,IERR)
836             IF (IERR>0) RETURN
837         ENDDO
838     ENDDO
839
840     DO K=OB%K1+1,OB%K2
841         DO J=OB%J1+1,OB%J2
842             I = OB%I2
843             IF (I==M%IBAR) CYCLE ! Don't assign wall cell index
                ! to obstruction face pointing out of the
                ! computational domain
844             IC = M%CELL_INDEX(I+1,J,K)
845             IF (M%SOLID(IC) .AND. .NOT.M%OBSTRUCTION(M%
                ! Permanently
                ! covered face
                OBST_INDEX_C(IC))%REMOVABLE) CYCLE
846             IOR = 1
847             SURF_INDEX = OB%SURF_INDEX(IOR)
848             IW = M%WALL_INDEX(IC,-IOR)
849             IF (IW==0) THEN

```

```

850           M%N_INTERNAL_WALL_CELLS = M%N_INTERNAL_WALL_CELLS +
            1
851           IW = M%N_EXTERNAL_WALL_CELLS + M%
            N_INTERNAL_WALL_CELLS
852           ENDIF
853           CALL INIT_WALL_CELL(NM, I , J ,K, N, IW, IOR, SURF_INDEX, IERR)
854           IF (IERR>0) RETURN
855       ENDDO
856 ENDDO
857
858 DO K=OB%K1+1,OB%K2
859     DO I=OB%I1+1,OB%I2
860       J = OB%J1+1
861       IF (J==1) CYCLE ! Don't assign wall cell index to
            obstruction face pointing out of the computational
            domain
862       IC = M%CELL_INDEX(I, J-1, K)
863       IF (M%SOLID(IC) .AND. .NOT.M%OBSTRUCTION(M%
            OBST_INDEX_C(IC))%REMOVABLE) CYCLE ! Permanently
            covered face
864       IOR = -2
865       SURF_INDEX = OB%SURF_INDEX(IOR)
866       IW = M%WALL_INDEX(IC, -IOR)
867       IF (IW==0) THEN
868         M%N_INTERNAL_WALL_CELLS = M%N_INTERNAL_WALL_CELLS +
            1
869         IW = M%N_EXTERNAL_WALL_CELLS + M%
            N_INTERNAL_WALL_CELLS
870       ENDIF
871       CALL INIT_WALL_CELL(NM, I , J ,K, N, IW, IOR, SURF_INDEX, IERR)
872       IF (IERR>0) RETURN
873     ENDDO
874 ENDDO
875
876 DO K=OB%K1+1,OB%K2
877     DO I=OB%I1+1,OB%I2
878       J = OB%J2
879       IF (J==M%JBAR) CYCLE ! Don't assign wall cell index
            to obstruction face pointing out of the
            computational domain
880       IC = M%CELL_INDEX(I, J+1, K)
881       IF (M%SOLID(IC) .AND. .NOT.M%OBSTRUCTION(M%
            OBST_INDEX_C(IC))%REMOVABLE) CYCLE ! Permanently

```

```

      covered face
882      IOR = 2
883      SURF_INDEX = OB%SURF_INDEX(IOR)
884      IW = M%WALL_INDEX(IC, -IOR)
885      IF (IW==0) THEN
886          M%N_INTERNAL_WALL_CELLS = M%N_INTERNAL_WALL_CELLS +
              1
887          IW = M%N_EXTERNAL_WALL_CELLS + M%
              N_INTERNAL_WALL_CELLS
888      ENDIF
889      CALL INIT_WALL_CELL(NM, I, J, K, N, IW, IOR, SURF_INDEX, IERR)
890      IF (IERR>0) RETURN
891  ENDDO
892 ENDDO
893
894 DO J=OB%J1+1,OB%J2
895   DO I=OB%I1+1,OB%I2
896     K = OB%K1+1
897     IF (K==1) CYCLE ! Don't assign wall cell index to
      obstruction face pointing out of the computational
      domain
898     IC = M%CELL_INDEX(I, J, K-1)
899     IF (M%SOLID(IC) .AND. .NOT.M%OBSTRUCTION(M%
      OBST_INDEX_C(IC))%REMOVABLE) CYCLE ! Permanently
      covered face
900     IOR = -3
901     SURF_INDEX = OB%SURF_INDEX(IOR)
902     IW = M%WALL_INDEX(IC, -IOR)
903     IF (IW==0) THEN
904         M%N_INTERNAL_WALL_CELLS = M%N_INTERNAL_WALL_CELLS +
              1
905         IW = M%N_EXTERNAL_WALL_CELLS + M%
              N_INTERNAL_WALL_CELLS
906     ENDIF
907     CALL INIT_WALL_CELL(NM, I, J, K, N, IW, IOR, SURF_INDEX, IERR)
908     IF (IERR>0) RETURN
909   ENDDO
910 ENDDO
911
912 DO J=OB%J1+1,OB%J2
913   DO I=OB%I1+1,OB%I2
914     K = OB%K2

```



```

915     IF (K==M%KBAR) CYCLE ! Don't assign wall cell index
      to obstruction face pointing out of the
      computational domain
916     IC = M%CELL_INDEX(I , J ,K+1)
917     IF (M%SOLID(IC) .AND. .NOT.M%OBSTRUCTION(M%
      OBST_INDEX_C(IC))%REMOVABLE) CYCLE ! Permanently
      covered face
918     IOR = 3
919     SURF_INDEX = OB%SURF_INDEX(IOR)
920     IW = M%WALL_INDEX(IC, -IOR)
921     IF (IW==0) THEN
922         M%N_INTERNAL_WALL_CELLS = M%N_INTERNAL_WALL_CELLS +
          1
923         IW = M%N_EXTERNAL_WALL_CELLS + M%
          N_INTERNAL_WALL_CELLS
924     ENDIF
925     CALL INIT_WALL_CELL(NM, I , J ,K, N, IW, IOR, SURF_INDEX, IERR)
926     IF (IERR>0) RETURN
927 ENDDO
928 ENDDO
929
930 ENDDO OBST_LOOP_2
931
932 ! Initialize PSUM for zone cases
933
934 IF (N_ZONE > 0) THEN
935     N_ZONE_LOOP: DO IPZ = 1 ,N_ZONE
936         PSUM(IPZ ,NM) = 0. _EB
937         IF (EVACUATION_ONLY(NM)) EXIT N_ZONE_LOOP
938         DO K=1,M%KBAR
939             DO J=1,M%JBAR
940                 DO I=1,M%IBAR
941                     IF (M%PRESSURE_ZONE(I , J ,K) /= IPZ) CYCLE
942                     IF (M%SOLID(M%CELL_INDEX(I , J ,K))) CYCLE
943                     VC = M%DX(I) *M%RC(I) *M%DY(J) *M%DZ(K)
944                     IF (N_TRACKED_SPECIES>0) ZZ_GET(1:
                        N_TRACKED_SPECIES) = M%ZZ(I , J ,K, 1:
                        N_TRACKED_SPECIES)
945                     CALL GET_SPECIFIC_HEAT(ZZ_GET ,CP,M%IMP(I , J ,K))
946                     RIRM = M%RSUM(I , J ,K) / (CP*M%PBAR(K, IPZ))
947                     PSUM(IPZ ,NM) = PSUM(IPZ ,NM) + VC*(1. _EB/M%PBAR(K
                        , IPZ) -RIRM)
948                 ENDDO
949             ENDDO
950         ENDDO
951     ENDIF

```

```

949         ENDDO
950     ENDDO
951     ENDDO N_ZONELOOP
952 ENDIF
953
954 ! Set up wall cell arrays for VIRTUAL boundaries
955
956 IW = M%N_EXTERNAL_WALL_CELLS + M%N_INTERNAL_WALL_CELLS
957
958 DEVICELOOP: DO N=1,N_DEVC
959     IF (EVACUATION_ONLY(NM)) CYCLE DEVICELOOP
960     DV => DEVICE(N)
961     IF (DV%MESH/=NM) CYCLE DEVICELOOP
962     IF (DV%QUANTITY/= 'CABLE_TEMPERATURE') CYCLE DEVICELOOP
963     IW = IW + 1
964     DV%VIRTUAL_WALL_INDEX = IW
965     I = DV%I
966     J = DV%J
967     K = DV%K
968     SURF_INDEX = DV%SURF_INDEX
969     CALL INIT_WALL_CELL(NM, I, J, K, 0, IW, 0, SURF_INDEX, IERR)
970 ENDDO DEVICELOOP
971
972 ! Determine back wall index for exposed surfaces
973
974 DO IW=M%N_EXTERNAL_WALL_CELLS+1,M%N_EXTERNAL_WALL_CELLS+M%
    N_INTERNAL_WALL_CELLS
975     IF (EVACUATION_ONLY(NM)) CYCLE
976     ! Only assign BACK_INDEX to wall cells that are not attached
        to the exterior boundary of the computational domain
977     SF=>SURFACE(M%WALL(IW)%SURF_INDEX)
978     IF (SF%BACKING==EXPOSED) THEN
979         II = M%WALL(IW)%II
980         JJ = M%WALL(IW)%JJ
981         KK = M%WALL(IW)%KK
982         IC = M%CELL_INDEX( II, JJ, KK)
983         IOR = M%WALL(IW)%IOR
984         IF (.NOT.M%SOLID(IC)) M%WALL(IW)%BACK_INDEX = M%
            WALL_INDEX(IC, IOR)
985         IF ( M%SOLID(IC)) THEN
986             SELECT CASE(IOR)
987                 CASE(-1)
988                     II=II+1

```

```

989         CASE( 1)
990             II=II-1
991         CASE(-2)
992             JJ=JJ+1
993         CASE( 2)
994             JJ=JJ-1
995         CASE(-3)
996             KK=KK+1
997         CASE( 3)
998             KK=KK-1
999         END SELECT
1000         IC = M%CELL_INDEX( II , JJ ,KK)
1001         M%WALL(IW)%BACK_INDEX = M%WALL_INDEX(IC ,IOR)
1002     ENDIF
1003 ENDIF
1004 ENDDO
1005
1006 ! Set clocks and counters related to frequency of solid phase
      conduction updates
1007
1008 M%BC_CLOCK      = T_BEGIN
1009 M%WALL_COUNTER = 0
1010
1011 ! Set clock for boudary fuel vegetation model
1012
1013 M%VEG_CLOCK_BC = T_BEGIN
1014
1015 ! Allocate arrays for storing velocity boundary condition info
1016
1017 N_EDGES_DIM = 4*(IBP1*JBP1+IBP1*KBP1+JBP1*KBP1)
1018 IF (EVACUATION_ONLY(NM)) N_EDGES_DIM = 4*(IBP1*KBP1+JBP1*KBP1)
1019 DO N=1,M%N_OBST
1020     OB=>M%OBSTRUCTION(N)
1021     IPTS = OB%I2-OB%I1
1022     JPTS = OB%J2-OB%J1
1023     KPTS = OB%K2-OB%K1
1024     IF (EVACUATION_ONLY(NM)) THEN
1025         N_EDGES_DIM = N_EDGES_DIM + 4*(IPTS*KPTS+JPTS*KPTS)
1026     ELSE
1027         N_EDGES_DIM = N_EDGES_DIM + 4*(IPTS*JPTS+IPTS*KPTS+JPTS*
      KPTS)
1028     ENDIF
1029 ENDDO

```

```

1030
1031 ALLOCATE(M%IJKE(16,N_EDGES_DIM),STAT=IZERO)
1032 CALL ChkMemErr('INIT','IJKE',IZERO)
1033 M%IJKE = 0
1034 ALLOCATE(M%OMEGA(0:N_EDGES_DIM,-2:2),STAT=IZERO)
1035 CALL ChkMemErr('INIT','OMEGA',IZERO)
1036 M%OMEGA = 0._EB
1037 ALLOCATE(M%TAU(0:N_EDGES_DIM,-2:2),STAT=IZERO)
1038 CALL ChkMemErr('INIT','TAU',IZERO)
1039 M%TAU = 0._EB
1040 ALLOCATE(M%EDGE_TYPE(N_EDGES_DIM,2),STAT=IZERO)
1041 CALL ChkMemErr('INIT','EDGE_TYPE',IZERO)
1042 M%EDGE_TYPE = SOLID_EDGE
1043 ALLOCATE(M%EDGE_INTERPOLATION_FACTOR(N_EDGES_DIM,2),STAT=IZERO)
1044 CALL ChkMemErr('INIT','EDGE_INTERPOLATION_FACTOR',IZERO)
1045 M%EDGE_INTERPOLATION_FACTOR = 1._EB
1046
1047 ! Initialize and allocate lagrangian particle/PARTICLE arrays
1048
1049 M%NLP = 0
1050 M%NLPDIM = 1000
1051 IF (PARTICLE_FILE .AND. .NOT.EVACUATION_ONLY(NM)) THEN
1052     ALLOCATE(M%LAGRANGIAN_PARTICLE(M%NLPDIM),STAT=IZERO)
1053     CALL ChkMemErr('INIT','PARTICLE',IZERO)
1054 ENDIF
1055
1056 ! Allocate array to hold character strings for Smokeview file
1057
1058 M%N_STRINGS = 0
1059 M%N_STRINGS_MAX = 100
1060 ALLOCATE(M%STRING(M%N_STRINGS_MAX),STAT=IZERO)
1061 CALL ChkMemErr('INIT','STRING',IZERO)
1062
1063 ! Set up arrays to hold velocity boundary condition info
1064
1065 CALL INITIALIZE_EDGES
1066
1067 ! Initialize Pressure solver
1068
1069 CALL INITIALIZE_POISSON_SOLVER
1070 IF (IERR/=0) RETURN
1071

```

```
1072 ! Determine which wall cells to assign for solid phase
      thermocouples and profiles
1073
1074 CALL INITIALIZE_DEVC
1075 IF (IERR/=0) RETURN
1076
1077 CALL INITIALIZE_PROF
1078 IF (IERR/=0) RETURN
1079
1080 ! Initialize Mesh Exchange
1081
1082 CALL INITIALIZE_INTERPOLATION
1083
1084
1085 CONTAINS
```

Appendix C

Flame Height Calculation, post-processing

```
1 program compute_flame_height
2
3 character(30) :: infile(16,3)
4 real :: z(0:200), hrrpul(200), height(16,3), qstar(16), diameter,
   sumold
5 integer :: i, n, npts
6
7 diameter = 1.13 ! Equivalent diameter of 1 m2 square
8
9 qstar(1) = 0.1
10 qstar(2) = 0.2
11 qstar(3) = 0.5
12 qstar(4) = 1.0
13 qstar(5) = 2.0
14 qstar(6) = 5.0
15 qstar(7) = 10.
16 qstar(8) = 20.
17 qstar(9) = 50.
18 qstar(10) = 100.
19 qstar(11) = 200.
20 qstar(12) = 500.
21 qstar(13) = 1000.
22 qstar(14) = 2000.
23 qstar(15) = 5000.
24 qstar(16) = 10000.
25
26 infile(1,1) = 'Qs=p1-RI=05_fds2ascii.csv'
```

```
27 infile (2,1) = 'Qs=p2_RI=05_fds2ascii.csv'
28 infile (3,1) = 'Qs=p5_RI=05_fds2ascii.csv'
29 infile (4,1) = 'Qs=1_RI=05_fds2ascii.csv'
30 infile (5,1) = 'Qs=2_RI=05_fds2ascii.csv'
31 infile (6,1) = 'Qs=5_RI=05_fds2ascii.csv'
32 infile (7,1) = 'Qs=10_RI=05_fds2ascii.csv'
33 infile (8,1) = 'Qs=20_RI=05_fds2ascii.csv'
34 infile (9,1) = 'Qs=50_RI=05_fds2ascii.csv'
35 infile (10,1) = 'Qs=100_RI=05_fds2ascii.csv'
36 infile (11,1) = 'Qs=200_RI=05_fds2ascii.csv'
37 infile (12,1) = 'Qs=500_RI=05_fds2ascii.csv'
38 infile (13,1) = 'Qs=1000_RI=05_fds2ascii.csv'
39 infile (14,1) = 'Qs=2000_RI=05_fds2ascii.csv'
40 infile (15,1) = 'Qs=5000_RI=05_fds2ascii.csv'
41 infile (16,1) = 'Qs=10000_RI=05_fds2ascii.csv'
42
43 infile (1,2) = 'Qs=p1_fds2ascii.csv'
44 infile (2,2) = 'Qs=p2_fds2ascii.csv'
45 infile (3,2) = 'Qs=p5_fds2ascii.csv'
46 infile (4,2) = 'Qs=1_fds2ascii.csv'
47 infile (5,2) = 'Qs=2_fds2ascii.csv'
48 infile (6,2) = 'Qs=5_fds2ascii.csv'
49 infile (7,2) = 'Qs=10_fds2ascii.csv'
50 infile (8,2) = 'Qs=20_fds2ascii.csv'
51 infile (9,2) = 'Qs=50_fds2ascii.csv'
52 infile (10,2) = 'Qs=100_fds2ascii.csv'
53 infile (11,2) = 'Qs=200_fds2ascii.csv'
54 infile (12,2) = 'Qs=500_fds2ascii.csv'
55 infile (13,2) = 'Qs=1000_fds2ascii.csv'
56 infile (14,2) = 'Qs=2000_fds2ascii.csv'
57 infile (15,2) = 'Qs=5000_fds2ascii.csv'
58 infile (16,2) = 'Qs=10000_fds2ascii.csv'
59
60 infile (1,3) = 'Qs=p1_RI=20_fds2ascii.csv'
61 infile (2,3) = 'Qs=p2_RI=20_fds2ascii.csv'
62 infile (3,3) = 'Qs=p5_RI=20_fds2ascii.csv'
63 infile (4,3) = 'Qs=1_RI=20_fds2ascii.csv'
64 infile (5,3) = 'Qs=2_RI=20_fds2ascii.csv'
65 infile (6,3) = 'Qs=5_RI=20_fds2ascii.csv'
66 infile (7,3) = 'Qs=10_RI=20_fds2ascii.csv'
67 infile (8,3) = 'Qs=20_RI=20_fds2ascii.csv'
68 infile (9,3) = 'Qs=50_RI=20_fds2ascii.csv'
69 infile (10,3) = 'Qs=100_RI=20_fds2ascii.csv'
```

```

70 infile (11,3) = 'Qs=200_RI=20_fds2ascii.csv '
71 infile (12,3) = 'Qs=500_RI=20_fds2ascii.csv '
72 infile (13,3) = 'Qs=1000_RI=20_fds2ascii.csv '
73 infile (14,3) = 'Qs=2000_RI=20_fds2ascii.csv '
74 infile (15,3) = 'Qs=5000_RI=20_fds2ascii.csv '
75 infile (16,3) = 'Qs=10000_RI=20_fds2ascii.csv '
76
77 write (6,"(a)") "Q*,L/D_(RI=5),L/D_(RI=10),L/D_(RI=20)"
78
79 file_loop: do n=1,16
80
81     resolution_loop: do i=1,3
82
83         if (i==1) npts=39
84         if (i==2) npts=76
85         if (i==3) npts=151
86
87         open(10,file=infile(n,i),form='formatted',status='old')
88         read(10,*)
89         read(10,*)
90         z = 0.
91         z(0) = 0.
92         do k=1,npts
93             read(10,*,end=20) z(k),hrrpul(k)
94         enddo
95     20 continue
96         sum = 0.
97         do k=1,npts
98             !! sum = sum + hrrpul(k)*(z(k)-z(k-1))
99             sum = sum + hrrpul(k)
100         enddo
101         sum1 = 0.
102         do k=1,npts
103             !! sum1 = sum1 + hrrpul(k)*(z(k)-z(k-1))
104             sumold = sum1
105             sum1 = sum1 + hrrpul(k)
106             if (sum1/sum>0.99) then
107                 height(n,i) = z(k-1) + (z(k)-z(k-1))*(0.99*sum-
108                     sumold)/(sum1-sumold)
109             endif
110         enddo
111

```



```
112     enddo resolution_loop
113
114     write(6,"(f8.1,' ',f8.2,' ',f8.2,' ',f8.2)") qstar(n),height
        (n,1)/diameter,height(n,2)/diameter,height(n,3)/diameter
115     close(10)
116
117 enddo file_loop
118
119 end program
```